

THE ORBITING GEOPHYSICAL  
OBSERVATORIES  
OGO  
PROGRAM  
SUMMARY

COPY FILE  
COPY

NATIONAL AERONAUTICS AND SPACE ADMINISTRATION



THE ORBITING GEOPHYSICAL  
OBSERVATORIES  
**OGO  
PROGRAM  
SUMMARY**

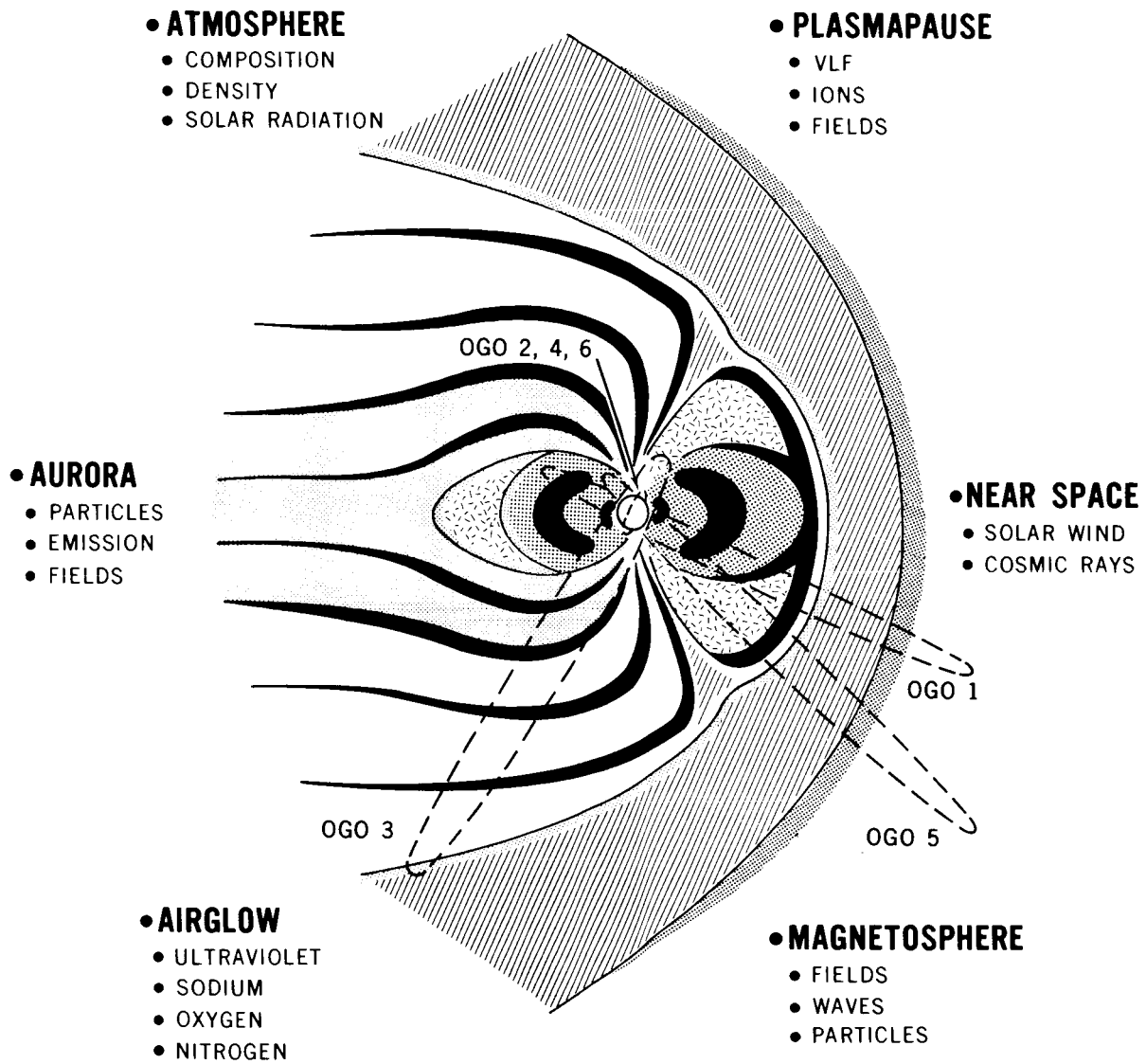
By  
John E. Jackson

Prepared by  
National Space Science Data Center  
NASA Goddard Space Flight Center



*Scientific and Technical Information Branch* 1978  
NATIONAL AERONAUTICS AND SPACE ADMINISTRATION  
*Washington, D.C.*

This document is available from the National Technical Information Service (NTIS),  
Springfield, Virginia 22161, at the price code A06 (\$6.50 domestic; \$13.00 foreign).



# ORBITING GEOPHYSICAL OBSERVATORIES 1964-1971

# CONTENTS

SECTION	PAGE
I. FOREWORD .....	I-1
II. INTRODUCTION .....	II-1
III. OVERVIEW OF THE OGO PROGRAM* .....	III-1
5. OGO 5 Results .....	III-1
6. OGO 6 Results .....	III-11
References .....	III-19
IV. SPACECRAFT AND EXPERIMENT LITERATURE REFERENCES .....	IV-1
A. OGO 1 .....	IV-1
B. OGO 2 .....	IV-4
C. OGO 3 .....	IV-7
D. OGO 4 .....	IV-10
E. OGO 5 .....	IV-13
F. OGO 6 .....	IV-18
V. ADDITIONAL LITERATURE CITATIONS AND ABSTRACTS .....	V-1
A. Literature Cited in IAA .....	V-1
B. Literature Cited in STAR .....	V-31
C. Literature Cited in Other Series .....	V-37
VI. INDEXES TO ADDITIONAL LITERATURE CITATIONS AND ABSTRACTS .....	VI-1
A. Subject Index .....	VI-1
B. Personal Author Index .....	VI-17
C. Corporate Source Index .....	VI-25

\* This is a continuation of part III-B of the *OGO Program Summary* (Jackson and Vette, 1975) in which the scientific results from the OGO 1-4 missions had been given under the headings III-B-1 through III-B-4, respectively.

# I. FOREWORD

A program summary provides a valuable but, unfortunately, seldom available final report for a major research undertaking, representing the combined efforts of hundreds of scientists, engineers, technicians, and administrators over a period of a decade or more. The concept of the program summary, as developed at the National Space Science Data Center (NSSDC)\*, includes not only a description of the objectives, spacecraft, experiments, and flight performance, but also a complete experiment-related bibliography along with a comprehensive assessment of the technological and scientific accomplishments. The program summary also provides abstracts of the bibliography, as well as author, subject, and corporate source indexes. Such a document should provide a useful management tool with which the cost effectiveness of a scientific program can be measured. This should be valuable for the planning of future efforts, as well as for historical purposes.

The NSSDC facilities are unusually well suited for the compilation of program summaries. The comprehensive approach used by NSSDC for the archiving and distribution of satellite data has led not only to an extensive collection of data tapes, films and prints but also to a very complete documentation on spacecraft and experiments. The spacecraft documentation is in fact more complete than the acquisition of data at NSSDC, because it is usually initiated for all missions during the prelaunch hardware phase and it is available for all missions, whether or not data are ever deposited at NSSDC. This supporting documentation is computerized and it includes complete descriptions of spacecraft and experiments. Also available at NSSDC is a computerized space science literature file containing some 30,000 literature citations coded according to satellite(s) and experiment(s). The task of producing a program summary can therefore be greatly simplified with the help of appropriate

computer printouts from the above NSSDC files. Program-related papers and reports, which have not been published in scientific journals, can usually be found in the NSSDC microfiche file.

The effort devoted to the NSSDC literature file is not as extensive and comprehensive as the aerospace literature acquisition and distribution program carried out by the NASA Scientific and Technical Information Facility. Consequently, to produce the bibliography for a program summary NSSDC relies heavily on the resources of the NASA Facility. A cooperative effort between NSSDC and the NASA Facility led to the production of the first program summary; namely, the OGO Program Summary (Jackson and Vette, 1975). The roles of each group and the rationale for such a document are explained in more detail in the Foreword and Introduction to the OGO Program Summary.

This Supplement to the OGO Program Summary has also been produced jointly by NSSDC and the NASA Facility. It was pointed out in the introduction of the OGO Program Summary that a Supplement would be needed, because the large number of OGO 5 and OGO 6 articles still appearing in the literature made it advisable to delay the writing of the OGO 5 and OGO 6 overviews. This Supplement provides an updating of the OGO Bibliography with approximately 200 additional citations and the scientific results of the OGO 5 and OGO 6 missions. Since the latest literature search was completed 8 years after the launch of the last OGO mission, the OGO Bibliography should now be very close to the definitive stage. Additional publications found later will be entered on a routine basis in the NSSDC literature file to make this information available if desired. Suggestions for the improvement of future summaries are solicited.

\*A glossary of acronyms and abbreviations used in this report is given in section VIII of the OGO Program Summary (Jackson and Vette, 1975).

## II. INTRODUCTION

The purpose of the Supplement to the OGO Program Summary is to provide a major updating of the OGO bibliography and a comprehensive summary of the scientific results from the OGO 5 and OGO 6 missions. These scientific results were not included in the original document, because a large number of OGO 5 and OGO 6 publications were still appearing in the literature when the OGO Program Summary (Jackson and Vette, 1975) was being finalized. The postponement turned out to be well justified, because the total OGO 5 and OGO 6 publications have increased substantially during the subsequent 3 years.

The Supplement follows the same format as that of the OGO Program Summary, but it does not repeat finalized information given in the original document. Thus, the reader must refer to the original document for spacecraft and experiment descriptions, for much of the literature citations and related indexes, for the general summary of the OGO program, for the scientific results from the OGO 1-4 missions, and for a detailed discussion of format and organization. The original document should also be consulted for indexes of experiments, experimenters, and associated institutions. The Glossary of Abbreviations and Acronyms is not repeated in the Supplement, because it was essentially complete in the original document.

The bibliography in the Supplement is again presented by experiment using the same (PM, PS, PC, OM, and OS) author code and the same (A, N, and B) document code as explained in the Introduction for the OGO Program Summary. The updated bibliography is cumulative and it shows the total productivity for each individual experiment. The updated cumulative list contains approximately 200 additional citations. The new A and N numbers within the cumulative list are in italics to indicate that the corresponding citations and abstracts appear in the Supplement. In order to obtain as complete a bibliography as possible, a final search for OGO publications was conducted in July 1977 at NSSDC and also at the NASA Scientific and Technical Information Facility. The present bibliography should be essentially complete as of that date.

The OGO bibliography given in the OGO Program Summary and its Supplement includes 1003 documents; 573 are articles in refereed scientific or technical journals; 163 are articles in proceedings of symposia (including proceedings in books; in special publications by NASA, universities, or industry; and in COSPAR publication *Space Research*). The remaining documents are classified as: Book Articles (9), Government Reports (82), University Reports (134) and Industry Reports (42). The journals in which most of the articles have been found and the number of articles are given in Table II-1.

TABLE II-1

### Journals Where Most OGO Experiment Articles Appear

Journal Name	No. of Articles
Annales de Géophysique	11
Astrophysical Journals Pts. 1, 2, & 3	28
Journal of Geophysical Research-Space Science	327
IEEE Proceedings (all)	23
Journal of Atmospheric & Terrestrial Physics	23
Physical Review Letters	7
Planetary and Space Science	37
Radio Science	14
Solar Physics	30
Space Research (COSPAR)	36
Space Science Reviews	12
Other Journals	61

Of the 964 documents which were related to experiments, as opposed to spacecraft, the distribution was PM = 742, OM = 56, PS = 74, OS = 83, and PC = 9. Since a given document could be related to more than one OGO experiment, a single code assignment was made on the basis of the hierarchy PM, OM, PS, OS, PC. As expected, the majority of documents cited were written by the PI group and discussed a major topic of an OGO experiment.

The status of the OGO Bibliography can be assessed in a quantitative manner with the aid of the data presented in Figure II-1 and Figure II-2. These figures show the total scientific publications from each of the 6 OGO missions as a function of time. Only experiment-related publications that appeared in scientific journals were used in compiling the data for these graphs. The data in Figure II-1 and Figure II-2 suggest that the present bibliography is now close to 100 percent complete for the OGO 1, 2, and 3 missions and about 80 percent complete for the OGO 4, 5, and 6 missions. These cumulative publication graphs are an updated version of Figure II-1 and Figure II-2 from the initial OGO Program Summary. A comparison with the original graphs shows that the OGO 5 and OGO 6 publications increased by 67 and 52 journal articles, respectively, showing that the scientific returns were far from being complete for the last two OGO missions when the initial OGO Program Summary was being assembled. Somewhat surprising is the increase in OGO 4 publications. With the 27 additional publications, which have now been identified, it is evident that the previously published summary of the OGO 4 results is now somewhat incomplete. In order to be consistent with Figures II-1 and II-2 from the OGO Program Summary, the corresponding figures in the Supplement include all identified journal publications in the PM, OM, PS and OS categories. From a total of 549 publications shown on the new Figures II-1 and II-2,

## INTRODUCTION

465 or 85 percent are in the PM or OM categories. The percentage of publications in the PM or OM categories varies from a minimum of 75 percent for the OGO 3 graph to a maximum of 91 percent for the OGO 2 graph.

The graphs in Figure II-1 and Figure II-2 also provide useful information concerning the time period required to produce the scientific results from the OGO missions. These graphs reveal that OGO papers have been published in scientific journals for a period of at least 10 years beyond launch, and in the case of OGO 4, 5, and 6 for about 6 to 8 years beyond the end of the data acquisition phase. The peak publication rate for all the OGO missions extends for a period of 2 to 3 years, beginning 2 to 3 years after launch. Allowing an average time of 6 months for publication, it is seen that about 50 percent of the publications occurred later than 4 years after launch. Thus, a large fraction of the important experimental results are produced well after prime data analysis funding has ended. OGO experimenters have frequently stressed in final reports submitted to NASA the fact that only a small fraction of their data could be analyzed with the resources available to them. Thus, potentially an even greater scientific output could have been achieved in many cases. Even without speculating on this possible loss of significant scientific results, it is evident from the graphs in Figure II-1 and Figure II-2 that additional support after prime data analysis is essential if most of the scientific results are to be understood and made accessible to the scientific community in an acceptable manner. Evidently, many OGO experimenters have managed to obtain this additional support and this has contributed in no small measure to the extraordinary success of the OGO program.



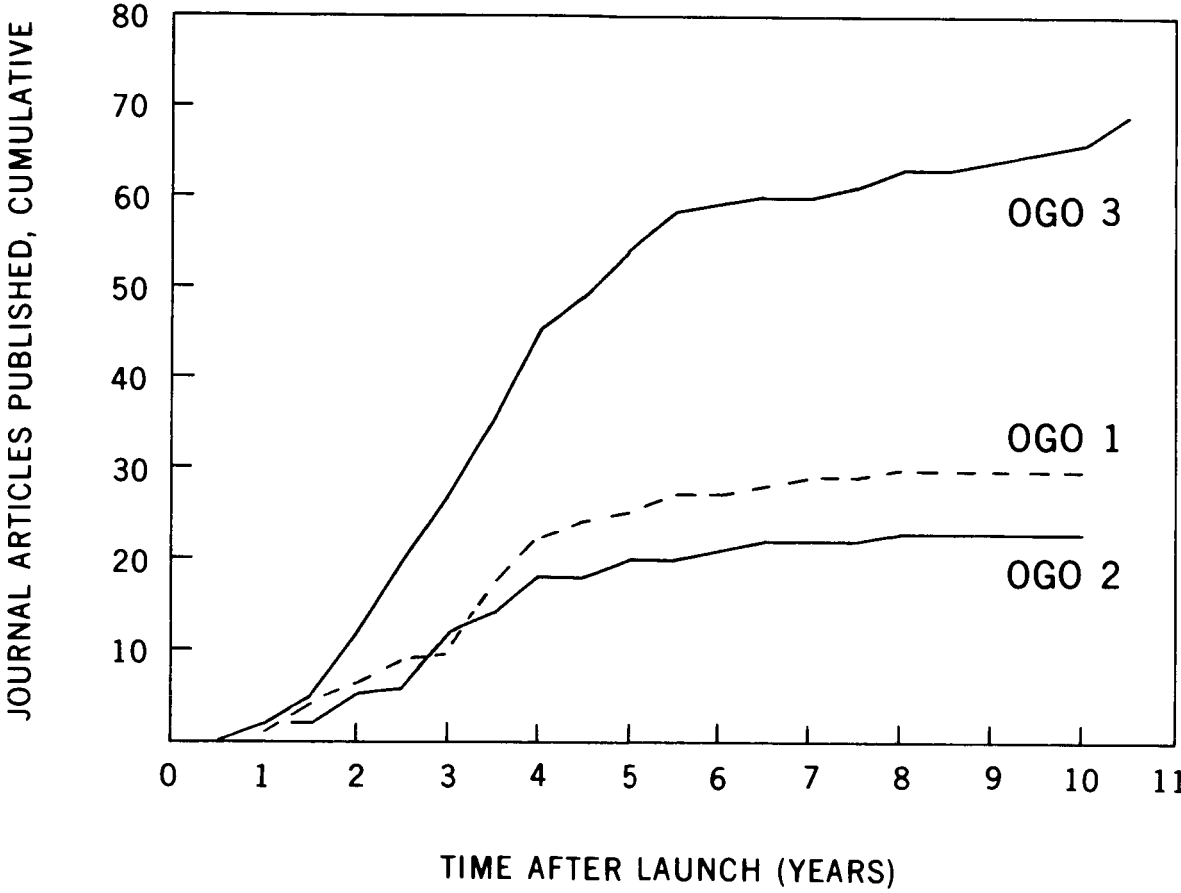


FIGURE II-1

INTRODUCTION

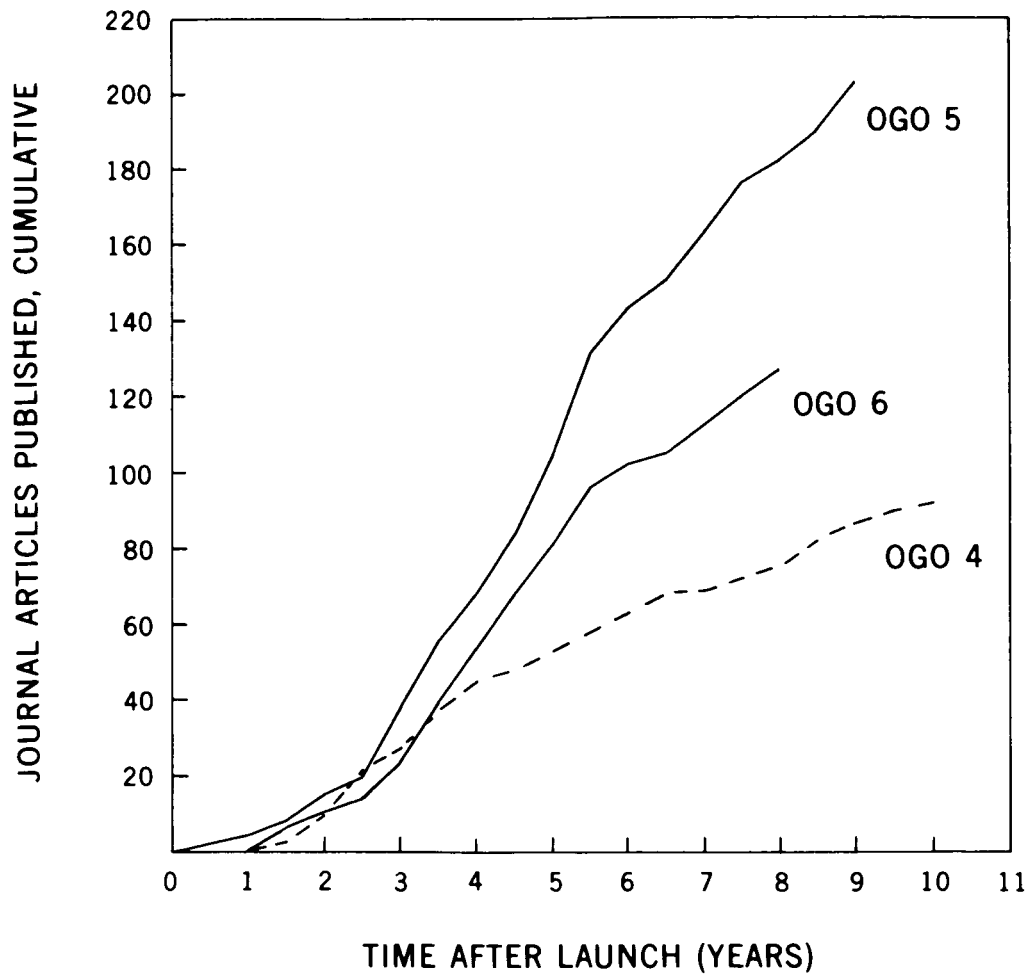


FIGURE II-2

# III. OVERVIEW OF THE OGO PROGRAM

## Scientific Results From the OGO 5 and OGO 6 Missions

### 5. OGO 5 Results

The OGO 5 mission was in many respects the most successful mission of the OGO program. The three-axis stabilization of OGO 5 was maintained for 41 months, a duration which was more than twice the combined total stabilized life of the first four OGOS. The OGO 5 spacecraft had the greatest number of successful experiments (22 out of 25) and it yielded the greatest number of experiment hours of data (636,000). The OGO 5 experiments had by July 1977 resulted in over 200 publications in refereed scientific journals. This number, which is by far the greatest of the OGO program, is comparable to the total combined journal publications from the first four OGO missions. The OGO 6 mission is in second place for attitude-controlled operation (24 months) and for journal publications (about 130). The OGO 3 mission, however, is in second place for the number of successful experiments (19 out of 23) and for the number of experiment hours of data (440,000).

Technologically, OGO 5 represents the last stage of the OGO spacecraft evolution. The OGO 5 spacecraft incorporated, for the first time, a capability of ejecting deployable experimental elements whose effect could not be adequately predicted and which might jeopardize the success of the mission. Thus, the de Havilland antennas, which caused oscillation problems on OGO 4, were not only shortened from 18.3 to 9.15 meters (60 to 30 feet), but also made ejectable. The OGO 5 spacecraft did experience a drop of power (by a factor of 10) in one wideband transmitter, 30 days after launch. There were also two partial failures in redundant assemblies. These failures, however, had very little impact upon the OGO 5 mission.

As indicated earlier, 22 of the 25 OGO 5 experiments can be considered successful. The three unsuccessful experiments were: E-07 (Frank), which failed 8 days after launch after yielding a small amount of useful data (see sections 5.1.3.4 and 5.1.4); E-02 (Sagalyn), which had a partial failure 2 weeks after launch, followed by very severe degradation preventing the acquisition of useful data; and E-26 (Aggson), which was severely handicapped by the shortening of the antennas from 18.3 to 9.15 meters (60 to 30 feet). Although the scientific objectives of experiment E-26 could not be achieved, some useful technological information was obtained concerning electrical field measurements in very low density plasma (Heppner, 1975).

The scientific results from OGO 5 have been summarized following the same organization as was used for the overview of the OGO 1, 2, 3, and 4 missions (Jackson and Vette, 1975). The OGO 5 accomplishments were, therefore, grouped according to the following disciplines: magnetic and electric fields, low-energy plasmas, energetic particles, radio physics, and optical experiments (airglow, aurora, Lyman-alpha, etc.). In many instances, however, it was necessary to modify the above organization in order to present more coherently various interdisciplinary investigations such as, for example, the study of the magnetospheric substorms of August 15, 1968. This substorm investigation was based upon correlative data from three of the above disciplines and from a total of seven OGO 5 experiments.

A comparison between OGO 5 and the previous OGO missions would show that the OGO 5 experiments were in general much more sophisticated and comprehensive than the earlier OGO experiments. For example, instead of simply measuring the bulk speed and density of the solar wind, the OGO 5 experiments were concerned with topics such as the directional variation of solar wind temperature (parallel vs perpendicular temperatures) or temperature differences between solar wind constituents (helium vs hydrogen temperatures). The OGO 5 techniques for examining waves included such refinements as the production of dynamic spectra, the determination of principal axes, and the performance of cross-correlation analyses. Significant improve-

ments were evidenced also in many other areas, particularly in the multidisciplinary approach to many of the magnetospheric problems.

### 5.1 Magnetic Field and Electric Field Measurements

Magnetic and electric field measurements have yielded a large number of important results concerning various magnetospheric regions and concerning various magnetospheric phenomena. The results are presented by regions insofar as is practical and by phenomena when this appears to be more appropriate. In many cases the results presented under the 5.1 headings were based in part upon low-energy plasma measurements (5.2) and upon energetic particle data (5.3). This is indicated by references to the appropriate experiments. No attempt, however, is made to include these results again under the 5.2 and 5.3 headings.

#### 5.1.1 Detailed Mapping of the Magnetic Field in the Magnetosphere (E-15, B-11)

Data from both OGO 3 (Experiment B-11) and OGO 5 (Experiment E-15) were used to conduct an extensive study of magnetospheric morphology at distances greater than  $4 R_E$  using the  $\Delta B$  method (Sugiura et al, 1971). Since this study was initiated using the OGO 3 data, the results were discussed under section 3.1.1 of the OGO 3 results. Subsequently, Sugiura (1973a) used the OGO 5 data near perigee to extend the  $\Delta B$  topology to the innermost magnetosphere (2.3 to  $3.6 R_E$ ). In this region, Sugiura (1973a) found that the equatorial  $\Delta B$  was related to the Dst magnetic activity index, according to the formula:  $\Delta B(\text{gammas}) = -45 + 0.83 \text{ Dst}$ . These results showed that magnetospheric equatorial currents have significant effects upon the magnetic field even at quiet times.

A study of magnetic inclination using data from experiment E-15 indicated that an appreciable dawn-dusk asymmetry existed in the configuration of the inner magnetospheric field (Sugiura, 1973b).

#### 5.1.2 Magnetopause Investigations

The magnetopause has been investigated extensively using magnetic field measurements from OGO 5. A recent and comprehensive summary of this work (Russell et al, 1974) shows that these investigations were concerned primarily with three major areas: structure, average shape, and motions.

##### 5.1.2.1 Magnetopause Structure (E-15, E-11, E-14, E-17)

The OGO 5 investigations of magnetopause structure using magnetic field data were basically an extension and a refinement of the magnetopause investigations, which had been conducted with the relatively inaccurate Explorer 12 data (Cahill and Amazeen, 1963; Sonnerup and Cahill, 1967). The Explorer 12 data showed that the magnetic field usually exhibited an abrupt reversal in direction at the magnetopause. This reversal sometimes resembled a simple rotation with no change in magnitude, and sometimes it resembled a simple tangential discontinuity. The rotational and tangential discontinuities were of interest because of their consistency, respectively, with the open and closed models of the magnetosphere.

Using magnetic field data obtained with experiment E-15 during magnetopause crossing, Sonnerup and Ledley (1974) were able to find two excellent examples of rotational discontinuities. Although these results provided the best evidence available to date of magnetic signatures consistent with an open magnetosphere model, the differential electron flux at 45 eV measured simultaneously with experiment E-11 (Ogilvie et al, 1971a) exhibited a change in amplitude corresponding more typically to a closed magnetosphere.

## OVERVIEW

A simple magnetopause structure corresponding to a tangential field discontinuity was investigated by Neugebauer et al (1974) using magnetic field data from experiment E-14 and the Faraday cup data from experiment E-17 (flux of positive ions having E/Q ratios between 100 and 11,000 V). Neugebauer et al (1974) found that the observations agreed fairly well (but not exactly) with the closed magnetosphere model of Chapman and Ferraro (1931, 1932, 1933, 1940).

In most cases, however, the magnetopause structures observed by Neugebauer et al (1974) and by Sonnerup and Ledley (1974) were more complex than simple rotational or simple tangential discontinuities.

### 5.1.2.2 Magnetopause Shape (E-15)

Ledley (1971) computed the unit vector perpendicular to the magnetopause for a number of OGO 5 crossings. This study was done using magnetic field data from experiment E-15 and the analysis technique of Sonnerup and Cahill (1967). The direction of the normal was compared to predictions based upon a simple model surface. Consistent differences were observed between outbound and inbound crossings suggesting that all measurements might have been made during periods of either expansion or contraction of the magnetopause.

### 5.1.2.3 Magnetopause Motions (E-14)

The first detailed evidence of an inward displacement of the magnetopause, as the interplanetary magnetic field reverses from northward to southward, was found in data from experiment E-14 obtained during an inbound pass of OGO 5 on March 27, 1968 (Aubry et al, 1970). This inward motion was interpreted by Aubrey et al (1970) as an "erosion" of the magnetopause. The "erosion" concept and nomenclature of Aubry et al (1970) are now fairly well accepted (see section 4.2.9 under the OGO 4 results for a more detailed discussion of magnetopause erosion). The OGO 5 data of March 27, 1968, also provided clear evidence of magnetopause oscillations with a period of about 10 minutes (Aubry et al, 1970).

The dependence of the magnetopause position upon the polarity of the interplanetary magnetic field was confirmed by Maezawa (1974), who conducted a statistical analysis of the data from experiment E-14 obtained during 29 magnetopause crossings. A refinement introduced by Maezawa was a normalization procedure which eliminated the effects of changing solar wind.

## 5.1.3 Bow Shock Investigations

In a recent and comprehensive review of the extensive literature dealing with observations of the Earth's bow shock, Formisano (1974) stated that: "Very recently, the available information on the bow shock structure has increased considerably, mainly through the extensive analysis of the data from the satellites OGO 5 and HEOS 1." Formisano's appraisal of the importance of the OGO 5 data is particularly significant, because Formisano was recognized in the U.S. National Report to the IUGG for the period 1971-1974, as one of the two individuals most responsible for the progress in the understanding of the terrestrial bow shock during the period 1971-1974 (Russell, 1975).

### 5.1.3.1 Bow Shock Velocity and Coherence (E-14)

Some very important information concerning bow shock motions was derived from the simultaneous measurements made on February 12, 1969, with OGO 5 (Experiment E-14) and HEOS 1 (field magnitude and solar wind data), when an almost ideal geometrical relationship existed between the two satellites. For the first time it was possible to measure shock velocities without the need to assume large-scale coherence and rotational symmetry for the shock motion. These measurements yielded shock velocities significantly higher than had previously been

reported. Simultaneous observations with Explorer 33 at 125  $R_E$  showed that the bow shock was behaving on this occasion (February 12, 1969) as a coherent surface over an enormous span (Greenstadt et al, 1972).

### 5.1.3.2 Laminar Bow Shock Structure (E-14, E-17, E-24)

The  $M$  and  $\beta$  parameters\* of the solar wind were both low enough ( $M \leq 2.5$  and  $\beta < 0.01$ ) on February 12, 1969, to produce the laminar shock structure expected from theory. A detailed study of the actual shock structure using data from experiments E-14, E-17, and E-24 yielded the most complete picture to date of the bow shock in its simplest laminar form (Greenstadt et al, 1975).

### 5.1.3.3 Turbulent Bow Shock Structure (E-14, E-17, E-18, E-24)

Turbulent structures, characterized by  $M > 3$  and  $0.1 < \beta < 10$ , are the most commonly observed at the bow shock. Turbulent shocks observed on March 12, 1968, were investigated in considerable detail by experiments E-14, E-17, E-18, and E-24. The electric field data from experiment E-24 provided the first observations of electrostatic turbulence in the Earth's bow shock (Fredricks et al, 1968) and the first frequency versus time spectra showing the microscopic details of this electrostatic turbulence (Fredricks et al, 1970).

Regions of large gradients in total magnetic field as measured by experiment E-14 were found to correlate with regions of electric field enhancements (Fredricks and Coleman, 1969). The data from experiment E-14 were also used to set an upper limit of 24 km for the shock thickness (Fredricks and Coleman, 1969). Simultaneous observations with experiment E-18 showed that solar protons experienced an increase in energy at (or after) the maximum of the electrostatic noise. The upstream parameters were measured by experiment E-17. A comprehensive summary of the above shock observations on March 12, 1968, has been given by Fredricks et al (1970).

### 5.1.3.4 Mixed Bow Shock Structure (E-7)

A special class of turbulent shock called "mixed structure" occurs when the angle  $\theta_{BN}$  between the magnetic field direction and the shock normal is small.\*\* Under this condition some particles of the incoming solar wind can be reflected with increased energy. An excellent example of electrons reflected at the bow shock was provided by experiment E-7 (Fredricks et al, 1971).

### 5.1.3.5 Quasi-Turbulent Bow Shock Structure (E-14, E-16, E-17)

The only observation of a shock structure corresponding to low  $M$  and high  $\beta$  values (quasi-turbulent case) was made with OGO 5 on March 5, 1969 (Neugebauer et al, 1971). The shock data were obtained by experiments E-14, E-16, and E-17. Since  $M$  was equal to 3 in this case, there is some doubt that  $M$  was truly subcritical.

\*  $M$  = magnetosonic (or Alfvén) Mach number, which is basically a velocity parameter.

$M$  is considered high if it is above a critical value of about 3.  
 $M$  is low if it is less than the critical value.

$\beta$  = ratio of plasma pressure to magnetic pressure.

$\beta$  is typically between 0.1 and 10.  $\beta$  is considered low if less than 0.1, high if greater than 0.1, and very high if greater than 10.

\*\* Shocks corresponding to small values of  $\theta_{BN}$  are also called "pulsating" and "quasi-parallel." The investigation of these shocks is continuing (Greenstadt et al, 1977).

### 5.1.3.6 Turbulent Bow Shock Structure with Very High $\beta$ Values (E-1, E-14, E-16, E-17, E-18, E-24)

Very high  $\beta$  values ( $\beta > 10$ ) are extremely rare and they usually last only a few minutes. On January 23, 1969, a very high  $\beta$  condition lasted for more than 90 minutes during which the OGO 5 satellite crossed the bow shock once under conditions of moderately high  $\beta$  ( $\beta = 8$ ) and twice under conditions of extremely high  $\beta$  ( $\beta = 170$  and  $\beta = 49$ ). A detailed study of these crossings using data from experiments E-1, E-14, E-16, E-17, E-18, and E-24 indicated that a steady state bow shock may not be able to form at very high  $\beta$  (Formisano et al, 1975).

### 5.1.4 Investigations of the Interplanetary Medium (E-14, E-24, E-17, E-7)

Early observations suggested that the bow shock was the outer boundary of the Earth's influence upon the solar wind. The upstream region beyond the bow shock was therefore assumed to represent the undisturbed interplanetary medium. It is now known that information on the presence of the bow shock is transmitted upstream as far as the orbit of the Moon. Part of this information propagates upstream as magnetohydrodynamic waves. A detailed investigation of these waves by experiment E-14 (Russell et al, 1971a) showed that these waves form discrete packets propagating toward the Sun, but blown back toward the shock. Simultaneous upstream observations on January 30, 1969, showed that (1) the MHD wave amplitude (measured by experiment E-14) was very closely correlated with the variations in local electron density (measured by experiment E-17) and (2) the instantaneous electron density could also be determined very accurately from the plasma wave emissions detected by experiment E-24 (Fredricks et al, 1972).

The data from experiment E-14 showed that the near-Earth region upstream from the bow shock is free from terrestrial contamination if the interplanetary magnetic field at the satellite does not intersect the bow shock (Childers and Russell, 1972). On the average, the interplanetary field lies along the Parker spiral, and the result would be for the afternoon side of the upstream region to be free of terrestrial contamination. Childers and Russell (1972) investigated the amplitude distribution of this contamination and found that the amplitudes were attenuated by a factor of 3 over a distance of about 4  $R_E$ . This study also revealed that deviations from the average field configuration occurred frequently enough, that even on the afternoon side contamination was seldom absent for periods of more than 5 hours (at the OGO 5 orbit).

Upstream evidence of the bow shock was also observed in the electric field data of experiment E-24, in the solar plasma flux data of experiment E-17, and in the 4- to 7-keV proton data of experiment E-7 (Scarf et al, 1970).

The data from experiment E-14, together with data from Mariners 2, 4, and 5, were also used to study the dominant polarity of the interplanetary magnetic field above and below the solar equatorial plane. This study indicated that the dominant polarity in a given "solar" hemisphere was basically that of the dipole component of the Sun's field in the same hemisphere (Rosenberg and Coleman, 1969).

### 5.1.5 Magnetotail and Substorm Studies (E-14, E-24, E-17, E-18, E-6, E-13)

One of the most fascinating problems of space science is the study of the transfer of energy from the solar wind to the magnetosphere and of the subsequent dissipation of this energy. Although a large number of topics are included in this multifaceted study, the magnetospheric substorm is perhaps the topic which has received the most attention.\* Significant

\* Substorm investigations have led to an overwhelming proliferation of scientific publications. A recent review of this topic by Rostoker (1972) lists a total of 173 references on substorms.

contributions have been made in this area by the OGO 5 experimenters. Yet, in spite of concerted efforts by many investigators from various satellite and ground-based programs, several important aspects of substorm behavior and theory remain unresolved (Vasyliunas and Wolf, 1973).

The classical description of the polar magnetic substorm, as derived from ground-based data, includes two phases: expansion and recovery (Akasofu, 1964). The beginning of the expansion phase is marked by a variety of phenomena, including the onset of sharp negative bays on auroral magnetograms. Some indication of a third (or growth) phase, preceding the expansion phase was detected in ground based data (McPherron, 1968). The best evidence for a growth phase, however, was found in the OGO 5 data obtained during the two substorms of August 15, 1968. The OGO 5 satellite was then traveling inbound on the midnight meridian through the cusp region of the geomagnetic tail. The beginning of each substorm expansion phase was determined from the ground-based observations, using the classical data analysis procedures. It was then shown, using the data from experiment E-14 on OGO 5 that the above expansion phase was preceded by a growth phase during which significant changes occurred in the near tail magnetic field (McPherron et al, 1973a). This conclusion was confirmed and extended by correlative particle observations made on OGO 5 by experiments E-13 (Kivelson et al, 1973) and E-6 (West et al, 1973b; Buck et al, 1973), and by the plasma wave data from experiment E-24 (Scarf et al, 1973b). These measurements showed that the geomagnetic tail acts as a temporary storage reservoir for energy transferred from the solar wind, prior to the release of this energy in substorms. These observations were used to develop a substorm model in which the substorm sequence is divided in three main phases: growth, expansion, and recovery (McPherron et al, 1973b). The growth phase concept has been criticized by Akasofu and Snyder (1972) and it remains one of the many controversial issues concerning substorms. It is now generally agreed, however, that the magnetotail plays an active and important role in the development of substorms (Russell and McPherron, 1973).

Magnetic field fluctuations in the magnetotail have been studied extensively, using data from experiment E-14, in an attempt to identify instabilities which might be related to the substorm process (Russell, 1972a). This study has led to the observation of a variety of magnetic wave phenomena in the tail, but the information was not complete enough to lead to final conclusions concerning these instabilities.

The field-aligned currents which flow on the plasma sheet boundary also appear to play a significant part in the development of instabilities in the plasma sheet. Aubry et al (1972), using data from experiments E-13 and E-14, showed that the currents flowing at the outer boundary had a magnitude large enough to drive these instabilities. Scarf et al (1973a), using data from several OGO 5 experiments (E-24, E-14, E-17, and E-18), discovered field-aligned currents of comparable magnitude flowing at the inner edge of the plasma sheet.

The above summary of the OGO 5 substorm investigations is by no means complete. At best, it indicates the magnitude of the OGO 5 effort devoted to the substorm problem. The pieces of the substorm puzzle have been and continue to be slowly assembled by investigators from many programs. At the present time many important questions concerning substorms remain unanswered (Schindler, 1975).

### 5.1.6 Study of the Polar Cusp during the Storm of November 1, 1968\* (E-13, E-14, E-17, E-18, E-24)

Although the polar cusp (see section 4.2.9 of the OGO Program Summary) is normally at higher magnetic latitudes than the OGO 5 orbit, during geomagnetic storms the cusp moves southward and it can be intersected by the OGO 5 orbit. This occurred during the storm of November 1, 1968.

\* The November 1, 1968, storm was one of the largest geomagnetic disturbances of the solar cycle.

## OVERVIEW

and led to a wealth of OGO 5 data on particle population and wave activity in the disturbed cusp. Data from experiments E-13, E-14, E-17, E-18, and E-24 showed that the polar cusp had indeed moved equatorward during the storm, that magnetosheath electrons and protons were present in this region, and that the stormtime cusp was highly turbulent at ULF and VLF frequencies (Russell et al, 1971b). A detailed analysis of the data from experiment E-24 showed that the polar cusp region is a major source of strong local magnetospheric wave activity and a region where wave-particle interactions control the plasma dynamics. The observed wave levels were particularly intense at the cusp boundaries, suggesting that a variety of instabilities are associated with the high gradients in plasma density and in thermal energy at the cusp boundaries (Scarf et al, 1972).

Further study of the November 1, 1968, polar cusp data showed (1) that the data of experiment E-14 were consistent with the presence of field-aligned current layers and (2) that the data of experiment E-24 were indicative of potential drops between OGO 5 (at about  $3 R_E$  geocentric) and the ionosphere on the order of 2 kilovolts (Fredricks et al, 1973).

The OGO 5 data of November 1, 1968, also provided a rare opportunity to observe the interface region between the polar cusp and the magnetosheath. Two transitions were detected. The first one resembled the magnetopause signature and corresponded to a slight depression in the magnetopause. The second one appeared to be a collisionless shock within the magnetosheath (Scarf et al, 1974).

### 5.1.7 Outer Radiation Zone-Plasma Sheet Boundary (E-13, E-14, E-17, E-18, E-24)

Coordinated OGO 5 measurements made by Scarf et al (1973a) at the outer radiation zone-plasma sheet boundary with experiments E-13, E-14, E-17, E-18, and E-24 revealed phenomena similar to those seen at the dayside polar cusp boundary (see section 5.1.6).

### 5.1.8 Polar Cap and Auroral Oval (E-15, E-13, E-14, E-17, E-18, E-24)

Analysis of ground-based data obtained during the International Geophysical Year 1957-1958 showed that auroral activity tends to be continuously present in a circular belt (auroral oval), centered approximately 4 deg South of the magnetic dipole axis toward the dark hemisphere, and approximately 30 deg in diameter. This auroral oval is fixed in geomagnetic dipole latitude versus local time coordinates. The discovery of the auroral oval was a major refinement of the earlier auroral zone concept, initially inferred in the 19th century from the accounts of polar explorers.

It is now generally accepted that the auroral oval corresponds to the projection on Earth of the polar cusp (dayside of oval) and of the plasma sheet (nightside of oval). The near-Earth plasma-sheet region is sometimes called the "nightside cusp." The region inside the oval is known as the polar cap and it corresponds to the termination on Earth of the tail geomagnetic field lines (for the given hemisphere).

Although the existence and location of the auroral oval was found consistent with subsequent developments in magnetospheric physics, some aspects of the auroral oval concept are currently being reexamined (Eather, 1973). Specifically, should the important magnetosphere-ionosphere interactions evidenced by the auroral oval be organized on the basis of auroral light, or should the auroral displays be recognized as one manifestation of the more fundamental geomagnetic field morphology and particle precipitation patterns? What are the significant boundaries? What criteria should be used to define these boundaries? How far into the magnetosphere do the boundaries extend? Some of these questions have been investigated by Sugiura (1975) who showed, using data from experiment E-15, that the polar cap and auroral belt boundaries could be identified in the magnetosphere at distances of typically 5 to  $7 R_E$ . Scarf et al (1975) in a paper, which was basically an extension of

their earlier studies discussed under sections 5.1.6 and 5.1.7, reached conclusions similar to those presented by Sugiura (1975), namely that the boundaries are revealed by field-aligned currents. The two papers (Scarf et al, 1975 and Sugiura, 1975) were published in the same issue of the Journal of Geophysical Research.

The polar cap and auroral oval problems have been presented in some detail because of their close (and unifying) relationships to many magnetospheric topics investigated extensively under the OGO program. (See, for example, sections 1.2.2, 4.2.8, 4.2.9, 4.2.10, 4.3.4, 5.1.4, 5.1.5, 5.1.6, 5.1.7, and various later sections of the OGO 5 and OGO 6 results.)

## 5.1.9 Magnetospheric Wave Phenomena

Experiments E-14, E-16, E-17, and E-24 on OGO 5 have detected a great variety of magnetic and electric waves, ranging in frequency from millihertz to kilohertz, occurring throughout the magnetosphere and in the near-Earth solar wind. Although many of these waves had been previously observed, several new wave phenomena were discovered by the OGO 5 investigators. The OGO 5 measurement of magnetic field and magnetospheric plasma have also led to an increased awareness of the importance of ULF, ELF, and VLF waves in the physical processes occurring in the magnetosphere (Russell, 1972b; Scarf and Fredricks, 1972).

This section (5.1.9) is concerned primarily with wave phenomena that were either discovered or extensively investigated by the OGO 5 investigators. It should be noted, however, that the earlier discussion of wave phenomena associated with the upstream region (section 5.1.4), the magnetotail (section 5.1.5), and the polar cusp (section 5.1.6) is not repeated under section 5.1.9.

### 5.1.9.1 Electrostatic Waves with $f = 3f_c/2$ (E-24)

The data from experiment E-24 led to the discovery of electrostatic waves having a frequency equal to  $3/2$  times the electron cyclotron frequency (Kennel et al, 1970a). The  $3f_c/2$  waves were observed at geomagnetic latitudes ranging from 50 deg South to 40 deg North, but the strongest emission tended to occur near the geomagnetic equator, near midnight and for  $5 < L < 7$ , i.e., near the base of the plasmashet (Fredricks and Scarf, 1973).

The large amplitude of the  $3f_c/2$  waves, together with their high frequency, suggested that these emissions could be responsible for pitch-angle diffusion and energization of auroral electrons (Scarf et al, 1973b). This is only one of many ways in which wave-particle interactions appear to be relevant to the development of magnetic storms and substorms. It is now believed that future progress in substorm theory requires that the effects of wave-particle interactions be included in theoretical substorm models (Fredricks, 1975).

### 5.1.9.2 Strong Impulsive Bursts (E-24)

Also discovered in the data from experiment E-24 were strong, impulsive, almost undispersed electric field bursts in the 1- to 10-kHz frequency range. These bursts tend to occur near current layers in the upstream solar wind, the bow shock region, and the magnetosheath (Scarf and Fredricks, 1972).

### 5.1.9.3 Lion Roars (E-16)

Data obtained in the magnetosheath with experiment E-16 led to the discovery of narrow-band emissions with center frequencies near 100 Hz. These emissions were named "lion roars" because they sound like roaring lions when played through a loudspeaker (Smith et al, 1969). Smith and Tsurutani (1976) conducted statistical studies of the center frequency, amplitude, and duration of lion-roar signals. The center frequency was found to be approximately one-half the local electron gyrofrequency. The maximum amplitudes were found to have an

average value of 85 milligammas. The probability of occurrence increased from 10 percent in magnetically quiet intervals to 75 percent during disturbed periods. The propagation of lion-roar emission was found to be essentially along the ambient magnetic field, and this field was seen to decrease in magnitude in the presence of lion roars. Although the generating mechanism for lion roars is still poorly understood, the lion-roar emission appears to be an important feature of the magnetosheath.

#### 5.1.9.4 Micropulsations (B-11, E-15, E-14)

The first comprehensive survey of continuous micropulsations in the magnetosphere was conducted by Heppner et al (1970), using data from OGO 3 (Experiment B-11) and OGO 5 (Experiment E-15) obtained within 20 deg of the magnetic equator. Micropulsations with Pc 3 periods (10-45 sec) were found to prevail in the daytime magnetosphere. The Pc 4 (45-150 sec) micropulsations were also seen throughout the daytime magnetosphere, but mainly between  $L = 5$  and  $L = 10$ . The frequency of occurrence of the Pc 4 waves was about one order of magnitude smaller than that of the Pc 3 waves. The Pc 2 (5-10 sec) and the Pc 1 (0.2-5 sec) waves were observed primarily close to the magnetopause. The above study by Heppner et al (1970) was a preliminary one and it did not yield a sufficient number of observations in the Pc 5 range (150-600 sec) to be statistically significant. A more extensive study of the Pc 5 range, based upon 22 months of OGO 5 fluxgate magnetometer data (Experiment E-14) was subsequently carried out by Kokubun et al (1976). The Pc 5 waves were observed primarily in the region  $L = 6-13$ , at magnetic latitudes 10-30 deg, and in the morning sector between 0300 and 1100 LT. The study by Kokubun et al (1976) included also a determination of the polarization properties of the Pc 5 waves. Simultaneous data from experiment E-14 on OGO 5 and from the fluxgate magnetometer on ATS-1 were used by Hughes et al (1977) to show that the Pc 4 waves exhibit their maximum amplitudes near  $L = 7$ . This result is consistent with the field line resonance theory of Chen and Hasegawa (1974).

The first observation in space of band-limited Pi 1 micropulsations was made with the data from experiment E-14 (McPherron and Coleman, 1971). These irregular pulsations had been observed on the ground for many years, but their existence above the ionosphere was in doubt. These Pi 1 pulsations were first observed on June 8, 1968, between 7 and 5  $R_E$  on the dawn meridian just below the magnetic equator during the recovery phase of a magnetospheric substorm. Micropulsations with comparable periods and amplitudes were simultaneously observed in the auroral zone near the (magnetic) subsatellite point. Additional parameters also obtained by McPherron and Coleman (1971) included polarization, ellipticity, and propagation characteristics of the Pi 1 micropulsations.

#### 5.1.9.5 Plasmaspheric Hiss (E-16, E-18)

It was found from the OGO 3 triaxial search coil magnetometer (Experiment B-10) that a relatively steady hiss band was present throughout the magnetosphere for  $L$  values less than 5. Using OGO 5 data collected simultaneously from experiments E-16 and E-18, Thorne et al (1973) showed that hiss emissions were contained almost exclusively within the high-density plasmasphere. In view of the remarkable agreement between the plasmopause position and the hiss cutoff, this hiss emission was named the plasmaspheric hiss. The main exception to the general rule was found in the afternoon sector at high geomagnetic latitude where hiss emission occurred well outside the plasmasphere. Hiss in this restricted zone outside the plasmasphere was called exohiss.

Using data from experiments E-16 and E-18, obtained inside the plasmasphere and for  $L > 2.5$ , Chan et al (1974) found that the hiss amplitude  $A$  was related to the ambient density  $N$  according to the formula:  $A = k \ln(N/N_0)$ , where  $k$  is a proportionality constant and  $N_0$  is a threshold value of density below which hiss will not occur. Localized hiss observed outside of the plasmasphere in regions of detached ion density

enhancements was shown to have an amplitude variation in excellent agreement with the above formula (Chan and Holzer, 1976). The above empirical relationship between hiss amplitude and plasma density suggests that the observed plasmaspheric hiss (for  $L > 2.5$ ) is generated near the point of observation, a conclusion that is consistent with the theory of magnetospheric ELF hiss developed by Etcheto et al (1973).

#### 5.1.9.6 Chorus in the Outer Magnetosphere (E-16)

The data from experiment E-16 made it possible to determine for the first time the wave normal direction of chorus in the outer magnetosphere (Burton and Holzer, 1974). It was found that the daytime wave normals were contained primarily within 20 deg from the geomagnetic field in the equatorial and midlatitude regions. At high latitudes the daytime wave normal distribution was less regular, and it extended to approximately 40 deg from the geomagnetic field. The only nighttime measurements were for equatorial conditions, and they agreed with the daytime measurements. The determinations of wave normal directions combined with simultaneous electron-energy and pitch-angle measurements showed that the chorus data were in qualitative agreement with existing theory (see Thorne and Kennel, 1967, and references therein for theoretical discussions of chorus generation). Specifically, these data were found to be consistent with (1) wave generation by cyclotron resonance with electrons in the 5- to 150-keV energy range, (2) wave generation only when the pitch-angle distribution is peaked at 90 deg and it exceeds a critical anisotropy, (3) wave generation in the vicinity of the geomagnetic equator, and (4) wave generation when the wave normal is at an angle of about 20 deg with respect to the geomagnetic field. Away from the source the data indicated that both ducted and unducted propagation of chorus could occur at different times. The analysis of the data from experiment E-16 was carried out one step further by Burton (1976), who showed (for the first time) that chorus generation occurs only when the pitch-angle anisotropy exceeds substantially the critical anisotropy defined by Kennel and Petschek (1966).

### 5.2 Low-Energy Plasma Experiments

A large number of OGO 5 investigations were based upon simultaneous data from the magnetic field measurements and from the low-energy plasma measurements. In many cases high-energy particle measurements were also included in these joint efforts. In such cases the scientific results could be given under two or three of the 5.1, 5.2, and 5.3 headings. To avoid duplications, results based upon data from two or more disciplines were presented only once and under the discipline which seemed the most appropriate. Since the participating experiments have been indicated under each topic discussed, a summary of contributions by experiments or by discipline could readily be compiled, if desired.

#### 5.2.1 Low-Energy Plasmas in the Magnetosphere (General)

One of the outstanding accomplishments of the OGO 5 mission is the comprehensive investigation made of the low-energy plasmas in the plasmasphere and in the trough region between the plasmasphere and the magnetopause. Discussed under the 5.2.1 headings are measurements that have provided the general characteristics of the electron and ion density variation versus the parameter  $L$  and measurements of plasma temperatures and satellite potential.

##### 5.2.1.1 Ion Density Versus $L$ (E-18, E-3)

The most complete study of the low-energy ion density in the magnetosphere was conducted with the OGO 5 mass spectrometer data (Experiment E-18). The data from experiment E-18 have provided numerous profiles of oxygen, hydrogen, and helium ion densities within the plasmasphere (Harris et al,

## OVERVIEW

1970). The smoothest plasma density variations were observed in the bulge (dusk) region where a  $1/R^4$  radial dependence was usually exhibited by the ion density profiles (Chappell et al, 1970b). The profiles in the nightside region were found to be less smooth because of their rapid response to magnetic activity changes (Chappell et al, 1970a). The dayside profiles were observed to be the most irregular. Chappell et al (1971b) concluded that the dayside profiles were influenced by effects occurring during the previous night and by filling from the daytime ionosphere. These effects sometime combined to produce a double plasmopause in the daytime profile. The ion density profiles exhibited quite consistently a wave-like structure at  $L = 6.5$ , independently of the plasmopause position (Harris et al, 1970). Chen et al (1976) used the data from experiment E-18 to investigate the diurnal variation of the equatorial thermal plasma at  $L = 2.4$  and  $L = 3.2$ . This work led to the discovery of a semidiurnal variation in the hydrogen ion density with peaks near noon and midnight. A few total ion density profiles were also obtained with experiment E-3, leading to observed plasmopause positions consistent with the results of experiment E-18 (Serbu and Maier, 1970).

### 5.2.1.2 Electron Density Versus L (E-1)

Electron densities versus L, measured within the plasmasphere by experiment E-1 (Freeman, 1973) were found to be consistent with the ion densities measured by experiment E-18 (see section 5.2.1.1). When detectable in the data of experiment E-1, the plasmopause position agreed with that found by experiment E-18. The electron density measurements made in the plasmatrough by experiment E-1 appear to suffer from vehicle potential effects.

### 5.2.1.3 Ion Temperature Versus L (E-3)

Experiment E-3 yielded the first measurements of ion temperature profiles in the magnetosphere. It was found that the ion temperature increased from about  $2 \times 10^4$  deg K inside the plasmasphere to about  $10^5$  deg K outside the plasmasphere. The temperature increase occurred typically within  $0.8 R_E$  at a location consistent with the plasmopause position (Serbu and Maier, 1970).

### 5.2.1.4 Satellite Potential Measurements (E-1, E-3)

Satellite potential measurements were made by experiments E-1 and E-3. The results, unfortunately, revealed inconsistencies which were left unresolved (Serbu, 1976). The disagreements between the satellite potential measurements and the apparent immunity of experiment E-18 to satellite potential effects (Harris, 1974) would indicate that the complex OGO 5 satellite surface was not at a uniform potential with respect to the ambient plasma.

## 5.2.2 Investigation of the Plasmopause

The ion data from experiment E-18 have yielded extensive information concerning the plasmopause position, making it possible to investigate this parameter in considerable detail.

### 5.2.2.1 Plasmopause Identification (E-18)

Since  $H^+$  is the major ion component of the outer plasmasphere, the plasmopause morphology was derived primarily from the  $H^+$  profiles. The plasmopause, however, could frequently be seen also in the  $He^+$  data and even occasionally in the  $O^+$  data (Harris et al, 1970). The ion density through the plasmopause was found to exhibit a great variability in its appearance; and, consequently, criteria had to be developed to achieve consistency in the identification of the plasmopause (Chappell et al, 1970a).

### 5.2.2.2 Plasmopause Position vs $K_p$ (E-18)

The data from experiment E-18 showed that the plasmopause position in the midnight to 0400 sector agreed fairly well with the formula  $L = 6 - 0.6 K_p$  of Binsack (1967). The best correlation between the L value of the plasmopause and the magnetic activity was obtained by allowing a 2- to 6-hour response time following changes in the values of  $K_p$  (Chappell et al, 1970a). The plasmopause position on the dayside (0400 to 1500 sector) seemed to be determined by the level of magnetic activity present during the previous corotation of the dayside sector through the formative nightside region (Chappell et al, 1971b). In the bulge region (1500 to 2200 sector) the plasmopause position was found to range from  $L > 9$  when  $K_p < 1$  to  $L = 4$  when  $K_p > 4$ . Because of greater variability, the plasmopause position was not as well defined in terms of  $K_p$  as it was in the nighttime sector (Chappell et al, 1970b).

### 5.2.3 Investigation of the Trough Region (E-18)

A particularly important result obtained from experiment E-18 was the first accurate measurement of the ion density ( $H^+$ ) in the trough region beyond the plasmopause (Harris, 1974). The trough densities were found to be typically between  $0.1$  and  $10$  ions/cm<sup>3</sup>. The analysis of one year of data from experiment E-18 showed that the minimum densities occurred near midnight, while the maximum densities occurred in the late morning and early afternoon. An unusual feature of these data was a substantial reduction in density near local noon.

Isolated regions of relatively dense plasma ( $10$ - $100$  ions/cm<sup>3</sup>) were frequently observed in the afternoon-dusk trough region and interpreted as detached plasmas (Chappell et al, 1970b; Chappell, 1974). These observations, however, could also be interpreted as plasmatail structures (see section 4.2.3).

### 5.2.4 Storm Effects on the Plasmasphere (E-18)

A combination of data from OGO 4 (see section 4.4.1), OGO 5 (Experiment E-18), and the ground whistler station at Byrd, Antarctica, led to new information concerning the variable magnetospheric convection, and the gradual erosion of the plasmasphere during the magnetospheric substorm of August 15, 1968 (Carpenter and Chappell, 1973). Much of the plasma removed from the plasmasphere in the dusk sector appeared to remain nearby as an irregular outlying structure in the ion density profile. From the combined observations it was inferred that westward electric fields of the order of  $0.5$  mV/m were present in the midnight sector during the substorm.

### 5.2.5 The Plasmasphere and Stable Auroral Red Arcs (E-18)

A phenomenon associated with some geomagnetic storms is the stable (or subauroral) red arc (SAR arc). Plasmaspheric ion densities were measured with experiment E-18 during observations of SAR arcs associated with the storm of October 29 to November 7, 1968, and with the storms of October 10 to 17, 1968. It was found that the plasmasphere was drastically reduced in size during these storms and that the SAR arcs were located at L value near the position of the plasmopause (Chappell et al, 1971a).

### 5.2.6 Magnetospheric Convection Model (E-18)

Chappell (1972) showed that the general characteristics of the plasmasphere measured by experiment E-18 during periods of steady magnetic activity were in general agreement with the steady-state (uniform) electric-field convection model originally proposed by Axford and Hines (1961). Chappell et al (1972) explained the plasmasphere dynamics inferred from the observations made with experiment E-18 by using an extension of the model of Axford and Hines (1961), which included the effects of nonuniform convection.



### 5.2.7 Magnetopause Study with the Low-Energy Electron Spectrometer (E-11)

Electron fluxes between 25 eV and several keV were measured near the dawn magnetopause with experiment E-11. It was found that the electron flux at 45 eV provides an accurate determination of the magnetopause location. A magnetopause thickness of about 200 km was derived from such observations. Simultaneous magnetic field measurements with experiment E-15 provided complementary data for the calculations of pressure balance across the magnetopause. These calculations showed that inside the magnetosphere near the magnetopause the plasma energy density was nearly equal to the magnetic field energy density. It was also concluded from this investigation that a significant contribution was made to the total plasma energy density by the particle population outside the 25 eV to several keV range measured by experiment E-11 (Ogilvie et al, 1971a).

### 5.2.8 Bow Shock Effects Measured with Low-Energy Plasma Experiments (E-11, E-17, E-18)

The data from experiment E-11 were used to conduct an extensive survey of electron temperature in the magnetosheath and nearby interplanetary medium. This survey, conducted by Scudder et al (1973), included 25,626 observations. The main conclusions were as follows. In the nearby interplanetary medium the mean electron temperature was  $1.55 \times 10^5$  deg K. The electron temperature anisotropy estimated from 6827 calculations was  $T_{\parallel}/T_{\perp} = 1.24$  on magnetic lines terminating at the bow shock and  $T_{\parallel}/T_{\perp} = 1.11$  on miss lines. Thirty-four observations of bow shock crossings (from the interplanetary medium to the sheath) showed mean electron density and temperature jumps of 2.1:1 and 4.2:1, respectively. Ogilvie et al (1971b), using data from experiment E-11, showed that the electron energy flux in the solar wind revealed a significant sunward component at energies greater than 210 eV whenever measurements were made on magnetic-field lines intersecting the bow shock surface. Since this effect was not seen on miss lines, it was concluded that electron acceleration occurred at the bow shock.

High time-resolution plasma measurements made with experiment E-17 during bow shock crossings showed that solar-wind positive ions often undergo a substantial deceleration just upstream of the bow shock (Neugebauer, 1970). Complementary observations with experiment E-18 showed that the solar wind proton flux increased in density and that its velocity distribution became randomized in passing through the bow shock from the upstream region to the magnetosheath (Ossakow et al, 1970). Using data from experiment E-18, Ossakow and Sharp (1973) showed that the predominant scale length for the above changes was  $c/\omega_{pi}$  (where  $c$  is the speed of light and  $\omega_{pi}$  is the proton plasma frequency).

### 5.2.9 Power Spectrum of the Solar Wind (E-17)

The first measurements of solar-wind positive-ion power spectra in the 0.0048 to 13.3 Hz range were obtained with experiment E-17 (Unti et al, 1973). Although 25 of the 32 power spectra presented by Unti et al were consistent with a power law distribution of the scale sizes of the irregularities, 7 of the spectra showed small power enhancements near the frequency expected for the convection of gyroradius size structures past the satellite. Using a much greater number of spectra from experiment E-17 (634 quiet spectra and 1094 disturbed spectra), Neugebauer (1975) extended the work of Unti et al and found that a power spectrum enhancement corresponding to gyroradius size irregularities was clearly seen when many spectra were amplitude-normalized, frequency-normalized (to the gyrofrequency), and averaged. Some doubts concerning the above interpretation of the spectral enhancements have been raised, however, by Unti and Russell (1976), who pointed out that spectral enhancements seen on individual spectra were not at the proper frequency and that several other explanations, including bow shock effects, could be given for the observations. The controversy is currently unresolved.

### 5.2.10 Temperature Differences in the Solar Wind (E-17)

Approximately 2000 hydrogen and helium spectra measured in the solar wind with experiment E-17 were used by Neugebauer (1976) to investigate  $T_{He}/T_H$ , the helium to hydrogen temperature ratio. This study confirmed the IMP 6 observations (Feldman et al, 1974) of the inverse dependence of  $T_{He}/T_H$  on the ratio of the solar wind expansion time scale to a Coulomb collision time scale. The analysis of Feldman et al was also extended to show that the velocity difference  $V_{He} - V_H$  also varies in a similar manner. Neugebauer (1976) concluded that the OGO 5 results suggest a model of continuous preferential acceleration and heating of helium (or deceleration and cooling of hydrogen) that is opposed by Coulomb collisions.

### 5.2.11 Comparison of Solar Wind at 0.7 and 1 AU (E-17)

Intriligator and Neugebauer (1975) compared solar wind velocity data obtained at 0.7 AU with Pioneer 9 and at 1 AU with OGO 5 (experiment E-17). There was no significant change seen in the average velocity; but the velocity fluctuations seemed somewhat smaller at 1 AU, suggesting that some equilibrium had been reached between low-speed and high-speed streams in the solar wind.

### 5.2.12 Shock Waves in the Solar Wind (E-17)

Successions of sharp discontinuities observed occasionally in the magnetic field intensity of the interplanetary medium (and seen also in the amplitudes of various solar wind plasma parameters) have been interpreted as evidence of shock systems in the solar wind (Colburn and Sonett, 1966). Theoretical explanations fall into two groups. One group explains the shocks by the movement of a fast solar wind stream into a slower one. The second one explains shocks by changes in solar wind velocity (or density) produced by flares. Unti et al (1973) conducted a detailed investigation of the shock system of February 2, 1969, using data from experiment E-17. Unti et al concluded that a solar flare was the most likely cause of this particular shock system. The study of Unti et al was extended by Dryer et al (1975) by including the Pioneer 9 observations of the same shock ensemble. It was found that the major features of the shock system (forward shock, tangential discontinuities, piston and reverse shocks) were retained during the 0.13 AU transit of the shock ensemble from Pioneer 9 to OGO 5. Dryer et al concluded that the shock ensemble of February 2, 1969, had been produced by a two-stream interaction. The two conflicting conclusions concerning the shock system of February 2, 1969, show that the genesis of shock ensembles is still poorly understood.

## 5.3 Energetic Particle and Photon Measurements

An unusually comprehensive set of energetic particle and energetic photon experiments was included in the OGO 5 mission. Experiment E-06 was used primarily to conduct surveys of energetic particles in the radiation belt, the magnetosphere, and the magnetosheath; experiments E-04 and E-23 yielded extensive observations of solar X-rays and of other energetic solar flare radiations; and a total of 6 experiments (E-05, -08, -09, -10, -12, and -27) were used to provide cosmic-ray data in the 2-MeV to 10-BeV energy range and for atomic numbers ranging from 2 to 50.

With the exception of experiment E-06, which also provided supporting data for the substorm studies discussed under section 5.1.5, the data from the above energetic particle experiments were used to investigate problems quite different from those presented under sections 5.1 and 5.2. Experiment E-13, not mentioned in the previous paragraph, belongs also under the 5.3 heading. Experiment E-13, however, was conducted almost exclusively in conjunction with experiment E-14 and the results from experiment E-13 can be found under section 5.1.6, 5.1.7, 5.1.8, and 5.1.9.6

## OVERVIEW

### 5.3.1 Radiation Belt Studies (E-06)

The most complete study to date (West and Buck, 1976b and 1976c) of the inner belt electron distribution and dynamics was conducted with the OGO 5 magnetic electron spectrometer (Experiment E-06). This study, based upon data from 1968, showed that only a small residual (at energies greater than 1 MeV) remained in the heart of the inner belt from the Starfish high-altitude nuclear detonation of July 9, 1962 (West and Buck, 1976c). The results for energies less than 1 MeV were therefore indicative of the normal inner belt. Storm-time injection and subsequent decay were investigated by West and Buck (1976b) for the mild storm of June 11, 1968, and for the more intense storms of October 31 and November 1, 1968. The data from experiment E-06 were used by Teague and Stassinopoulos (1972) to confirm their model of the Starfish flux decay in the inner radiation zone. A partial study was also carried out using E-06 data covering the electron pitch-angle distribution and dynamics in the slot and outer belt regions (Lyons et al, 1972).

### 5.3.2 Outer Magnetosphere Studies (E-06)

The data from experiment E-06 were used to conduct a complete survey of electron pitch-angle distributions in the equatorial regions of the outer magnetosphere (West et al, 1973a). It was shown that the normal loss-cone distribution prevails in much of the magnetosphere on the dayside of the Earth. Pitch-angle distributions with minimums at 90 deg (called butterfly distributions) were observed in the early afternoon near the magnetopause and on the nightside at distances beyond 5.5  $R_E$ . West et al (1973) explained the butterfly distribution by a mechanism that they called "magnetopause shadowing," according to which the equatorially mirroring particles drift eastward from the nightside to the dayside until they encounter the magnetopause, at which point field discontinuities cause the particles to leave the trapping region. This mechanism is quite different from the well known loss process due to drift shell splitting resulting from magnetic field configuration, and which occurs well within the magnetosphere.

### 5.3.3 Magnetosheath Protons (E-06)

The first comprehensive study of energetic protons in the magnetosheath was conducted by West and Buck (1976a) using data from experiment E-06. These magnetosheath protons were found to be directional with the peak flux directed downstream. The proton fluxes showed a fairly good correlation with  $K_p$ , and the proton spectra were often quite similar to those observed in the nearby magnetosphere. These proton fluxes appear to be generated within or near the magnetosheath.

### 5.3.4 Low-Energy Solar Flare Radiation (E-23)

Solar X-ray measurements in the 3- to 10-keV energy range (Experiment E-23) have led to a number of papers aimed at determining the relative importance of thermal (collision heating of ambient gas) and non-thermal (bremsstrahlung) emission in the generation of low-energy solar flare X-rays (Kahler et al, 1970; Kahler, 1973). The main conclusion reached was that both mechanisms are probably present and that it is very difficult to distinguish a thermal from a non-thermal event in the low-energy X-ray range (Kahler and Kreplin, 1971). The X-ray data from experiment E-23 also showed that numerous small flares were occurring during periods when no flares or subflares were reported from the routine monitoring of solar activity (Kahler and Kreplin, 1970).

Perhaps the most significant study conducted with the data from experiment E-23 was the correlation between type III bursts and the 4-keV X-ray emission (Kahler, 1972). This study included a total of 151 type III events, a number which exceeded the combined total of all previous investigations. The highest X-ray correlation was found to occur with bursts observed

in the decimetric band and when bursts are more intense. It was concluded that the energetic electrons, which produce both phenomena, can (depending upon the relative effectiveness of the electron acceleration mechanism in the chromosphere and of the fractional electron escape in the corona) produce either X-rays, type III bursts, or both.

### 5.3.5 Energetic Solar Flare Radiation (E-04, E-06)

A comprehensive study of the angular distribution of solar protons and electrons over a wide rigidity range (300 kV to 300 MV) was conducted with experiment E-06 during the solar flare of November 18, 1968 (Nielsen et al, 1975). These interplanetary measurements of solar flare emissions at 1 AU revealed unusually large and long-lasting anisotropies for both electrons and protons. These observations did not lead to a unique interpretation, but they were consistent with a solar emission lasting over an extended period, a weak scattering region between the Sun and the Earth, and a strong scattering region beyond the Earth's orbit. Correlative ground-based measurements in both polar regions made during the flare of November 18, 1968 (Nielsen and Pomerantz, 1975) showed that the initial stage of a Polar Cap Absorption event coincided with the strongly anisotropic distribution observed beyond the magnetopause by Nielsen et al (1975).

Solar flare X-ray data at energies greater than 10 keV, obtained with experiment E-04 during its two years of operation, have provided new insights into the solar flare process. These data supplement the X-ray measurements at energies below 10 keV made by experiment E-23 and discussed under section 5.3.4. Kane (1969) showed that the hard X-ray emission from a large number of solar flares consisted of two components, namely: (1) an impulsive non-thermal component which coincided with the microwave emission and (2) a slower component of thermal origin. The impulsive component was shown to correlate well with EUV emission (Kane and Donnelly, 1971), H alpha emission (Vorpahl and Zirin, 1970; Vorpahl, 1972), and type III bursts (Kane, 1972). From a study of 129 impulsive X-ray bursts, Kane (1971) showed that the impulsive X-ray spectrum was consistent with bremsstrahlung emission from electrons with energies greater than 10 keV and having a spectrum of the form  $KE^{-\delta}$  where  $1 < \delta < 4$ . Since values of  $\delta$  less than 1 were not observed, it was concluded that  $\delta = 1$  represented an upper limit on the hardness of the non-thermal electron spectrum.

### 5.3.6 Cosmic-Ray Electrons and Positrons in the 2- to 9-MeV Range (E-05)

Experiment E-05 on OGO 5 represented the first search for cosmic-ray positrons in the region from 3 to 12 MeV, and it incorporated the lowest energy threshold (2 MeV) used up to that time for the detection of cosmic-ray electrons. Differential energy spectra of cosmic-ray electrons and positrons in the 2- to 9.5-MeV interval obtained with experiment E-05 have shown that the positron-to-electron ratio totaled for this energy interval, was only 1.8 percent. This was the lowest  $e^+/e^-$  ratio ever measured in any energy interval, and it suggested that this electron component of the cosmic-ray spectrum was of knock-on or directly accelerated origin (Cline and Porreca, 1969).

### 5.3.7 Cosmic-Ray Electrons in the 10- to 200-MeV range (E-09)

The first investigation of cosmic-ray electrons in the 10- to 200-MeV energy range was conducted with the data from experiment E-09 on OGO 5. This experiment produced data continuously for three and one-half years from which a large number of new and significant results were obtained. The preliminary results from experiment E-09 were presented by Fan et al (1969). A more comprehensive report based upon the first year of data was published by L'Heureux et al (1972). Two papers published in 1975 (L'Heureux and Meyer, 1975a and 1975b) are based upon the full three and one-half years of

data. The above studies were aimed at measuring the primary cosmic-ray spectrum with a minimum contribution from emissions within the solar system. To achieve this objective, only data obtained during quiet solar periods were used. It was discovered, however, that this procedure yielded an "uncontaminated" cosmic-ray spectrum only for energies greater than 30 MeV (L'Heureux and Meyer, 1975b). The electron flux for energies below 30 MeV exhibited frequent and large increases, which were not correlated with solar activity, but which appeared to originate from Jupiter's magnetosphere. The implication is that the interstellar flux of electrons with energies less than 30 MeV will not be known until it can be measured outside the solar cavity. The data for electrons with energies greater than 30 MeV were used to study the solar modulation of cosmic rays during the period 1968-1971. This study revealed a hysteresis effect following the June 9, 1969, Forbush decrease, suggesting a sudden and lasting change in the rigidity dependence of solar modulation (L'Heureux and Meyer 1975a).

Solar emission of electrons in the 10- to 200-MeV range was first observed with the data from experiment E-09 (Datlowe et al, 1969). This was followed by a detailed study of solar electrons in the above energy range based upon data from 30 solar flares (Datlowe, 1971). It was found that electrons with energies greater than 10 MeV are a normal feature of major solar particle events. The electron propagation is diffusive, but not isotropic. The electron spectra fit a power law  $AE^{-\gamma}$  with  $2.5 < \gamma < 3.8$ . Experiment E-09 was also used by L'Heureux (1974) to verify the existence of gamma-ray bursts, a phenomenon first detected by instruments in the Vela satellite (Klebesadel et al, 1973).

### 5.3.8 Cosmic-Ray Electrons in the 500-MeV to 10-BeV Range (E-12)

The data from experiment E-12 have provided a continuous monitoring of the cosmic-ray electron spectrum between 0.5 and 10 GeV from March 1968 until August 1971. These observations have permitted detailed assessments of both the long-term intensity variations (11-year cycle) and the short-term fluctuations (Forbush decreases). The results have revealed a smaller rigidity dependence for Forbush decreases than for the long-term variation (Burger and Swanenburg, 1973b). A hysteresis effect, similar to the one discussed under section 5.3.7 was also observed by Burger and Swanenburg (1973a) in the long-term intensity variation (caused by solar modulation). The cosmic-ray diffusion coefficient, a parameter which plays an important role in the modulation mechanism, was investigated extensively by the scientific team responsible for experiment E-12. Most models of the modulation mechanism are based upon a diffusion coefficient which is a separable function of rigidity and of heliocentric distance. Theoretical considerations and the data from experiment E-12, however, led Burger and Swanenburg (1971) to conclude that the diffusion coefficient is nonseparable. Winkler and Bedijn (1976) then developed a model based upon a nonseparable diffusion coefficient, which explained the observed intensity variations not only for the electronic component, but also for the proton and helium components. Although these results lent strong support to the nonseparable model, Winkler and Bedijn (1976) did not conclude that other models were necessarily ruled out. Some questions still remain unresolved, but the above efforts have undoubtedly led to a better understanding of the solar modulation mechanism, which in turn has resulted in an improved knowledge of the interstellar cosmic-ray spectrum.

### 5.3.9 Low-Z Cosmic-Ray Nuclei (E-10)

The data from experiment E-10 were used to measure the spectra and charge composition of galactic cosmic radiation in the energy range 5-800 MeV/nucleon and charge range 1 to 14. These measurements revealed an overabundance of low-energy carbon and oxygen nuclei and a carbon/oxygen ratio that were not consistent with the usual assumption that cosmic rays pass through the same average amount of interstellar gas (Teegarden

et al, 1969). These observations, however, lent support to the hypothesis of a two-source model for the origin of galactic cosmic rays. These two sources are presumed to be quite different, both in their relative composition and in their degree of remoteness from the solar cavity.

Data obtained with experiment E-10 during a series of three solar flares during the period May 28-29, 1969, have yielded the two largest  $^3\text{He}/^4\text{He}$  ratios ever reported for a solar event. A preliminary account of these observations was given by Balasubrahmanyam and Serlemitsos (1974). In a subsequent and more detailed analysis of these solar events Serlemitsos and Balasubrahmanyam (1975) also reported an unusually low abundance of protons during the above solar events. These  $^3\text{He}$  and  $^1\text{H}$  observations have placed new limitations upon theoretical models of " $^3\text{He}$ -rich" flares.

### 5.3.10 High-Z, Low-Energy Cosmic-Ray Nuclei (E-27)

Data on cosmic-ray particles in the energy range 2- to 50-MeV/nucleon and charge range  $5 \leq Z \leq 50$  were acquired with experiment E-27 during the entire operational life of OGO 5. Measurements made in the Earth's radiation belt (Mogro-Campero and Simpson, 1970) led to the discovery of a very pronounced flux enhancement in the CNO region ( $Z = 6, 7, \text{ and } 8$ ). The observed CNO enhancement was characterized by prominent peaks at  $Z = 6$  and  $8$ , which tended to overlap and hide a smaller and less definite peak at  $Z = 7$ . These observations represent the first identification of carbon and oxygen nuclei in the Earth's radiation belt, as well as the first suggestion for the presence of a significant quantity of nitrogen nuclei. The measured oxygen-to-carbon abundance ratio indicated that these nuclei were of extraterrestrial origin. A subsequent and more detailed study by Mogro-Campero (1972) yielded the variation of the CNO flux as a function of the magnetic parameter  $L$  and showed that the results on C and O had placed a new value for the observed high-energy limit of trapping.

Experiment E-27 was also used to investigate the relative abundance of solar flare nuclei in the charge range  $6 \leq Z \leq 26$ . By summing together the data from several flares, Mogro-Campero and Simpson (1972a) found an overabundance of solar accelerated nuclei relative to solar system abundances, which tended to increase with increasing atomic number. This initial study was followed by a more comprehensive investigation in which Mogro-Campero and Simpson (1972b) compared the results from six different flares. This comparison showed that the abundance ratio of the iron group nuclei (Ti-Ni) to oxygen nuclei (O) varied by as much as two orders of magnitude for these six flares.

Similar heavy nuclei measurements were conducted with experiment E-27 during quiet interplanetary periods. These measurements showed that the energy spectra of C and O nuclei during quiet times behaved as the H and He spectra during quiet times as low energies. This behavior, together with results concerning relative abundances and flux variations, indicated that these low-energy heavy nuclei were of galactic origin (Mogro-Campero and Simpson, 1975).

### 5.3.11 Energetic Photons in Cosmic Rays (E-08)

Experiment E-08 represents the first application of the spark chamber technique to satellite gamma-ray astronomy. This experiment had an angular resolution of 3 deg, and it was sensitive to photons of energy 25 to 100 MeV. The experiment, however, produced only 3 months of useful data during which gamma rays were detected 195 times. Hutchinson et al (1969) analyzed the first 88 of these events, which were observed while the gamma-ray telescope was pointed toward Cygnus. A variation in intensity as a function of galactic latitude was derived, which showed a maximum in the direction of the galactic plane.

## OVERVIEW

### 5.4 Radio Physics

Experiment E-20 was the only Radio Physics experiment included in the OGO 5 mission. This experiment was used to conduct extensive investigations of type III solar bursts at frequencies between 3.5 MHz and 50 kHz. Significant progress was achieved in the theoretical understanding of type III solar bursts and in the empirical modeling of the electron density distribution between the Sun and the Earth.

#### 5.4.1 Production of Type III Solar Bursts (E-20)

The data from experiment E-20 were used to resolve a major difficulty in the electron-stream hypothesis for the generation of type III radio bursts. The basis for the theory is the fact that solar electron events, exhibiting electron energies greater than 40 keV, are always accompanied by type III bursts. The theory, however, did not explain why so many type III bursts were observed without corresponding solar electron events. Alvarez and Haddock (1972) explained this apparent contradiction by assuming that the exciter electrons traveled along the Archimedean spirals of the interplanetary magnetic field. This assumed propagation mechanism would cause the exciter electrons to reach the Earth only when they originate from flares on the western half of the solar disk. The results from experiment E-20 were shown to be completely consistent with this explanation.

Further support for this explanation was provided by Alvarez et al (1973), who showed that the frequency spectrum of type III bursts exhibited increasingly lower frequencies as the solar flare longitude became increasingly westward. This result was again consistent with the proposed spiral paths for the exciter electrons.

#### 5.4.2 Arrival Times and Decay of Type III Solar Bursts (E-20)

The type III burst spectra observed with experiment E-20 were used also to determine the velocity of the exciter particles and the burst decay rates. By showing that the type III spectra below 1 MHz were due primarily to second harmonic emission, Haddock and Alvarez (1973) were able to measure burst arrival times with improved accuracy. Their measurements showed that the exciter particles (in 32 cases) traveled at very nearly one-third the velocity of light. Alvarez and Haddock (1973b) showed that the decay times of bursts increased with decreasing frequency at a rate considerably slower than predicted by electron-proton Coulomb collisions. At 50 kHz measured and predicted values differed by about a factor of 100. A new theory was not proposed, but it was shown that existing theories were inadequate.

#### 5.4.3 Solar Wind Density Model (E-20)

Alvarez and Haddock (1973a) used the data from experiment E-20 to derive a model of the electron density distribution of the solar wind to 1 AU, which was consistent with optically determined values near the Sun and with direct measurements near the Earth. This experimental model, in effect, filled the gap in observational data in the region from 20 to 200 solar radii.

### 5.5. Optical Experiments

The two optical experiments (E-21 and E-22) included in the OGO 5 mission were based upon different principles, and they were operated by different investigators. Their objectives, however, were very similar. Both experiments measured the intensity of the hydrogen Lyman-alpha airglow (1216 Å) and used these measurements to derive information concerning neutral hydrogen densities in the Earth's magnetosphere and beyond. Experiment E-21 could also measure the atomic oxygen emission at 1304 Å, and experiment E-22 could measure the width of the 1216-Å line from which hydrogen temperature

could be inferred. These additional capabilities were useful only for the first month of operation, and consequently the two optical experiments were used primarily to investigate the 1216-Å airglow intensity.

This apparent duplication of effort turned out to be extremely beneficial. It not only enhanced the motivation of the two scientific groups involved to analyze and publish their results promptly, but it also led to one of the most spectacular scientific and technological accomplishments of the entire OGO program. The two scientific teams were able (through their joint efforts) to convince the NASA management that unique and valuable information could be obtained by placing the OGO 5 spacecraft temporarily in a spinning mode. This was done not only once, but on six different occasions. One cannot help wondering whether these very difficult and risky spacecraft maneuvers would have been attempted based upon data from only one optical experiment. Since the results and implications of the measurements in the spinning mode turned out to be quite startling (see section 5.5.2), it was fortunate indeed that the findings were completely corroborated by two independent experiments.

#### 5.5.1 The Inner Geocorona (E-21, E-22)

The major objective of the optical experiments on OGO 5 was to investigate the geocorona, which is the outermost atomic hydrogen atmosphere of the Earth, a region extending approximately from 2 to 15  $R_E$ . The optical experiments measured the 1216-Å airglow produced by solar Lyman-alpha scattering in the geocorona. The hydrogen density is derived from the airglow data. At altitudes greater than 6  $R_E$  the celestial background radiation introduced large uncertainties in the 1216-Å measurements, a situation which led to the somewhat arbitrary distinction between the inner geocorona (distances less than 6  $R_E$ ) and the outer geocorona (beyond 6  $R_E$ ). Experiments E-21 (Thomas, 1970) and E-22 (Bertaux and Blamont, 1970) yielded a number of Lyman-alpha airglow profiles and pointed out the need for a mapping of the celestial background radiation at 1216 Å.

#### 5.5.2 Celestial Background Radiation at 1216 Å (E-21, E-22)

To permit a mapping of the celestial background at 1216 Å, the OGO 5 spacecraft was placed in a spinning mode (see introduction to section 5.5) during the periods September 12-14, 1969, December 15-17, 1969, and April 1-3, 1970. The data from experiment E-21 (Thomas and Krassa, 1971) and E-22 (Bertaux and Blamont, 1971) led to the discovery of a prominent source of Lyman-alpha radiation located at a distance of 3 AU at the intersection of the ecliptic and galactic planes along the projection of the solar apex.\* The presence of this Lyman-alpha source at 3 AU suggested that it was due to an interstellar wind of neutral hydrogen penetrating deeply into the heliosphere until it was ionized by charge exchange and extreme ultraviolet radiation. The parameters of this postulated interstellar wind were calculated by Bertaux et al (1971). A confirmation of the celestial background measurements was provided by three additional spin-up operations on September 4, 1970; March 18, 1971; and May 23, 1971 (Thomas and Krassa, 1974). The broad survey of the background radiation during the spin-up operations was supplemented by continuous monitoring (over a 3-year period) of the limited celestial region which could be studied with the stabilized spacecraft. The continuous monitoring revealed two variations on the background emission, one due to solar activity and the other due to the Earth's orbital motion causing an annual variation in the distance from the Earth to the source (Thomas and Bohlin, 1972).

#### 5.5.3 The Outer Geocorona (E-21, E-22)

The detailed mapping of the celestial background and the monitoring of its variations made it possible for the first time

\* The solar apex is the point in the celestial sphere toward which the Sun appears to be moving.

to measure accurately the outer geocorona airglow at 1216 Å and to deduce the hydrogen density distribution between 5 and 16  $R_E$  (Bertaux and Blamont, 1973). These measurements led also to the discovery of the "geotail," an anti-solar enhancement in the density of the hydrogen geocorona, reminiscent of a cometary tail (Thomas and Bohlin, 1972; Bertaux and Blamont, 1973).

#### 5.5.4 Observations of Comet Bennett (E-21, E-22)

On five separate occasions during March 1970, the OGO 5 satellite passed through the Lyman-alpha coma of Comet Bennett. Data from experiments E-21 and E-22 showed that the comet (including its tail) was surrounded by a huge cloud of hydrogen having a diameter of approximately 13 million kilometers (Bertaux, 1970). From the curvature of the extended hydrogen tail, it was estimated that the mean flux of the inner blue wing\* of the solar Lyman-alpha radiation had a value of about  $9.5 \times 10^{11}$  photons  $\text{cm}^{-2} \text{S}^{-1} \text{Å}^{-1}$  (Keller and Thomas, 1973).

### 6. OGO 6 Results

The OGO 6 spacecraft was the last stage of a continuous evolution, during which each OGO mission made significant contributions to the design of the next mission. Thus, the wideband transmitter that failed on OGO 5 was redesigned for OGO 6. Other changes made on OGO 6 included improvements in the design of the 9.15-meter (30-ft) antennas and in the design of the VLF electric-field experiment antenna. Also, as a natural desire to optimize the use of the expensive OGO spacecraft, the weight, power, data output, and command requirements increased steadily during the OGO program. The weight of experiments increased from 86 kg (190 lb) on OGO 1 to 168 kg (370 lb) on OGO 6. Experiment power rose from 60 to 230 W, and redesigns of the OGO 6 spacecraft increased the number of experiment commands by 60 percent over the original design.

Yet, although the OGO 6 mission represents the culmination of the OGO spacecraft technology, this mission was also somewhat of an anticlimax. The entire OGO program came to an abrupt termination less than 30 months after the launch of OGO 6 (see Figure III-5 of the OGO Program Summary). The operational life of the relatively well-behaved OGO 6 spacecraft was only 24 months compared to 63 months for the crippled OGO 1. A large number of OGO 6 experiments failed to yield published results for a number of reasons; one reason being undoubtedly the general loss of interest in the OGO program after 1971. Seeking a more promising research environment, a number of OGO experimenters transferred to other projects and agencies; and, because of new responsibilities, their OGO efforts had to be interrupted.

Reorientation in NASA priorities after 1971 was undoubtedly a factor in the almost complete lack of scientific results based upon experiments F-15 (Evans) and F-16 (Farley). The absence of scientific publications based upon experiments F-08 (Kreplin), F-09 (Bedo), F-10 (Regener), and F-11 (Blamont) is due partly to the decreasing NASA support and partly to severe degradation, which these four experiments suffered shortly after launch. Several OGO 6 experiments (F-02, Nagy; F-03, Hanson; F-05, Taylor; and F-23, Aggson) were severely affected by the solar-array failure that developed on the OGO 6 spacecraft. This gave the vehicle a negative potential of more than 20 V when the solar paddles were exposed to sunlight. Experiments F-02, F-03, F-05, and F-23 were nevertheless quite successful because of their excellent nighttime performances. The failure of experiment F-06 (Hanson), which occurred at the time of initial turn-on, was not related to any of the above-mentioned factors. Experiment F-07 (McKeown) failed to achieve its scientific objectives because of severe surface contamination;

some engineering data were obtained, however, concerning this contamination and the feasibility of the new measuring techniques used in experiment F-07. Experiment F-24 (Helliwell) failed to achieve one of its major objectives (measurements of electric field to magnetic field ratio) because of the loss of the magnetic field data shortly after launch. Thus, eight experiments on OGO 6 (F-06, F-07, F-08, F-09, F-10, F-11, F-15, and F-16) failed to yield significant scientific results, and five additional experiments (F-02, F-03, F-05, F-23, and F-24) were partially disabled. It should be noted, however, that the latter five experiments were used to conduct a large number of very significant investigations.

In spite of the above mentioned deficiencies, the OGO 6 mission was quite successful, resulting by July 1977 in about 130 publications in refereed journals. The OGO 6 mission was certainly outstanding in many respects; and were it not for the fact that it was overshadowed by the extraordinary success of the OGO 5 mission, the OGO 6 mission would certainly have been an appropriate climax for the OGO program.

The scientific results from OGO 6 have been summarized following the same organization as was used for the overview of the OGO 1, 2, 3, 4, and 5 missions. The OGO 6 accomplishments were, therefore, grouped according to the following disciplines: Magnetic and Electric Fields, Low-Energy Plasmas, Energetic Particles, Radio Physics, Optical Experiments, and Neutral-Atmospheric Measurements.

#### 6.1 Magnetic Fields and Electric Fields

##### 6.1.1 Magnetic Field Measurements

Some results from the OGO 6 magnetic field measurements have already been presented under the OGO 4 overview. For example, the data from experiment F-21 on OGO 6 were combined with data from experiment D-06 on OGO 4 to investigate crustal anomalies (section 4.1.3) and the equatorial electrojet (section 4.1.4). Conversely, some of the results given under 6.1 are based partly upon OGO 2 and 4 data. The polar orbiting OGO 2, 4, and 6 satellites were known as the POGO series.

##### 6.1.1.1 Geomagnetic Field Models (C-06, D-06, F-21)

Data from experiment F-21 on OGO 6 were used to continue the World Magnetic Survey discussed under section 4.1.1. The POGO (8/71) model of the terrestrial magnetic field was developed by adding the OGO 6 data for the period June 1969 to March 1970 to the POGO (8/69) data base. The POGO (8/71) model used 12,773 OGO 2 points (experiment C-06), 18,431 OGO 4 points (experiment D-06), and 20,019 OGO 6 points (experiment F-21) selected from especially quiet days (Langel, 1974a). The POGO (8/71) model was used extensively to investigate disturbances  $\Delta B$  in the total field magnitude,  $\Delta B$  being defined as the measured field minus the model field.

##### 6.1.1.2 High-Latitude $\Delta B$ (C-06, D-06, F-21)

The data from experiments C-06, D-06 and F-21 were used to measure the high-latitude  $\Delta B$  in the 400- to 1510-km altitude range (Langel, 1974a). These near-Earth measurements showed that  $\Delta B$  was positive on the dawnside from near 2200 to near 1000 MLT (magnetic local time\*) and negative on the duskside from near 1000 to 2200 MLT. This basic pattern was found present for all seasons and for all levels of magnetic disturbances. Langel (1974b) derived equivalent ionospheric currents that could cause the negative  $\Delta B$  region and called these HLS (high-latitude sunlit). The HLS currents are latitudinally broad as opposed to jet-type currents. Since the positive  $\Delta B$  region could not be explained by ionospheric currents only, it was concluded that the positive  $\Delta B$  region was due to at least two sources, the

\* The solar Lyman-alpha profile (flux versus wavelength) resembles the wings of a butterfly. The blue wing corresponds to  $\lambda < 1215.664 \text{ Å}$ . The other wing is known as the red wing.

\* For a definition of coordinate systems, see J. H. King, "Handbook of Correlative Data," NSSDC 71-05, Feb. 1971, p. 170-175 and references therein.

## OVERVIEW

westward electrojet and an unidentified non-ionospheric source.

The maximum positive and negative  $\Delta B$  values ( $B_p$  and  $B_n$ , respectively) were investigated with respect to various parameters of the interplanetary magnetic field (Langel, 1975). The best correlation (0.79) was shown by  $B_p$  versus  $\sum B_z/T$ , for times when  $B_z$  was negative and for  $T = 120$  min. The summation represents the integrated effect of southward  $B_z$  over a time interval  $T$  preceding the measurement of  $B_p$ . Langel (1975) also compared  $\Delta B$  with DP2 fluctuations (polar magnetic disturbance corresponding to twin vortex currents) and concluded that the two phenomena were not correlated. Langel (1974c) showed that the area above the Earth's surface covered by the positive  $\Delta B$  region was the largest in summer and when the interplanetary magnetic field was directed toward the Sun. This result indicated that the variable portion of the positive  $\Delta B$  region was due to variations in latitudinally narrow electrojet currents and not due to variations in the non-ionospheric source of  $\Delta B$ .

### 6.1.1.3 Low-Latitude $\Delta B$ (C-06, D-06, F-21)

Using the same data base as was used for the studies discussed under sections 6.1.1.1 and 6.1.1.2, Cain and Davis (1973) investigated the geomagnetic field at low latitudes to determine the effect of external fluctuations during quiet times. This study served two purposes: first, it improved the magnetic field model; and second, it led to more accurate measurements and identification of the external fluctuations.

### 6.1.1.4 Global Anomaly Map (C-06, D-06, F-21)

The data reduction procedures used to show that crustal anomalies could be detected in the POGO data (see section 4.1.3) were applied to the entire set of POGO magnetic measurements, resulting in a detailed global magnetic anomaly map. Although more work was needed to fully interpret the map and to determine the cause of the anomalies, many of the anomalies appeared to be of geological origin with a source in the lithospheric region of the Earth (Regan et al, 1973).

### 6.1.1.5 Investigation of Proton Whistlers (F-22)

The VLF studies conducted with the first five OGO satellites were concerned with VLF phenomena (whistlers) in which the wave propagation characteristics are determined primarily by the electron density along the propagation paths. The electron whistler is by far the most common and it is the only kind of whistler seen on the ground. At the OGO 6 satellite altitudes, an electron whistler can be converted into a proton whistler, i.e., a wave that interacts primarily with positively charged particles (in this case protons). Theoretically, this conversion depends upon  $\theta$ , the angle between the magnetic field and the direction of propagation. Since different theories led to different values of  $\theta$ , it became necessary to measure  $\theta$ . The measurement of  $\theta$  was first accomplished using data from experiment F-22 (Chan et al, 1972). The results were in good agreement with Wang's (1971) collisionless mode-coupling model.

### 6.1.1.6 Investigation of ELF Chorus (F-22, F-16)

New insights concerning the propagation of ELF chorus were gained from a correlated study of ELF chorus data from experiment F-22 and electron precipitation data from experiment F-16. Chorus signals were typically accompanied by electron precipitation, but chorus peaks and precipitation peaks did not coincide. These observations were consistent with the following model. The chorus signals originate near the geomagnetic equator (see section 5.1.9.6) as a result of plasma instability (Kennel and Petschek, 1966). The generation mechanism leads to electron precipitation along the field lines on which the chorus originated. The observed chorus signals travel initially on ducts centered on the same field line. At altitudes ranging from 0.2 to 1  $R_E$ , the duct ends and the chorus signals

diverge from the field line. The correlation between chorus and precipitation peaks is, therefore, only approximate at the OGO 6 satellite altitude (Holzer et al, 1974).

### 6.1.1.7 Investigation of ELF Hiss (F-22)

A study (using data from experiment F-22) of ELF hiss amplitude during geomagnetic storms (Smith et al, 1974) showed that hiss exhibits a pronounced intensification during the recovery phase of geomagnetic storms as the plasmasphere expands into the intensified belt of the outer zone electrons. This behavior is as expected from the theory of hiss generation, which states that hiss occurs when energetic electrons encounter an abrupt increase in ambient (cold) plasma density. The hiss variations observed during magnetic storms are also consistent with the experimental results given under section 5.1.9.5; namely, that hiss is proportional to  $\ln(N/N_0)$  where  $N$  is the ambient electron density and  $N_0$  is the density below which hiss will not occur.

The data from experiment F-22 were also used by Thorne et al (1977) to extend the above study by Smith et al (1974). Thorne et al investigated the local time variation of ELF emissions during periods of substorm activity and concluded that ELF emission enhancements are controlled by substorm activity.

A comprehensive study of hiss in the inner zone for  $L < 2$  was conducted for the first time using data from experiment F-22 (Tsurutani et al, 1975). This study showed that inner zone hiss occurs almost exclusively during the recovery phase of magnetic storms and substorms. It was also found that the inner zone hiss is primarily a daytime phenomenon and that its intensity is related to the magnitude of the geomagnetic activity. These features suggest that the inner zone hiss originates near the plasmapause as plasmaspheric hiss, which then propagates to the inner zone. This mechanism can occur during magnetic storms because the plasmasphere is displaced inward, causing the plasmaspheric hiss to be generated at lower  $L$  values with a corresponding reduction in the propagation distance to the inner zone. Theoretical calculations (Tsurutani et al, 1975) indicated that the observed inner zone hiss could cause a significant loss of relativistic electrons from the inner zone.

The data from experiment F-22 also revealed extensive hiss activity at high latitudes, well outside the plasmasphere. This was a somewhat surprising result in view of the usual plasmaspheric confinement of hiss signals. A study of these observations by Kelley et al (1975) led to the conclusion that the high-latitude hiss was plasmaspheric hiss, which propagated downward along field lines and leaked out of the plasmasphere into the high-latitude lower ionosphere.

### 6.1.2 Electric Field Measurements (F-23)

Theoretical considerations (e.g., Axford and Hines, 1961) predict that circulatory plasma motions produced by the solar wind in the distant magnetosphere should be transferred via the magnetic field lines down to the polar ionosphere. This ionospheric convection would be accompanied by strong electric fields at all altitudes in the polar ionosphere and, as a result of differential ion-electron drag, would cause the polar electrojet at an altitude of about 100 km.

A completely different mechanism is involved in the production of the equatorial electrojet and of its associated electric field. The basic driving forces are gravitational (solar and lunar tides) and solar-heating effects that produce air motions in the upper atmosphere. In the E region, where electrical conductivity is appreciable, the motion across the geomagnetic field induces electric fields that eventually cause the electrojet. The electric fields associated with the equatorial electrojet are, therefore, primarily in the E region.

The most comprehensive measurements of electric fields in the ionosphere were conducted with experiment F-23 on OGO 6 (double probe floating potential technique). The resolution of the measurements was limited by the accuracy with which the spacecraft orientation was known because this orientation had

to be known in order to calculate the required  $V \times B$  correction\*. The dc fields in the equatorial and midlatitude regions could not be measured at OGO 6 altitudes because their amplitudes were comparable to the  $V \times B$  correction. Excellent data were obtained, however, in the polar regions where strong electric fields are present at all ionospheric altitudes.

#### 6.1.2.1 High-Latitude Electric Fields (F-23)

Based upon the data from experiment F-23 (Heppner, 1972a), it appears that strong convective electric fields are always present over a broad expanse of polar latitudes at ionospheric altitudes. The convection exhibits a basic pattern, featuring antisolar flow in the central polar cap region and an east-west return flow in the adjacent evening and morning auroral regions. The corresponding electric field is oriented from dawn to dusk in the polar cap, equatorward in the morning auroral region, and polarward in the afternoon auroral belt. The dawn-dusk potential drop across the polar cap was found to be typically between 40 and 70 kV and it appeared to be equal to the total dawn-dusk potential drop across the auroral belt.

Heppner (1972b) showed that the dawn-dusk electric field distribution exhibited a number of typical patterns or signatures. Well-defined signatures were found to correlate strongly with the azimuthal angle of the interplanetary magnetic field. This correlation constitutes the best available proof that the solar wind is indeed the primary driving force producing the polar electric fields.

The convection flow in the auroral belt exhibits a sharp east-west separation along a boundary known as the Harang discontinuity. The Harang discontinuity was studied extensively, using the data from experiment F-23 (Maynard, 1974). This study showed that the discontinuity extends typically from 2300 MLT at 60-deg invariant latitude to 2150 MLT at 70-deg invariant latitude. It was also found that the discontinuity moved southward, steepening its latitudinal profile as magnetic activity increased. A well-defined boundary was not seen near noon where the auroral belt convection flow returns to the polar cap (Heppner, 1973). Data in this region are characterized by a multiplicity of field reversals and large irregularities in the dawn-dusk components.

#### 6.1.2.2 High-Latitude Electric Field Model (F-23)

An important conclusion reached from the analysis of the data from experiment F-23 was that existing models of the high-latitude magnetospheric electric field were not in agreement with observations. This lack of representative models provided the motivation for generating empirical models based primarily upon the OGO 6 data. The results from this modeling effort (Heppner, 1977) include quantitative models of typical high-latitude dawn-dusk electric field profiles and typical model convection patterns to show boundary locations at other magnetic local times.

#### 6.1.2.3 Variational (ELF) Electric Fields (F-23)

Experiment F-23 was designed to measure electric fields from dc up to 4 kHz in seven frequency bands. The dc measurements were discussed earlier in sections 6.1.2.1 and 6.1.2.2. Electric fields measured at frequencies above 500 kHz corresponded to well-known electromagnetic phenomena such as whistlers, hiss, and chorus. Electric fields measured at frequencies below 64 Hz were in most cases due to electrostatic waves. The amplitudes of these ELF fields were found to be large, not only in polar regions (where strong dc fields were observed), but also in the equatorial regions (where dc fields were too weak to be observed). It was shown that the electric fields due to electrostatic waves could be grouped in three different classes,

\* Experiment F-23 monitored the potential difference  $\phi$  between two collinear 4.5-meter antennas. The quantity  $\phi$  was related to the electric field  $E$  by the formula:  $\phi = (E + V \times B) \cdot d$  where  $V$  was the satellite velocity,  $B$  was the geomagnetic field, and  $d$  was the vector distance between the antenna midpoints. Consequently, the  $V \times B$  term had to be known in order to calculate  $E$  from the measurements of  $\phi$ .

based upon their spectral characteristics: type A - strong signals with a  $1/f$  spectrum, type B - weak signals with a flat spectrum, and type C - weak signals with a rising spectrum. Comparisons with ground-based ionosonde data showed that the low-latitude type A signals were correlated with low-latitude spread F. Type A signals were also correlated with the fluctuations in electron densities measured by experiment F-03 on OGO 6 (Holtet et al, 1977).

## 6.2 Low-Energy Plasma Experiments

Useful data were acquired throughout the OGO 6 mission by three low-energy plasma experiments: the Langmuir probes (F-02), the retarding potential analyzer (F-03), and the ion mass spectrometer (F-05). Experiments F-02 and the ion analysis mode of experiment F-03, however, became restricted almost exclusively to nighttime observations after the OGO 6 spacecraft potential problem developed 2 weeks after launch. Experiment F-05 was basically a continuation of experiment D-05 on OGO 4. The two experiments (D-05 and F-05) have provided essentially a continuous data base for the period July 1967 to June 1971, and in many cases the scientific results obtained were based upon data from both experiments. A number of results based upon both D-05 and F-05 were given in sections 4.2.1 and 4.2.2. of the OGO 4 Overview. These results are not repeated here.

### 6.2.1 Solar Geomagnetic Control of the Ionosphere (F-05)

Preliminary studies with experiment D-05 on OGO 4 revealed strong longitudinal variations in the pole-to-pole profiles of ion composition obtained as the Earth rotates beneath the relatively fixed satellite orbit. Taylor (1972a) used data from experiment F-05 to investigate the longitudinal effects and found that the average longitudinal variation was closely related to the angle in the noon local time plane between the Earth-Sun line and the magnetic dipole equator. Taylor (1972a) then showed that the proper investigation of seasonal, diurnal, and annual variations requires that the data be ordered in terms of the solar-geomagnetic geometry. Taylor (1972a) concluded that this selective approach to data analysis was required for the development of realistic models of ion composition distribution.

### 6.2.2 The High-Latitude Light-Ion Trough (F-05)

Taylor (1972b) applied the data-selection approach discussed in section 6.2.1 to the study of the high-latitude, light-ion trough (see sections 2.2.2 and 4.2.2). The improved data analysis technique led to the first clear identification of diurnal variations and magnetic storm effects. It was found that the steepness of the trough is much greater at night than during the day. In response to magnetic storms, the light-ion trough minimum moves equatorward and deepens. Taylor and Cordier (1974) showed that the light-ion trough is smooth and well defined during quiet magnetic conditions. Considerable structure is exhibited, however, during and following magnetic storm periods. The location and properties of these irregularities were found to be consistent with the concept of plasmasphere distortions in the form of "plasmatails" (see section 4.2.3). These results showed that the light-ion trough is indeed a fundamental parameter for studies of the formation and maintenance of the plasmasphere.

### 6.2.3 High-Latitude Minor-Ion Enhancements (F-05)

Perhaps the most surprising result from experiment F-05 was the discovery of abrupt and pronounced enhancements of the thermal molecular ions  $NO^+$ ,  $O_2^+$ , and  $N_2^+$  at mid- and high latitudes (Taylor, 1974). Normally, trace constituents with densities less than 2 ions/cm<sup>3</sup> (for  $L > 4$  and altitudes  $> 600$  km), these minor ions, following magnetic storms, can reach concentration levels exceeding  $10^3$  ions/cm<sup>3</sup> at altitudes as great as 1000 km. These enhancements are highly localized in time and space. Taylor et al (1975) have shown that the minor-ion enhancements are accompanied by a significant

## OVERVIEW

depletion in the concentration of atomic ions  $H^+$ ,  $O^+$ ,  $N^+$ , and  $He^+$ . This depletion, which can be by a factor of 3 or more, has been called by Taylor et al (1975) the high-latitude ion trough. The high-latitude ion trough is distinct and at a higher latitude than the light-ion trough. Grebowsky et al (1976) showed that the high-latitude trough was usually near or on the polar cap boundary as defined by experiments F-17 and F-23. This showed clearly that the high-latitude trough was not associated with the plasmopause. Grebowsky et al (1976) concluded that the high-latitude trough had to be related to magnetospheric processes occurring at the polar cap boundary, such as the precipitation of soft electrons or the reversal of the dc convection field.

### 6.2.4 Discovery of $Fe^+$ Ions in the Upper F-Region (F-03)

Experiment F-03 led to the discovery of heavy ions in the equatorial ionosphere at heights well above the F2 peak (Hanson and Sanatani, 1970). These ions with mass of about 56 amu were tentatively identified as iron ions. Further investigations by Hanson et al (1972) corroborated the  $Fe^+$  identification, both experimentally and theoretically. Although this somewhat startling conclusion was initially met with some skepticism, the  $Fe^+$  hypothesis has now been fully confirmed by recent measurements on Explorer satellites (Brinton, 1976).

Hanson and Sanatani (1971) showed that there is a high correlation between the presence of equatorial spread F and  $Fe^+$  ions. Iron ions, however, were sometimes observed without corresponding spread F. It was concluded that  $Fe^+$  was a "nearly" necessary condition for the formation of equatorial irregularities. A mechanism based partly upon the presence of  $Fe^+$  ions was proposed by Hanson et al (1973b) to explain the production of equatorial spread F.

### 6.2.5 Supercooled Plasma near the Magnetic Equator (F-03, F-02)

Using data from experiments F-03 and F-02, Hanson et al (1973a) showed that near the magnetic equator the ion temperature often exhibits deep depressions at altitudes above 600 km. The measured temperatures, which are well below the expected neutral gas temperatures, have been explained by Bailey et al (1973) in terms of expansion cooling brought about by the flow of plasma from the summer to the winter hemisphere.

### 6.2.6 Large Ion Depletions at Magnetic Equator (F-03)

The data from experiment F-03 also revealed that near the magnetic equator the F-region below the F2 peak is often drastically depleted in ion concentration, with the ion density decreasing by as much as 3 orders of magnitude in only a few vertical kilometers. These ion depletions were found to be associated with enhancements in heavier ions such as  $NO^+$  and  $Fe^+$  (Hanson and Sanatani, 1973).

### 6.2.7 Irregularities in the F-Region (F-03)

The duct mode data from experiment F-03 have provided a spectacular view of the small-scale irregularities in the F-region. These data made it possible to describe for the first time the general nature of these irregularities, their many different characteristic forms, and their geographic distribution (McClure and Hanson, 1973). The spectral characteristics of the F-region irregularities were investigated by Dyson et al (1974) who found that the irregularities were typically random with a power distribution varying as  $(1/q)^2$  where  $q$  = satellite velocity/irregularity scale size. These observations have provided some of the basic information required for a theoretical explanation of ionospheric irregularities. For example, the frequency spread  $2\Delta f/f$  in the ionogram phenomenon of spread F was shown to be proportional to the ion concentration fluctuation  $\Delta N/N$  measured at OGO 6 altitude with experiment F-03 (Wright et al, 1977). The implication is that the frequency spreading is caused by  $\Delta N/N$  irregularities.

### 6.2.8 Midlatitude Red Arcs (F-02, F-03)

The data from experiments F-02 and F-03 were used to show that the position of midlatitude red arcs coincides with a peak in electron temperature and minimum in electron density. These conditions, however, do not necessarily result in a visible red arc, because the red-line emission is an extremely nonlinear function of electron temperature (Nagy et al, 1972; Nagy et al, 1974).

### 6.2.9 Accuracy of Plasma Temperature Measurements (F-02, F-03)

As mentioned under section 4.2.5 of the OGO 4 Results, plasma temperature measurements have sometimes yielded conflicting results. This problem was investigated by comparing temperature data from experiments F-02 and F-03 to similar measurements made with the worldwide incoherent scatter network. Electron temperatures from the OGO 6 experiments were typically 15 percent greater than the radar data. Ion temperatures, however, seemed to agree within 5 percent. It was noted, however, that the comparisons were made during nighttime hours at altitudes between 400 and 600 km, i.e., under conditions when suspected errors are minimum (McClure et al, 1973).

## 6.3 Energetic Particle Measurements

Useful data were obtained for 14 months from three of the four energetic particle experiments on OGO 6: F-17 (Trapped and Precipitating Electrons, Williams), F-19 (Low-Energy Solar Cosmic-Ray Measurements, Masley), and F-20 (Cosmic-Ray Experiment, Stone). These experiments functioned normally from launch until August 29, 1970, at which time a spacecraft failure prevented the transmission of further useful data from F-17, F-19, and F-20. The fourth experiment, F-18 (Neutron Monitor, Lockwood) performed normally for 6 months until its power supply failed.

### 6.3.1 Solar-Flare Particles and Polar-Cap Absorption (F-19)

Greatly enhanced radio-wave absorption is observed in the polar cap (see section 5.1.8) beginning a few hours after a solar flare and lasting several days. This absorption is mostly due to increases in D-region electron concentration produced by energetic solar particles. These particles reach the D-region only over the polar caps, because at other latitudes the particles are deviated by the geomagnetic field. An instrument called a riometer is used for routine absorption measurements at various ground-based sites.

Baker et al (1974) used proton, alpha particle, and electron data from experiment F-19 on OGO 6 to compute the expected polar cap absorption of 30-MHz cosmic noise. These calculations were performed for the solar particle events of June 7, September 25, and November 2, 1969, and compared with ground-based riometer data. It was found that electrons contributed most of the absorption before the peak of the November 2, 1969, event. In the other two events protons produced most of the absorption. The alpha particle contribution was negligible in all cases. Measured and calculated absorption were in excellent agreement. These measurements were particularly significant, because OGO 6 was essentially directly above the ground-based riometer sites when the correlative data were obtained.

### 6.3.2 Solar Particle Entry and Propagation (F-19)

Using data from experiment F-19 for the period June 1969 to September 1970, Masley and Satterblom (1971) located the first tail field line at low latitude on the noon side. This location was monitored for 30 crossings during quiet geomagnetic conditions. The average value of the invariant latitude was 76 deg for the northern hemisphere and 75 deg for the southern hemisphere. The location of the first tail line was indicated by a sharp increase in the intensity of the 270-keV solar electrons.



### 6.3.3 Solar Proton/Alpha Ratio (F-19)

Satterblom and Masley (1971) derived the ratio of proton to alpha particle intensities at 5 to 21 MeV for the nine largest cosmic-ray events observed during the period June 1969 to September 1970. The ratios (obtained from experiment F-19) ranged from 25 to 1000 for these events.

### 6.3.4 Cosmic-Ray Abundances and Spectra (F-20)

The data from experiment F-20 were used to make the first comprehensive satellite measurement of the abundances and spectra of cosmic-ray nuclei using the geomagnetic field as a spectral analyzer (Brown et al, 1974). It was found that the nuclei in the charge range  $2 \leq Z \leq 10$  have similar integral rigidity spectra over the range of cutoff rigidities 2 to 15 GV, approaching a power law with exponent -1.6 at rigidities greater than 8 GV. Brown et al pointed out that their observations were not consistent with many of the leading theoretical treatments of cosmic-ray propagation. The data, however, could be explained by assuming a rigidity-dependent confinement of cosmic rays within the Galaxy.

### 6.3.5 Beryllium/Boron Ratio (F-20)

The cosmic-ray Be/B ratio depends upon the confinement time of cosmic rays in the Galaxy. The isotope  $^{10}\text{Be}$  provides a natural clock since it decays with a half-life of  $1.5 \times 10^6$  years. It has been shown theoretically (O'Dell et al, 1971) that the Be/B ratio should be  $0.42 \pm 0.06$  if there is no decay of  $^{10}\text{Be}$ , decreasing to  $0.29 \pm 0.05$  if there is complete decay. From the analysis of data from experiment F-20, Brown et al (1974) derived a ratio of  $0.41 \pm 0.02$ . Although the measurements of Brown et al represented an improvement over previous measurements of this type, the results could only be used to place an upper limit (of  $10^7$  years) upon the age of cosmic rays. The determination of cosmic-ray age continues to be a very challenging problem in experimental physics.

### 6.3.6 Isotopes of H and He in Solar Cosmic Rays (F-20)

Using data from experiment F-20 obtained during seven flare events, Garrard et al (1973) derived the ratios  $^3\text{He}/^4\text{He} = 0.10 \pm 0.02$ ,  $^2\text{H}/^1\text{H} < 3 \times 10^{-4}$ , and  $^3\text{H}/^1\text{H} = 1 \times 10^{-4}$  in the 4 to 5 MeV/nucleon energy range. This study extended earlier results by making measurements at significantly lower energies and by providing simultaneous  $^2\text{H}$ ,  $^3\text{H}$ , and  $^3\text{He}$  data permitting consistency tests. Furthermore, individual flare results were compared with the average solar flare event abundances. The results indicated that additional refinements were necessary in the calculations of the origin of  $^3\text{He}$ ,  $^2\text{H}$ , and  $^3\text{H}$  in solar flares.

### 6.3.7 Neutron Measurements (F-18)

Neutrons are produced in the Earth's atmosphere by the interactions of energetic particles (galactic cosmic rays and solar protons) with air nuclei. The fraction of these neutrons that leak out of the atmosphere is referred to as the Earth's neutron albedo. Some of the near-Earth neutrons could be produced by solar flare protons interacting with the solar atmosphere. Theoretical calculations (Lingenfelter, 1963; Lingenfelter and Flamm, 1964; Newkirk, 1963) have yielded estimates of the neutron leakage flux versus neutron energy (at fixed latitudes) and of the total neutron flux as a function of latitude.

The primary purposes of neutron measurements in space with experiment F-18 have been to determine the near-Earth neutron flux originating in the terrestrial atmosphere and the near-Earth neutron flux originating in the solar atmosphere. These measurements showed that the total neutron leakage flux versus latitude (Jenkins et al, 1970) was 0.7 times the intensity predicted by Lingenfelter (1963) and Newkirk (1963). The latitude dependence of the total neutron flux (Lockwood et al,

1973) was found to vary with galactic cosmic-ray modulation during the period July to October 1969, in a manner consistent with the predictions of Lingenfelter (1963). The neutron energy spectrum in the 1 to 10 MeV range was measured by Jenkins et al (1971) for both the polar regions and the equatorial regions. The measured spectrum in the equatorial region agrees with the spectral shape calculated by Newkirk (1963) for a geomagnetic latitude of 57 deg N. The measured polar spectrum was found to be flatter (i.e., with a greater fraction of fast neutrons) than indicated by Newkirk's spectrum. The data from experiment F-18 did not yield any indication of a quiet time solar neutron flux, but some evidence was found for a solar neutron flux during solar flares (Hedili, 1974).

### 6.3.8 Field-Aligned Precipitations of $> 30$ keV Electrons (F-17)

The data from experiment F-17 on OGO 6 have provided the first experimental evidence of field-aligned precipitation of  $> 30$  keV electrons (Williams and Trefall, 1976). A search through about 2 months of data from experiment F-17 revealed 10 examples of such precipitation events. Preliminary indications were that these events usually occurred poleward of the trapping boundary for  $> 30$ -keV electrons and mainly in the late afternoon to early morning sectors. A more complete survey of the 14 months of data available from experiment F-17 is in progress, with a view to studying in detail the location of these events and their relationship to geomagnetic activity.

## 6.4 Radio Physics Experiments

Experiment F-25 (Whistler and Low-Frequency Electric Field Study, Laaspere) has provided comprehensive data on whistlers and other low-frequency phenomena over an extended range of frequencies (20 Hz to 1000 kHz). Some useful results were also obtained with experiment F-24 (VLF Noise and Propagation, Helliwell) in spite of its very brief operational lifetime.

### 6.4.1 Auroral Hiss (F-25)

Auroral hiss, the most prominent emission in the auroral zone, was investigated extensively by Laaspere et al (1971) using data from experiment F-25. It was found that auroral hiss is truly a broadband phenomenon, extending from a few kHz to at least 540 kHz. Under geomagnetically quiet conditions the center of the auroral hiss zone extends from about 70 deg invariant at magnetic midnight, through 75 deg invariant latitude at 0600 and 1800 MLT to about 78 deg invariant latitude at magnetic noon. The zone moves on the average about 5 deg toward the equator under disturbed conditions.

### 6.4.2 Global Distribution of 200- and 540-kHz Signals (F-25)

The data from experiment F-25 revealed the following worldwide distribution of 200- and 540-kHz signals: (1) naturally generated hiss at polar latitudes; (2) nighttime midlatitude enhancements; (3) signal peaks associated with individual ground stations; (4) conjugate region signals of low-latitude, 200-kHz stations; and (5) signal enhancements at the equator (Laaspere and Semprebon, 1974).

### 6.4.3 Lower Hybrid Resonance (LHR) Noise (F-25)

One of the most intense phenomena observed with experiment F-25 was the LHR noise seen below auroral latitudes in the range from a few to about 20 kHz. The LHR emissions were found to occur mostly at night in the invariant latitude range from 45 deg to 65 deg (Laaspere et al, 1971). The observed LHR phenomena were frequently associated with whistlers, suggesting that the LHR hiss could derive its energy from whistler waves (Laaspere and Johnson, 1973).

## OVERVIEW

### 6.4.4 Miscellaneous ELF-VLF Phenomena (F-25)

Additional ELF-VLF phenomena observed with experiment F-25 and investigated by Laaspere and Johnson (1973) include triggered emissions, banded chorus, saucers, and the accidental demodulation of radio-frequency signals. It was found that emissions in the ELF-VLF bands can be triggered by VLF stations and by proton whistlers. Banded chorus, which is one of the most common emissions at altitudes of a few Earth radii, is relatively rare at OGO 6 altitudes. However, when present, banded chorus can be the most intense emission observed. Emissions with saucer-shaped, frequency-versus-time characteristics were observed only when the spacecraft altitude was greater than 930 km, indicating that this is the approximate lower boundary of the region in which saucers originate. The experiment F-25 receiver operating in the lowest frequency band (20 Hz to 15 kHz) has also detected the audio modulation of radio-frequency signals from the Voice of Australia and from the Voice of America. Tentative explanations for the demodulation mechanism include (1) plasma-sheath detection and (2) overloading of the receiver input stage.

### 6.4.5 Polarization Measurements of Whistlers (F-24)

Experiment F-24 was designed to provide a substantially greater amount of detailed information than had previously been available from satellite-borne VLF receivers. The new and more advanced design concepts incorporated in experiment F-24 included the broadband measurements of wave polarization, wave normal, and wave impedance. Although the fully operational life of experiment F-24 lasted less than 4 weeks, the feasibility of the more advanced measurements was thoroughly demonstrated (Helliwell et al, 1973). A major achievement of the F-24 experiment on OGO 6 was the experimental verification of the polarization of proton whistlers (Smith, 1970). As predicted theoretically, the electron whistler was found to be right-hand polarized and the proton whistler left-hand polarized.

## 6.5 Optical Experiments

The OGO 6 mission has provided extensive optical data at 1216 Å (Experiments F-12 and F-13), at 1304 Å (Experiment F-13), at 5577 Å (Experiment F-26), at 5890 Å (Experiment F-26), and at 6300 Å (Experiment F-14). The measurement of these emissions has typically yielded their global distributions and a number of derived parameters such as neutral densities, neutral temperatures, and electron densities. The remote sensor techniques for obtaining these parameters are often more difficult to use than the direct *in situ* techniques. The development of these remote sensor techniques is important; however, because in some cases, such as planetary flyby missions, the remote sensing techniques are the only ones that can be used.

In presenting the results of the OGO 6 optical experiments one could proceed according to regions investigated (lower thermosphere or E-region, upper thermosphere or F-region, exosphere or region above 500 km, geocorona, etc.) parameters measured (atomic oxygen and atomic hydrogen densities, electron density, neutral temperatures, etc.) or wavelengths used in measurements. An organization according to wavelengths seems the simplest and it is used in the following summary.

### 6.5.1 Celestial Lyman-Alpha Measurements (F-12)

In spite of its short operational life (June 6-18, 1969), experiment F-12 yielded important data that were used to produce a global survey of the 1216-Å emission across the whole sky. By fitting the observed absorption (produced by the hydrogen-cell resonance filter of experiment F-12) as a function of Doppler shift (due to satellite motion combined with the F-12 scanner direction), the spectral width of the emission line was obtained and the corresponding emission temperature was derived. These results constitute the first measurements by a

hydrogen-resonance filter technique of the spectral character of the Lyman-alpha emission over the complete celestial sphere. These measurements revealed: (1) a dawn-to-dusk difference of 200 deg K in the emission temperature, (2) a rather surprising antisolar "hot" region that appeared to be aligned with the Earth's magnetotail, and (3) a number of weak stellar sources in the UV continuum (Clark and Metzger, 1971; Metzger and Clark, 1972).

### 6.5.2 Exospheric 1216-Å Airglow (F-13)

The vertical intensity of the 1216-Å airglow was measured at altitudes ranging from 400 to 1100 km for the period June 1969 to June 1970 using data from experiment F-13 (Thomas and Anderson, 1976). From these measurements the atomic hydrogen density at the exobase, taken to be 500 km, was determined for 286 orbits throughout the 1-year period. The solar flux at 1216 Å, which was also derived from the data analysis, was found to vary linearly with the sunspot number. Both the magnitude and the variation of the hydrogen density at the exobase as a function of the exospheric temperature are in excellent agreement with the OGO 5 results of Vidal-Madjar et al (1974) obtained by a totally different technique. Since very complicated procedures have to be used to analyze the data from experiment F-13, the above agreement is an important (and very successful) test of the data analysis techniques used (see also comments preceding section 6.5.1).

### 6.5.3 Exospheric 1304-Å Airglow (F-13)

The vertical intensity of 1304-Å airglow was measured at altitudes ranging from 400 to 1100 km for the period September 15 - October 25, 1969, using data from experiment F-13. From these measurements Strickland and Thomas (1976) calculated the vertical atomic oxygen column density above the satellite altitude. Because of uncertainties in the various parameters involved in these calculations the airglow data were of limited value for determining oxygen densities. Relative density variations, however, could be determined reliably over short periods of time (such as two or three orbits). Thus, it could be shown that the exospheric atomic oxygen density decreased prior to the geomagnetic storm of late September 1969 and increased during the storm with the largest changes occurring at low latitudes. The calculation of oxygen density from the 1304-Å airglow data requires the use of very complicated analysis techniques. Although simpler *in situ* measuring techniques can be used in the terrestrial atmosphere, the development of airglow remote-sensing techniques is important for planetary flyby and orbiter missions.

### 6.5.4 Tropical F-Region 5577-Å Airglow (F-26)

The 5577-Å emission is excited in the nighttime F-region as a result of the formation of  $O_2^+$  ions in charge transfer reactions between  $O^+$  and  $O_2$  and the subsequent dissociative recombination of the molecular ions. The 5577-Å emission is therefore proportional to both the  $O_2$  and the  $O^+$  densities. Since the  $O_2$  density is known fairly well from neutral atmosphere models, a measurement of the F-region 5577-Å emission yields a measurement of the  $O^+$  density, which is essentially equal to the electron density. Since much of the emission is generated below the peak of the F2 region, the 5577-Å data is equivalent to a bottomside sounding of the ionosphere from a satellite. This technique can provide synoptic data about the bottomside of the ionosphere that are otherwise impractical to obtain. A successful test of the above concepts was conducted by comparing the satellite data with ground-based data from Huancayo, Peru. Thomas and Donahue (1972) applied the above analysis technique to the data from experiment F-26 and derived a number of synoptic electron density maps for the equatorial region. Because of significantly lesser nighttime densities at mid- and lower latitudes (and a corresponding much weaker 5577-Å emission in the F-region), the above technique could be applied only for the tropical regions.

### 6.5.5 E-Region 5577-A Airglow (F-26)

An intense 5577-A airglow layer is observed near 100 km at latitudes ranging from -60 to +60 deg. This E-region layer airglow is due to a mechanism that is quite different from that which produces the F-region airglow. The classical theory of the E-region 5577-A airglow is due to Chapman (1931) and it relates (in a somewhat complicated manner) the emission rate to the density of atomic oxygen. This relationship involves three reaction rate parameters, which unfortunately are not accurately known, and this leads to some uncertainty in the calculation of atomic oxygen density from the airglow data. Using 5577-A airglow data obtained with experiment F-26 during the period August 1969 to April 1970, Donahue et al (1973) derived the first comprehensive picture of the global distribution of atomic oxygen density in the E-region. The oxygen density was calculated assuming the Chapman mechanism and the results are subject to the above-mentioned uncertainties. The resulting maps of the atomic oxygen density near 97 km (Donahue et al, 1974) revealed a strong variation in latitude, longitude, universal time, and time of year. Donahue and Carignan (1975) showed that the variation of the oxygen density between 100 and 120 km was inconsistent with the temperature gradients assumed in the Jacchia 1971 model atmosphere and an eddy diffusion coefficient  $K$  that reaches its maximum value below 115 km. It was concluded that the temperature gradients had to be increased from the model values by factors of 2 to 5, depending upon possible revisions in the values of  $K$ .

### 6.5.6 E-Region 5890-A Airglow (F-26)

The 5890-A airglow results from the reaction of NO and O to form NO<sub>2</sub>. The 5890-A airglow intensity is therefore proportional to the product of NO and O densities. Donahue (1974) used the 5890-A airglow data from experiment F-26 to derive an upper limit for the product (NO)(O) and found that near 110 km, during the nights of 1969-1970, the product (NO)(O) was less by a factor of 5 than the product of observed NO densities and Jacchia 1971 O model densities.

### 6.5.7 Noctilucent Clouds in Polar Regions (F-26)

Simultaneous observations over the polar regions of an intense airglow at 5577 A and at 5890 A, originating from an altitude of about 85 km, led to the discovery of an extensive scattering layer present over the geographic poles during the local summer. It was concluded that this scattering layer was probably an extension poleward of noctilucent clouds (Donahue et al, 1972).

### 6.5.8 Global Temperature at 270 km from 6300-A Airglow (F-14)

Blamont et al (1974) used the data from experiment F-14 (Spectral Profile Measurements of the 6300-A Airglow Line) to conduct a global survey of the neutral temperature at 270 km. This work was based upon an averaging of data for the altitude region 240 to 300 km obtained under daytime conditions ranging from sunrise to sunset. It was found that the maximum temperature occurred close to the summer pole at the solstices, and that the changeover occurred within a period of about 20 days close to the equinoxes. The diurnal variation was the greatest near the equator. The annual variation was nearly sinusoidal with an amplitude of about 300 deg K.

Blamont and Luton (1972) investigated the geomagnetic effects on the neutral temperature at 270 km and found that changes in excess of 300 deg K occurred in the polar regions under disturbed magnetic conditions. The 270-km temperature data obtained from experiment F-14 also revealed systematic differences between the hemispheres at the time of equinox (Barlier et al, 1974). These differences have the same sign for spring and fall conditions, showing that the southern hemisphere is warmer than the northern hemisphere.

### 6.5.9 Exospheric Temperature Model (F-14)

At altitudes greater than about 500 km (exosphere) the atmospheric temperature is essentially independent of altitude. The exospheric temperature depends, however, upon the latitude, local time, day of the year (seasonal effects), solar flux, and magnetic activity. A model of the exospheric temperature, including the effects of the above parameters, was derived by Thuillier et al (1976) using the 6300-A airglow data from experiment F-14. The resulting model was found to agree fairly well with the model of Hedin et al (1974), which is based upon the N<sub>2</sub> density data from experiment F-04 on OGO 6, and the model of Salah et al (1974), which is based upon ion temperature data obtained with the Millstone Hill ionospheric radar.

## 6.6 Neutral Atmosphere Measurements

The OGO 6 mission included three experiments designed to measure the density and composition of the Earth's thermosphere.\* These were experiment F-01 (Microphone Atmospheric Density Gauge, Sharp), experiment F-04 (Neutral Atmospheric Composition, Reber), and experiment F-07 (Energy Transfer Probe for Atmospheric Density, McKeown). Experiment F-01 experienced in flight a significant loss in sensitivity that limited its usefulness to altitudes less than 440 km, i.e., near perigee. Experiment F-07 yielded no geophysical data because of severe contamination by outgassing from the OGO 6 solar cell panels. Experiment F-04, however, turned out to be one of the most successful experiments of the entire OGO program. It yielded 2 years of excellent data from which very significant new results were obtained. These results, according to Jacchia (1974), include "one of the most remarkable discoveries in upper atmosphere physics;" namely, "that all the known types of thermospheric variation are accompanied by large variations in composition that are not accounted for by static diffusion models, thus clearly indicating the presence of large-scale convection phenomena."

### 6.6.1 Results from Experiment F-01

#### 6.6.1.1 Geomagnetically Aligned Neutral Density Peaks (F-01)

Analysis of the data from experiment F-01 for the period July 12-15, 1969, revealed a persistent pair of density peaks present on seven successive orbits during July 13 and July 14 (both geomagnetically disturbed days). The density peaks were observed in the daytime at geomagnetic latitudes near 52 deg and 60 deg North, and at altitudes near 400 km. Since the density peaks occurred at latitudes and altitudes characteristic of red arcs, the experimental technique used might provide a red-arc monitoring technique that is not limited by daylight, moonlight, or clouds (Anderson and Sharp, 1972).

#### 6.6.1.2 Atmospheric Density Variation with Kp (F-01)

Longitudinal density profiles were measured with experiment F-01 during the period September 27-30, 1969, at 406 km and 1600 hr local time from about 0 to 40 deg North for Kp values ranging from 0 to 8. The results showed that the neutral density increased with Kp at all latitudes between 10 and 30 deg North. A least-squares fit to the density data versus the magnetic index Ap gave best results at low latitudes when the Ap values were for a time 3 hours earlier than the time corresponding to the density values (Anderson, 1973).

\*The term, thermosphere, refers to the neutral atmosphere in the altitude range from about 100 to about 500 km, i.e., immediately below the exosphere.

## OVERVIEW

### 6.6.2 Results from Experiment F-04

Analysis of the data from experiment F-04 on OGO 6 has led to about 20 papers in refereed scientific journals, including 16 papers in the *Journal of Geophysical Research*. From this work a new and more complex picture of the whole thermosphere has gradually evolved.

#### 6.6.2.1 Global Morphology of the Undisturbed Thermosphere (F-04)

Measurements of neutral  $N_2$ , O, and He densities with experiment F-04 over the south polar regions during magnetically quiet periods in late August and early September 1969 revealed some unexpected variations in thermospheric composition. The most surprising result was the presence near 70 deg invariant latitude of a maximum in the  $N_2$  density and a minimum in the He density, suggesting the existence of: (1) a high-latitude heat input, (2) a thermospheric wind system, and (3) a possible correlation with similar features observed in the polar ionosphere (Hedin and Reber, 1972). A subsequent study based upon the analysis of data covering a 2-year-period showed that  $N_2$  enhancements with similar amplitudes occurred in both north and south polar regions under quiet magnetic conditions (Reber and Hedin, 1974). Approximately 500 orbits of  $N_2$  data corresponding to  $K_p < 3$  were subsequently examined on an individual basis to ascertain the general characteristics of the quiet polar thermosphere. This study revealed two persistent but variable regions of enhanced  $N_2$  densities, one located around noon magnetic local time at about 80 deg invariant latitude and one located near midnight magnetic local time at about 70 deg invariant latitude (Tausch and Hinton, 1975).

#### 6.6.2.2 Global Morphology of the Disturbed Thermosphere (F-04)

Concurrently with the results described under section 6.6.2.1, a picture of the disturbed thermosphere was gradually emerging from the data of experiment F-04. An initial study of the effects of geomagnetic storms on the neutral atmospheric composition was carried out by Tausch et al (1971) using data for the period September 27 through October 3, 1969. This study showed that the major portion of the energy deposition occurred at high latitude, causing enhancements in  $N_2$  densities with temperature increases on the order of 400 to 500 deg K. These results suggested dynamic processes causing a thermospheric circulation that is upward at the poles and downward at the equator. A more comprehensive study of geomagnetic storm effects was made subsequently by Marubashi et al (1976), using both ion and neutral density data obtained with OGO 6 during the period August 25-28, 1969. The overall behavior of the neutral atmosphere was the same as observed in the earlier study. In addition, both ion and neutral density variations seemed to be closely correlated. A storm-time decrease in  $H^+$  density occurred in two distinct regions separated by the low-latitude boundary of the light-ion trough. It was concluded that the  $H^+$  decrease was caused principally by the decrease in H density for both regions. The  $O^+$  density showed an increase during the storm, the pattern of which was similar to that for O, suggesting that the change in  $O^+$  density might have been controlled by the change in O density.

The local time and invariant latitude dependence of the  $N_2$  enhancements during elevated magnetic activity was determined by Tausch (1977), using data from eight families of polar perigee passes during 1969 and 1970. The greatest  $N_2$  enhancements (increases by a factor of 3 to 4 over the quiet time densities) were observed in the 2250-0300 MLT sector extending from the pole down to at least 50 deg invariant latitude.

#### 6.6.2.3 Equatorial Phenomena in Thermospheric Composition (F-04)

Reber et al (1973) reported several interesting phenomena related to the equatorial thermosphere. The diurnal variation during equinox showed the  $N_2$  and O densities peaking near 1500 LMT, while the He density peaked near 1000 LMT. The latitudinal variation in  $N_2$  during the day was very similar to the F-region electron density variation exhibiting the features of the ionospheric anomaly (see section 4.2.4 of the Overview). During periods of intense geomagnetic disturbances the low-latitude thermospheric temperature increased by only 100 deg K compared to increases of more than 1000 deg K at midlatitudes.

#### 6.6.2.4 Global Thermospheric Models (F-04)

Tausch and Carignan (1972) compared the data obtained from experiment F-04 with that predicted by the Jacchia (1965, 1971) models. These models, based on satellite drag data, had been used extensively for comparison and prediction purposes. The comparison made by Tausch and Carignan showed good agreement in the mean values of the total density but revealed significant discrepancies in the O/ $N_2$  constituent ratio. The need for a new model of the thermosphere was therefore indicated.

Hedin et al (1974), using data from experiment F-04 for the period June 1969 to May 1971, derived an empirical model of the thermosphere for magnetically quiet conditions. The OGO 6 model also included the exospheric temperatures inferred from the  $N_2$  densities. The global characteristics of the thermosphere, which are revealed by the OGO 6 model, have been discussed by Mayr et al (1974). The special features of the OGO 6 model correspond basically to the morphology described under section 6.6.2.1.

The OGO 6 data were used by Jacchia (1974) to improve his earlier models and by Wydra (1975) to provide a model of exospheric temperatures that include both quiet and disturbed magnetic conditions.

The OGO 6 model, which was basically a sunspot maximum model, has recently been extended by Hedin et al (1977a, 1977b) using mass spectrometer data from OGO 6, San-Marco 3, AEROS-A, and AE-C obtained under conditions of declining and minimum solar activity. The extended model also used incoherent scatter data from four ground stations (Arecibo, Jicamarca, Millstone Hill, and St. Santin).

## REFERENCES

- Akasofu, S. I., "The Development of the Auroral Substorm," *Planet. Space Sci.*, 12, 4, 273-282, Apr. 1964.
- Akasofu, S. I., and A. L. Snyder, "Comments on the Growth Phase of Magnetospheric Substorms," *J. Geophys. Res.*, 77, 31, 6275-6277, Nov. 1972.
- Alvarez, H., and F. T. Haddock, "Evidence for Electron Excitation of Type III Radio Burst Emission," *Solar Phys.*, 26, 2, 468-473, Oct. 1972.
- Alvarez, H., and F. T. Haddock, "Solar Wind Density Model from km-Wave Type III Bursts," *Solar Phys.*, 29, 1, 197-209, Mar. 1973a.
- Alvarez, H., and F. T. Haddock, "Decay Time of Type III Solar Bursts Observed at Kilometric Wavelengths," *Solar Phys.*, 30, 1, 175-182, May 1973b.
- Alvarez, H., F. T. Haddock, and W. H. Potter, "Heliographic Longitude Distribution of the Flares Associated with Type III Bursts Observed at Kilometric Wavelengths," *Solar Phys.*, 31, 2, 493-500, Aug. 1973.
- Anderson, A. D., "The Relation Between Low-Latitude Neutral Density Variations Near 400 km and Magnetic Activity Indices," *Planet. Space Sci.*, 21, 12, 2049-2060, Dec. 1973.
- Anderson, A. D., and G. W. Sharp, "Neutral Density Measurements near 400 Kilometers by a Microphone Density Gage on OGO 6 during July 12-15, 1969," *J. Geophys. Res.*, 77, 10, 1878-1884, April 1972.
- Aubry, M. P., C. T. Russell, and M. G. Kivelson, "Inward Motion of the Magnetopause before a Substorm," *J. Geophys. Res.*, 75, 34, 7018-7031, Dec. 1970.
- Aubry, M. P., M. C. Kivelson, R. L. McPherron and C. T. Russell, "Outer Magnetosphere near Midnight at Quiet and Disturbed Times," *J. Geophys. Res.*, 77, 28, 5487-5502, Oct. 1972.
- Axford, W. I., and C. O. Hines, "A Unifying Theory of High-Latitude Geophysical Phenomena and Geomagnetic Storms," *Can. J. Phys.*, 39, 7, 1433-1464, July 1961.
- Bailey, G. J., R. J. Moffett, W. B. Hanson, and S. Sanatani, "Effects of Interhemisphere Transport on Plasma Temperatures at Low Latitudes," *J. Geophys. Res.*, 78, 25, 5597-5610, Sept. 1973.
- Baker, M. B., A. J. Masley, and P. R. Satterblom, "Simultaneous Satellite and Riometer Studies," in *Proc. of the 13th Int. Cosmic Ray Conf.*, 2, 1440-1445, Univ. of Denver, Denver, Co., 1974.
- Balasubrahmanyam, V. K., and A. T. Serlemitsos, "A Solar Energetic Particle Event with  ${}^3\text{He}/{}^4\text{He} > 1$ ," *Nature*, 252, 5483, 460-462, Dec. 1974.
- Barlier, F., P. Bauer, C. Jaeck, G. Thuillier, and G. Kockarts, "North-South Asymmetries in the Thermosphere During the Last Maximum of the Solar Cycle," *J. Geophys. Res.*, 79, 34, 5273-5285, Dec. 1974.
- Bertaud, Ch., "Observations de la comète Bennett" (in French), *L'Astronomie*, 84, 361-374, Sept. 1970.
- Bertaux, J. L., and J. E. Blamont, "OGO 5 Measurements of Lyman-Alpha Intensity Distribution and Linewidth up to 6 Earth Radii," *Space Res.*, 10, 591-601, 1970. (Proc. of the 12th COSPAR Plenary Meeting, Prague, Czech., May 11-14, 1969.)
- Bertaux, J. L., and J. E. Blamont, "Evidence for a Source of an Extraterrestrial Hydrogen Lyman-Alpha Emission - The Interstellar Wind," *Astron. and Astrophys.*, 11, 2, 200-217, Mar. 1971.
- Bertaux, J. L., and J. E. Blamont, "Interpretation of OGO 5 Lyman-Alpha Measurements in the Upper Geocorona," *J. Geophys. Res.*, 78, 1, 80-91, Jan. 1973.
- Bertaux, J. L., A. Ammar, and J. E. Blamont, "OGO 5 Determination of the Local Interstellar Wind Parameters," *Space Res.*, 12, 1559-1567, 1972. (Proc. of the 14th COSPAR Meeting, Seattle, Wa., June 21-July 2, 1971.)
- Binsack, J. H., "Plasmapause Observations with the M.I.T. Experiment on IMP 2," *J. Geophys. Res.*, 72, 21, 5231-5237, Nov. 1967.
- Blamont, J. E., and J. M. Luton, "Geomagnetic Effect on the Neutral Temperature of the F Region during the Magnetic Storm of September 1969," *J. Geophys. Res.*, 77, 19, 3534-3556, July 1972.
- Blamont, J. E., J. M. Luton, and J. S. Nisbet, "Global Temperature Distributions from OGO 6300 Å Airglow Measurements," *Radio Sci.*, 9, 2, 247-251, Feb. 1974.
- Brinton, H. C., "F-Region Meteoric Ions as Tracers of Ionospheric Dynamics," (abstract), *EOS*, 975, Dec. 1976.
- Brown, J. W., E. C. Stone, and R. E. Vogt, "Measurements of the Cosmic-Ray Be/B Ratio and the Age of Cosmic Rays," in *Proc. of the 13th Int. Cosmic Ray Conf.*, 1, 484-489, Univ. of Denver, Denver, Co., 1974a.
- Brown, J. W., E. C. Stone, and R. E. Vogt, "The Elemental Abundance Ratios of Interstellar Secondary and Primary Cosmic Rays," in *Proc. of the 13th Int. Cosmic Ray Conf.*, 1, 556-561, Univ. of Denver, Denver, Co., 1974b.

## REFERENCES

- Buck, R.M., H.I. West, Jr., and R. G. D'Arcy, Jr., "Satellite Studies of Magnetospheric Substorms on August 15, 1968, 7, OGO 5 Energetic Proton Observations - Spatial Boundaries," *J. Geophys. Res.*, 78, 16, 3103-3118, June 1973.
- Burger, J. J., and B. N. Swanenburg, "Long Term Solar Modulation of Cosmic Ray Electrons with Energies Above 0.5 GeV," in *Proc. of the 12th Int. Cosmic Ray Conf.*, MOD-4, 1858-1863, Hobart, Tasmania, 1971.
- Burger, J. J., and B. N. Swanenburg, "Energy Dependent Time Lag in the Long-Term Modulation of Cosmic Rays," *J. Geophys. Res.*, 78, 1, 292-305, Jan. 1973a.
- Burger, J. J., and B. N. Swanenburg, "Short Term Intensity Fluctuations of Cosmic-Ray Electrons Between 0.5 and 10 GeV," in *Proc. of the 13th Int. Cosmic Ray Conf.*, 5, 3117-3122, Univ. of Denver, Denver, Co., 1973b.
- Burton, R. K., "Critical Electron Pitch Angle Anisotropy Necessary for Chorus Generation," *J. Geophys. Res.*, 81, 25, 4779-4781, Sept. 1976.
- Burton, R. K., and R. E. Holzer, "The Origin and Propagation of Chorus in the Outer Magnetosphere," *J. Geophys. Res.*, 79, 7, 1014-1023, Mar. 1974.
- Cahill, L. J., and P. G. Amazeen, "The Boundary of the Geomagnetic Field," *J. Geophys. Res.*, 68, 7, 1835-1844, Apr. 1963.
- Cain, J. C., and W. M. Davis, "Low Latitude Variations of the Magnetic Field," in *Symposium on Low Level Satellite Surveys*, 67-83, ed. J. C. Cain, NASA-GSFC, Unnumbered, Greenbelt, Md., Sept. 1973.
- Carpenter, D. L. and C. R. Chappell, "Satellite Studies of Magnetospheric Substorms on August 15, 1968, 3, Some Features of Magnetospheric Convection," *J. Geophys. Res.*, 78, 16, 3062-3067, June 1973.
- Chan, K. W., and R. E. Holzer, "A Relation Between ELF Hiss Amplitude and Plasma Density in the Outer Plasmasphere," *J. Geophys. Res.*, 79, 13, 1989-1993, May 1974.
- Chan, K. W. and R. E. Holzer, "ELF Hiss Associated With Plasma Density Enhancements in the Outer Magnetosphere," *J. Geophys. Res.*, 81, 13, 2267-2274, May 1976.
- Chan, K. W., R. K. Burton, and R. E. Holzer, "Measurement of the Wave-Normal Vector of Proton Whistlers on OGO 6," *J. Geophys. Res.*, 77, 4, 635-639, Feb. 1972.
- Chapman, S., "Some Phenomena of the Upper Atmosphere," *Royal Soc. of London, Proceedings*, Ser. A, 132, 820, 353-374, Aug. 1931.
- Chapman, S., and V. C. A. Ferraro, "A new theory of magnetic storms - I. The initial phase," *Terrest. Magn. Atmospheric Elec.*, 36, 2, 77-97, June 1931; and *Terrest. Magn. Atmospheric Elec.*, 36, 3, 171-186, Sept. 1931.
- Chapman, S., and V. C. A. Ferraro, "A new theory of magnetic storms - I. The initial phase," *Terrest. Magn. Atmospheric Elec.*, 37, 147-156, 1932.
- Chapman, S., and V. C. A. Ferraro, "A new theory of magnetic storms - II. The main phase," *Terrest. Magn. Atmospheric Elec.*, 38, 79-96, 1933.
- Chapman, S., and V. C. A. Ferraro, "Theory of First Phase of Geomagnetic Storm," *Terrest. Magn. Atmospheric Elec.*, 45, 3, 245-268, Sept. 1940.
- Chappell, C. R., "Recent Satellite Measurements of the Morphology and Dynamics of the Plasmasphere," *Rev. of Geophys. and Space Phys.*, 10, 4, 951-979, Nov. 1972.
- Chappell, C. R., "Detached Plasma Regions in the Magnetosphere," *J. Geophys. Res.*, 79, 13, 1861-1870, May 1974.
- Chappell, C. R., K. K. Harris, and G. W. Sharp, "A Study of the Influence of Magnetic Activity on the Location of the Plasmopause as Measured by OGO 5," *J. Geophys. Res.*, 75, 1, 50-56, Jan. 1970a.
- Chappell, C. R., K. K. Harris, and G. W. Sharp, "The Morphology of the Bulge Region of the Plasmasphere," *J. Geophys. Res.*, 75, 19, 3848-3861, July 1970b.
- Chappell, C. R., K. K. Harris, and G. W. Sharp, "OGO 5 Measurements of the Plasmasphere during Observations of Stable Auroral Red Arcs," *J. Geophys. Res.*, 76, 10, 2357-2365, Apr. 1971a.
- Chappell, C. R., K. K. Harris, and G. W. Sharp, "The Dayside of the Plasmasphere," *J. Geophys. Res.*, 76, 31, 7632-7647, Nov. 1971b.
- Chappell, C. R., K. K. Harris, and G. W. Sharp, "Plasmasphere Dynamics Inferred from OGO 5 Observations," *Space Research*, 12, Pt. 2, 1513-1521, 1972 (Proc. of the 14th COSPAR Plenary Meeting, Seattle, Wa., June 21-July 2, 1971).
- Chen, L., and A. Hasegawa, "A Theory of Long-Period Magnetic Pulsations, I, Steady State Excitation of Field Line Resonance," *J. Geophys. Res.*, 79, 7, 1024-1032, Mar. 1974.
- Chen, A. J., J. M. Grebowsky, and K. Marubashi, "Diurnal Variation of Thermal Plasma in the Plasmasphere," *Planet. Space Sci.*, 24, 8, 765-769, Aug. 1976.

## REFERENCES

- Childers, D. D., and C. T. Russell, "Power Spectra of the Interplanetary Magnetic Field Near the Earth," in *Solar Wind*, NASA SP-308, 375-381, Wash. D. C., 1972.
- Clark, M. A., and P. H. Metzger, "Observation of Early-Type Stars from OGO 6," *Astron. and Astrophys.*, 10, 1, 155-158, Jan. 1971.
- Cline, T. L., and G. Porreca, "Cosmic Ray Electrons and Positrons of Energies 2 to 9.5 MeV Observed in Interplanetary Space," *Acta Phys.*, 29, Suppl. 1, 145-149, 1970. (Proc. of the 11th Int. Conf. on Cosmic Rays, Budapest, Hungary, Aug. 25-Sept. 4, 1969.)
- Colburn, D. S., and C. P. Sonett, "Discontinuities in the Solar Wind," *Space Sci. Rev.*, 5, 439-506, June 1966.
- Datlowe, D., "Relativistic Electrons in Solar Particle Events," *Solar Physics*, 17, 2, 436-458, Apr. 1971.
- Datlowe, D., J. L'Heureux, and P. Meyer, "Electrons from Solar Flares in the 10 to 200 MeV Region," *Acta Phys.*, 29, Suppl. 2, 643-648, 1970. (Proc. of the 11th Int. Conf. on Cosmic Rays, Vol. 2, Budapest, Hungary, Aug. 25-Sept. 4, 1969.)
- Donahue, T. M., "An Upper Limit to the Product of NO and O Densities from 105 to 120 km," *J. Geophys. Res.*, 79, 28, 4337-4339, Oct. 1974.
- Donahue, T. M., and G. R. Carignan, "The Temperature Gradient Between 100 and 120 km," *J. Geophys. Res.*, 80, 34, 4565-4569, Dec. 1975.
- Donahue, T. M., B. Guenther, and J. E. Blamont, "Noctilucent Clouds in the Daytime: Circumpolar Particulate Layers near the Summer Mesopause," *J. of the Atmos. Sci.*, 29, 6, 1205-1209, Sept. 1972.
- Donahue, T. M., B. Guenther, and R. J. Thomas, "Distribution of Atomic Oxygen in the Upper Atmosphere Deduced from OGO 6 Airglow Observations," *J. Geophys. Res.*, 78, 28, 6662-6689, Oct. 1973.
- Donahue, T. M., B. Guenther, and R. J. Thomas, "Spatial and Temporal Behavior of Atomic Oxygen Determined by OGO 6 Airglow Observations," *J. Geophys. Res.*, 79, 13, 1959-1964, May 1974.
- Dryer, M., Z. K. Smith, T. Unti, J. D. Mihalov, B. F. Smith, J. H. Wolfe, D. S. Colburn, and C. P. Sonett, "Pioneer 9 and OGO 5 Observations of an Interplanetary Multiple Shock Ensemble on February 2, 1969," *J. Geophys. Res.*, 80, 22, 3225-3234, Aug. 1975.
- Dyson, P. L., J. P. McClure, and W. B. Hanson, "In Situ Measurements of the Spectral Characteristics of F Region Ionospheric Irregularities," *J. Geophys. Res.*, 79, 10, 1497-1502, Apr. 1974.
- Eather, R. H., "The Auroral Oval - A Reevaluation," *Rev. of Geophys. and Space Phys.*, 11, 1, 157-167, Feb. 1973.
- Etcheto, J., R. Gendrin, J. Solomon, and A. Roux, "A Self-Consistent Theory of Magnetospheric ELF Hiss," *J. Geophys. Res.*, 78, 34, 8150-8166, Dec. 1973.
- Fan, C. Y., J. L'Heureux, and P. Meyer, "Primary Cosmic-Ray Electron Energy Spectrum from 10 to 200 MeV Observed in Interplanetary Space," *Phys. Rev. Letters*, 23, 877-880, Oct. 1969.
- Feldman, W. C., J. R. Asbridge, and S. J. Bame, "The Solar Wind He<sup>2+</sup> to H<sup>+</sup> Temperature Ratio," *J. Geophys. Res.*, 79, 16, 2319-2323, June 1974.
- Formisano, V., "The Earth's Bow Shock Fine Structure" in *Correlated Interplanet. and Magnetospheric Obs.*, 187-223, ed. D. E. Page, D. Reidel Pub. Co., Dordrecht, Holland, 1974.
- Formisano, V., C. T. Russell, J. D. Means, E. W. Greenstadt, F. L. Scarf, and M. Neugebauer, "Collisionless Shock Waves in Space: A Very High Beta Structure," *J. Geophys. Res.*, 80, 16, 2013-2022, June 1975.
- Fredricks, R. W., "Wave-Particle Interactions and their Relevance to Sub-Storms," *Space Sci. Rev.*, 17, 2, 449-480, Mar. 1975.
- Fredricks, R. W., and P. J. Coleman, Jr., "Observations of the Microstructure of the Earth's Bow Shock" in *Plasma Instabilities in Astrophysics*, 199-228, Gordon and Breach, New York, NY, 1969.
- Fredricks, R. W., and F. L. Scarf, "Recent Studies of Magnetospheric Electric Field Emissions above the Electron Gyrofrequency," *J. Geophys. Res.*, 78, 1, 310-314, Jan. 1973.
- Fredricks, R. W., C. F. Kennel, F. L. Scarf, G. M. Crook, and I. M. Green, "Detection of Electric-field Turbulence in the Earth's Bow Shock," *Phys. Rev. Lett.*, 21, 24, 1761-1764, Dec. 1968.
- Fredricks, R. W., F. V. Coronoti, C. F. Kennel, and F. L. Scarf, "Fast Time-resolved Spectra of Electrostatic Turbulence in the Earth's Bow Shock," *Phys. Rev. Lett.*, 24, 18, 994-998, May 1970a.
- Fredricks, R. W., G. M. Crook, C. F. Kennel, I. M. Green, F. L. Scarf, P. J. Coleman, and C. T. Russell, "OGO 5 Observations of Electrostatic Turbulence in Bow Shock Magnetic Structures," *J. Geophys. Res.*, 75, 19, 3751-3768, July 1970b.

## REFERENCES

- Fredricks, R. W., F. L. Scarf, and L. A. Frank, "Nonthermal Electrons and High-Frequency Waves in the Upstream Solar Wind - 2, Analysis and Interpretation," *J. Geophys. Res.*, **76**, 28, 6691-6699, Oct. 1971.
- Fredricks, R. W., F. L. Scarf, C. T. Russell, and M. Neugebauer, "Detection of Solar-Wind Electron Plasma Frequency Fluctuations in an Oblique Nonlinear Magnetohydrodynamic Wave," *J. Geophys. Res.*, **77**, 19, 3598-3601, July 1972.
- Fredricks, R. W., F. L. Scarf, and C. T. Russell, "Field-Aligned Currents, Plasma Waves, and Anomalous Resistivity in the Disturbed Polar Cusp," *J. Geophys. Res.*, **78**, 13, 2133-2141, May 1973.
- Freeman, R. M. "Langmuir Probe Studies of Low-energy Magnetospheric Plasma," Univ. of London, Ph.D. Thesis, 1973.
- Garrard, T. L., E. C. Stone, and R. E. Vogt, "The Isotopes of H and He in Solar Cosmic Rays," in *High Energy Phenomena*, NASA SP-342, 341-354, Wash. D.C., 1973.
- Grebowsky, J. M., A. J. Chen, and H. A. Taylor, Jr., "High-Latitude Troughs and the Polar Cap Boundary," *J. Geophys. Res.*, **81**, 4, 690-694, Feb. 1976.
- Greenstadt, E. W., P. C. Hedgecock, and C. T. Russell, "Large-Scale Coherence and High Velocities of the Earth's Bow Shock on February 12, 1969," *J. Geophys. Res.*, **77**, 7, 1116-1122, Mar. 1972.
- Greenstadt, E. W., C. T. Russell, F. L. Scarf, V. Formisano, and M. Neugebauer, "Structure of the Quasi-Perpendicular Laminar Bow Shock," *J. Geophys. Res.*, **80**, 4, 502-514, Feb. 1975.
- Greenstadt, E. W., C. T. Russell, V. Formisano, P. C. Hedgecock, F. L. Scarf, M. Neugebauer, and R. E. Holzer, "Structure of a Quasi-Parallel, Quasi-Laminar Bow Shock," *J. Geophys. Res.*, **82**, 4, 651-666, Feb. 1977.
- Haddock, F. T., and H. Alvarez, "The Prevalence of Second Harmonic Radiation in Type III Bursts Observed in Kilometric Wavelengths," *Solar Phys.*, **29**, 1, 183-196, Mar. 1973.
- Hanson, W. B., and S. Sanatani, "Meteoric Ions above the F<sub>2</sub> Peak," *J. Geophys. Res.*, **75**, 28, 5503-5509, Oct. 1970.
- Hanson, W. B., and S. Sanatani, "Relationship between Fe<sup>+</sup> Ions and Equatorial Spread F," *J. Geophys. Res.*, **76**, 31, 7761-7768, Nov. 1971.
- Hanson, W. B., and S. Sanatani, "Large N<sub>i</sub> Gradients below the Equatorial F Peak," *J. Geophys. Res.*, **78**, 7, 1167-1173, Mar. 1973.
- Hanson, W. B., D. L. Sterling, and R. F. Woodman, "Source and Identification of Heavy Ions in the Equatorial F Layer," *J. Geophys. Res.*, **77**, 28, 5530-5541, Oct. 1972.
- Hanson, W. B., A. F. Nagy, and R. J. Moffett, "OGO 6 Measurements of Supercooled Plasma in the Equatorial Exosphere," *J. Geophys. Res.*, **78**, 4, 751-756, Feb. 1973a.
- Hanson, W. B., J. P. McClure, and D. L. Sterling, "On the Cause of Equatorial Spread F," *J. Geophys. Res.*, **78**, 13, 2353-2356, May 1973b.
- Harris, K. K., "The Measurement of Cold Ion Densities in the Plasma Trough," *J. Geophys. Res.*, **79**, 31, 4654-4660, Nov. 1974.
- Harris, K. K., G. W. Sharp, and C. R. Chappell, "Observations of the Plasmopause from OGO 5," *J. Geophys. Res.*, **75**, 1, 219-224, Jan. 1970.
- Hedin, A. E., and C. A. Reber, "Longitudinal Variations of Thermospheric Composition Indicating Magnetic Control of Polar Heat Input," *J. Geophys. Res.*, **77**, 16, 2871-2879, June 1972.
- Hedin, A. E., H. G. Mayr, C. A. Reber, N. W. Spencer, and G. R. Carignan, "Empirical Model of Global Thermospheric Temperature and Composition Based on Data From the OGO 6 Quadrupole Mass Spectrometer," *J. Geophys. Res.*, **79**, 1, 215-225, Jan. 1974.
- Hedin, A. E., J. E. Salah, J. V. Evans, C. A. Reber, G. P. Newton, N. W. Spencer, D. C. Kayser, D. Alcaide, P. Bauer, and J. P. McClure, "A Global Thermospheric Model Based on Mass Spectrometer and Incoherent Scatter Data: MSIS Part 1 - N<sub>2</sub> Density and Temperature," *J. Geophys. Res.*, **82**, 16, 2139-2147, June 1977a.
- Hedin, A. E., C. A. Reber, G. P. Newton, N. W. Spencer, H. C. Brinton, H. G. Mayr, and W. E. Potter, "A Global Thermospheric Model Based on Mass Spectrometer and Incoherent Scatter Data: MSIS Part 2 - Composition," *J. Geophys. Res.*, **82**, 16, 2148-2156, June 1977b.
- Helliwell, R. A., R. L. Smith and J. J. Angerami, "Measurements of VLF Polarization and Wave Normal Direction on OGO F," Final Rept., Stanford Univ., Radioscience Lab., Unnumbered, Stanford, Ca., 1973.
- Hepner, J. P., "Electric Fields in the Magnetosphere," in *Critical Problems of Magnetospheric Physics*, 107-122, ed. E. R. Dyer, IUCSTP, Wash., D. C., Nov. 1972a (Proc. of COSPAR/IAGA/URSI Symp., Madrid, Spain, 11-13 May 1972).
- Hepner, J. P., "Polar-Cap Electric Field Distributions Related to the Interplanetary Magnetic Field Direction," *J. Geophys. Res.*, **77**, 25, 4877-4887, Sept. 1972b.



## REFERENCES

- Heppner, J. P., "High Latitude Electric Fields and the Modulations Related to Interplanetary Magnetic Field Parameters," *Radio Sci.*, 8, 11, 933-948, Nov. 1973.
- Heppner, J. P., Private Communication, 1975.
- Heppner, J. P., "Empirical Models of High-Latitude Electric Fields," *J. Geophys. Res.*, 82, 7, 1115-1125, Mar. 1977.
- Heppner, J. P., B. G. Ledley, T. L. Skillman, and M. Sugiura, "A Preliminary Survey of the Distribution of Micropulsations in the Magnetosphere from OGO's 3 and 5," *Ann. de Geophys.*, 26, 709-717, July-Sept. 1970.
- Holtet, J. A., N. C. Maynard, and J. P. Heppner, "Variational Electric Fields at Low Latitudes and their Relation to Spread F and Plasma Irregularities," to be published in *J. Atmos. Terr. Phys.*, 1977.
- Holzer, R. E., T. A. Farley, R. K. Burton, and M. C. Chapman, "A Correlated Study of ELF Waves and Electron Precipitation on OGO 6," *J. Geophys. Res.*, 79, 7, 1007-1013, Mar. 1974.
- Hughes, W. J., R. L. McPherron, and C. T. Russell, "Multiple Satellite Observations of Pulsation Resonance Structure in the Magnetosphere," *J. Geophys. Res.*, 82, 4, 492-498, Feb. 1977.
- Hutchinson, G. W., A. J. Pearce, D. Ramsden, and R. D. Wills, "Spark-Chamber Observation of Galactic Gamma Radiation," in *Non-Solar X- and Gamma-Ray Astronomy*, 300-305, ed. L. Gratton, Springer-Verlag, New York, N.Y., 1970. (Proc. of Symp. No. 37 of the Int. Astron. Union, Rome, Italy, May 8-10, 1969.)
- Ifedili, S. O., "A Search for Solar Neutrons During Solar Flares," *Solar Phys.*, 39, 1, 233-241, Nov. 1974.
- Intriligator, D. S., and M. Neugebauer, "A Search for Solar Wind Velocity Changes Between 0.7 and 1 AU," *J. Geophys. Res.*, 80, 10, 1332-1334, Apr. 1975.
- Jacchia, L. G., "Static Diffusion Models of the Upper Atmosphere with Empirical Temperature Profiles," *Smithson. Contrib. Astrophys.*, 8, 9, 215-257, 1965.
- Jacchia, L. G., "Revised Static Models of the Thermosphere and Exosphere with Empirical Temperature Profiles," *Smithson. Astrophys. Observatory, Special Rept. 332*, Cambridge, Ma., May 1971.
- Jacchia, L. G., "Variations in Thermospheric Composition: A Model Based on Mass Spectrometer and Satellite Drag Data," *J. Geophys. Res.*, 79, 13, 1923-1927, May 1974.
- Jackson, J. E., and J. I. Vette, "OGO Program Summary," NASA SP-7601, Washington, D.C., 1975.
- Jenkins, R. W., J. A. Lockwood, S. O. Ifedili, and E. L. Chupp, "Latitude and Altitude Dependence of the Cosmic Ray Albedo Neutron Flux," *J. Geophys. Res.*, 75, 22, 4197-4204, Aug. 1970.
- Jenkins, R. W., S. O. Ifedili, J. A. Lockwood, and H. Razdan, "The Energy Dependence of the Cosmic-Ray Neutron Leakage Flux in the Range 0.01-10 MeV," *J. Geophys. Res.*, 76, 31, 7470-7478, Nov. 1971.
- Kahler, S. W., "The Role of Energetic Electrons in the Correlation of Meter and Decimeter Type III Bursts with 4 KeV X-Ray Emission," *Solar Physics*, 25, 2, 435-451, Aug. 1972.
- Kahler, S. W., "Possible Low Energy ( $E < 10$  keV) Nonthermal X-Ray Events," in *High Energy Phenomena*, NASA SP-342, 124-131, Wash. D.C., May 1973.
- Kahler, S. W., and R. W. Kreplin, "Thermal Runaway as the Solar Flare Trigger Mechanism," *Solar Phys.*, 14, 2, 372-383, Oct. 1970.
- Kahler, S. W., and R. W. Kreplin, "The Observations of Nonthermal Solar X-Radiation in the Energy Range  $3 < E < 10$  KeV," *Astrophys. J.*, 168, 2, 531-541, Sept. 1971.
- Kahler, S. W., J. F. Meekins, R. W. Kreplin, and C. S. Bowyer, "Temperature and Emission Measure Profiles of Two Solar X-Ray Flares," *Astrophys. J.*, 162, 1, 293-304, Oct. 1970.
- Kane, S. R., "Observations of Two Components in Energetic Solar X-Ray Bursts," *Astrophys. J.*, 157, 2, L139-L142, Aug. 1969.
- Kane, S. R., "An Upper Limit on the Hardness of the Nonthermal Electron Spectra Produced During the Flash Phase of Solar Flares," *Astrophys. J.*, 170, 2, 587-591, Dec. 1971.
- Kane, S. R., "Evidence for a Common Origin of the Electrons Responsible for the Impulsive X-Ray and Type III Radio Bursts," *Solar Phys.*, 27, 1, 174-181, Nov. 1972.
- Kane, S. R., and R. F. Donnelly, "Impulsive Hard X-Ray and Ultraviolet Emission During Solar Flares," *Astrophys. J.*, 164, 1, 151-163, Feb. 1971.
- Keller, H. U., and G. E. Thomas, "Determination of Solar Lyman-Alpha Flux Independent of Calibration by Ultraviolet Observations of Comet Bennett," *Astrophys. J.*, 186, 2, L87-L90, Dec. 1973.
- Kelley, M. C., B. T. Tsurutani, and F. S. Mozer, "Properties of ELF Electromagnetic Waves in and Above the Earth's Ionosphere Deduced From Plasma Wave Experiments on the OV1-17 and OGO 6 Satellites," *J. Geophys. Res.*, 80, 34, 4603-4611, Dec. 1975.

## REFERENCES

- Kennel, C. F. and H. E. Petschek, "Limit on Stably Trapped Particle Fluxes," *J. Geophys. Res.*, 71, 1, 1-28, Jan. 1966.
- Kennel, C. F., R. W. Fredricks, and F. L. Scarf, "High Frequency Electrostatic Waves in the Magnetosphere," in *Particles and Fields in the Magnetosphere*, 257-265, ed. B. M. McCormac, D. Reidel Pub. Co. Dordrecht, Holland, 1970.
- King, J. H., "Coordinate Systems" in *National Space Science Data Center Handbook of Correlative Data*, 170-175, ed. J. H. King, NSSDC 71-05, Greenbelt, Md., Feb. 1971.
- Kivelson, M. G., T. A. Farley, and M. P. Aubry, "Satellite Studies of Magnetospheric Substorms on August 15, 1968, 5, Energetic Electrons, Spatial Boundaries, and Wave-Particle Interactions at OGO 5," *J. Geophys. Res.*, 78, 16, 3079-3092, June 1973.
- Klebesadel, R. W., I. B. Strong, and R. A. Olson, "Observations of Gamma Ray Bursts of Cosmic Origin," *Astrophys. J.*, 182, 2, L85-L88, June 1973.
- Kokubun, S., R. L. McPherron, and C. T. Russell, "OGO 5 Observations of Pc 5 Waves: Ground-Magnetosphere Correlations," *J. Geophys. Res.*, 81, 28, 5141-5149, Oct. 1976.
- Laaspere, T., and W. C. Johnson, "Additional Results from an OGO 6 Experiment concerning Ionospheric Electric and Electromagnetic Fields in the Range 20 Hz to 540 kHz," *J. Geophys. Res.*, 78, 16, 2926-2944, June 1973.
- Laaspere, T., and L. C. Semprebon, "The Global Distribution of Natural and Man-Made Ionospheric Electric Fields at 200 kHz and 540 kHz as Observed by OGO 6," *J. Geophys. Res.*, 79, 16, 2393-2401, June 1974.
- Laaspere, T., W. C. Johnson, and L. C. Semprebon, "Observations of Auroral Hiss, LHR Noise, and Other Phenomena in the Frequency Range 20 Hz-540 kHz on OGO 6," *J. Geophys. Res.*, 76, 19, 4477-4493, July 1971.
- Langel, R. A., "Near-Earth Magnetic Disturbance in Total Field at High Latitudes, 1, Summary of Data from OGO 2, 4, and 6," *J. Geophys. Res.*, 79, 16, 2363-2371, June 1974a.
- Langel, R. A., "Near-Earth Magnetic Disturbance in Total Field at High Latitudes, 2, Interpretation of Data From OGO 2, 4, and 6," *J. Geophys. Res.*, 79, 16, 2373-2392, June 1974b.
- Langel, R. A., "Variation with Interplanetary Sector of the Total Magnetic Field Measured at the OGO 2, 4 and 6 Satellites," *Planet. Space Sci.*, 22, 10, 1413-1425, Oct. 1974c.
- Langel, R. A., "Relation of Variations in Total Magnetic Field at High Latitude With the Parameters of the Interplanetary Magnetic Field and With DP 2 Fluctuations," *J. Geophys. Res.*, 80, 10, 1261-1270, Apr. 1975.
- Ledley, B. G., "Magnetopause Attitudes during OGO 5 Crossings," *J. Geophys. Res.*, 76, 28, 6736-6742, Oct. 1971.
- L'Heureux, J., "Cosmic Gamma-Ray burst Detected with an Instrument on Board the OGO 5 Satellite," *Astrophys. J.*, 187, 2, L53-L56, Jan. 1974.
- L'Heureux, J., and P. Meyer, "On the Quiet Time Increases of Low Energy Cosmic Ray Electrons," in *Proc. of the 14th Int. Cosmic Ray Conf.*, 2, 748-751, Max-Planck-Institut für Extraterr. Phys., Munich, Germany, 1975a.
- L'Heureux, J., and P. Meyer, "Modulation of Low Energy Electrons and Protons Near Solar Maximum," in *Proc. of the 14th Int. Cosmic Ray Conf.*, 3, 979-984, Max-Planck-Institut für Extraterr. Phys., Munich, Germany, 1975b.
- L'Heureux, J., C. Y. Fan, and P. Meyer, "The Quiet Time Spectra of Cosmic-Ray Electrons of Energies Between 10 and 200 MeV Observed on OGO-5," *Astrophys. J.*, 171, 2, 363-376, Jan. 1972.
- Lingenfelter, R. E., "The Cosmic-Ray Neutron Leakage Flux," *J. Geophys. Res.*, 68, 20, 5633-5639, Oct. 1963.
- Lingenfelter, R. E., and E. J. Flamm, "Neutron Leakage Flux from Interactions of Solar Protons in the Atmosphere," *J. Geophys. Res.*, 69, 11, 2199-2207, June 1964.
- Lockwood, J. A., S. O. Ifedili, and R. W. Jenkins, "Measurements of the Atmospheric Neutron Leakage Rate," *J. Geophys. Res.*, 78, 34, 7978-7985, Dec. 1973.
- Lyons, L. R., R. M. Thorne, and C. F. Kennel, "Pitch-Angle Diffusion of Radiation Belt Electrons within the Plasmasphere," *J. Geophys. Res.*, 77, 19, 3455-3474, July 1972.
- Maizawa, K., "Dependence of the Magnetopause Position on the Southward Interplanetary Magnetic Field," *Planet. Space Sci.*, 22, 10, 1443-1453, Oct. 1974.
- Marubashi, K., C. A. Reber, and H. A. Taylor, Jr., "Geomagnetic Storm Effects on the Thermosphere and the Ionosphere Revealed by in situ Measurements from OGO 6," *Planet. Space Sci.*, 24, 11, 1031-1041, Nov. 1976.
- Masley, A. J., and P. R. Satterblom, "Determination of First Open Field Line Location and Particle Access," *EOS*, 52, 11, 892, Nov. 1971.
- Maynard, N. C., "Electric Field Measurements Across the Harang Discontinuity," *J. Geophys. Res.*, 79, 31, 4620-4631, Nov. 1974.
- Mayr, H. G., A. E. Hedin, C. A. Reber, and C. R. Carignan, "Global Characteristics in the Diurnal Variations of the Thermospheric Temperature and Composition," *J. Geophys. Res.*, 79, 4, 619-628, Feb. 1974.

## REFERENCES

- McClure, J. P., and W. B. Hanson, "A Catalog of Ionospheric F Region Irregularity Behavior Based on OGO 6 Retarding Potential Analyzer Data," *J. Geophys. Res.*, **78**, 31, 7431-7440, Nov. 1973.
- McClure, J. P., W. B. Hanson, A. F. Nagy, R. J. Cicerone, L. H. Brace, M. Baron, P. Bauer, H. C. Carlson, J. V. Evans, G. N. Taylor, and R. F. Woodman, "Comparison of  $T_e$  and  $T_i$  from OGO 6 and from Various Incoherent Scatter Radars," *J. Geophys. Res.*, **78**, 1, 197-205, Jan. 1973.
- McPherron, R. L., "Relation of Auroral Zone Micropulsations to Magnetospheric Substorms," Univ. of Calif., Ph.D. Thesis, Berkeley, Ca., 1968.
- McPherron, R. L., and P. J. Coleman, Jr., "Satellite Observations of Band-Limited Micropulsations during a Magnetospheric Substorm," *J. Geophys. Res.*, **76**, 13, 3010-3021, May 1971.
- McPherron, R. L., M. P. Aubry, C. T. Russell, and P. J. Coleman, Jr., "Satellite Studies of Magnetospheric Substorms on August 15, 1968, 4, OGO 5 Magnetic Field Observations," *J. Geophys. Res.*, **78**, 16, 3068-3078, June 1973a.
- McPherron, R. L., C. T. Russell, and M. P. Aubry, "Satellite Studies of Magnetospheric Substorms on August 15, 1968, 9, Phenomenological Model for Substorms," *J. Geophys. Res.*, **78**, 16, 3131-3149, June 1973b.
- Metzger, P. H., and M. A. Clark, "Spectral Variations of the Lyman-Alpha Sky: A Final Report of Observations from OGO 6," Aerospace Corp., Rept. No. TR-0172(2260-10)-4, El Segundo, Ca., Mar. 1972.
- Mogro-Campero, A., "Geomagnetically Trapped Carbon, Nitrogen, and Oxygen Nuclei," *J. Geophys. Res.*, **77**, 16, 2799-2818, June 1972.
- Mogro-Campero, A., and J. A. Simpson, "Identification and Relative Abundances of C, N and O Nuclei Trapped in the Geomagnetic Field," *Physical Rev. Lett.*, **25**, 23, 1631-1635, Dec. 7, 1970.
- Mogro-Campero, A., and J. A. Simpson, "Enrichment of Very Heavy Nuclei in the Composition of Solar Accelerated Particles," *Astrophys. J.*, **171**, 1, L5-L9, Jan. 1972a.
- Mogro-Campero, A., and J. A. Simpson, "The Abundances of Solar Accelerated Nuclei from Carbon to Iron," *Astrophys. J.*, **177**, 1, L37-L41, Oct. 1972b.
- Mogro-Campero, A., and J. A. Simpson, "Origin and Composition of Heavy Nuclei Between 10 and 60 MeV per Nucleon During Interplanetary Quiet Times in 1968-1972," *Astrophys. J.*, **200**, 3, 773-786, Sept. 1975.
- Nagy, A. F., W. B. Hanson, R. J. Hoch, and T. L. Aggson, "Satellite and Ground-Based Observations of a Red Arc," *J. Geophys. Res.*, **77**, 19, 3613-3617, July 1972.
- Nagy, A. F., L. H. Brace, N. C. Maynard, and W. B. Hanson, "Is the Red Arc a Good Indicator of Ionosphere-Magnetosphere Conditions?," *J. Geophys. Res.*, **79**, 28, 4331-4333, Oct. 1974.
- Neugebauer, M., "Initial Deceleration of Solar Wind Positive Ions in the Earth's Bow Shock," *J. Geophys. Res.*, **75**, 4, 717-733, Feb. 1970.
- Neugebauer, M., "The Enhancement of Solar Wind Fluctuations at the Proton Thermal Gyroradius," *J. Geophys. Res.*, **80**, 7, 998-1002, Mar. 1975.
- Neugebauer, M., "The Role of Coulomb Collisions in Limiting Differential Flow and Temperature Differences in the Solar Wind," *J. Geophys. Res.*, **81**, 1, 78-82, Jan. 1976.
- Neugebauer, M., C. T. Russell, and J. V. Olson, "Correlated Observations of Electrons and Magnetic Fields at the Earth's Bow Shock," *J. Geophys. Res.*, **76**, 19, 4366-4380, July 1971.
- Neugebauer, M., C. T. Russell, and E. J. Smith, "Observations of the Internal Structure of the Magnetopause," *J. Geophys. Res.*, **79**, 4, 499-510, Feb. 1974.
- Newkirk, L. L., "Calculation of Low-Energy Neutron Flux in the Atmosphere by the  $S_n$  Method," *J. Geophys. Res.*, **68**, 7, 1825-1833, Apr. 1963.
- Nielsen, E., and M. A. Pomerantz, "Access of Solar Electrons to the Polar Regions," *Planet. Space Sci.*, **23**, 6, 945-954, June 1975.
- Nielsen, E., M. A. Pomerantz, and H. I. West, Jr., "Angular Distributions of Solar Protons and Electrons," *Planet. Space Sci.*, **23**, 8, 1179-1194, Aug. 1975.
- O'Dell, F. W., M. M. Shapiro, R. Silverberg, and C. H. Tsao, "New Observations and Calculations of Primary Be/B in the Cosmic Rays," in *Proc. of the 12th Int. Cosmic Ray Conf.*, **1**, 197, Hobart, Tasmania, Australia, 1971.
- Ogilvie, K. W., J. D. Scudder, and M. Sugiura, "Magnetic Field and Electron Observations near the Dawn Magnetopause," *J. Geophys. Res.*, **76**, 16, 3574-3586, June 1971a.
- Ogilvie, K. W., J. D. Scudder, and M. Sugiura, "Electron Energy Flux in the Solar Wind," *J. Geophys. Res.*, **76**, 34, 8165-8173, Dec. 1971b.
- Ossakow, S. L., and G. W. Sharp, "Proton Scattering in the Region near the Earth's Bow Shock," *J. Geophys. Res.*, **78**, 4, 607-616, Feb. 1973.

## REFERENCES

- Ossakow, S. L., G. W. Sharp, and K. K. Harris, "Spectrometer Observations in the Region near the Bow Shock on March 12, 1968," *J. Geophys. Res.*, **75**, 31, 6024-6036, Nov. 1970.
- Reber, C. A., and A. E. Hedin, "Heating of the High-Latitude Thermosphere During Magnetically Quiet Periods," *J. Geophys. Res.*, **79**, 16, 2457-2461, June 1974.
- Reber, C. A., A. E. Hedin, and S. Chandra, "Equatorial Phenomena in Neutral Thermospheric Composition," *J. Atmos. and Terr. Phys.*, **35**, 6, 1223-1228, June 1973.
- Regan, R. D., J. C. Cain, and W. M. Davis, "A Global Magnetic Anomaly Map," in *Symposium on Low Level Satellite Surveys*, 95-120, ed. J. C. Cain, NASA-GSFC, Unnumbered, Greenbelt, Md., Sept. 1973.
- Rosenberg, R. L., and P. J. Coleman, Jr., "Heliographic Latitude Dependence of the Dominant Polarity of the Interplanetary Magnetic Field," *J. Geophys. Res.*, **74**, 24, 5611-5622, Nov. 1969.
- Rostoker, G., "Polar Magnetic Substorms," *Rev. of Geophys. and Space Phys.*, **10**, 1, 157-211, Feb. 1972.
- Russell, C. T., "Noise in the Geomagnetic Tail," *Planet. Space Sci.*, **20**, 9, 1541-1553, Sept. 1972a.
- Russell, C. T., "Magnetic and Electric Waves in Space," in *Earth's Magnetospheric Processes*, 39-50, ed. B. M. McCormac, D. Reidel Pub. Co., Dordrecht, Holland, 1972b.
- Russell, C. T., "Magnetospheric Physics: Magnetic Fields," *Rev. of Geophys. and Space Phys.*, **13**, 3, 952-955, July 1975.
- Russell, C. T., and R. L. McPherron, "The Magnetotail and Substorms," *Space Sci. Rev.*, **15**, 2, 205-266, Nov. 1973.
- Russell, C. T., D. D. Childers, and P. J. Coleman, Jr., "OGO 5 Observations of Upstream Waves in the Interplanetary Medium: Discrete Wave Packets," *J. Geophys. Res.*, **76**, 4, 845-861, Feb. 1971a.
- Russell, C. T., C. R. Chappell, M. D. Montgomery, M. Neugebauer, and F. L. Scarf, "OGO 5 Observations of the Polar Cusp on November 1, 1968," *J. Geophys. Res.*, **76**, 28, 6743-6764, Oct. 1971b.
- Russell, C. T., M. Neugebauer, and M. G. Kivelson, "OGO 5 Observations of the Magnetopause," in *Correlated Interplanetary and Magnetospheric Observations*, 139-157, ed. D. E. Page, D. Reidel Publ. Co., Dordrecht, Holland, 1974.
- Salah, J. E., J. V. Evans, and R. H. Wand, "Seasonal Variations in the Thermosphere above Millstone Hill," *Radio Sci.*, **9**, 2, 231-238, Feb. 1974.
- Satterblom, P. R., and A. J. Masley, "Proton-Alpha Particle Ratios during 1969-1970," *EOS*, **52**, 11, 888, Nov. 1971.
- Scarf, F. L., and R. W. Fredricks, "Electrostatic Waves in the Magnetosphere," in *Earth's Magnetospheric Processes*, 329-339, ed. B. M. McCormac, D. Reidel Pub. Co., Dordrecht, Holland, 1972.
- Scarf, F. L., R. W. Fredricks, L. A. Frank, C. T. Russell, P. J. Coleman, Jr., and M. Neugebauer, "Direct Correlations of Large-Amplitude Waves with Suprathermal Protons in the Upstream Solar Wind," *J. Geophys. Res.*, **75**, 34, 7316-7322, Dec. 1970.
- Scarf, F. L., R. W. Fredricks, and I. M. Green, "Plasma Waves in the Dayside Polar Cusp, 1, Magnetospheric Observations," *J. Geophys. Res.*, **77**, 13, 2274-2293, May 1972.
- Scarf, F. L., R. W. Fredricks, C. T. Russell, M. Kivelson, M. Neugebauer, and C. R. Chappell, "Observation of a Current-Driven Plasma Instability at the Outer Zone - Plasma Sheet Boundary," *J. Geophys. Res.*, **78**, 13, 2150-2165, May 1973a.
- Scarf, F. L., R. W. Fredricks, C. F. Kennel, and F. V. Coroniti, "Satellite Studies of Magnetospheric Substorms on August 15, 1968, 8, OGO 5 Plasma Wave Observations," *J. Geophys. Res.*, **78**, 16, 3119-3130, June 1973b.
- Scarf, F. L., R. W. Fredricks, M. Neugebauer, and C. T. Russell, "Plasma Waves in the Dayside Polar Cusp, 2, Magnetopause and Polar Magnetosheath," *J. Geophys. Res.*, **79**, 4, 511-520, Feb. 1974.
- Scarf, F. L., R. W. Fredricks, C. T. Russell, M. Neugebauer, M. Kivelson, and C. R. Chappell, "Current-Driven Plasma Instabilities at High Latitudes," *J. Geophys. Res.*, **80**, 16, 2030-2040, June 1975.
- Schindler, K., "Plasma and Fields in the Magnetospheric Tail," *Space Sci. Rev.*, **17**, 2, 589-614, Mar. 1975.
- Scudder, J. D., D. L. Lind, and K. W. Ogilvie, "Electron Observations in the Solar Wind and Magnetosheath," *J. Geophys. Res.*, **78**, 28, 6535-6548, Oct. 1973.
- Serbu, G. P., Private Communication, 1976.
- Serbu, G. P., and E. J. R. Maier, "Observations from OGO 5 of the Thermal Ion Density and Temperature within the Magnetosphere," *J. Geophys. Res.*, **75**, 31, 6102-6113, Nov. 1970.
- Serlemitsos, A. T., and V. K. Balasubrahmayan, "Solar Particle Events With Anomalously Large Relative Abundance of  $^3\text{He}$ ," *Astrophys. J.*, **198**, 1, 195-204, May 1975.

## REFERENCES

- Smith, E. J., and B. T. Tsurutani, "Magnetosheath Lion Roars," *J. Geophys. Res.*, **81**, 73, 2261-2266, May 1976.
- Smith, E. J., R. E. Holzer, and C. T. Russell, "Magnetic Emissions in the Magnetosheath at Frequencies Near 100 Hz," *J. Geophys. Res.*, **74**, 11, 3027-3036, June 1969.
- Smith, E. J., A. M. A. Frandsen, B. T. Tsurutani, R. M. Thorne, and K. W. Chan, "Plasmaspheric Hiss Intensity Variations During Magnetic Storms," *J. Geophys. Res.*, **79**, 16, 2507-2510, June 1974.
- Smith, R. L., "Polarization of Proton Whistlers," *J. Geophys. Res.*, **75**, 34, 7261-7266, Dec. 1970.
- Sonnerup, B. U. O., and L. J. Cahill, Jr., "Magnetopause Structure and Attitude from Explorer 12 Observations," *J. Geophys. Res.*, **72**, 1, 171-183, Jan. 1967.
- Sonnerup, B. U. O., and B. G. Ledley, "Magnetopause Rotational Forms," *J. Geophys. Res.*, **79**, 28, 4309-4314, Oct. 1974.
- Strickland, D. J., and G. E. Thomas, "Global Atomic Oxygen Density Derived from OGO 6 1304Å Airglow Measurements," *Planet. Space Sci.*, **24**, 4, 313-326, Apr. 1976.
- Sugiura, M., "Quiet Time Magnetospheric Field Depression at 2.3-3.6 R<sub>E</sub>," *J. Geophys. Res.*, **78**, 16, 3182-3185, June 1973a.
- Sugiura, M., "Magnetospheric Field Morphology at Magnetically Quiet Times," *Radio Sci.*, **8**, 11, 921-928, Nov. 1973b.
- Sugiura, M., "Identification of the Polar Cap Boundary and the Auroral Belt in the High-Altitude Magnetosphere: A Model for Field-Aligned Currents," *J. Geophys. Res.*, **80**, 16, 2057-2068, June 1975.
- Sugiura, M., B. G. Ledley, T. L. Skillman, and J. P. Heppner, "Magnetospheric-Field Distortions Observed by OGO 3 and 5," *J. Geophys. Res.*, **76**, 31, 7552-7565, Nov. 1971.
- Tausch, D. R., "Structure of Electrodynamical and Particle Heating in the Disturbed Polar Thermosphere," *J. Geophys. Res.*, **82**, 4, 455-460, Feb. 1977.
- Tausch, D. R., and G. R. Carignan, "Neutral Composition in the Thermosphere," *J. Geophys. Res.*, **77**, 25, 4870-4876, Sept. 1972.
- Tausch, D. R., and B. B. Hinton, "Structure of Electrodynamical and Particle Heating in the Undisturbed Polar Thermosphere," *J. Geophys. Res.*, **80**, 31, 4346-4350, Nov. 1975.
- Tausch, D. R., G. R. Carignan, and C. A. Reber, "Neutral Composition Variation above 400 Kilometers during a Magnetic Storm," *J. Geophys. Res.*, **76**, 34, 8318-8325, Dec. 1971.
- Taylor, Jr., H. A., "Observed Solar Geomagnetic Control of the Ionosphere: Implications for Reference Ionospheres," *Space Res.*, **12**, Pt. 2, 1275-1290, 1972a (Proc. of the 14th COSPAR Plenary Meeting, Seattle, Wa., June 21-July 2, 1971).
- Taylor, Jr., H. A., "The Light Ion Trough," *Planet. Space Sci.*, **20**, 10, 1593-1605, Oct. 1972b.
- Taylor, Jr., H. A., "High Latitude Minor Ion Enhancements: A Clue for Studies of Magnetosphere-Atmosphere Coupling," *J. Atmos. Terr. Phys.*, **36**, 11, 1815-1823, Nov. 1974.
- Taylor, Jr., H. A., and G. R. Cordier, "In-Situ Observations of Irregular Ionospheric Structure Associated with the Plasmopause," *Planet. Space Sci.*, **22**, 9, 1289-1296, Sept. 1974.
- Taylor, Jr., H. A., J. M. Grebowsky, and A. J. Chen, "Ion Composition Irregularities and Ionosphere - Plasmasphere Coupling: Observations of a High Latitude Ion Trough," *J. Atmos. Terr. Phys.*, **37**, 4, 613-623, Apr. 1975.
- Teague, M. J., and E. G. Stassinopoulos, "A Model of the Starfish Flux in the Inner Radiation Zone," NASA/GSFC TM-X-66211, Greenbelt, Md., Dec. 1972.
- Teegarden, B. J., F. B. McDonald, and V. K. Balasubrahmanyam, "Spectra and Charge Composition of the Low Energy Galactic Cosmic Radiation from Z = 2 to 14," *Acta Phys.*, **29**, Suppl. 1, 345-351, 1970. (Proc. of the 11th Int. Conf. on Cosmic Rays, Budapest, Hungary, Aug. 25-Sept. 4, 1969.)
- Thomas, G. E., "Ultraviolet Observations of Atomic Hydrogen and Oxygen from the OGO Satellites," *Space Res.*, **10**, 602-607, 1970. (Proc. of the 12th COSPAR Plenary Meeting, Prague, Czech., May 11-14, 1969.)
- Thomas, G. E., and D. E. Anderson Jr., "Global Atomic Hydrogen Density Derived from OGO 6 Lyman Alpha Measurements," *Planet. Space Sci.*, **24**, 4, 303-312, Apr. 1976.
- Thomas, G. E., and R. C. Bohlin, "Lyman-Alpha Measurements of Neutral Hydrogen in the Outer Geocorona and in Interplanetary Space," *J. Geophys. Res.*, **77**, 16, 2752-2761, June 1972.
- Thomas, G. E., and R. F. Krassa, "OGO 5 Measurements of the Lyman-Alpha Sky Background," *Astron. and Astrophys.*, **11**, 2, 218-233, Mar. 1971.
- Thomas, G. E., and R. F. Krassa, "OGO 5 Measurements of the Lyman-Alpha Sky Background in 1970 and 1971," *Astron. and Astrophys.*, **30**, 2, 223-232, Jan. 1974.
- Thomas, R. J., and T. M. Donahue, "Analysis of OGO 6 Observations of the OI 5577-A Tropical Nightglow," *J. Geophys. Res.*, **77**, 19, 3557-3565, July 1972.
- Thorne, R. M., and C. F. Kennel, "Quasi-Trapped VLF Propagation in the Outer Magnetosphere," *J. Geophys. Res.*, **72**, 3, 857-870, Feb. 1967.

## REFERENCES

- Thorne, R. M., E. J. Smith, R. K. Burton, and R. E. Holzer, "Plasmaspheric Hiss," *J. Geophys. Res.*, **78**, 10, 1581-1596, Apr. 1973.
- Thorne, R. M., S. R. Church, W. J. Malloy, and B. T. Tsurutani, "The Local Time Variation of ELF Emissions during Periods of Substorm Activity," *J. Geophys. Res.*, **82**, 10, 1585-1590, Apr. 1977.
- Thuillier, G., J. L. Falin, and C. Wachtel, "Experimental Model of the Exospheric Temperature based on Optical Measurements on board the OGO 6 Satellite," Paper presented at the 19th COSPAR Plenary Meeting, Philadelphia, Pa., June 8-19, 1976.
- Tsurutani, B. T., and E. J. Smith, "Electromagnetic Hiss and Relativistic Electron Losses in the Inner Zone," *J. Geophys. Res.*, **80**, 4, 600-607, Feb. 1975.
- Unti, T., and M. Neugebauer, "Shock System of February 2, 1969," *J. Geophys. Res.*, **78**, 31, 7237-7256, Nov. 1973.
- Unti, T., and C. T. Russell, "On the Causes of Spectral Enhancements in Solar Wind Power Spectra," *J. Geophys. Res.*, **81**, 4, 469-482, Feb. 1976.
- Unti, T. W. J., M. Neugebauer, and B. E. Goldstein, "Direct Measurements of Solar-Wind Fluctuations Between 0.0048 and 13.3 Hz," *Astrophys. J.*, **180**, 3, 591-598, Mar. 1973.
- Vasyliunas, V. M., and R. A. Wolf, "Magnetospheric Substorms: Some Problems and Controversies," *Rev. of Geophys. and Space Phys.*, **11**, 1, 181-189, Feb. 1973.
- Vidal-Madjar, A., J. E. Blamont, and B. Phissamay, "Evolution with Solar Activity of the Atomic Hydrogen Density at 100 Kilometers of Altitude," *J. Geophys. Res.*, **79**, 1, 233-241, Jan. 1974.
- Vorpahl, J. A., "Optical, Hard X-Ray, and Microwave Emission During the Impulsive Phase of Flares," in *High Energy Phenomena on the Sun*, NASA SP-342, 221-227, Wash. D.C., 1973.
- Vorpahl, J. A. and H. Zirin, "Identification of the Hard X-Ray Pulse in the Flare of September 11-12, 1968," *Solar Phys.*, **11**, 2, 285-290, Feb. 1970.
- Wang, T., "Intermode Coupling at Ion Whistler Frequencies in a Stratified Collisionless Ionosphere," *J. Geophys. Res.*, **76**, 4, 947-959, Feb. 1971.
- West, Jr., H. I., and R. M. Buck, "Observations of Greater than 100-keV Protons in the Earth's Magnetosheath," *J. Geophys. Res.*, **81**, 4, 569-584, Feb. 1976a.
- West, Jr., H. I., and R. M. Buck, "Energetic Electrons in the Inner Belt in 1968," *Planet. Space Sci.*, **24**, 7, 643-655, July 1976b.
- West, Jr., H. I., and R. M. Buck, "A Study of Electron Spectra in the Inner Belt," *J. Geophys. Res.*, **81**, 25, 4696-4700, Sept. 1976c.
- West, Jr., H. I., R. M. Buck, and J. R. Walton, "Electron Pitch Angle Distributions throughout the Magnetosphere as Observed on OGO 5," *J. Geophys. Res.*, **78**, 7, 1064-1081, March 1973a.
- West, Jr., H. I., R. M. Buck, and J. R. Walton, "Satellite Studies of Magnetospheric Substorms on August 15, 1968, 6, OGO 5 Energetic Electron Observations - Pitch Angle Distributions in the Nighttime Magnetosphere," *J. Geophys. Res.*, **78**, 16, 3093-3102, June 1973b.
- Williams, D. J., and H. Trefall, "Field-Aligned Precipitation of > 30-keV Electrons," *J. Geophys. Res.*, **81**, 16, 2927-2930, June 1976.
- Winkler, C. N., and P. J. Bedijn, "Long-Term Cosmic Ray Modulation in the Period 1966-1972 and Interplanetary Magnetic Fields," *J. Geophys. Res.*, **81**, 19, 3198-3206, July 1976.
- Wright, J. W., J. P. McClure, and W. B. Hanson, "Comparisons of Ionogram and OGO 6 Satellite Observations of Small-Scale F Region Inhomogeneities," *J. Geophys. Res.*, **82**, 4, 548-554, February 1977.
- Wydra, B. J., "Global Exospheric Temperatures and Densities Under Active Solar Conditions," Penn. State Univ., Ionos. Res. Lab., PSU-IRL-SCI-436, University Park, Pa., Oct. 1975.

# IV. SPACECRAFT AND EXPERIMENT

## LITERATURE REFERENCES

### OGO 1

#### SPACECRAFT/MISSION BIBLIOGRAPHY

Papers with major discussion of spacecraft, mission, testing, subsystems, or ground systems prepared by NASA project or project support personnel.

A63-10333, A63-21527, A65-14349, A65-19503,  
A65-22431, A69-36674, A70-35303.  
N62-15053, N64-27251, N65-21656, N65-29296,  
N66-21006, N74-76913, N74-76932.

Papers with minor discussion of spacecraft, mission, testing, subsystems, or ground systems prepared by NASA project or project support personnel.

N65-29783, N74-76912.

Papers about spacecraft, mission, testing, subsystems, or ground systems prepared by NASA contractor personnel.

A63-13537, A63-13629, A63-21528, A63-23249,  
A64-10864, A64-11240, A64-24447, A64-27303,  
A65-19528, A66-15919.  
N67-22257, N69-33977, N74-74623.

#### EXPERIMENTS

##### OGO 1, Anderson

EXPERIMENT NAME ..... Solar Cosmic Rays  
NSSDC ID ..... 64-054A-12

#### BIBLIOGRAPHY

PM: A67-41233, A69-31967, A71-19825.  
N68-33302.  
B03937-000.

OS: N69-34536.

##### OGO 1, Bohn

EXPERIMENT NAME ..... Interplanetary Dust  
Particles  
NSSDC ID ..... 64-054A-07

#### BIBLIOGRAPHY

PM: A66-15266.  
N67-32070.

PS: A68-29467.

### OGO 1, Bridge

EXPERIMENT NAME ..... Plasma Probe, Faraday  
Cup  
NSSDC ID ..... 64-054A-14

#### BIBLIOGRAPHY

PM: A68-17768, A68-28348, A69-19373, A71-30029.  
N72-18715.

PS: A73-33436.

OS: N70-27302.

### OGO 1, Cline

EXPERIMENT NAME ..... Positron Search and  
Gamma Ray Spectrum  
NSSDC ID ..... 64-054A-15

#### BIBLIOGRAPHY

PM: A68-41427.  
N74-77446.

PS: A74-30149.

### OGO 1, Haddock

EXPERIMENT NAME ..... Radio Astronomy  
NSSDC ID ..... 64-054A-09

#### BIBLIOGRAPHY

PM: N69-31345, N74-74631.

PS: N69-25437.

### OGO 1, Hargreaves

EXPERIMENT NAME ..... Radio Propagation  
NSSDC ID ..... 64-054A-05

#### BIBLIOGRAPHY

PM: A68-38439.  
N66-12993, N69-24521.  
B18548-000.

OM: A66-10892.

SPACECRAFT AND EXPERIMENT LITERATURE REFERENCES

OGO 1, Helliwell

EXPERIMENT NAME ..... VLF Noise and Propagation  
NSSDC ID ..... 64-054A-08

BIBLIOGRAPHY

PM: A68-17728, A69-25153, A69-31981, A70-15117, A70-27183, A75-42748, A76-19854, N67-30831, N67-37021, N70-15678, N70-33156, N73-16344, N75-20195.

PS: A68-38428.

PC: N74-74765.

OS: A68-14098, A70-30078, A70-40479, A72-21189, A75-24400, B00969-000.

OGO 1, Heppner

EXPERIMENT NAME ..... Magnetic Survey Using Two Magnetometers  
NSSDC ID ..... 64-054A-02

BIBLIOGRAPHY

PM: A68-11011, A68-12172, A72-12084.

PS: N70-19313.

OS: A71-30028, A75-19138

OGO 1, Konradi

EXPERIMENT NAME ..... Trapped Radiation Scintillation Counter  
NSSDC ID ..... 64-054A-16

BIBLIOGRAPHY - None found

OGO 1, Mange

EXPERIMENT NAME ..... Geocoronal Lyman-Alpha Scattering  
NSSDC ID ..... 64-054A-10

BIBLIOGRAPHY - None found

OGO 1, McDonald

EXPERIMENT NAME ..... Cosmic-Ray Isotopic Abundance  
NSSDC ID ..... 64-054A-17

BIBLIOGRAPHY

PM: A63-20022, A66-26348, A66-34847, A67-19913, A68-41421, A68-41431, A71-18137, B01634-000.

OGO 1, Sagalyn

EXPERIMENT NAME ..... Spherical Ion and Electron Trap  
NSSDC ID ..... 64-054A-03

BIBLIOGRAPHY

PM: A72-23011.

PC: N70-28003.

OGO 1, Simpson

EXPERIMENT NAME ..... Cosmic-Ray Spectra and Fluxes  
NSSDC ID ..... 64-054A-18

BIBLIOGRAPHY

PM: A66-34754, A66-34833, A67-11687, A67-27249, A67-37412, A68-41420, A68-41434, A69-20067, A69-20068, B03716-000.

OM: A76-35348.

OGO 1, Smith

EXPERIMENT NAME ..... Triaxial Search Coil Magnetometer  
NSSDC ID ..... 64-054A-01

BIBLIOGRAPHY

PM: A66-23148, A67-40804, A69-36675, A70-15127, A72-44857.

PS: A68-13469, N73-10791.

PC: N69-72494.

OS: A70-27594, A72-21189.



## SPACECRAFT AND EXPERIMENT LITERATURE REFERENCES

### OGO 1, Taylor

OS: A69-33055, A69-34227, A70-30059, A71-27654,  
A73-14962.

EXPERIMENT NAME ..... Positive Ion  
Composition  
NSSDC ID ..... 64-054A-06

#### BIBLIOGRAPHY

PM: A63-12209, A66-14781, A68-19744, A68-37114,  
A69-23777, A70-26568.

PS: A68-41673.

OM: A69-25153, A69-25157.

OS: A68-37940, A70-41087, A71-30951.  
N74-74635.

### OGO 1, Van Allen

EXPERIMENT NAME ..... Trapped Radiation and  
High-Energy Protons  
NSSDC ID ..... 64-054A-19

#### BIBLIOGRAPHY

PM: N67-31362, N67-40126, N69-12899, N74-76911.

### OGO 1, Whipple

EXPERIMENT NAME ..... Planar Ion and Electron  
Trap  
NSSDC ID ..... 64-054A-04

#### BIBLIOGRAPHY

PM: N74-74638.

PS: A69-31976, A70-13994, A73-33436.

### OGO 1, Winckler

EXPERIMENT NAME ..... Ionization Chamber  
NSSDC ID ..... 64-054A-20

#### BIBLIOGRAPHY

PM: A65-33664, A67-25807, A67-41232, A68-22450,  
A68-35480, A69-12740, A69-22182, A70-15106,  
A71-18128,  
N67-13710, N68-10422, N68-23026, N70-17448,  
N70-17624, N72-28802, N74-18420, N74-21445,  
N74-74639.

PS: A66-34768.

### OGO 1, Winckler

EXPERIMENT NAME ..... Electron Spectrometer  
NSSDC ID ..... 64-054A-21

#### BIBLIOGRAPHY

PM: A67-25807, A68-41697, A70-30090,  
N67-13710, N69-19899, N70-17448, N70-17624,  
N72-28802, N74-74639.

OM: N73-20842, N74-20502, N74-20503.

OS: A70-30358, A71-33948.  
N66-35685, N67-19899, N74-74636.

### OGO 1, Wolfe

EXPERIMENT NAME ..... Electrostatic Plasma  
Analysis (Protons  
0.1-18keV)  
NSSDC ID ..... 64-054A-13

#### BIBLIOGRAPHY

PM: A65-25921, A65-29239.

### OGO 1, Wolff

EXPERIMENT NAME ..... Gegenschein  
Photometry  
NSSDC ID ..... 64-054A-11

#### BIBLIOGRAPHY

PM: A67-12055.

PS: N64-27813.

SPACECRAFT AND EXPERIMENT LITERATURE REFERENCES

OGO 2

SPACECRAFT/MISSION BIBLIOGRAPHY

Papers with major discussion of spacecraft, mission, testing, subsystems, or ground systems prepared by NASA project or project support personnel.

A63-10333, A63-21527, A65-14349, A69-36674, A70-35303, N64-23517, N65-18269, N74-76913, N74-76932.

Papers with minor discussion of spacecraft, mission, testing, subsystems, or ground systems prepared by NASA project or project support personnel.

N67-18763.

Papers about spacecraft, mission, testing, subsystems, or ground systems prepared by NASA contractor personnel.

A63-13537, A63-13629, A63-21528, A64-10864, A65-19528, N64-13388, N74-74623, N74-74661, B00570-000.

EXPERIMENTS

OGO 2, Anderson

EXPERIMENT NAME ..... Cosmic-Ray Ionization

NSSDC ID ..... 65-081A-06

BIBLIOGRAPHY

PM: A68-43450, A69-28950, A69-31967, A70-31902, A70-31903, N74-74624, N74-76923.

PS: N69-34536.

OGO 2, Barth

EXPERIMENT NAME ..... UV Spectrometer, 1100-3400A

NSSDC ID ..... 65-081A-12

BIBLIOGRAPHY

OS: N69-18074.

OGO 2, Cain

EXPERIMENT NAME ..... Magnetic Survey, Rubidium Vapor Magnetometer

NSSDC ID ..... 65-081A-05

BIBLIOGRAPHY

PM: A67-23244, A67-36513, A67-36901, A68-26625, A68-42083, A69-11125, A69-37490, A69-42428, A70-39349, A71-29903, A71-33946, A72-12081, A74-34019, A75-12368, A75-24043, A75-28743, N67-30147, N67-37398, N71-32190, N74-17058, N76-71877, N76-71880, N77-13587.

PS: A73-41374, N64-27355, N72-23341.

OS: A74-28723.

OGO 2, Donley

EXPERIMENT NAME ..... Positive Ion Study

NSSDC ID ..... 65-081A-19

BIBLIOGRAPHY - None found

OGO 2, Haddock

EXPERIMENT NAME ..... Radio Astronomy

NSSDC ID ..... 65-081A-01

BIBLIOGRAPHY

PM: A71-26144, N69-14393, N70-23999.

PS: N69-25437.

OGO 2, Haddock

EXPERIMENT NAME ..... Electron Density Measurements

NSSDC ID ..... 65-081A-21

BIBLIOGRAPHY

PM: A70-35771, A73-34783, N70-23999.

SPACECRAFT AND EXPERIMENT LITERATURE REFERENCES

**OGO 2, Helliwell**

EXPERIMENT NAME ..... VLF Noise and Propagation  
 NSSDC ID ..... 65-081A-02

**BIBLIOGRAPHY**

PM: A68-19752, A68-31481, A69-14029, A69-28958, A69-34939, A70-15116, A70-29924, A71-31757, A75-16440, N67-30831, N70-15525, N70-32928, B01263-000.  
 PS: A68-37940.  
 PC: N74-74765.  
 OS: A69-11125, A69-38495, A70-30078, A72-21189, B00969-000.

**OGO 2, Hinteregger**

EXPERIMENT NAME ..... Solar UV Emissions  
 NSSDC ID ..... 65-081A-17

**BIBLIOGRAPHY**

PM: A66-27326, N65-29678.  
 PC: N65-14504.

**OGO 2, Hoffman**

EXPERIMENT NAME ..... Scintillation Detector  
 NSSDC ID ..... 65-081A-09

**BIBLIOGRAPHY** - None found

**OGO 2, Jones**

EXPERIMENT NAME ..... Neutral Particle and Ion Composition  
 NSSDC ID ..... 65-081A-13

**BIBLIOGRAPHY**

PM: N70-14425, N74-77537.

**OGO 2, Kreplin**

EXPERIMENT NAME ..... Solar X-ray Emissions  
 NSSDC ID ..... 65-081A-16

**BIBLIOGRAPHY** - None found

**OGO 2, Mange**

EXPERIMENT NAME ..... Lyman-Alpha and UV Airglow Study  
 NSSDC ID ..... 65-081A-11

**BIBLIOGRAPHY** - None found

**OGO 2, Morgan**

EXPERIMENT NAME ..... Whistler and Audio-Frequency Electromagnetic Waves  
 NSSDC ID ..... 65-081A-03

**BIBLIOGRAPHY**

PM: A69-16257, N69-17928.  
 OM: N67-30831.  
 OS: A72-21189, B00969-000.

**OGO 2, Newton**

EXPERIMENT NAME ..... Neutral Particle Study  
 NSSDC ID ..... 65-081A-20

**BIBLIOGRAPHY** - None found

**OGO 2, Nilsson**

EXPERIMENT NAME ..... Interplanetary Dust Particles  
 NSSDC ID ..... 65-081A-14

**BIBLIOGRAPHY**

PM: A66-41213, A68-35397, A70-10444, N69-23367.  
 PS: A68-29467.

# SPACECRAFT AND EXPERIMENT LITERATURE REFERENCES

## OGO 2, Reed

EXPERIMENT NAME ..... Airglow and Auroral  
Study  
NSSDC ID ..... 65-081A-10

### BIBLIOGRAPHY

PM: A67-23278,  
N67-27576, N67-27578, N72-27423.  
PS: N69-18074.

## OGO 2, Simpson

EXPERIMENT NAME ..... Low-Energy Proton,  
Alpha Particle  
Measurement  
NSSDC ID ..... 65-081A-07

### BIBLIOGRAPHY

OS: N69-34536.

## OGO 2, Smith

EXPERIMENT NAME ..... Triaxial Search-Coil  
Magnetometer  
NSSDC ID ..... 65-081A-04

### BIBLIOGRAPHY

PM: A69-36675.  
PC: B21207-000.  
OS: A72-21189.

## OGO 2, Taylor

EXPERIMENT NAME ..... Positive Ion  
Composition  
NSSDC ID ..... 65-081A-15

### BIBLIOGRAPHY

PM: A68-37114, A68-41673, A69-31326, A69-34939,  
A71-33762, A73-11904, A73-15533.  
PS: A68-38423, A71-30037.  
OS: A72-10361.

## OGO 2, Van Allen

EXPERIMENT NAME ..... Corpuscular Radiation  
Experiment  
NSSDC ID ..... 65-081A-18

### BIBLIOGRAPHY

PM: N69-20849, N74-76909.

## OGO 2, Webber

EXPERIMENT NAME ..... Galactic and Solar  
Cosmic Ray  
NSSDC ID ..... 65-081A-08

### BIBLIOGRAPHY

PM: A66-23684, A68-41562.  
PS: N74-19088.

# SPACECRAFT AND EXPERIMENT LITERATURE REFERENCES

## OGO 3

### SPACECRAFT/MISSION BIBLIOGRAPHY

Papers with major discussion of spacecraft, mission, testing, subsystems or ground systems prepared by NASA project or project support personnel.

A63-10333, A69-36674, A70-35303.  
N74-74630, N74-76932.

Papers with minor discussion of spacecraft, mission, testing, subsystems or ground systems prepared by NASA project or project support personnel.

A71-33663.  
N74-76912.

Papers about spacecraft, mission, testing, subsystems, or ground systems prepared by NASA contractor personnel.

A63-21528, A64-10864.  
N69-33977, N74-74623.

### EXPERIMENTS

#### OGO 3, Anderson

EXPERIMENT NAME ..... Solar Cosmic Rays  
NSSDC ID ..... 66-049A-01

#### BIBLIOGRAPHY

PM: A68-37148, A69-22181, A69-37555, A71-19825.  
N69-23730, N69-29659.  
B03937-000, B03943-000.

OS: A68-31924.

#### OGO 3, Bohn

EXPERIMENT NAME ..... Interplanetary Dust  
Particles  
NSSDC ID ..... 66-049A-21

#### BIBLIOGRAPHY

PM: A68-29457, A68-29468, A71-14014, A71-33741.  
A72-31937.  
N71-33768.

PS: A68-29467.

OM: N74-29255.

#### OGO 3, Bridge

EXPERIMENT NAME ..... Plasma Probe, Faraday  
Cup  
NSSDC ID ..... 66-049A-06

#### BIBLIOGRAPHY

PM: A68-28348, A69-14027, A69-19373, A71-30029.  
N72-18715.

OS: A73-33436.

#### OGO 3, Cline

EXPERIMENT NAME ..... Positron Search and  
Gamma-Ray Spectrum  
NSSDC ID ..... 66-049A-04

#### BIBLIOGRAPHY

PM: A68-17769, A68-41427, A69-23753, A70-38098.

PS: A74-30149.

#### OGO 3, Evans

EXPERIMENT NAME ..... Low-Energy Proton  
Experiment  
NSSDC ID ..... 66-049A-07

BIBLIOGRAPHY - None found

#### OGO 3, Frank

EXPERIMENT NAME ..... Low-Energy Electrons  
and Protons  
NSSDC ID ..... 66-049A-08

#### BIBLIOGRAPHY

PM: A67-19926, A67-26312, A67-37401, A68-17771,  
A68-34245, A68-41684, A69-19358, A70-23490,  
A70-23491, A70-30089, A70-43834, A71-17261,  
A71-24781.  
N66-13640, N68-15232.

PS: A69-29565.

OS: A69-37967, A70-30358, A70-31905, A70-37487,  
A71-17263.  
B18378-000.

SPACECRAFT AND EXPERIMENT LITERATURE REFERENCES

OGO 3, Fritz

EXPERIMENT NAME ..... Radio Propagation  
NSSDC ID ..... 66-049A-16

PS: A71-17258,  
N70-19313.

OM: A73-13871, A77-16238.

OS: A71-17686, A71-34777, A72-42902.

BIBLIOGRAPHY

PM: B18548-000.

OGO 3, Konradi

OGO 3, Haddock

EXPERIMENT NAME ..... Radio Astronomy  
NSSDC ID ..... 66-049A-18

EXPERIMENT NAME ..... Trapped Radiation  
Scintillation Counter  
NSSDC ID ..... 66-049A-10

BIBLIOGRAPHY

PM: A69-21699.

BIBLIOGRAPHY

PM: A70-34835, A71-19724, A71-43176,  
N70-11147, N70-12221, N74-74631, N74-74660,  
N74-76907.

PS: N69-25437.

OS: N70-33175.

OGO 3, Mange

OGO 3, Helliwell

EXPERIMENT NAME ..... VLF Noise and  
Propagation  
NSSDC ID ..... 66-049A-17

EXPERIMENT NAME ..... Geocoronal  
Lyman-Alpha Scattering  
NSSDC ID ..... 66-049A-19

BIBLIOGRAPHY

PM: A70-27181, A71-14028.

PS: A69-30191.

OS: A71-24439.

BIBLIOGRAPHY

PM: A69-25153, A69-31981, A70-27183, A71-11499,  
A72-42043, A73-41912, A75-42748, A77-16238,  
N67-30831, N68-14025, N70-15678, N70-33156,  
N73-16344, N75-20195, N75-22959,  
B01263-000, B01265-000.

PS: A68-37940,  
N68-17981.

OS: A70-30078, A70-40479, A71-30952, A72-21189,  
B00969-000.

OGO 3, McDonald

OGO 3, Heppner

EXPERIMENT NAME ..... Magnetic Survey Using  
Two Magnetometers  
NSSDC ID ..... 66-049A-11

EXPERIMENT NAME ..... Cosmic-Ray Isotopic  
Abundance  
NSSDC ID ..... 66-049A-02

BIBLIOGRAPHY - None found

OGO 3, Sagalyn

BIBLIOGRAPHY

PM: A69-11226, A70-30076, A71-23635, A72-10886,  
A72-12084, A73-11732, A73-43693, A74-14270,  
N71-25271, N71-32436, N73-17947.

EXPERIMENT NAME ..... Spherical Ion and  
Electron Trap  
NSSDC ID ..... 66-049A-13

BIBLIOGRAPHY

PM: A68-29421.

# SPACECRAFT AND EXPERIMENT LITERATURE REFERENCES

## OGO 3, Simpson

EXPERIMENT NAME ..... Cosmic-Ray Spectra  
and Fluxes  
NSSDC ID ..... 66-049A-03

### BIBLIOGRAPHY

PM: A68-41420, A71-18127,  
B03716-000.  
OM: A76-35348.

## OGO 3, Smith

EXPERIMENT NAME ..... Triaxial Search-Coil  
Magnetometer  
NSSDC ID ..... 66-049A-12

### BIBLIOGRAPHY

PM: A68-41693, A69-18834, A69-31985, A69-36675,  
A69-40501, A70-21380, A74-24759.  
PS: A70-30078,  
N73-10791.  
PC: N69-72494.  
OM: A75-27679.  
OS: A72-21189.

## OGO 3, Taylor

EXPERIMENT NAME ..... Positive Ion  
Composition  
NSSDC ID ..... 66-049A-15

### BIBLIOGRAPHY

PM: A68-19744, A68-37114, A69-23777, A70-26568,  
A70-29185, A70-38377, A72-17453, A77-21513.  
PS: A68-41673, A77-21504.  
OM: A69-25153, A69-25157.  
OS: A70-30358.

## OGO 3, Whipple

EXPERIMENT NAME ..... Planar Ion and Electron  
Trap  
NSSDC ID ..... 66-049A-14

### BIBLIOGRAPHY

PM: A74-18372,  
N74-74638.  
PS: A69-31976, A70-13994, A73-33436.

## OGO 3, Winckler

EXPERIMENT NAME ..... Electron Spectrometer  
NSSDC ID ..... 66-049A-22

### BIBLIOGRAPHY

PM: A68-41697, A69-40508, A69-43172, A70-30090,  
N67-13710, N69-19899, N70-17448, N70-17624,  
N72-28802, N74-74639.  
OM: N73-20842, N74-20502, N74-20503.  
OS: N74-74636.

## OGO 3, Winckler

EXPERIMENT NAME ..... Ionization Chamber  
NSSDC ID ..... 66-049A-23

### BIBLIOGRAPHY

PM: A67-41232, A68-22450, A68-35480, A69-12740,  
A69-22182, A69-40508, A69-43172, A70-15106,  
A71-18128,  
N67-13710, N68-10422, N68-23026, N70-17448,  
N70-17624, N72-28802, N74-18420, N74-21445,  
N74-74639.  
OS: A69-33055, A69-34227, A70-30059, A71-17918,  
A71-27654, A73-14962.

## OGO 3, Wolfe

EXPERIMENT NAME ..... Electrostatic Plasma  
Analysis (Protons 0.1-18  
keV)  
NSSDC ID ..... 66-049A-05

### BIBLIOGRAPHY

PM: A65-29239.

## OGO 3, Wolff

EXPERIMENT NAME ..... Gegenschein Photometry  
NSSDC ID ..... 66-049A-20

### BIBLIOGRAPHY

PM: A68-12548,  
N67-35595.

SPACECRAFT AND EXPERIMENT LITERATURE REFERENCES

OGO 4

SPACECRAFT/MISSION BIBLIOGRAPHY

Papers with major discussion of spacecraft, mission, testing, subsystems, or ground systems prepared by NASA project or project support personnel.
A63-10333, A69-36674, A70-35303.
N74-76932.

Papers about spacecraft, mission, testing, subsystems, or ground systems prepared by NASA contractor personnel.
A63-21528, A64-10864.
N69-33977.
N78-70070.

EXPERIMENTS

OGO 4, Anderson

EXPERIMENT NAME ..... Cosmic-Ray Ionization
NSSDC ID ..... 67-073A-07

BIBLIOGRAPHY

PM: A70-31903, A73-10878.
N74-74624, N74-76923.
PS: N69-34536.

OGO 4, Barth

EXPERIMENT NAME ..... UV Spectrometer,
1100-3400 A
NSSDC ID ..... 67-073A-14

BIBLIOGRAPHY

PM: A69-31400, A69-32645, A69-36682, A70-39338,
A73-41925, A75-46289, A76-19839, A77-16243,
A77-23222.
N69-26549.
N78-12583.
OM: A72-26402, A77-27318.
OS: A69-34957, A70-39344, A72-42418.

OGO 4, Cain

EXPERIMENT NAME ..... Magnetic Survey,
Rubidium Vapor
Magnetometer
NSSDC ID ..... 67-073A-06

BIBLIOGRAPHY

PM: A69-37490, A69-42428, A70-39349, A71-29903,
A72-12081, A73-31768, A73-31773, A74-34019,
A75-12368, A75-24043, A75-28743.
N71-32190, N72-30823, N73-20866, N74-13566,
N74-17058, N76-71877, N76-71880, N77-13587.
PS: A73-31772, A73-41374.
N72-23341.
OM: A73-31771.

OGO 4, Chandra

EXPERIMENT NAME ..... Positive Ion Study
NSSDC ID ..... 67-073A-19

BIBLIOGRAPHY

PM: A70-36016, A71-19663, A71-33956, A73-38939,
A75-20360, A75-35040, A76-28486.
N68-35999.
PS: A71-30037, A71-30951.
PC: N74-76910.
OS: A72-26411, A73-33436.

OGO 4, Haddock

EXPERIMENT NAME ..... Radio Astronomy
NSSDC ID ..... 67-073A-01

BIBLIOGRAPHY

PM: A71-26144.
N70-42352.
PS: N69-25437.

OGO 4, Helliwell

EXPERIMENT NAME ..... VLF Noise and
Propagation
NSSDC ID ..... 67-073A-02



SPACECRAFT AND EXPERIMENT LITERATURE REFERENCES

BIBLIOGRAPHY

PM: A69-14029, A70-15116, A70-18532, A71-31757, A71-39746, A72-23008, A73-33451, A73-33876, A75-16440, A76-16522, N68-14025, N70-15525, N70-15768, N70-32928, N73-16126, N73-22079, N74-12109.

PS: N74-15857.

OM: A70-18534, A76-14838.

OS: A70-30078, A72-19149, A72-21189.

OGO 4, Hinteregger

EXPERIMENT NAME ..... Solar UV Emissions  
NSSDC ID ..... 67-073A-20

BIBLIOGRAPHY

PM: N65-29678.

PC: N65-14504.

OGO 4, Hoffman

EXPERIMENT NAME ..... Low-Energy Auroral Particle Detector  
NSSDC ID ..... 67-073A-11

BIBLIOGRAPHY

PM: A68-43443, A69-28964, A71-27911, A71-30032, A72-19149, A72-39541, A73-15531, A73-26988, A73-33434, A73-41914, A73-45114, A74-14274, A74-43679, A75-19330, A76-22086, A76-22107, N70-29987, N71-25272, N73-10392, N73-11345, N74-74628, N75-12873.

PS: N74-28251.

OGO 4, Jones

EXPERIMENT NAME ..... Neutral Particle and Ion Composition  
NSSDC ID ..... 67-073A-15

BIBLIOGRAPHY

PM: A69-36681, N71-21544, N71-23238, B05000-000.

OGO 4, Kreplin

EXPERIMENT NAME ..... Solar X-ray Emissions  
NSSDC ID ..... 67-073A-21

BIBLIOGRAPHY

PM: A69-43611, A71-14046, A71-14212, A71-20318, A72-29722, N74-74629.

PS: A70-16719, A70-43301, A72-20013, N69-32730.

OS: A70-34943, A71-20944, A72-35089, N69-17412, N71-36131.

OGO 4, Mange

EXPERIMENT NAME ..... Lyman-Alpha and UV Airglow Study  
NSSDC ID ..... 67-073A-13

BIBLIOGRAPHY

PM: A70-15128, A70-23493, A70-35764, A71-11503, A71-11504, A71-14028, A71-17279, A71-33964, A75-35040, A76-42683, N76-10603, N77-86006.

PS: A69-30191.

OM: A73-38939, A75-22671.

OS: A69-34957, A72-42418, A77-27318, N71-34333.

OGO 4, Morgan

EXPERIMENT NAME ..... Whistler and Audio-Frequency Electromagnetic Waves  
NSSDC ID ..... 67-073A-03

BIBLIOGRAPHY

PM: A70-18534, A72-19149, A76-22086.

OM: A70-19630.

OS: A72-21189, A72-39541



SPACECRAFT AND EXPERIMENT LITERATURE REFERENCES

OGO 5

SPACECRAFT/MISSION BIBLIOGRAPHY

Papers with major discussion of spacecraft, mission, testing, subsystems, or ground systems prepared by NASA project or project support personnel. A63-10333, A69-36674, A70-35303. N74-76932.

Papers with minor discussion of spacecraft, mission, testing, subsystems, or ground systems prepared by NASA project or project support personnel. N74-76912.

Papers about spacecraft, mission, testing, subsystems, or ground systems prepared by NASA contractor personnel. A63-21568, A64-10864. N69-33977.

EXPERIMENTS

OGO 5, Aggson

EXPERIMENT NAME ..... Electric Field Measurement
NSSDC ID ..... 68-014A-26

BIBLIOGRAPHY - None found

OGO 5, Anderson

EXPERIMENT NAME ..... Energetic Radiations from Solar Flares
NSSDC ID ..... 68-014A-04

BIBLIOGRAPHY

PM: A69-40775, A71-15937, A71-19825, A72-14561, A72-32790, A73-11389, A73-20766, A74-30287, A74-38468, A75-35537, A75-37352, A77-16850, A77-18572, A78-10580. N72-28812, N74-21445, N74-21458, N75-17277, N75-18144. B03940-000

PS: A70-25746, A71-43849, A73-17041, A74-30908, A75-16217.

OM: A75-43792, A76-10136. N75-17281.

OS: A71-20945, A72-13507, A74-37631.

OGO 5, Blamont

EXPERIMENT NAME ..... Geocoronal Lyman-Alpha Measurements
NSSDC ID ..... 68-014A-22

BIBLIOGRAPHY

PM: A69-31412, A70-42468, A71-24438, A71-33834, A73-19233, A75-13173, A75-23721, A75-28032, A77-11488. N73-10812. N78-71246.

PS: N65-30651.

OM: A76-31317.

OS: A73-12323, A73-39074. N73-10813, N76-21066.

OGO 5, Boyd

EXPERIMENT NAME ..... Electron Temperature and Density
NSSDC ID ..... 68-014A-01

BIBLIOGRAPHY

PM: A70-37513, A74-17648.

OM: A75-35003, A75-36977.

OS: A72-35599, A75-23707.

OGO 5, Cline

EXPERIMENT NAME ..... Interplanetary, Electrons, Positrons, and Protons
NSSDC ID ..... 68-014A-05

BIBLIOGRAPHY

PM: A70-38096. N69-38983.

PS: A74-30149. N71-25288

OGO 5, Coleman

EXPERIMENT NAME ..... Hydromagnetic Waves and Trapped Particles
NSSDC ID ..... 68-014A-13

# SPACECRAFT AND EXPERIMENT LITERATURE REFERENCES

## BIBLIOGRAPHY

- PM: A71-43162, A72-42406, A72-44513, A73-29964, A73-33437, A73-33453, A73-33457, A73-36273, A75-35005, A77-21512, A77-42295, N74-35223.
- PS: A74-14283, A74-17742, A74-24766, A75-19349.
- OM: A73-33449.
- OS: A72-44850, A73-33454, A76-33058, A76-41914, N74-17126.

### OGO 5, Coleman

EXPERIMENT NAME ..... Triaxial Fluxgate Magnetometer  
 NSSDC ID ..... 68-014A-14

## BIBLIOGRAPHY

- PM: A67-15724, A69-42693, A70-36006, A70-37483, A70-43851, A71-14515, A71-14550, A71-19656, A71-21631, A71-21643, A71-27913, A71-33943, A71-43162, A72-19145, A72-23004, A72-29379, A72-29380, A72-35599, A72-35610, A72-44513, A72-44856, A72-44857, A73-13855, A73-29964, A73-29966, A73-33437, A73-33449, A73-33450, A73-33452, A73-33457, A73-36273, A74-14285, A74-21679, A74-21680, A75-19134, A75-19349, A75-23707, A75-28015, A75-35003, A75-35005, A76-22081, A77-11219, A77-16868, A77-21093, A77-21512, A77-23205, A77-23220, A77-42295, N73-10792, N73-20498, N74-35223, N74-74633, N75-76086, B18269-000.
- PS: A69-14681, A70-13980, A70-21377, A70-29111, A70-30078, A71-33944, A72-42406, A72-42902, A73-22054, A73-33453, A74-14283, A74-17742, A75-19127, N69-33963, N73-10791.
- OM: A70-30069, A72-29378, A72-44511, A74-12627, A74-30677, A75-12370, A75-19138, A75-22613, A75-41805, A75-42744, A75-46232, A76-33057, A76-41914, N72-11325, N74-30528, N76-33787, N76-33788, N76-33793, N76-33795, N78-11543.
- OS: A69-33452, A71-11491, A71-17263, A71-30952, A72-44850, A73-24744, A73-33454, A73-33455, A73-33456, A73-36275, A74-18364, A74-43688, A75-22774, A75-46238, A76-22092, A76-33058, A76-44665, N74-17126, B14580-000.

### OGO 5, Crook

EXPERIMENT NAME ..... Plasma Wave Detector  
 NSSDC ID ..... 68-014A-24

IV-14

## BIBLIOGRAPHY

- PM: A69-14681, A69-36683, A69-42693, A70-17376, A70-29111, A70-30069, A70-30085, A70-36005, A70-36006, A70-37483, A71-11500, A71-14550, A71-23711, A71-24788, A71-30956, A71-37353, A71-43158, A71-43162, A72-23019, A72-26399, A72-29380, A72-35610, A72-44523, A73-13883, A73-19254, A73-26985, A73-29964, A73-29966, A73-33437, A73-33456, A73-36273, A74-21680, A75-23707, A75-35003, A76-41914, A77-23220, N72-22383, N73-10789, N73-10795, N74-74626, N74-77109, B18269-000.
- PS: A69-33452, A70-17376, A70-30083, A71-37368, A74-43688, A75-35005.
- OM: A72-35599, A73-33457, A75-38275, A76-12272, N78-11543, B14583-000.
- OS: A71-11491, A71-30952, A71-31774, A72-21189, A72-44850, A73-22069, A74-14283, A75-19134, A75-19138.

### OGO 5, Frank

EXPERIMENT NAME ..... Low-Energy Proton and Electron Differential Energy Analyzer (LEPEDEA)  
 NSSDC ID ..... 68-014A-07

## BIBLIOGRAPHY

- PM: A71-14550, A71-37353, A71-43158, N66-13640.
- PS: A69-29565.
- OS: A75-19138.

### OGO 5, Haddock

EXPERIMENT NAME ..... Radio Astronomy  
 NSSDC ID ..... 68-014A-20

## BIBLIOGRAPHY

- PM: A73-17047, A73-32964, A73-32965, A73-41497, A74-14811, A75-35005, N69-14392, N72-23118, N75-19114, N75-24593, B14718-000.
- PS: N69-25437.

## SPACECRAFT AND EXPERIMENT LITERATURE REFERENCES

### OGO 5, Heppner

EXPERIMENT NAME ..... Magnetic Survey Using  
Two Magnetometers  
NSSDC ID ..... 68-014A-15

#### BIBLIOGRAPHY

PM: A70-30045, A70-30076, A71-23635, A71-31754,  
A71-43161, A72-10886, A73-11732, A73-33464,  
A73-43693, A74-14270, A75-11221, A75-35007,  
A77-17124.  
N71-25271, N71-32519, N73-17947.

PS: A72-13507.

OM: A73-13871, A76-33057.  
N78-11543.

OS: A71-17686, A71-34777, A72-42902, A73-45112.

### OGO 5, Meyer

EXPERIMENT NAME ..... Cosmic-Ray Electrons  
NSSDC ID ..... 68-014A-09

#### BIBLIOGRAPHY

PM: A70-12902, A71-18170, A71-29057, A72-16719,  
A73-33293, A74-30204, A74-31942, A76-26886,  
A76-26907.  
N75-32995  
B08373-000.

OM: A74-37632.  
B13262-000.

### OGO 5, Ogilvie

EXPERIMENT NAME ..... Triaxial Electron  
Analyzer  
NSSDC ID ..... 68-014A-11

#### BIBLIOGRAPHY

PM: A66-23689, A67-33595, A68-25969, A71-31754,  
A72-13507, A73-45112.  
N71-25273.

OM: N78-11543.

### OGO 5, Hutchinson

EXPERIMENT NAME ..... Energetic Photons in  
Primary Cosmic Rays  
NSSDC ID ..... 68-014A-08

#### BIBLIOGRAPHY

PM: A70-40691.  
B18277-000.

### OGO 5, Kreplin

EXPERIMENT NAME ..... Solar X-ray Emissions  
NSSDC ID ..... 68-014A-23

#### BIBLIOGRAPHY

PM: A70-45768, A71-12761, A71-40425, A73-11391,  
A76-10136.  
N74-21450.

### OGO 5, Sagalyn

EXPERIMENT NAME ..... Thermal and Epithermal  
Plasma  
NSSDC ID ..... 68-014A-02

BIBLIOGRAPHY - None found

### OGO 5, McDonald

EXPERIMENT NAME ..... Galactic and Solar  
Cosmic-Ray Studies  
NSSDC ID ..... 68-014A-10

#### BIBLIOGRAPHY

PM: A67-25852, A70-38127, A75-15342, A75-34018,  
A77-11692.  
N69-38984.

### OGO 5, Serbu

EXPERIMENT NAME ..... Thermal Ions and  
Electrons  
NSSDC ID ..... 68-014A-03

#### BIBLIOGRAPHY

PM: A71-11498, A72-26399, A75-16437.

OM: A75-36977.

## SPACECRAFT AND EXPERIMENT LITERATURE REFERENCES

### OGO 5, Sharp

EXPERIMENT NAME ..... Light-Ion Magnetic  
Mass Spectrometer  
NSSDC ID ..... 68-014A-18

#### BIBLIOGRAPHY

PM: A69-36679, A70-18530, A70-18546, A70-30074,  
A70-36014, A70-43851, A71-11491, A71-24787,  
A71-39833, A71-43162, A72-10892, A72-39544,  
A73-12320, A73-13709, A73-13879, A73-22054,  
A73-26985, A73-29966, A73-33451, A73-33876,  
A74-30660, A75-16637, A75-35005, A77-23220,  
N73-16432, N74-76914, N75-17877.

PS: N74-17126.

OM: A70-36006, A72-21223, A73-20652, A73-33457,  
A74-30677, A74-43691, A75-16437, A75-35003,  
A75-36977, A76-12272, A76-33058, A76-41210,  
A77-21512, A77-23205, A77-42295.  
N74-30528.

OS: A69-33452, A71-14515, A73-26984, A74-14283,  
A74-18364, A75-23707, A75-36982, A75-46285,  
A76-44665.  
N70-27302.

### OGO 5, Simpson

EXPERIMENT NAME ..... Low-Energy Heavy  
Cosmic-Ray Particles  
(High-Z Low-E)  
NSSDC ID ..... 68-014A-27

#### BIBLIOGRAPHY

PM: A71-13475, A72-15366, A72-32959, A73-13719,  
A74-30156, A75-46822.  
N73-25870.

OS: A73-23538.

### OGO 5, Smith

EXPERIMENT NAME ..... Triaxial Search-Coil  
Magnetometer  
NSSDC ID ..... 68-014A-16

#### BIBLIOGRAPHY

PM: A69-31985, A69-36675, A70-37483, A71-33943,  
A72-26399, A72-29378, A73-26984, A74-18364,  
A74-21679, A74-24767, A74-30677, A75-19134,  
A75-35003, A76-33057, A76-33058, A76-44665,  
A77-21512, A77-23220  
N74-30528.

PS: A70-30078, A74-14283.  
N73-10791.

PC: N69-72494.

OM: A70-43851, A73-33457, A74-12627, A76-12272,  
A77-21523, A77-42295.  
N78-11543.

OS: A69-33452, A71-11491, A72-21189, A73-13855,  
A73-33453, A75-23707, A75-36988, A75-46238,  
A76-41914.  
N74-17126.

### OGO 5, Snyder

EXPERIMENT NAME ..... Plasma Spectrometer  
NSSDC ID ..... 68-014A-17

#### BIBLIOGRAPHY

PM: A68-42739, A70-21377, A70-36005, A71-14550,  
A71-33943, A71-37353, A71-43162, A72-29378,  
A72-29380, A72-35610, A73-23539, A73-29966,  
A73-36273, A74-12627, A74-21679, A74-21680,  
A75-19134, A75-23707, A75-27387, A75-28004,  
A75-28038, A75-28750, A75-35003, A75-35005,  
A75-42744, A76-19838, A76-22081, A77-23220.  
N72-14808.

OM: A70-29111, A70-36006, A73-29964, A73-33437.  
N78-11543.

OS: A71-14515, A71-19656, A71-33944, A75-16631,  
A75-19138

### OGO 5, Thomas

EXPERIMENT NAME ..... UV Photometer  
NSSDC ID ..... 68-014A-21

#### BIBLIOGRAPHY

PM: A69-31400, A71-24439, A72-32955, A74-15496,  
A74-22345, A75-32382.

PS: N73-10813, N76-21066.

OM: A76-31317.

OS: A71-35409, A73-12323, A73-39074.

### OGO 5, Van De Hulst

EXPERIMENT NAME ..... Measurement of the  
Absolute Flux and  
Energy Spectra of  
Electrons  
NSSDC ID ..... 68-014A-12

## SPACECRAFT AND EXPERIMENT LITERATURE REFERENCES

### BIBLIOGRAPHY

PM: A69-19198, A70-37522, A70-38105, A70-38106,  
A70-40690, A70-45769, A72-33869, A73-19252,  
A74-27700, A74-31903.  
N77-84176, N77-84177.  
B14744-000, B14745-000

PS: A76-39130.

### OGO 5, West

EXPERIMENT NAME ..... Electron and Proton  
Spectrometer  
NSSDC ID ..... 68-014A-06

### BIBLIOGRAPHY

PM: A66-23690, A71-21037, A73-12442, A73-24732,  
A73-33454, A73-33455, A75-22759, A75-37031,  
A75-41805, A76-22092, A76-35289, A76-44653,  
A77-16868, A77-42295.  
N70-28103, N73-31150, N74-13165, N74-74662,  
N74-74663, N75-17020.  
B07587-000, B15152-000.

PS: N67-30930.

OM: A73-33449, A73-33457, A76-47884.  
N73-20842.

OS: A72-35597, A73-33453, A74-17742.  
N71-25273, N74-30528.

# SPACECRAFT AND EXPERIMENT LITERATURE REFERENCES

## OGO 6

### SPACECRAFT/MISSION BIBLIOGRAPHY

Papers with major discussion of spacecraft, mission, testing, subsystems, or ground systems prepared by NASA project or project support personnel.  
A69-36674, A69-43132, A70-35303.  
N74-76932.

Papers about spacecraft, mission, testing, subsystems, or ground systems prepared by NASA contractor personnel.  
A63-21528, A64-10864.  
N78-70070.

### EXPERIMENTS

#### OGO 6, Aggson

EXPERIMENT NAME ..... DC Electric Field Measurements  
NSSDC ID ..... 69-051A-23

#### BIBLIOGRAPHY

PM: A70-30082, A72-35989, A72-39980, A72-42432, A72-44854, A73-15333, A74-14272, A75-11226, A75-16634, A76-16514, A77-27317, A77-34326, N74-29091, N74-74627.  
PS: A72-39543.  
OM: A72-42901, A76-22105.  
OS: A75-35036, A76-42697, N74-74632.

#### OGO 6, Barth

EXPERIMENT NAME ..... UV Photometer  
NSSDC ID ..... 69-051A-13

#### BIBLIOGRAPHY

PM: A75-16634, A76-28988, A76-28989.

#### OGO 6, Bedo

EXPERIMENT NAME ..... Solar UV Emissions, 160-1600 A  
NSSDC ID ..... 69-051A-09

IV-18

## BIBLIOGRAPHY

PM: N71-10358.

PC: N74-16940.

#### OGO 6, Blamont

EXPERIMENT NAME ..... Airglow and Auroral Emissions  
NSSDC ID ..... 69-051A-11

#### BIBLIOGRAPHY

PM: A74-11523.

#### OGO 6, Blamont

EXPERIMENT NAME ..... Line Shape of the 6300-A Airglow Emission  
NSSDC ID ..... 69-051A-14

#### BIBLIOGRAPHY

PM: A72-35603, A74-23679, A75-16449, A76-42390.  
OM: A77-25183, A77-34901, N76-10610.  
OS: A73-36150, A75-46269.

#### OGO 6, Cain

EXPERIMENT NAME ..... Magnetic Survey, Rubidium Vapor Magnetometer  
NSSDC ID ..... 69-051A-21

#### BIBLIOGRAPHY

PM: A70-39349, A71-29903, A73-31768, A74-34019, A75-12368, A75-24043, A75-28743, A76-16514, N72-30823, N73-20866, N74-17058, N76-71877, N76-71880, N77-13587.  
PS: A73-31772, A73-41374, N72-23341.  
OM: A73-31771, A73-31773, A75-13176, N76-71883.  
OS: A73-31769.



SPACECRAFT AND EXPERIMENT LITERATURE REFERENCES

OGO 6, Clark

EXPERIMENT NAME ..... Celestial Lyman-Alpha Measurement  
NSSDC ID ..... 69-051A-12

BIBLIOGRAPHY

PM: A70-43852, A71-17975.  
N71-36136, N72-23429, N74-74625.  
OS: A71-24439.

OGO 6, Donahue

EXPERIMENT NAME ..... Sodium Airglow Photometer  
NSSDC ID ..... 69-051A-26

BIBLIOGRAPHY

PM: A72-35604, A72-42515, A73-45121, A74-30670,  
A75-11227, A76-16501, A76-18436.  
N73-16436, N75-19882, N75-27744.  
OM: A76-39128.  
OS: N75-24202.

OGO 6, Evans

EXPERIMENT NAME ..... Auroral Particle Measurement  
NSSDC ID ..... 69-051A-15

BIBLIOGRAPHY - None found

OGO 6, Farley

EXPERIMENT NAME ..... Trapped and Precipitating Electrons UCLA  
NSSDC ID ..... 69-051A-16

BIBLIOGRAPHY

PM: A74-24766.  
N73-15863.

OGO 6, Hanson

EXPERIMENT NAME ..... Planar Ion and Electron Trap  
NSSDC ID ..... 69-051A-03

BIBLIOGRAPHY

PM: A70-43840, A70-43841, A72-10902, A72-35989,  
A72-42016, A72-44516, A73-19241, A73-22066,  
A73-24738, A73-41919, A74-12640, A74-18754,  
A74-27695, A75-11226, A77-23211.  
N73-32286, N74-20542.  
B20340-000.  
PS: A72-26411, A73-29988.  
OM: A75-30005, A77-12057, A77-15786, A77-24016,  
A77-34326.  
OS: A72-42416, A76-42697.  
N71-35437.

OGO 6, Hanson

EXPERIMENT NAME ..... Ion Mass Spectrometer, UTD  
NSSDC ID ..... 69-051A-06

BIBLIOGRAPHY

PM: N71-10588.

OGO 6, Helliwell

EXPERIMENT NAME ..... VLF Noise and Propagation  
NSSDC ID ..... 69-051A-24

BIBLIOGRAPHY

PM: A71-14538, A75-11226.  
N74-12842.  
OS: A72-21189.

OGO 6, Kreplin

EXPERIMENT NAME ..... Solar X-ray Emissions  
NSSDC ID ..... 69-051A-08

BIBLIOGRAPHY - None found

# SPACECRAFT AND EXPERIMENT LITERATURE REFERENCES

## OGO 6, Laaspere

EXPERIMENT NAME ..... Whistler and  
Audio-Frequency  
NSSDC ID ..... Electromagnetic Waves  
69-051A-25

### BIBLIOGRAPHY

PM: A69-36677, A71-33951, A72-29384, A73-33438,  
A74-34020, A77-42297.  
B17973-000.  
PS: A72-23520.  
OS: A72-21189.

## OGO 6, Nagy

EXPERIMENT NAME ..... Electron Temperature  
and Density  
NSSDC ID ..... 69-051A-02

### BIBLIOGRAPHY

PM: A72-35989, A73-19241, A75-11226.  
N73-13376.  
OS: A73-41919, A76-42697.

## OGO 6, Lockwood

EXPERIMENT NAME ..... Neutron Monitor  
NSSDC ID ..... 69-051A-18

### BIBLIOGRAPHY

PM: A69-36678, A70-39326, A72-10877, A73-41498,  
A74-15356, A75-18717.  
N73-19841, N73-32639.  
PS: A73-36645.

## OGO 6, Masley

EXPERIMENT NAME ..... Low-Energy Solar  
Cosmic-Ray  
NSSDC ID ..... Measurement  
69-051A-19

### BIBLIOGRAPHY

PM: A68-27616, A71-18158, A72-31965, A74-30263.  
N73-16795.  
B11181-000.

## OGO 6, McKeown

EXPERIMENT NAME ..... Energy Transfer Probe  
for Atmospheric  
NSSDC ID ..... Density  
69-051A-07

### BIBLIOGRAPHY

PM: A66-15922, A69-36680.  
N71-20207, N74-25869, N74-74659.  
B20296-000, B20953-000, B20954-000.  
PS: N74-10255.  
B20297-000.

## OGO 6, Reber

EXPERIMENT NAME ..... Neutral Atmospheric  
Composition  
NSSDC ID ..... 69-051A-04

### BIBLIOGRAPHY

PM: A71-21647, A71-39711, A72-13518, A72-32964,  
A72-42431, A73-26997, A73-27602, A73-31767,  
A73-33441, A73-38941, A74-18376, A74-21693,  
A74-27713, A74-34027, A76-14318, A76-26524,  
A77-11489, A77-16240, A77-23201, A77-37153,  
A77-37154.  
N71-20638, N71-25267, N73-17946, N73-33320  
N75-32651.  
B16248-000.  
PS: A72-24957, A73-15538, A73-29975, A74-12645,  
A74-36747, A75-12453.  
PC: N70-11727.  
OM: A74-29960, A74-30667, A77-23987, A77-25183.  
N76-10610, N77-23648.  
OS: A72-45593, A73-25753, A74-36735, A76-28990.  
N73-33321, N76-31814.

## OGO 6, Regener

EXPERIMENT NAME ..... Solar UV Survey,  
1850 - 3500 A  
NSSDC ID ..... 69-051A-10

### BIBLIOGRAPHY

PM: N77-86268.

## SPACECRAFT AND EXPERIMENT LITERATURE REFERENCES

### OGO 6, Sharp

EXPERIMENT NAME ..... Microphone  
Atmospheric Density  
Gauge  
NSSDC ID ..... 69-051A-01

#### BIBLIOGRAPHY

PM: A72-26407, A74-14219,  
N72-28467, N72-32390.  
OS: A71-33802, A74-23676.

### OGO 6, Smith

EXPERIMENT NAME ..... Triaxial Search-Coil  
Magnetometer  
NSSDC ID ..... 69-051A-22

#### BIBLIOGRAPHY

PM: A69-36675, A72-19148, A74-24766, A74-34038,  
A74-44202, A75-23716, A76-16507, A77-31391.  
PC: B21207-000.  
OM: A75-13176, A77-34326.  
OS: A72-21189, A75-36988.

### OGO 6, Stone

EXPERIMENT NAME ..... Cosmic-Ray Experiment  
NSSDC ID ..... 69-051A-20

#### BIBLIOGRAPHY

PM: A68-27615, A71-22801, A73-15526, A73-24727,  
A74-30187, A74-30190,  
N72-27829, N72-29818, N73-15837, N73-33777,  
N74-21466,  
B10763-000.  
PS: A72-21510, A72-39401.

### OGO 6, Taylor

EXPERIMENT NAME ..... Ion Mass Spectrometer,  
GSFC  
NSSDC ID ..... 69-051A-05

#### BIBLIOGRAPHY

PM: A71-33762, A73-11904, A73-15533, A73-19255,  
A74-18376, A75-11853, A75-12439, A75-28356,  
A76-22105, A77-16240, A77-42297,  
N71-25265, N74-16064.  
PS: A71-43166, A74-14224.  
OM: A77-34326.  
OS: A74-28723, A75-20360.

### OGO 6, Williams

EXPERIMENT NAME ..... Trapped and  
Precipitating Electrons,  
GSFC  
NSSDC ID ..... 69-051A-17

#### BIBLIOGRAPHY

PM: A68-34540, A69-36676, A74-14848, A76-36276.  
OM: A76-22105.  
OS: N74-16072.

## V. Additional Literature Citations and Abstracts

An updated version of the OGO program bibliography has been given in Section IV of this Supplement in terms of accession numbers. The accession numbers that did not appear in the bibliography for the original *OGO Program Summary* have been shown in italics. The literature citations and abstracts corresponding to the new (italicized) accession numbers are given in this section.

The accession number at the beginning of a citation is a unique number assigned for identification to each document processed into the NASA system. The letter starting an accession number indicates the series to which it belongs, and the two-digit number immediately following the letter consists of the last two digits of the year in which the document was processed.

### A. Literature Cited in IAA

The "A" at the beginning of these accession numbers represents a series announced in *International Aerospace Abstracts (IAA)*. This series contains journal articles and books, meeting papers and conference proceedings issued by professional societies and academic organizations, and translations of journals. No meeting papers are used in the OGO Bibliography unless the actual written paper is available through the professional society or a document distribution center.

**A63-21528\***

#### THE ENGINEERING DESIGN OF THE ORBITING GEOPHYSICAL OBSERVATORIES.

G. J. Gleghorn (Space Technology Laboratories, Inc., Redondo Beach, Calif.) 1963 26 p (NASA, American Association for the Advancement of Science, and American Astronautical Society, Symposium on Scientific Satellites-Mission and Design, Philadelphia, Pa., Dec. 27, 1962.) In: Scientific Satellites. Advances in the Astronautical Sciences, vol. 12. Edited by Irving E. Jeter. North Hollywood, Calif., Western Periodicals Co., 1963, p. 149-174. (NSSDC-ID-64-054A-00-PC; NSSDC-ID-65-081A-00-PC)

Description of the systems and subsystems design of the OGO, an attitude-stabilized spacecraft designed to provide support for 150 lb of scientific experiments when placed in a variety of orbits around earth. The spacecraft incorporates an active thermal-control system, a wideband telemetry system with both real-time and data-storage capability, and a silicon solar-cell power supply. Stabilization techniques provide for specific orientations which are part of experiment requirements, and for removal of sensors when necessary from the immediate vicinity of the spacecraft. The system test station and checkout provisions are detailed, and the completed mobile ground-support station is illustrated.

**A69-31985\***

#### MAGNETIC EMISSIONS IN THE MAGNETOSHEATH AT FREQUENCIES NEAR 100 HZ.

R. E. Holzer, C. T. Russell (California, U., Inst. of Geophysics and Planetary Physics, Los Angeles, Calif.), and E. J. Smith (California Inst. of Tech., Jet Propulsion Lab., Pasadena, Calif.) 1 Jun. 1969 10 p refs In: Journal of Geophysical Research, vol. 74, p. 3027-3036. (Contract JPL-950403)

Report of intense, sporadic bursts of narrow-band magnetic noise in the earth's magnetosheath at frequencies near 100 Hz. The bursts have peak signal amplitudes of tenths of gammas, and durations from less than one second to tens of seconds. It is concluded that the signals are probably transverse electromagnetic waves propagating within the magnetosheath in the whistler mode, and may provide evidence concerning wave-particle instabilities in the turbulent magnetosheath plasma.

**A70-16719#**

#### SOLAR X-RAYS - DEVELOPING BACKGROUND FOR COMPREHENSIVE THEORY

R. W. Kreplin (U.S. Navy, E. O. Hulburt Center for Space Research, Washington, D. C.) Dec. 1969 8 p ref In: Astronautics and Aeronautics, vol. 7, p. 58-65.

Study of solar-activity phenomena based on observations of solar X-ray emission. Techniques developed to measure X-ray spectra are described, and solar X-ray spectra and

their relation to solar activity are discussed. X-ray images of the sun are presented. Investigations of location, size, and morphology of the X-ray emitting regions are considered. A picture of the solar-flare mechanism as it emerges on the basis of the obtained data is given. G.R.

**A70-34943\***

#### SOLAR X-RAY CONTROL OF THE E-LAYER OF THE IONOSPHERE

P. R. Sengupta (Iowa, U., Iowa City, Iowa) Jul. 1970 10 p ref In: Journal of Atmospheric and Terrestrial Physics, vol. 32, p. 1273-1282.

(Grants NSG-233-62; NGR-16-001-002)

Investigation of solar X-ray control of the E-layer of the ionosphere, with calculation of electron production rates between 100 and 140 km above the earth due to 31 to 100 Å solar X-ray flux extrapolated from X-ray data to show that about 70% of the E-layer ionization is contributed by the X-rays. Calculated E-layer electron densities due to solar X-ray flux on two typical days are compared with the E-layer electron density profile. Effective recombination coefficients of the layer calculated from the term coefficients are in agreement with accepted values. F.R.L.

**A71-12761**

#### THERMAL RUNAWAY AS THE SOLAR FLARE TRIGGER MECHANISM

S. W. Kahler and R. W. Kreplin (U.S. Navy, E. O. Hulburt Center for Space Research, Washington, D. C.) Oct. 1970 12 p refs In: Solar Physics, vol. 14, p. 372-383. (Grant NSF GP-11406)

It is postulated that the solar flare 'trigger' mechanism is a thermal runaway which occurs in the inner corona. This runaway is the result of a radiative power function which decreases with increasing temperature. Relationships of the onsets of H alpha flares, hard X-ray, soft X-ray and centimeter radio bursts are consistent with the model. Flares are shown to be common solar phenomena which occur preferentially in hot and dense active regions. Author

**A71-20944**

ON THE EXISTENCE OF SOLAR-FLARE PLASMAS OF TEMPERATURE GREATER THAN .1 BILLION DEG K S. Kahler (U.S. Navy, E. O. Hulburt Center for Space Research, Washington, D. C.) 1 Mar. 1971 4 p refs In: Astrophysical Journal, vol. 164, pt. 1, p. 365-368. (Grant NSF GP-20117)

The steady-state rate of energy loss from a solar-flare plasma at .1 billion deg K as proposed by Chubb to explain hard X-ray observations is considered. For large electron densities (greater than or equal to 10 billion per cu cm), the total energy requirement is shown to be excessively large; and for small densities (less than 10 billion per cu cm), the

Note: An asterisk (\*) denotes a NASA supported document. A pound sign (#) denotes microfiche availability.

distribution of electron energies may not be thermally relaxed. Author

## A71-33663#

## RING CURRENT ASYMMETRY [K ASIMMETRII KOL'TSEVOGO TOKA]

IA. I. Feldshtein and O. A. Troshichev Jun. 1971 5 p refs In: RUSSIAN. In: Kosmicheskie Issledovaniia, vol. 9, p. 408-412.

Proton measurements in a ring current carried out on Sept. 8, 1966 by the OGO-3 satellite are compared with geomagnetic field data of low-latitude and high-latitude observations. A geomagnetic field depression linked with the occurrence of ring current protons is established by low-latitude observations over a period from 3 to 4 UT in the nightfall and day sectors. Intensive polar magnetic disturbances occurred simultaneously at high latitudes. V.Z.

## A71-33964\*

## OBSERVATIONS OF THE O I 1304-A AIRGLOW FROM OGO 4

R. R. Meier (U.S. Navy, E. O. Hulburt Center for Space Research, Washington, D. C.) and D. K. Prinz (U.S. Navy, E. O. Hulburt Center for Space Research, Washington, D. C.) 1 Jul. 1971 13 p refs In: Journal of Geophysical Research, vol. 76, p. 4608-4620. (NASA Order S-32327-G; Grants NSF GP-11336; NSF GP-21346)

Summary of the main features of the atomic oxygen 1304-A day airglow as observed from the OGO 4 spacecraft. The subsolar emission rates from the nadir lie in the range from 10 to 17 kR for August 1967 and vary approximately as the cosine of the solar zenith angle. Day-to-day variations (for observations fixed relative to the sun) can typically be of the order of 10 to 20% and occasionally as much as 40% over a period of several days. Long-term variations (of the order of weeks) correlate with solar activity. Photoelectron impact excitation of atomic oxygen is apparently the only process sufficient to account for the observed emission rates. Resonant scattering of sunlight is too small to account for the observations. Author

## A71-40425

## THE OBSERVATION OF NONTHERMAL SOLAR X-RADIATION IN THE ENERGY RANGE 3 LESS THAN E LESS THAN 10 KEV

S. W. Kahler and R. W. Kreplin (U.S. Navy, E. O. Hulburt Center for Space Research, Washington, D. C.) 15 Sep. 1971 11 p refs In: Astrophysical Journal, vol. 168, pt. 1, p. 531-541. (Grant NSF GP-20117)

Analysis of the low-energy (3 to 10 keV) X-ray spectra observed during solar impulsive bursts of E greater than 10 keV X-rays reported by Kane and Anderson (1970). In two of these bursts the total low-energy X-ray emission can be separated into thermal and nonthermal components. The inferred nonthermal electron spectrum is discussed in relation to acceleration by electric fields. The electron spectrum allows a determination of the minimum value of the ratio of electric field strength to electron density. Author

## A71-43849\*

## MAGNETIC FIELDS, BREMSSTRAHLUNG AND SYNCHROTRON EMISSION IN THE FLARE OF 24 OCTOBER 1969

G. Pruss (Big Bear Observatory, Pasadena, Calif.), J. Vorpahl (California, U., Berkeley, Calif.), and H. Zirin Sep. 1971 9 p ref In: Solar Physics, vol. 19, p. 463-471. (Contract NAS5-9094 Grants NGR-05-002-034; NGL-05-003-017; NSF GA-24015)

An impulsive flare Oct. 24, 1969, produced two bursts with virtually identical time profiles of 8800 MHz emission and X-rays above 48 keV. The two spikes of hard X-rays correspond in time to the times of sharp brightening and expansion in the H alpha flare. The first burst was not observed at frequencies below 3000 MHz. This cutoff is

ascribed to plasma cutoff above the lowlying flare. A model of the flare based on H alpha observations at Big Bear shows that the density of electrons with energy above 10 keV is  $5 \times 10$  to the 7th power if the field density is 10 to the 11th power. The observed radio flux would be produced by this electron distribution with the observed field of 200 G. The H alpha emission accompanying the hard electron acceleration is presumed to be due to excitation of the field atoms by the hard electrons. Author

## A72-20013

## EVIDENCE THAT SOLAR X-RAY EMISSION IS OF PURELY THERMAL ORIGIN (ALSO OBSERVATION OF FAR UV FLASH DURING 28 AUGUST 1966 PROTON FLARE)

T. A. Chubb (U.S. Navy, E. O. Hulburt Center for Space Research, Washington, D. C.) 1972 20 p refs In: Solar-terrestrial physics/1970; Proceedings of the International Symposium, Leningrad, USSR, May 11-19, 1970, Dordrecht, D. Reidel Publishing Co.,

X-ray emission from the sun, as thus far observed, is fully interpretable as thermal plasma emission from sets of hot plasmas at different temperatures. Solar minimum conditions are characterized by the presence of only a few plage regions, which dominate X-ray emission below 20 A. Activity events under these conditions can cause a large increase in flux below 20 A in coincidence with a decrease in emission between 44 and 60 A, as the silicon and magnesium ions that dominate 44-60 A emission move to higher stages of ionization. Under flare conditions, temperatures rise to the 10-30 million degree regime, with the higher temperature portions of the plasma dominating the shorter wavelength portions of the spectrum. Thus, flare temperatures calculated from the ratio of SiXV and SiXVI lines are slightly higher than values calculated from the SiXIII and SiXIV lines, and no major discrepancy exists between these temperatures and temperatures calculated from X-ray continuum emission in the 4-6 A part of the spectrum. (Author)

## A72-29722

## ELECTRON TEMPERATURE AND EMISSION MEASURE VARIATIONS DURING SOLAR X-RAY FLARES. D. M. Horan (U.S. Navy, E. O. Hulburt Center for Space Research, Washington, D. C.) Dec. 1971 10 p refs Solar Physics, vol. 21, Dec. 1971, p. 188-197.

X-ray emission from seventeen X-ray flares was analyzed to obtain electron temperatures and emission measures associated with the source region in the solar corona. The source region was assumed to be isothermal with a Maxwellian electron velocity distribution. Flares which were characterized by a rapid initial X-ray flux increase were found to also have a rapid initial rise in electron temperature and emission measure. Flares which were characterized by a gradual initial X-ray energy flux increase were found to have a less rapid initial rise in electron temperature and emission measure. In all X-ray flares studied the peak temperature chronologically preceded the peak X-ray flux and the peak flux never came after the peak emission measure. (Author)

## A72-31937\*#

## FOUR YEARS OF DUST PARTICLE MEASUREMENTS IN CISLUNAR AND SELENOCENTRIC SPACE FROM LUNAR EXPLORER 35 AND OGO 3.

W. M. Alexander, J. C. Smith (Baylor University, Waco, Tex.), C. W. Arthur (California, University, Los Angeles, Calif.), and J. L. Bohn (Temple University, Philadelphia, Pa.) May 1972 17 p refs COSPAR, Plenary Meeting, 15th, Madrid, Spain, May 10-24, 1972, Paper. 17 p. (Grant NGR-39-012-001)

Since July 1967, knowledge concerning the distributions of picogram size particulate matter in selenocentric space has been obtained from the Lunar Explorer 35 dust particle experiment. For almost 40% of the time, the mean sporadic cumulative flux is quite similar to the flux in interplanetary space. However, there are fluctuations of an order of magnitude during major meteor showers. The coincident

increase of the flux in selenocentric space during the shower periods has been observed for the fourth year. The 100-picogram sensor does not show an increase during shower times, indicating a mass threshold of less than 100 picograms for particles with velocities equal to or greater than lunar escape velocity. The flux values from Lunar Explorer 35 are compared to other long-lifetime measurements in selenocentric, cislunar and interplanetary space with excellent agreement for masses less than one nanogram. (Author)

A72-32790\*

#### LOCATION OF THE ELECTRON ACCELERATION REGION IN SOLAR FLARES.

S. R. Kane and R. P. Lin (California, University, Berkeley, Calif.) Apr. 1972 10 p refs Solar Physics, vol. 23, Apr. 1972, p. 457-466.

(Contracts NAS5-9094; NAS5-9091; Grant NGL-05-003-017)

Observations of impulsive solar flare X rays (energy greater than 10 keV) by the OGO-5 satellite and the measurements of energetic solar electrons made with the Explorer-35 and Explorer-41 (IMP-5) satellites during the period March 1968-September 1969 have been analyzed in order to determine the ion density in the X-ray source region as well as the location of the electron acceleration region in the solar atmosphere. The ion density in the X-ray source region varies from event to event and lies between 1 and 100 billion ions per cu cm for those events in which the impulsive X-ray emission could be detected; for those events in which no impulsive emission was detected above threshold, the ion density in the X-ray source was less than one billion ions per cu cm. At least in some small solar flares, the region where the electrons are accelerated during the flash phase is located in the lower corona. (Author)

A72-39543\*

#### ELECTRIC FIELDS IN THE IONOSPHERE AND MAGNETOSPHERE.

N. C. Maynard (NASA, Goddard Space Flight Center, Laboratory for Space Physics, Greenbelt, Md.) 1972 14 p refs In: Magnetosphere-ionosphere interactions; Proceedings of the Advanced Study Institute, Dalseter, Norway, April 14-23, 1971. Oslo, Universitetsforlaget, 1972, p. 155-168.

Review of current techniques for measuring ionospheric and magnetospheric electric fields and existing measurements. Considerable progress in understanding electric fields has been made in the auroral regions where fields originating basically from convection patterns in the magnetosphere and modified by ionospheric interaction have been detected by both the barium ion cloud and double floating probe techniques and have been compared against predictions. The anticorrelation of electric fields and auroral arcs, the establishment of the auroral electrojet currents as Hall currents, the irregular nature of the electric fields, and the reversal of the electric fields between the eastward and westward electrojet regions have been some of the important observations. Recent barium ion cloud observations in the polar cap have indicated that the long assumed electrojet return current across the polar cap does not exist. (Author)

A72-42515\*#

#### NOCTILUCENT CLOUDS IN DAYTIME - CIRCUMPOLAR PARTICULATE LAYERS NEAR THE SUMMER MESOPAUSE.

T. M. Donahue, B. Guenther (Pittsburgh, University, Pittsburgh, Pa.), and J. E. Blamont (Paris, Universite, Faculte des Sciences, Paris, France) Sep. 1972 5 p refs Journal of the Atmospheric Sciences, vol. 29, Sept. 1972, p. 1205-1209.

(Contract NAS5-511077)

A72-44511\*

#### BINARY INDEX FOR ASSESSING LOCAL BOW SHOCK OBLIQUITY.

E. W. Greenstadt (TRW Systems Group, Redondo Beach,

Calif.) 1 Oct. 1972 13 p refs Journal of Geophysical Research, vol. 77, Oct. 1, 1972, p. 5467-5479.

(Contract NASw-2186)

The earth's collisionless plasma bow shock has, overall, a nonuniform structure whose magnetic profile is simultaneously that of a monotonic or laminar perpendicular shock and of a multigradient oblique shock, depending on the local orientation of the interplanetary field to the nominal shock surface. A 'pulsation index'  $I_p$  has been devised from empirical results to provide a simple convenient means of assessing the probable local character of the shock's structure;  $I_p = 0$  or 1, according to whether local field geometry favors perpendicular or oblique structure, respectively, at a chosen point of observation on the nominal shock surface. (Author)

A73-13709\*

#### RECENT SATELLITE MEASUREMENTS OF THE MORPHOLOGY AND DYNAMICS OF THE PLASMASPHERE.

C. R. Chappell (Lockheed Research Laboratories, Palo Alto, Calif.) Nov. 1972 29 p refs Reviews of Geophysics and Space Physics, vol. 10, Nov. 1972, p. 951-979. Research supported by the Lockheed Independent Research Fund. (Contract NAS5-9092)

The characteristic morphology and dynamics of the plasmasphere vary with local time and with geomagnetic conditions. On the nightside the plasmopause position changes predictably with changing magnetic activity. Once established at a specific L-shell value, the steep density gradient on the nightside corotates into the dayside, where filling from the ionosphere takes place. In the duskside bulge region the characteristic density profile inside the plasmopause displays a smooth decrease proportional to  $1/R$  to the fourth power where R is radial distance. Plasmasphere morphology and dynamics can be understood in terms of a time-varying convection electric-field model of the magnetosphere that includes the bulge region as part of the main circulation pattern of the plasmasphere. (Author)

A73-13879\*

#### THERMAL IONS IN THE MAGNETOSPHERE.

C. R. Chappell (Lockheed Research Laboratories, Palo Alto, Calif.) 1972 11 p refs In: Earth's magnetospheric processes; Proceedings of the Symposium, Cortina, Italy, August 30-September 10, 1971. Dordrecht, D. Reidel Publishing Co., 1972, p. 280-290.

(Contract NAS5-9092)

The distribution and dynamics of thermal (approximately 1 eV) plasma are of fundamental importance for understanding many magnetospheric processes. Above the ionosphere the bulk of the thermal plasma is found in the plasmasphere, which displays varying characteristics in the different LT regions. These different characteristics are reviewed with specific interest placed on the  $H(+)$  ion density profiles, since the  $H(+)$  ions are the main component of the plasmasphere. Plasmasphere dynamics and morphology can be explained in terms of a time-varying convection model of the magnetosphere which incorporates the bulge region as part of the main flow pattern of the plasmasphere. (Author)

A73-15333\*#

#### ELECTRIC FIELDS IN THE MAGNETOSPHERE.

J. P. Heppner (NASA, Goddard Space Flight Center, Greenbelt, Md.) 1972 16 p ref In: Critical problems of magnetospheric physics; Proceedings of the Symposium, Madrid, Spain, May 11-13, 1972. Washington, D.C., IUCSTP Secretariat, 1972, p. 107-120; Discussion, p. 121, 122.

Two techniques, tracking the motions of  $Ba(+)$  clouds and measuring the differences in floating potential between symmetric double probes, have been highly successful in: (1) demonstrating the basic convective nature of magnetospheric electric fields, (2) mapping the global patterns of convection at upper ionosphere levels, and (3) revealing the physics of electric currents in the ionosphere and the

importance of magnetosphere-ionosphere feedback in altering the imposed convection. The basic pattern of anti-solar convection across the polar cap and night toward day convection in both the evening and morning sectors at auroral belt latitudes persists at all levels of activity. The dawn-dusk potential drop across the polar cap (anti-solar convection) ranges from 20 to 100 kilovolts with the most typical values in the center of this range. The sum of morning and evening (night toward day convection) potential drops in the adjacent auroral belts roughly equals the polar cap drop in the opposite sense as expected. (Author)

A73-26984\*

**PLASMASPHERIC HISS.**

R. M. Thorne, R. K. Burton, R. E. Holzer (California, University, Los Angeles, Calif.), and E. J. Smith (California Institute of Technology, Jet Propulsion Laboratory, Pasadena, Calif.) 1 Apr. 1973 16 p refs *Journal of Geophysical Research*, vol. 78, Apr. 1, 1973, p. 1581-1596. (Contracts NAS7-100; JPL-950403; Grants NGR-05-007-276; NSF GA-28045;)

A relatively steady band of ELF hiss has been detected by the OGO 5 search coil magnetometer on almost every passage through the plasmasphere; except for an anomalous region of the dayside at high geomagnetic latitudes, the emissions terminate abruptly at the plasmapause and are therefore referred to as 'plasmaspheric hiss.' A preliminary statistical study of the properties of the observed whistler mode turbulence has yielded the following characteristics: the waves are band limited with a sharp lower-frequency cutoff and a more diffuse upper-frequency cutoff; power spectra show a well-defined maximum near a few hundred hertz, the peak intensities generally ranging between 10 to the minus 7th power and 0.00001 gamma squared/Hz; the wave energy is spread over a bandwidth of a few hundred Hertz, and corresponding wideband amplitudes are 5 to 50 milligamma; the waves are highly turbulent in nature and show little tendency toward definite polarization. (Author)

A73-31771

**CORRELATION OF 'SATELLITE ESTIMATES' OF THE EQUATORIAL ELECTROJET INTENSITY WITH GROUND OBSERVATIONS AT ADDIS ABABA.**

P. Gouin (Haile Selassie I University, Addis Ababa, Ethiopia) Jun. 1973 8 p (International Symposium on Equatorial Aeronomy, 4th, Ibadan, Nigeria, Sept. 4-9, 1972.) *Journal of Atmospheric and Terrestrial Physics*, vol. 35, June 1973, p. 1257-1264.

Of the 2000 OGO-4 and OGO-6 equatorial passes, 112 were within 10 deg either side of Addis Ababa. Twenty-five passes happened during magnetically quiet periods when the index Ap was less than 4. Correlations were sought between the effect of the equatorial electrojet at satellite altitude and ground measurements. When the ground values Delta-H (AA) were read at the LT corresponding to the local time at the longitude of the satellite, the correlation is very good for 80 per cent of the observations. The inverse slope of the ground effect versus satellite effect is about 3.8 for Addis Ababa. A Delta-H (AA) threshold of about 40 gammas was found below which the satellite did not register any electrojet effect. (Author)

A73-33434\*

**ELECTRON PRECIPITATION PATTERNS AND SUBSTORM MORPHOLOGY.**

R. A. Hoffman and J. L. Burch (NASA, Goddard Space Flight Center, Greenbelt, Md.) 1 Jun. 1973 18 p refs *Journal of Geophysical Research*, vol. 78, June 1, 1973, p. 2867-2884.

(NSSDC-ID-67-073A-11-PM)

Statistical analysis of data from the auroral particles experiment aboard OGO 4, performed in a statistical framework interpretable in terms of magnetospheric substorm morphology, both spatial and temporal. Patterns of low-energy electron precipitation observed by polar satellites are examined as functions of substorm phase. The implications of the precipitation boundaries identifiable at the low-latitude edge of polar cusp electron precipitation and at the poleward edge of precipitation in the premidnight sector are discussed. M.V.E.

A73-36150#

**NEUTRAL WIND VELOCITIES CALCULATED FROM TEMPERATURE MEASUREMENTS DURING A MAGNETIC STORM AND THE OBSERVED IONOSPHERIC EFFECTS.**

O. P. Saxena and K. K. Mahajan (National Physical Laboratory, New Delhi, India) May 1973 17 p COSPAR, Plenary Meeting, 16th, Konstanz, West Germany, May 23-June 5, 1973, Paper. 17 p.

A73-45114\*

**HIGH-LATITUDE PROTON PRECIPITATION AND LIGHT ION DENSITY PROFILES DURING THE MAGNETIC STORM INITIAL PHASE.**

J. L. Burch (NASA, Goddard Space Flight Center, Laboratory for Space Physics, Greenbelt, Md.) 1 Oct. 1973 10 p refs *Journal of Geophysical Research*, vol. 78, Oct. 1, 1973, p. 6569-6578.

(NSSDC-ID-67-073A-11-PM; NSSDC-ID-67-073A-16-OS;

NSSDC-ID-67-073A-19-PM; NSSDC-ID-69-051A-05-OS)

Measurements of precipitating protons and light ion densities by experiments on OGO 4 indicate that widespread proton precipitation occurs in predawn hours during the magnetic storm initial phase from the latitude of the high-latitude ion trough, or plasmapause, up to latitudes greater than 75 deg. A softening of the proton spectrum is apparent as the plasmapause is approached. The separation of the low-latitude precipitation boundaries for 7.3-keV and 23.8-keV protons is less than about 1 deg, compared with a 3.6-deg separation that has been computed by using the formulas of Gendrin and Eather and Carovillano. Consideration of probable proton drift morphology leads to the conclusion that protons are injected in predawn hours, widespread precipitation occurring in the region outside the plasmapause. Protons less energetic than 7 keV drift eastward, whereas the more energetic protons drift westward, producing the observed dawn-dusk asymmetry for the lower-energy protons. (Author)

A74-11523

**VERTICAL RED LINE 6300 A DISTRIBUTION AND TROPICAL NIGHTGLOW MORPHOLOGY IN QUIET**

**MAGNETIC CONDITIONS**

G. Thuillier and J. E. Blamont (CNRS, Service d'Aeronomie, Verrieres-le-Buisson, Essonne, France) 1973 13 p refs In: Physics and chemistry of upper atmospheres; Proceedings of the Symposium, Orleans, France, July 31-August 11, 1972. Dordrecht, D. Reidel Publishing Co., 1973, p. 219-231.

**A74-12645\*****THEORY OF THE PHASE ANOMALY IN THE THERMOSPHERE**

H. G. Mayr, I. Harris, and H. Volland (NASA, Goddard Space Flight Center, Thermosphere and Exosphere Branch, Greenbelt, Md.) 1 Nov. 1973 10 p ref Journal of Geophysical Research, vol. 78, Nov. 1, 1973, p. 7480-7489.

Discussion of the temperature-density phase anomaly on the basis of a quasi-three-dimensional model in which the thermosphere dynamics associated with wind circulation is considered in a self-consistent form. Included in this analysis are the first three harmonics, which involve nonlinear coupling between diurnal and semidiurnal tides. It is shown that the phase anomaly with exospheric temperature peaks near 1600 LT and mass density peaks between 1400 and 1445 LT can be reproduced in a self-consistent theory without invoking ad hoc assumptions and boundary conditions that would mask the physical processes to be explored. A number of factors and processes are found to contribute to the phase anomaly, including the semidiurnal and particularly the terdiurnal components, heat advection, diffusion, and energy coupling with the lower atmosphere. A.B.K.

**A74-14224\*****DENSITY AND TEMPERATURE DISTRIBUTIONS IN NON-UNIFORM ROTATING PLANETARY EXOSPHERES WITH APPLICATIONS TO EARTH**

R. E. Hartle (NASA, Goddard Space Flight Center, Laboratory for Planetary Atmospheres, Greenbelt, Md.) Dec. 1973 15 p refs Planetary and Space Science, vol. 21, Dec. 1973, p. 2123-2137.

**A74-14270\*****MAGNETOSPHERIC FIELD MORPHOLOGY AT MAGNETICALLY QUIET TIMES**

M. Sugiura (NASA, Goddard Space Flight Center, Laboratory for Space Physics, Greenbelt, Md.) Nov. 1973 7 p (AGU, NCAR, and NOAA, Chapman Memorial Symposium on Magnetospheric Motions, Boulder, Colo., June 18-22, 1973.) Radio Science, vol. 8, Nov. 1973, p. 921-927.

Review of the magnetospheric morphology, using the method of the Delta B topology, where Delta B is the difference between the observed and a reference field. It is confirmed that Delta B continuously decreases inward to close distances from the earth at all local times. Extrapolating the statistical relation between Dst at the ground and the equatorial Delta B obtained from OGO-5 near perigee, it is shown that Dst is 54 gammas, when Delta B is zero at approximately 2 to 3 earth radii. Conversely, for a magnetically quiet condition as defined by Dst = 0, the average equatorial Delta B at these distances is -45 gammas. These results demonstrate the significance of the effects of the magnetospheric equatorial current that exists even at quiet times. A preliminary study of inclination shows that the field lines on the dusk side are more stretched out than on the dawn side. A comparison of declination on both sides indicates that the bending of the field lines toward the tail is greater near dusk than near dawn. These results suggest an appreciable dawn-dusk asymmetry in the configuration of the inner magnetospheric field. A.B.K.

**A74-14272\*****HIGH LATITUDE ELECTRIC FIELDS AND THE MODULATIONS RELATED TO INTERPLANETARY MAGNETIC FIELD PARAMETERS**

J. P. Heppner (NASA, Goddard Space Flight Center,

Laboratory for Space Physics, Greenbelt, Md.) Nov. 1973 16 p refs (AGU, NCAR, and NOAA, Chapman Memorial Symposium on Magnetospheric Motions, Boulder, Colo., June 18-22, 1973.) Radio Science, vol. 8, Nov. 1973, p. 933-948.

The meaning and characteristics of basic and average convection (i.e., electric field) patterns are described. The continuous existence of the basic convection pattern argues against treating magnetic field merging mechanisms as the fundamental cause of magnetospheric convection. However, whether related to merging or to some other mechanism, interplanetary magnetic field conditions significantly modulate the distribution, magnitudes, and boundaries of the convection pattern. A previous correlation between azimuthal angles of the interplanetary magnetic field and asymmetries in polar cap electric field distributions as seen by OGO-6 is reviewed. A new approach is taken to reveal correlations with the north-south angle and magnitude of the interplanetary field as well as additional features which correlate with the azimuthal angle. Both significant correlations and conditions which show a lack of correlation are found. Several aspects of the correlations appear to be particularly important. (Author)

**A74-14285\*****SUBSTORMS IN SPACE - THE CORRELATION BETWEEN GROUND AND SATELLITE OBSERVATIONS OF THE MAGNETIC FIELD**

R. L. McPherron, C. T. Russell, M. G. Kivelson, and P. J. Coleman, Jr. (California, University, Los Angeles, Calif.) Nov. 1973 18 p refs (AGU, NCAR, and NOAA, Chapman Memorial Symposium on Magnetospheric Motions, Boulder, Colo., June 18-22, 1973.) Radio Science, vol. 8, Nov. 1973, p. 1059-1076. (Grant NGL-05-007-004; Contract N00014-69-4016; Grant NSF GA-34148X; )

Several of the events criticized by Akasofu (1972) are reexamined. It is concluded that there is no simple one-to-one relationship between polar magnetic substorms and magnetospheric substorms as defined by midlatitude magnetograms. It appears that in some cases polar magnetic substorms occur during the growth phase of a magnetospheric substorm. Magnetospheric observations are more systematically organized by midlatitude onsets than by auroral zone onsets. The determination of onset times is discussed together with the determination of substorm similarity, the phenomenological model of magnetic variations during magnetospheric substorms, the event of February 25, 1967, and the complex event of February 13, 1968. G.R.

**A74-23676\*****RECENT IMPROVEMENTS IN OUR KNOWLEDGE OF NEUTRAL ATMOSPHERE STRUCTURE FROM SATELLITE DRAG MEASUREMENTS**

M. Roemer (Bonn, Universitaet, Bonn, West Germany) Feb. 1974 7 p ref (Union Radio Scientifique Internationale, Symposium on Incoherent Scatter, Tromso, Norway, June 12-16, 1973.) Radio Science, vol. 9, Feb. 1974, p. 223-229. Bundesministerium fuer Forschung und Technologie (Contract NAS1-11707-19) (BMBW-WRK-226; BMBW-SE-11)

Observational results on the density in the thermosphere and lower exosphere (i.e., within the altitude range from about 150 to about 1000 km) are discussed in this paper. Most observational results on total gas density were obtained from orbital drag and more recently also from in-situ drag analysis. The primary parameter measured is atmospheric density, with temperature as a secondary structural parameter deduced with the help of theory and/or atmospheric models. Both the merits and shortcomings of the drag analysis method are outlined in view of a comparison of temperature deduced from total density and kinetic gas temperature measured by incoherent scatter. Recent improvements of our knowledge of the known density variations are presented. (Author)



A74-24759\*

**ON THE LOCAL TIME DEPENDENCE OF THE BOW SHOCK WAVE STRUCTURE**

J. V. Olson and R. E. Holzer (California, University, Los Angeles, Calif.) 1 Mar. 1974 9 p ref Journal of Geophysical Research, vol. 79, Mar. 1, 1974, p. 939-947. Research supported by the National Research Council of Canada. (Grant NGR-05-007-276; Contract JPL-950403)

In the first 6 months after its launch, OGO 3 crossed the earth's bow shock over 500 times. From this group, a set of 494 shock crossings were chosen for analysis. These crossings, as they were recorded by the UCLA/JPL search coil magnetometer, were scanned and classified according to the nature of the plasma waves detected near the shock. More than 85% of the shocks detected fell into a single category showing the predominance of two independent wave trains near the shock, the higher frequency appearing upstream and the lower downstream. The other 15%, which constitute an upper limit, appear to be composed of shocks dominated by a single wave pattern and of chaotic shocks showing no orderly progression of wave frequencies as the shock was penetrated. This division of wave pattern was found to occur at all local times, that is, in all regions where the satellite penetrated the shock. (Author)

A74-28723

**EXOSPHERIC MODELS OF THE TOPSIDE IONOSPHERE**

J. Lemaire and M. Scherer (Institut d'Aeronomie Spatiale de Belgique, Brussels, Belgium) Mar. 1974 50 p Space Science Reviews, vol. 15, Mar. 1974, p. 591-640.

The historical evolution of the study of escape of light gases from planetary atmospheres is delineated, and the application of kinetic theory to the ionosphere is discussed. Ionospheric plasma becomes collisionless above the ion exobase, which is located near 1000 km altitude in the trough and polar regions and coincides with the plasmopause at lower latitudes. When the boundary conditions at conjugate points of a closed magnetic field line are different, interhemispheric particle fluxes exist from the high temperature point to the low temperature point, and from the point of larger concentrations to the point of smaller concentrations. Therefore the charge separation electric field in the exospheres is no longer given by the Pannekoek-Rosseland field. For nonuniform number densities and temperatures at the exobase, the observed  $r$  to the minus 4th power variation of the equatorial density distribution is recovered in the calculated density distributions. Taking account of plasma-sheet particle precipitation does not change the electric field and ionospheric ion distributions very much, at least for reasonable densities and temperatures of the plasma-sheet electrons and protons. (Author)

A74-30187\*#

**MEASUREMENTS OF THE COSMIC-RAY Be/B RATIO AND THE AGE OF COSMIC RAYS**

J. W. Brown, E. C. Stone, and R. E. Vogt (California Institute of Technology, Pasadena, Calif.) 1974 6 p refs In: International Cosmic Ray Conference, 13th, Denver, Colo., August 17-30, 1973, Proceedings. Volume 1. Denver, University of Denver, 1974, p. 484-489. NSF-supported research;

(Contract NASS-9312; Grant NGR-05-002-160)

The ratio Be/B depends on whether the confinement time of cosmic rays in the Galaxy is long or short compared to the radioactive half-life of Be-10. We report observations of this ratio which were obtained with a dE/dx-Cerenkov detector launched into a polar orbit on OGO-6 as part of the Caltech Solar and Galactic Cosmic Ray Experiment. Be/B ratios were determined for various rigidity thresholds up to 15 GV. We find no statistically significant rigidity dependence of the ratio, which is 0.41 plus or minus 0.02 when averaged over all observed cutoffs. Additional calculations suggest that if the present fragmentation parameters are correct, then the lifetime of cosmic rays in the Galaxy is less than 10 m.y. (Author)

A74-30660

**DETACHED PLASMA REGIONS IN THE MAGNETOSPHERE**

C. R. Chappell (California, University, La Jolla; Lockheed Research Laboratories, Palo Alto, Calif.) 1 May 1974 10 p refs Journal of Geophysical Research, vol. 79, May 1, 1974, p. 1861-1870.

(Contract N00014-73-C-0130)

Regions of high-density cold plasma have been observed outside the plasmasphere in the plasma trough region of the magnetosphere. These detached plasma regions may have densities as high as several hundred ions per cubic centimeter in the normally low-density plasma trough. The detached plasma regions are found across the day side of the magnetosphere, particular concentrations being in the afternoon-dusk sector. The regions are located at the plasmopause at dusk and progressively farther away for earlier local times in the early afternoon and morning. Detached plasma regions are observed during moderate to disturbed magnetic activity conditions. They exhibit a very complex spatial structure with sizes varying from thousands of kilometers down to less than 50 km in extent. The detached regions may be generated by variations in the magnetospheric convection electric field, which occurs during substorm activity. (Author)

A74-30667\*

**VARIATIONS IN THERMOSPHERIC COMPOSITION - A MODEL BASED ON MASS SPECTROMETER AND SATELLITE DRAG DATA**

L. G. Jacchia (Harvard College Observatory and Smithsonian Astrophysical Observatory, Cambridge, Mass.) 1 May 1974 5 p Journal of Geophysical Research, vol. 79, May 1, 1974, p. 1923-1927.

(Grant NGR-09-015-002)

The seasonal-latitudinal and the diurnal variations of composition observed by mass spectrometers on the OGO 6 satellite are represented by two simple empirical formulas. The formulas are of a very general nature and predict the behavior of these variations at all heights and for all levels of solar activity; they yield a satisfactory representation of the corresponding variations in total density, as derived from satellite drag. It is suggested that a seasonal variation of hydrogen may explain the abnormally low hydrogen densities at high northern latitudes in July 1964. (Author)

A74-30677\*

**A RELATION BETWEEN ELF HISS AMPLITUDE AND PLASMA DENSITY IN THE OUTER PLASMASPHERE**

K.-W. Chan, R. E. Holzer (California, University, Los Angeles, Calif.), and E. J. Smith (California Institute of Technology, Jet Propulsion Laboratory, Pasadena, Calif.) 1 May 1974 5 p refs Journal of Geophysical Research, vol. 79, May 1, 1974, p. 1989-1993.

(Grant NGR-05-007-276; Contracts JPL-950403; N00014-73-C-0130; )

Simultaneous observations of ELF hiss amplitude and plasma density on OGO 5 have been investigated. Passes through the region of variable plasma density in the outer plasmasphere have yielded a quantitative relation between the hiss amplitude, the plasma density, and the plasma density corresponding to the threshold of wave detection. It is suggested that this dependence of wave amplitude on plasma density is a source effect and is related to the wave-particle interaction in the outer plasmasphere that gives rise to hiss. (Author)

A74-36735

**DIURNAL VARIATION OF THE NEUTRAL THERMOSPHERIC WINDS DETERMINED FROM INCOHERENT SCATTER RADAR DATA**

R. G. Roble (National Center for Atmospheric Research, Boulder, Colo.), B. A. Emery (MIT, Cambridge, Mass.), J. E. Salah (MIT, Lexington, Mass.), and P. B. Hays (Michigan, University, Ann Arbor, Mich.) 1 Jul. 1974 9 p ref Journal of Geophysical Research, vol. 79, July 1, 1974, p. 2868-2876.

A technique is described to derive the pressure forces in terms of the latitudinal and longitudinal variation of the exospheric temperature that will reproduce the measured values of both the exospheric temperature and the wind component along the geomagnetic field line when it is used in a dynamic model of the neutral thermosphere. The atmospheric response to various harmonic forcing functions is determined from a three-dimensional dynamic model of the neutral thermosphere, the ion drag being specified by the electron density measurements. The calculated response for a number of runs with the dynamic model is used to construct the appropriate diurnal forcing function through a least squares fit of the measured and calculated diurnal variation of the longitudinal gradient of the exospheric temperature and the neutral wind vector in the geomagnetic declination direction. F.R.L.

A74-36747\*

**THERMOSPHERIC 'TEMPERATURES'**

H. G. Mayr, I. Harris, and N. W. Spencer (NASA, Goddard Space Flight Center, Greenbelt, Md.) 1 Jul. 1974 4 p refs Journal of Geophysical Research, vol. 79, July 1, 1974, p. 2921-2924.

The present work attempts to illustrate some of the differences one would expect to find between inferred thermospheric temperatures (i.e., inferred from satellite drag observation of mass density or from molecular nitrogen in situ mass spectrometer measurements) and direct gas temperature measurements (as have been made on board the San Marco satellite). The various temperatures are simulated with theoretical models for the diurnal and annual variations in the thermosphere. P.T.H.

A74-37631\*

**NON-RELATIVISTIC SOLAR ELECTRONS**

R. P. Lin (California, University, Berkeley, Calif.) Jul. 1974 68 p refs Space Science Reviews, vol. 16, June-July 1974, p. 189-256.

(Grant NGL-05-003-017)

(NSSDC-ID-68-014A-04-0S)

Summary of both the direct spacecraft observations of nonrelativistic solar electrons, and observations of the X-ray and radio emission generated by these particles at the sun and in the interplanetary medium. These observations bear on three physical processes basic to energetic particle phenomena: (1) the acceleration of particles in tenuous plasmas; (2) the propagation of energetic charged particles in a disordered magnetic field, and (3) the interaction of energetic charged particles with tenuous plasmas to produce electromagnetic radiation. Because these electrons are frequently accelerated and emitted by the sun, mostly in small and relatively simple flares, it is possible to define a detailed physical picture of these processes. In many small solar flares nonrelativistic electrons accelerated during flash phase constitute the bulk of the total flare energy. Thus the basic flare mechanism in these flares essentially converts the available flare energy into fast electrons. Nonrelativistic electrons exhibit a wide variety of propagation modes in the interplanetary medium, ranging from diffusive to essentially scatter-free. This variability in the propagation may be explained in terms of the distribution of interplanetary magnetic field fluctuations. (Author)

A74-37632\*

**RELATIVISTIC ELECTRON EVENTS IN INTERPLANETARY SPACE**

G. M. Simnett (California, University, Riverside, Calif.) Jul. 1974 67 p refs Space Science Reviews, vol. 16, June-July 1974, p. 257-323.

(Grant NGR-05-008-002; Contract N00014-69-A-0200-5004)

Review of relativistic electron events observed in interplanetary space. The different types of event are identified and illustrated. The relationships between solar X-ray and radio emissions and relativistic electrons are examined, and the relevance of the observations to solar flare acceleration

models is discussed. A statistical analysis of electron spectra, the electron/proton ratio and propagation from the flare site to the earth is presented. A model is outlined which can account for the release of electrons from the sun in a manner consistent with observations of energetic solar particles and electromagnetic solar radiation. (Author)

A74-43679\*

**DEPENDENCE OF FIELD-ALIGNED ELECTRON PRECIPITATION OCCURRENCE ON SEASON AND ALTITUDE**

F. W. Berko and R. A. Hoffman (NASA, Goddard Space Flight Center, Greenbelt, Md.) 1 Sep. 1974 6 p Journal of Geophysical Research, vol. 79, Sept. 1, 1974, p. 3749-3754.

An examination of factors affecting the occurrence of field-aligned 2.3-keV electron precipitation has been performed by using data from more than 7500 orbits of the polar-orbiting satellite OGO 4. Both season and altitude were found to be parameters that are directly related to the probability of occurrence. The highest probabilities occurred when the measurements were made at altitudes from 800 km to apogee (914 km), except during summer. In this altitude interval, the electron precipitation was more likely to be field-aligned during winter than during any other season. The analysis suggests the establishment by electrostatic charge layers of localized electric fields parallel to the magnetic field. The resulting potential distribution focuses the electron beam along the field lines in the region between the charge layers but destroys the focused beam below the lower layer, and thus an altitude dependence is created. (Author)

A74-43691\*

**PLASMA TAIL INTERPRETATIONS OF PRONOUNCED DETACHED PLASMA REGIONS MEASURED BY OGO 5**

A. J. Chen and J. M. Grebowsky (NASA, Goddard Space Flight Center, Greenbelt, Md.) 1 Sep. 1974 5 p refs Journal of Geophysical Research, vol. 79, Sept. 1, 1974, p. 3851-3855.

Measurements of the light ion thermal plasma distribution in the magnetosphere frequently show apparent isolated patches of enhanced plasma density in the trough region beyond the main plasmasphere. These patches of light ions viewed along a satellite orbit appear detached from the main plasmasphere. By using a simple time-dependent convection model to determine the length of time a magnetic flux tube has been closed and in daylight (a rough indicator of the expected equatorial plasma density variation), the most prominent 'detached' regions measured by the mass spectrometer on OGO 5 in the noon-dusk quadrant are seen on a global scale to be readily interpreted as filamentary extensions of the plasmasphere, called plasma tails. Hence on a global scale the pronounced detached regions may be attached to the main plasmasphere. (Author)

A74-44202\*

**INTENSITY VARIATION OF ELF HISS AND CHORUS DURING ISOLATED SUBSTORMS**

R. M. Thorne, K. F. Fiske, S. R. Church (California, University, Los Angeles, Calif.), and E. J. Smith (California Institute of Technology, Jet Propulsion Laboratory, Pasadena, Calif.) Sep. 1974 4 p refs Geophysical Research Letters, vol. 1, Sept. 1974, p. 193-196.

(Contract NAS7-100; Grants NSF GA-34148; NSF GA-28045)

(NSSDC-ID-69-051A-22-PM)

Electromagnetic ELF emissions (100-1000 Hz) observed on the polar-orbiting OGO-6 satellite within three hours of the dawn-dusk meridian consistently exhibit a predictable response to isolated substorm activity. Near dawn, the emissions intensify during the substorm and then subside following the magnetic activity; the waves are most intense at L greater than 4, exhibit considerable structure and have been primarily identified as chorus. At dusk the response is entirely different; the wave intensity falls to background levels

during substorm activity but subsequently intensifies, usually reaching levels well in excess of that before the disturbance. The emissions near dusk extend to low L, are relatively featureless, and have been identified as plasmaspheric hiss. These features are interpreted in terms of changes in the drift orbits of outer-zone electrons which cyclotron resonate with ELF waves. (Author)

## A75-11221\*

**MAGNETOPAUSE ROTATIONAL FORMS**

B. U. O. Sonnerup (Dartmouth College, Hanover, N.H.) and B. G. Ledley (NASA, Goddard Space Flight Center, Greenbelt, Md.) 1 Oct. 1974 6 p refs *Journal of Geophysical Research*, vol. 79, Oct. 1, 1974, p. 4309-4314. (Grant NGR-30-001-040) (NSSDC-ID-68-014A-15-PM)

Magnetic field data from the Goddard Space Flight Center magnetometer experiment on board OGO 5 are analyzed by the minimum-variance technique for two magnetopause crossings, believed to provide the best evidence presently available of magnetopause rotational discontinuities. Approximate agreement with predictions from MHD and first-order orbit theory is found, but available low-energy electron data suggest the presence of significant non-MHD effects. The paper also illustrates an improved method for data interval selection, a new magnetopause hodogram representation, and the utility of data simulation. (Author)

## A75-11226\*

**IS THE RED ARC A GOOD INDICATOR OF IONOSPHERE-MAGNETOSPHERE CONDITIONS**

A. F. Nagy (Michigan, University, Ann Arbor, Mich.), L. H. Brace, N. C. Maynard (NASA, Goddard Space Flight Center, Greenbelt, Md.), and W. B. Hanson (Texas, University, Richardson, Tex.) 1 Oct. 1974 3 p refs *Journal of Geophysical Research*, vol. 79, Oct. 1, 1974, p. 4331-4333. (NSSDC-ID-69-051A-02-PM; NSSDC-ID-69-051A-03-PM)

Weak red arcs were observed on the two consecutive nights of July 12-13 and July 13-14, 1969, at Richland, Washington, whereas no red arcs were detectable on the nights preceding and following the observations. Satellite (OGO 6) data of electron temperature and density, low-frequency ac electric field, and suprathermal electron flux corresponding to the conjugate region of Richland show no significant variations during these days. The data show elevated electron temperatures and enhanced low-frequency ac noise levels at the expected red arc position in the neighborhood of the density trough, as indicated by previous observations. The data appear to indicate that the optical criterion of red arc occurrence would lead to the conclusion of significantly different ionosphere-magnetosphere conditions during these four nights, whereas the more detailed in situ data show that the conditions were very similar. (Author)

## A75-11227\*

**AN UPPER LIMIT TO THE PRODUCT OF NO AND O DENSITIES FROM 105 TO 120 KM**

T. M. Donahue (Pittsburgh, University, Pittsburgh, Pa.) 1 Oct. 1974 3 p refs *Journal of Geophysical Research*, vol. 79, Oct. 1, 1974, p. 4337-4339. (Grant NGR-39-011-155; NSF GA-37744) (NSSDC-ID-69-051A-26-PM)

From the OGO 6 horizon-scanning-photometer data a useful upper limit can be set to the radiance of nightglow in the O-NO afterglow continuum above 105 km. The upper limit is a factor of about 5 less than the product of observed NO densities and Jacchia (1971) O model densities. (Author)

## A75-11853\*

**IN-SITU OBSERVATIONS OF IRREGULAR IONOSPHERIC STRUCTURE ASSOCIATED WITH THE PLASMAPAUSE**

H. A. Taylor, Jr. (NASA, Goddard Space Flight Center, Laboratory for Planetary Atmospheres, Greenbelt, Md.) and

G. R. Cordier (Aero Geo Astro Co., College Park, Md.) Sep. 1974 8 p ref (Union Radio Scientifique Internationale, Conference on Incoherent Scatter, Tromso, Norway, June 12-16, 1973.) *Planetary and Space Science*, vol. 22, Sept. 1974, p. 1289-1296.

Additional studies of the ion composition results obtained from the OGO-6 satellite support earlier observations of irregularities in the distribution of H(+) and He(+) within the light ion trough near L = 4, which has been associated with the plasmopause. These irregularities are in the form of sub-troughs superimposed upon the major midlatitude decrease of the light ions. In the sub-troughs, ionization depletions and recoveries of as much as an order of magnitude are observed within a few degrees of latitude, usually exhibited in a pattern which changes significantly with longitude as the earth rotates beneath the relatively fixed satellite orbit. The location and properties exhibited by these sub-troughs appear to be consistent with the concept of a plasmasphere distortion in the form of 'plasmatails' resulting from the combined effects of magnetospheric convection plus corotation. F.R.L.

## A75-12368\*

**VARIATION WITH INTERPLANETARY SECTOR OF THE TOTAL MAGNETIC FIELD MEASURED AT THE OGO 2, 4 AND 6 SATELLITES**

R. A. Langel (NASA, Goddard Space Flight Center, Greenbelt, Md.) Oct. 1974 13 p refs *Planetary and Space Science*, vol. 22, Oct. 1974, p. 1413-1425.

## A75-12370

**DEPENDENCE OF THE MAGNETOPAUSE POSITION ON THE SOUTHWARD INTERPLANETARY MAGNETIC FIELD**

K. Maezawa (Tokyo, University, Tokyo, Japan) Oct. 1974 11 p refs *Planetary and Space Science*, vol. 22, Oct. 1974, p. 1443-1453.

Statistical analysis of the distance to the dayside magnetopause, aimed at detecting the possible dependence of the dayside magnetic flux on the polarity of the interplanetary magnetic field. It is found that the normalized size of the dayside magnetosphere at the time of southward interplanetary magnetic field direction is smaller than at the time of northward interplanetary field direction. The difference in the magnetopause position between the two interplanetary field polarity conditions ranges from 0 to 2 earth radii. The implications of this finding and of other ones are discussed. M.V.E.

## A75-12439\*

**HIGH LATITUDE MINOR ION ENHANCEMENTS - A CLUE FOR STUDIES OF MAGNETOSPHERE-ATMOSPHERE COUPLING**

H. A. Taylor, Jr. (NASA, Goddard Space Flight Center, Thermosphere and Exosphere Center, Greenbelt, Md.) Nov. 1974 9 p refs (International Association of Geomagnetism and Aeronomy, Symposium on Dynamics, Chemistry and Thermal Processes in the Ionosphere and Thermosphere, Kyoto, Japan, Sept. 18-20, 1973.) *Journal of Atmospheric and Terrestrial Physics*, vol. 36, Nov. 1974, p. 1815-1823.

An investigation is conducted of upper ionosphere molecular ion composition data, which because of the unexpected, abrupt enhancements sometimes exhibited at high latitudes, may indirectly offer additional clues to understanding the processes by which the lower atmosphere becomes perturbed. It is found that molecular ion irregularities are sometimes localized in a relatively narrow region of time and space. The abruptness of these events suggests that lower atmosphere energetic processes presumed responsible for the ion enhancements may also be narrowly distributed. G.R.

## A75-12453\*

**MAGNETIC STORM DYNAMICS OF THE THERMOSPHERE**

H. G. Mayr (NASA, Goddard Space Flight Center,

Laboratory for Planetary Atmospheres, Greenbelt, Md.) and H. Volland (NASA, Goddard Space Flight Center, Laboratory for Planetary Atmospheres, Greenbelt, Md.; Bonn, Universitaet, Bonn, West Germany) Nov. 1974 12 p refs (International Association of Geomagnetism and Aeronomy, Symposium on Dynamics, Chemistry and Thermal Processes in the Ionosphere and Thermosphere, Kyoto, Japan, Sept. 18-20, 1973.) Journal of Atmospheric and Terrestrial Physics, vol. 36, Nov. 1974, p. 2025-2036.

A theoretical study of the Dst component of magnetic storms is presented. The dynamic characteristics are found significantly different for Joule dissipation and electron precipitation, leading to the conclusion that the former is probably the predominant heat source for the upper thermosphere. Composition measurements on OGO-6, which reveal markedly different characteristics in N<sub>2</sub>, O and He, can be explained on the basis of energy advection and diffusive mass transport by thermospheric winds. Essential features in the F<sub>2</sub>-region response are explicable in terms of these dynamic processes. Electric field induced motions are estimated and it is concluded that resultant adiabatic heating could be significant. (Author)

**A75-13173#**  
**SOLAR RADIATION ASYMMETRIES AND HELIOSPHERIC GAS HEATING INFLUENCING EXTRATERRESTRIAL UV DATA**

H. J. Fahr and G. Lay (Bonn, Universitaet, Bonn, West Germany) 1974 7 p ref In: Space research XIV; Proceedings of the Sixteenth Plenary Meeting, Konstanz, West Germany, May 23-June 5, 1973. Berlin, East Germany, Akademie-Verlag GmbH, 1974, p. 567-573.

Up to now the interpretation of extraterrestrial Lyman alpha data of the satellite OGO 5 has been based on the assumption of spherically symmetric solar radiation fields. This assumption, however, turns out to be very crude and it is shown that appreciable improvement in the interpretation of OGO 5 Lyman-alpha data can be achieved if actual solar radiation asymmetries both in the corpuscular and in the electromagnetic fluxes are taken into account. Methods of correcting for asymmetries in heliographic latitude and longitude are developed and facilitate the deduction of interstellar parameters. The galactic Lyman-alpha background is found to be below 10R; the density and temperature of the nearby interstellar gas have been obtained as 0.1 per cu cm and 4,000 to 6,000 K. The higher temperatures indicated by the OGO 5 data are shown to be due to the fact that the interstellar hydrogen penetrating into the solar system is subjected to a heliospheric heating process caused by elastic collisions with solar protons. (Author)

**A75-13176#**  
**RECENT ADVANCES IN COMETARY PHYSICS AND CHEMISTRY**

L. Biermann (Max-Planck-Institut fuer Physik und Astrophysik, Munich, West Germany) 1974 7 p ref In: Space research XIV; Proceedings of the Sixteenth Plenary Meeting, Konstanz, West Germany, May 23-June 5, 1973. Berlin, East Germany, Akademie-Verlag GmbH, 1974, p. 593-599.

This review discusses mainly the observations of some recent comets by OAO 2 and OGO 5 and their interpretation in terms of the physical processes and the chemical constitution of comets. The most important finding is that hydrogen atoms are much more abundant in cometary atmospheres than those molecules which make up the ordinary coma; from the intensity of the OH emissions it is concluded that ordinary water is a main constituent. The brightness in Lyman-alpha is at least as large as that due to emission bands in the ordinary optical range, and particularly the size of the hydrogen atmosphere greatly exceeds that of the ordinary coma. Finally, some plans for fly-by missions to comets are dealt with, and their potential and promise is discussed. (Author)

**A75-15342\***

**SOLAR ENERGETIC PARTICLE EVENT WITH HE-3/HE-4 GREATER THAN 1**

V. K. Balasubrahmanyam (NASA, Goddard Space Flight Center, Greenbelt, Md.) and A. T. Serlemitsos (Computer Sciences Corp., Silver Spring, Md.) 6 Dec. 1974 3 p refs Nature, vol. 252, Dec. 6, 1974, p. 460-462.

An unusual solar event involving the detection of a He-3/He-4 ratio of about 1.5 was observed with the aid of the cosmic-ray telescopes of OGO-V on May 28, 1969. A theory dealing with the production of H-2, H-3, and He-3 in solar events is considered together with the conditions which would have to be satisfied in order to explain the observed very high helium isotope ratio in terms of the theory. G.R.

**A75-16217\***

**ACCELERATION OF ELECTRONS IN ABSENCE OF DETECTABLE OPTICAL FLARES DEDUCED FROM TYPE III RADIO BURSTS, H ALPHA ACTIVITY AND SOFT X-RAY EMISSION**

S. R. Kane (California, University, Berkeley, Calif.), R. W. Kreplin (U.S. Navy, Naval Research Laboratory, Washington, D.C.), M.-J. Martres, M. Pick, and I. Soru-Escout (Paris, Observatoire, Meudon, Hauts-de-Seine, France) Oct. 1974 15 p refs Solar Physics, vol. 38, Oct. 1974, p. 483-497.

(Grant NGR-05-003-510)

(NSSDC-ID-68-014A-04-PS; NSSDC-ID-69-051A-18-PM)

**A75-16437**

**CORRELATED SATELLITE MEASUREMENTS OF PROTON PRECIPITATION AND PLASMA DENSITY**

F. Soraas and L. E. Berg (Bergen, Universitet, Bergen, Norway) 1 Dec. 1974 10 p refs Journal of Geophysical Research, vol. 79, Dec. 1, 1974, p. 5171-5180. Research supported by the Royal Norwegian Council for Scientific and Industrial Research.

The main experimental findings relating plasma densities in the equatorial plane (OGO 5) to proton precipitation at high latitudes (Esro 1A), obtained from nearly simultaneous observations in the evening/midnight local time sector, are summarized. When the plasma density is high out to large L values, most common during quiet geomagnetic conditions, the greater than 100-keV protons precipitation has no sharp equatorward boundary. The change from an anisotropic pitch angle distribution peaked at 90 deg with the magnetic field lines to an isotropic one is gradual with increasing L. When a sharp plasmopause is detected and the plasma density outside the plasmopause is low, there is a region outside the plasmopause where the proton flux is highly anisotropic. A rather abrupt transition to an isotropic pitch angle distribution takes place at approximately 1 earth radius outside the plasmopause. There is thus a region outside the plasmopause where the proton population is stable to precipitation losses. (Author)

**A75-16440\***

**'HISSLERS' - QUASI-PERIODIC (T APPROXIMATELY EQUAL TO 2 SEC) VLF NOISE FORMS AT AURORAL LATITUDES**

I. M. Ungstrup and D. L. Carpenter (Stanford University, Stanford, Calif.) 1 Dec. 1974 6 p refs Journal of Geophysical Research, vol. 79, Dec. 1, 1974, p. 5196-5201. (Grants NGL-05-020-008; NSF GA-32590X; NSF GA-28042; NSF GV-28840X)

**A75-16449**

**NORTH-SOUTH ASYMMETRIES IN THE THERMOSPHERE DURING THE LAST MAXIMUM OF THE SOLAR CYCLE**

F. Barlier, C. Jaeck (Centre d'Etudes et de Recherches Geodynamiques et Astronomiques, Grasse, Alpes-Maritimes, France), P. Bauer (CNET, Issy-les-Moulineaux,

Hauts-de-Seine, France), G. Thullier (CNRS, Service d'Aeronomie, Verrieres-le-Buisson, Essonne, France), and G. Kockarts (Institut d'Aeronomie Spatiale de Belgique, Brussels, Belgium) 1 Dec. 1974 13 p Journal of Geophysical Research, vol. 79, Dec. 1, 1974, p. 5273-5285.

A large volume of data (temperatures, densities, concentrations, winds) has been accumulated showing that in addition to seasonal changes in the thermosphere, annual variations are present and have a component that is a function of latitude. It appears that the helium concentrations have much larger variations in the southern hemisphere than in the northern hemisphere; the same holds true for the exospheric temperatures deduced from OGO 6 data. The bulge of density tends to stay over the southern hemisphere, whereas winds show a tendency to blow northward across the equator. More energy seems to be available for the thermosphere in the southern hemisphere during the equinoxes; this may be the result of an asymmetry in the geomagnetic field or an asymmetrical dissipation of tidal waves induced by an asymmetrical worldwide ozone distribution. (Author)

**A75-16631\***  
**THE SOLAR CYCLE VARIATION OF THE SOLAR WIND HELIUM ABUNDANCE**

K. W. Ogilvie (NASA, Goddard Space Flight Center, Greenbelt, Md.) and J. Hirshberg (High Altitude Observatory, Boulder, Colo.) 1 Nov. 1974 8 p ref Journal of Geophysical Research, vol. 79, Nov. 1, 1974, p. 4595-4602. (NSSDC-ID-68-014A-17-OS)

**A75-16634\***  
**ELECTRIC FIELD MEASUREMENTS ACROSS THE HARANG DISCONTINUITY**

N. C. Maynard (NASA, Goddard Space Flight Center, Laboratory for Planetary Atmospheres, Greenbelt, Md.) 1 Nov. 1974 12 p refs Journal of Geophysical Research, vol. 79, Nov. 1, 1974, p. 4620-4631.

The Harang discontinuity, the area separating the positive and negative bay regions in the midnight sector of the auroral zone, is a focal point for changes in behavior of many phenomena. Through this region the electric field, in a frame corotating with the earth, rotates through the west from a basically northward field in the positive bay region to a basically southward field in the negative bay region, appearing as a reversal in a single-axis measurement of the north-south component. Thirty-two of these reversals have been identified in the OGO 6 data from November and December 1969. The discontinuity is dynamic in nature, moving southward and steepening its latitudinal profile as magnetic activity is increased. As activity decreases, it relaxes poleward and spreads out in latitudinal width. It occurs over several hours of magnetic local time. (Author)

**A75-16637\***  
**THE MEASUREMENT OF COLD ION DENSITIES IN THE PLASMA TROUGH**

K. K. Harris (Lockheed Research Laboratories, Palo Alto, Calif.) 1 Nov. 1974 7 p refs Journal of Geophysical Research, vol. 79, Nov. 1, 1974, p. 4654-4660. Research supported by the Lockheed Independent Research Program; (Contracts NAS5-23106; NASw-2551) (NSSDC-ID-68-014A-18-PM)

The cold ion density in the plasma trough region is an important fundamental parameter in the currently proposed mechanisms to describe magnetospheric dynamics. Direct in situ measurements of the cold ion density are generally difficult owing to uncertainties in vehicle potentials and ion temperatures. It is shown that the light ion mass spectrometer from OGO 5 was very successful in acquiring these data and that vehicle potentials appear not to have been a prohibitive factor. The cold ion plasma trough data show a great deal of variability, indicating a strong dependence on the state of the convection electric field; consequently, average values of cold ion densities in the

plasma trough may be significantly different from the actual time-dependent values. The local time plot of plasma trough densities at  $L = 7$  for data acquired over a 1-year period shows the anticipated increase in cold ion density during the daytime and the expected decrease in cold ion density during dusk and early nighttime. (Author)

**A75-18717\***  
**A SEARCH FOR SOLAR NEUTRONS DURING SOLAR FLARES**

S. O. Ifedili (New Hampshire, University, Durham, N.H.) Nov. 1974 9 p ref Solar Physics, vol. 39, Nov. 1974, p. 233-241.

(Contract NAS5-9313; Grant NGR-30-002-088)

A new upper limit to the 1-20 MeV neutrons produced at the sun during large solar flares was obtained as a result of measurements made by a neutron detector on board the OGO-6 satellite. It was found that the 1-20 MeV solar neutron flux for the Nov. 2, June 13, June 15, Sept. 25, and Dec. 19, 1969, solar flare events cannot be greater than 0.05 n per sq cm per sec at the 95% confidence level. These measurements are consistent with the models proposed by Lingenfelter (1969) and Lingenfelter and Ramaty (1967) for solar neutron production during solar flares. P.T.H.

**A75-19127\***  
**THE SOLAR WIND AND MAGNETOSPHERIC DYNAMICS**

C. T. Russell (California, University, Los Angeles, Calif.) 1974 45 p refs In: Correlated interplanetary and magnetospheric observations; Proceedings of the Seventh ESLAB Symposium, Saugau, West Germany, May 22-25, 1973. Dordrecht, D. Reidel Publishing Co., 1974, p. 3-47. (Contract NAS5-9098; Grant NGR-05-007-004; NSF GA-34148X; )

The dynamic processes involved in the interaction between the solar wind and the earth's magnetosphere are reviewed. The evolution of models of the magnetosphere is first surveyed. The existence of the auroral substorm and the cyclical polar magnetic substorm is evidence that the magnetosphere is a dynamic system. The dynamic changes occurring in the magnetosphere, including erosion of the magnetopause, changes in the size of the polar cap, variations in the flaring angle of the tail, neutral point formation, plasma sheet motions, and the inward collapse of the midnight magnetosphere, are discussed. The cyclical variations of geomagnetic activity are explained in terms of the control of the solar wind-magnetosphere interaction by the north-south component of the interplanetary magnetic field. Present phenomenological models allow prediction of geomagnetic activity from interplanetary measurements, but modeling of detailed magnetospheric processes is still in its infancy. A.T.S.

**A75-19134\***  
**OGO-5 OBSERVATIONS OF THE MAGNETOPAUSE**  
C. T. Russell, M. G. Kivelson (California, University, Los Angeles, Calif.), and M. Neugebauer (California Institute of Technology, Jet Propulsion Laboratory, Pasadena, Calif.) 1974 19 p In: Correlated interplanetary and magnetospheric observations; Proceedings of the Seventh ESLAB Symposium, Saugau, West Germany, May 22-25, 1973. Dordrecht, D. Reidel Publishing Co., 1974, p. 139-157. (Contract NAS7-100; Grant NGL-05-007-004)

OGO-5 observations show not only that the average position of the magnetopause boundary moves in response to changes in dynamic pressure, but also that it moves in response to changes in the north-south component of the interplanetary field. Further, the boundary often oscillates about its average position as waves propagate along the boundary away from the nose region. The variation of the magnetic field through the boundary at times can be a simple rotation with no change in magnitude, and at other times can resemble a simple tangential discontinuity. However, it often displays complex patterns such as field enhancements on the magnetospheric side of the boundary or apparently

uncorrelated field strength and direction changes. One particularly simple boundary crossing has been studied in detail with both positive ion data and magnetic field data. In this case, the electron and ion currents could be separately deduced and the structure agreed with that expected for a Chapman-Ferraro boundary with almost complete neutralization. (Author)

A75-19138

**THE EARTH'S BOW SHOCK FINE STRUCTURE**

V. Formisano (CNR, Laboratorio di Ricerca e Tecnologia per lo Studio del Plasma nello Spazio, Rome, Italy) 1974 37 p refs In: Correlated interplanetary and magnetospheric observations; Proceedings of the Seventh ESLAB Symposium, Saugau, West Germany, May 22-25, 1973. Dordrecht, D. Reidel Publishing Co., 1974, p. 187-223. Research supported by the Consiglio Nazionale delle Ricerche.

Review of the information on the earth's bow shock structure obtained with the aid of the OGO 5 and HEOS 1 satellites. The experimental results concerning the downstream plasma and the fluid-parameter jump across the shock are compared with the predictions of the fluid model, in order to test the validity of the Rankine-Hugoniot relations for the earth's bow shock. Following a discussion of the determination of the shock velocity, which is the fundamental quantity needed in order to estimate the typical lengths associated with bow shock phenomena, a schematic classification of the data available is introduced on the basis of whether the Alfvén Mach number is above or below a critical value and the plasma beta is of the order of unity or smaller. Detailed observations of the shock structures and the associated wave phenomena are then reported for each of the possible regimes, including bow shocks with laminar, quasi-laminar, turbulent, quasi-turbulent, and mixed structures. In the case of the turbulent bow shock the essential question seems to be the way in which the strong anomalous ion dissipation takes place in the shock transition. In the mixed structures the low-frequency upstream waves appear to determine the essential structural features. A.B.K.

A75-19330\*

**SIMULTANEOUS PARTICLE AND FIELD OBSERVATIONS OF FIELD-ALIGNED CURRENTS**

F. W. Berko, R. A. Hoffman (NASA, Goddard Space Flight Center, Greenbelt, Md.), R. K. Burton, and R. E. Holzer (California, University, Los Angeles, Calif.) 1 Jan. 1975 10 p refs Journal of Geophysical Research, vol. 80, Jan. 1, 1975, p. 37-46. (Grant NGR-05-007-276; Contract JPL-950403)

Simultaneous measurements of low-energy precipitating electrons and magnetic fluctuations from the low-altitude polar-orbiting satellite OGO 4 have been compared. Analysis of the two sets of experimental data for isolated events led to the classification of high-latitude field-aligned currents as purely temporal or purely spatial variations. Magnetic field disturbances calculated by using these simple current models and the measured particle fluxes were in good agreement with measured field values. Although fluxes of electrons of greater than 1 keV were detected primarily on the night side, magnetometer disturbances indicative of field-aligned currents were seen at all local times, in both the visual auroral regions and the day side polar cusp. Thus electrons with energies of less than about 1 keV are the prime charge carriers in high-latitude day side field-aligned currents. (Author)

A75-19349\*

**SUBSTORM AND INTERPLANETARY MAGNETIC FIELD EFFECTS ON THE GEOMAGNETIC TAIL LOBES**

M. N. Caan, McPherron, and C. T. Russell (California, University, Los Angeles, Calif.) 1 Jan. 1975 4 p refs Journal of Geophysical Research, vol. 80, Jan. 1, 1975, p. 191-194.

(Grant NGR-05-007-004; Contract N00014-6-A-200-4016; Grant NSF GA-34148X; )

A75-20360\*

**THE EQUATORIAL HELIUM ION TROUGH AND THE GEOMAGNETIC ANOMALY**

S. Chandra (NASA, Goddard Space Flight Center, Laboratory for Planetary Atmospheres, Greenbelt, Md.) Feb. 1975 10 p ref Journal of Atmospheric and Terrestrial Physics, vol. 37, Feb. 1975, p. 359-367.

The latitudinal characteristics of He<sup>+</sup> in the equatorial region are compared with those of O<sup>+</sup> and H<sup>+</sup>. These ions, in different altitude regions, exhibit certain features which are characteristics of the ionospheric geomagnetic anomaly. It is shown that the latitudinal distributions of these ions are related to their vertical distribution at the equator via their respective scale heights and the geomagnetic dipole geometry. To a first order, the positions of the latitudinal maxima of a given ion may be related to its peak altitude at the equator by a proposed expression.

(Author)

A75-22613#

**MAGNETOSPHERIC SUBSTORM ASSOCIATED WITH SC**

T. Ondoh (Ministry of Posts and Telecommunications, Radio Research Laboratories, Tokyo, Japan) 1974 6 p In: International Symposium on Solar-Terrestrial Physics, Sao Paulo, Brazil, June 17-22, 1974, Proceedings. Volume 2. Sao Jose dos Campos, Brazil, Instituto de Pesquisas Espaciais, 1974, p. 16-21.

The present work describes on the basis of magnetograms at Kiruna and Honolulu and OGO-5 magnetograms a magnetospheric substorm which occurred simultaneously with the sudden commencement of 2345 UT, September 30, 1968. The storm occurred following a gradual development of the plasma sheet thinning under a continuation of the southward interplanetary B<sub>z</sub> field. Gradual increases of B and B<sub>x</sub> fields and gradual decrease of the B<sub>z</sub> field were observed at the OGO-5 during plasma sheet thinning. A large increase of the B<sub>y</sub> field began simultaneously with a southward turning of the northward B<sub>z</sub> field at the OGO-5 during sudden commencement rise time. This increase, which amounted to 30 gammas, may be explained by the field-aligned current of 0.024 A/m flowing into the dawn-side auroral zone. P.T.H.

A75-22671\*#

**F REGION WIND COMPONENTS IN THE MAGNETIC MERIDIAN FROM OGO 4 TROPICAL AIRGLOW OBSERVATIONS**

J. A. Bittencourt (Texas, University, Dallas, Tex.; Instituto de Pesquisas Espaciais, Sao Jose dos Campos, Brazil), G. T. Hicks (U.S. Navy, Naval Research Laboratory, Washington, D.C.), and B. A. Tinsley (Texas, University, Dallas, Texas) 1974 10 p In: International Symposium on Solar-Terrestrial Physics, Sao Paulo, Brazil, June 17-22, 1974, Proceedings. Volume 3. Sao Jose dos Campos, Brazil, Instituto de Pesquisas Espaciais, 1974, p. 328-337. (Grant NGR-44-004-142)

A75-22759\*

**PITCH ANGLE DISTRIBUTIONS OF ENERGETIC ELECTRONS IN THE EQUATORIAL REGIONS OF THE OUTER MAGNETOSPHERE - OGO-5 OBSERVATIONS**

H. I. West, Jr. and R. M. Buck (California, University, Livermore, Calif.) 1974 12 p ref In: Magnetospheric physics; Proceedings of the Summer Advanced Study Institute, Sheffield, England, August 13-24, 1973. (A75-22752 08-46) Dordrecht, D. Reidel Publishing Co., 1974, p. 93-104. AEC-sponsored research (NASA ORDER S-7001-G)

A75-22774\*

**PLASMA INSTABILITY MODES RELATED TO THE**

**EARTH'S BOW SHOCK**

W. W. Greenstadt and R. W. Fredricks (TRW Systems Group, Redondo Beach, Calif.) 1974 10 p refs In: Magnetospheric physics; Proceedings of the Summer Advanced Study Institute, Sheffield, England, August 13-24, 1973. Dordrecht, D. Reidel Publishing Co., 1974, p. 281-290.

(Contracts NASw-2398; NAS5-9278)

The present work examines the status of physical interpretations of some of the microscopic phenomena occurring in bow shock structures. A categorization of microscopic phenomena is given, and it is examined how various modes may or may not be invoked in explaining spacecraft measurements on bow structure. The macroscopic and observational context of the bow shock as presently understood is first defined, and then some of the microscopic plasma physical phenomena which might be expected to be found associated with certain macroscopic structures are outlined. Some problems in the use of the bow shock to test plasma shock theory are then discussed. P.T.H.

**A75-23707\*****STRUCTURE OF THE QUASI-PERPENDICULAR LAMINAR BOW SHOCK**

E. W. Greenstadt, F. L. Scarf (TRW Systems Group, Redondo Beach, Calif.), C. T. Russell (California, University, Los Angeles, Calif.), V. Formisano (CNR, Laboratorio de Plasma nello Spazio, Frascati, Italy), and M. Neugebauer (California Institute of Technology, Jet Propulsion Laboratory, Pasadena, Calif.) 1 Feb. 1975 13 p refs Journal of Geophysical Research, vol. 80, Feb. 1, 1975, p. 502-514. (Contracts NAS-2398; NAS-2513; NAS7-100; Grant NGR-05-007-004; NASw-2659)

It was found that low solar wind parameters  $M$  (less than or around 2.5) and  $\beta$  (much less than 1) and high angles to the local shock normal,  $\theta$  (greater than or around 65 deg), produced oblique laminar shock profiles as expected from theory, with marginal or vanishing upstream standing whistlers probably damped by acoustic or other plasma wave instabilities. The whistler mode appeared to dominate the electromagnetic spectrum. The laminar shock ramp thickness was several hundred kilometers and equal to  $(2-4)c/\omega\pi$ . Composition of the shock as an accumulation of near-standing waves and an evidently reproducible varying flux pattern was discernible. Electron thermalization occurred early in, or just before, the magnetic ramp, while proton thermalization appeared to occur later in the ramp. Instantaneous shock velocities derived from the standing whistler wavelength were consistent with average velocities derived from the elapsed time estimates and were as high as 200 km/sec. S.J.M.

**A75-23716\*****ELECTROMAGNETIC HISS AND RELATIVISTIC ELECTRON LOSSES IN THE INNER ZONE**

B. T. Tsurutani, E. J. Smith (California Institute of Technology, Jet Propulsion Laboratory, Pasadena, Calif.), and R. M. Thorne (California, University, Los Angeles, Calif.) 1 Feb. 1975 8 p refs Journal of Geophysical Research, vol. 80, Feb. 1, 1975, p. 600-607. (Contract NAS7-100)

It is shown that ELF hiss is present in the inner radiation zone ( $L$  less than 2) during both storms and substorms. This presence is ascribed to propagation of waves into this region from a distributed source located at high altitude near the equatorial plasmapause. Two major effects allow hiss to reach the inner zone during storms and substorms: (1) the observed tendency for plasmaspheric hiss to be greatly intensified during the recovery phase as the outward-moving plasmapause encounters the electrons that have been freshly injected into the magnetosphere; (2) the displacement of the plasmapause, and the presumed source region, to low altitudes during high levels of magnetic activity. S.J.M.

**A75-23721****OBSERVED VARIATIONS OF THE EXOSPHERIC****HYDROGEN DENSITY WITH THE EXOSPHERIC TEMPERATURE**

J. L. Bertaux (CNRS, Service d'Aeronomie, Verrieres-le-Buisson, Essonne, France) 1 Feb. 1975 4 p refs Journal of Geophysical Research, vol. 80, Feb. 1, 1975, p. 639-642. Centre National d'Etudes Spatiales (Contract CNES-71-201)

**A75-24043\*****A GLOBAL MAGNETIC ANOMALY MAP**

R. D. Regan, W. M. Davis (U.S. Geological Survey, Reston, Va.), and J. C. Cain (NASA, Goddard Space Flight Survey, Greenbelt, Md.) 10 Feb. 1975 9 p refs Journal of Geophysical Research, vol. 80, Feb. 10, 1975, p. 794-802.

A subset of POGO satellite magnetometer data has been formed that is suitable for analysis of crustal magnetic anomalies. Through the use of a thirteenth-order field model fit to these data, magnetic residuals have been calculated over the world to latitude limits of plus or minus 50 deg. These residuals, averaged over 1-degree latitude-longitude blocks, represent a detailed global magnetic anomaly map derived solely from satellite data. The occurrence of these anomalies on all individual satellite passes independent of local time and their decay as altitude increases imply a definite internal origin. Their wavelength structure and their correlation with known tectonic features further suggest that these anomalies are primarily of geologic origin and have their sources in the lithosphere. (Author)

**A75-27383\*****DYNAMICS OF MID-LATITUDE LIGHT ION TROUGH AND PLASMA TAILS**

A. J. Chen, J. M. Grebowsky, and H. A. Taylor, Jr. (NASA, Goddard Space Flight Center, Greenbelt, Md.) 1 Mar. 1975 9 p refs Journal of Geophysical Research, vol. 80, Mar. 1, 1975, p. 968-976.

Light ion trough measurements near midnight made by the Bennett RF ion mass spectrometer on OGO 4 operating in the high-resolution mode reveal the existence of irregular structure on the low-latitude side of the mid-latitude trough. By using two different relations between the equatorial convection electric field, assumed to be spatially invariant and directed from dawn to dusk, and  $K_p$ , a model development was made of the outer plasmasphere. The model calculations produced multiple plasma tails that compare favorably with the observed thermal proton irregularities. The model development produces an outer plasmasphere boundary location that varies similarly to the observed minimum density point of the light ion trough. However, the measurements are not extensive enough to yield conclusive proof that one of the electric field models is better than the other. (Author)

**A75-27387\*****THE ENHANCEMENT OF SOLAR WIND FLUCTUATIONS AT THE PROTON THERMAL GYRORADIUS**

M. Neugebauer (California Institute of Technology, Jet Propulsion Laboratory, Pasadena, Calif.) 1 Mar. 1975 5 p refs Journal of Geophysical Research, vol. 80, Mar. 1, 1975, p. 998-1002. (Contract NAS7-100)

Average power spectra of solar wind fluctuations at frequencies up to 0.87 Hz are calculated from OGO 5 measurements of positive ion flux. Although the general spectral trend follows the power law spectrum observed at lower frequencies, a small but statistically significant power enhancement is observed at the frequency  $v/2(\pi)R$ , where  $v$  is the solar wind velocity and  $R$  is the gyroradius of proton thermal motions in the solar wind. The measured power spectrum is in rough agreement with that deduced from radio scintillation observations. (Author)

**A75-27679****EXCITATION OF MAGNETOSONIC WAVES WITH**

**DISCRETE SPECTRUM IN THE EQUATORIAL VICINITY OF THE PLASMAPAUSE**

A. V. Gulemi, B. I. Klaine (Geofizicheskaia Observatoriia, Borok, USSR), and A. S. Potapov (Akademiia Nauk SSSR, Institut Zemnogo Magnetizma, Ionosfery i Rasprostraneniia Radiovoln, Irkutsk, USSR) Feb. 1975 8 p refs Planetary and Space Science, vol. 23, Feb. 1975, p. 279-286.

**A75-28004\*****RELATION OF SOLAR WIND FLUCTUATIONS TO DIFFERENTIAL FLOW BETWEEN PROTONS AND ALPHAS**

M. Neugebauer (California Institute of Technology, Jet Propulsion Laboratory, Pasadena, Calif.) 1974 2 p refs In: Solar wind three: Proceedings of the Third Conference, Pacific Grove, Calif., March 25-29, 1974. Los Angeles, University of California, 1974, p. 33, 34. (Contract NAS7-100)

An analysis is made of the difference between the alpha particle and proton flow velocities in the solar wind as observed by the OGO 5 satellite. The alpha and proton velocities from each of 962 spectral scans are compared with the variance of 32 solar wind flux measurements made during the scans. The average velocity difference is plotted for each of 10 logarithmic variance intervals and is seen to decrease and approach zero when the variance is high. It is shown that such an anticorrelation may be due to the fact the wave/particle interactions provide the drag force between two streams of different velocity in a collisionless plasma. F.G.M.

**A75-28015\*****INSTABILITIES CONNECTED WITH NEUTRAL SHEETS IN THE SOLAR WIND**

V. Formisano (CNR, Laboratorio per il Plasma nello Spazio, Frascati, Italy), P. C. Hedgecock (Imperial College of Science and Technology, London, England), C. T. Russell, and J. D. Means (California, University, Los Angeles, Calif.) 1974 7 p refs In: Solar wind three; Proceedings of the Third Conference, Pacific Grove, Calif., March 25-29, 1974. Los Angeles, University of California, 1974, p. 180-186. Research supported by the Consiglio Nazionale delle Ricerche, National Research Council of England, and NASA.

A preliminary study is presented of two sets of data obtained by HEOS 1 and OGO 5 in the solar wind, which reveal the internal structure of two neutral sheets and their two-dimensional structure. HEOS 1 observations of the effects of the tearing mode instability in one of the sheets are described, including complicated structures connected with the sector boundary, sharp increases and decreases in the magnetic field intensity, and the presence of closed loops. HEOS 1 and OGO 5 observations of large oscillations due to plasma pressure imbalances are discussed, and it is concluded that an interchange instability may have been observed. F.G.M.

**A75-28032****VARIATION OF THE SOLAR WIND FLUX WITH HELIOGRAPHIC LATITUDE, DEDUCED FROM ITS INTERACTION WITH INTERPLANETARY HYDROGEN**

J. Blamont (CNRS, Service d'Aeronomie, Verrieres-le-Buisson, Essonne, France) 1974 8 p refs In: Solar wind three; Proceedings of the Third Conference, Pacific Grove, Calif., March 25-29, 1974. Los Angeles, University of California, 1974, p. 321-328.

**A75-28038\*****THE ENHANCEMENT OF SOLAR WIND FLUCTUATIONS WITH SCALE SIZE NEAR THE PROTON GYORADIUS**

M. Neugebauer (California Institute of Technology, Jet Propulsion Laboratory, Pasadena, Calif.) 1974 2 p In: Solar wind three; Proceedings of the Third Conference, Pacific

Grove, Calif., March 25-29, 1974. Los Angeles, University of California, 1974, p. 373, 374. (Contract NAS7-100)

**A75-28356\*****ION COMPOSITION IRREGULARITIES AND IONOSPHERE-PLASMAPHERE COUPLING - OBSERVATIONS OF A HIGH LATITUDE ION TROUGH**

H. A. Taylor, Jr., J. M. Grebowsky, and A. J. Chen (NASA, Goddard Space Flight Center, Laboratory for Planetary Atmospheres, Greenbelt, Md.) Apr. 1975 11 p refs Journal of Atmospheric and Terrestrial Physics, vol. 37, Apr. 1975, p. 613-623.

**A75-28743\*****RELATION OF VARIATIONS IN TOTAL MAGNETIC FIELD AT HIGH LATITUDE WITH THE PARAMETERS OF THE INTERPLANETARY MAGNETIC FIELD AND WITH DP 2 FLUCTUATIONS**

R. A. Langel (NASA, Goddard Space Flight Center, Geophysics Branch, Greenbelt, Md.) 1 Apr. 1975 10 p refs Journal of Geophysical Research, vol. 80, Apr. 1, 1975, p. 1261-1270.

**A75-28750\*****A SEARCH FOR SOLAR WIND VELOCITY CHANGES BETWEEN 0.7 AND 1 AU**

D. S. Intriligator (Southern California, University, Los Angeles, Calif.) and M. Neugebauer (California Institute of Technology, Jet Propulsion Laboratory, Pasadena, Calif.) 1 Apr. 1975 3 p refs Journal of Geophysical Research, vol. 80, Apr. 1, 1975, p. 1332-1334. Research supported by the California Institute of Technology. (Contract NAS7-100; Grants NGR-05-002-165; NGR-05-002-059; NGR-05-018-181)

Observations are presented concerning the radial variations of the solar wind velocity between 0.7 and 1 au in late 1968 and early 1969. The observations were made with instruments carried by Pioneer 9 and the earth-orbiting satellite OGO 5. The Pioneer and OGO velocity measurements are compared. It is found that the same basic solar wind velocity structure was seen at both spacecraft. No statistically significant dependence of average velocity on the radial distance from the sun could be observed. G.R.

**A75-32382\*****A COMETARY HYDROGEN MODEL - COMPARISON WITH OGO-5 MEASUREMENTS OF COMET BENNETT (1970 II)**

H. U. Keller and G. E. Thomas Feb. 1975 13 p Astronomy and Astrophysics, vol. 39, no. 1, Feb. 1975, p. 7-19. (Contract NAS5-9327; Grants NGR-06-003-201; NGL-06-003-052)

A model is constructed for the hydrogen cloud of Comet Bennett (1970 II) based on highly sensitive observations of its Lyman alpha emission by a photometer on board OGO-5 and taking into account the cometary motion, field gradients, solar L-alpha profile, and finite lifetime of the H atoms along their trajectories. The solar L-alpha flux is determined independently of instrumental calibration using the strong curvature of the hydrogen cloud in the orbital plane of the comet, and the cometary production rate of hydrogen atoms is calculated. The combination of two equally weighted Maxwellian velocity distributions with mean velocities of 7 and 21 km/sec is found to match the photometer scans across the comet better than any single Maxwellian distribution. A complete L-alpha isophote map is presented for the model hydrogen cloud on Mar. 20, 1970. F.G.M.

**A75-34018\*****SOLAR PARTICLE EVENTS WITH ANOMALOUSLY LARGE RELATIVE ABUNDANCE OF HE-3**



A. T. Serlemitsos (NASA, Goddard Space Flight Center, Laboratory for High Energy Astrophysics, Greenbelt; Computer Sciences Corp., Silver Spring, Md.) and V. K. Balasubrahmanyam (NASA, Goddard Space Flight Center, Laboratory for High Energy Astrophysics, Greenbelt, Md.) 15 May 1975 10 p ref Astrophysical Journal, vol. 198, May 15, 1975, pt. 1, p. 195-204.

Energetic particle data are presented from a series of solar flares with a relative abundance of He-3 much higher than that of any previous events. The abundance of protons relative to He nuclei was significantly low in these events; not more than four H-2 and three H-3 were detected during the entire period under study, compared with 1110 He-3 nuclei. Results from these experiments are compared with data available from other investigations, and the limitations the former observations place on theoretical models to explain He-3-rich flares are discussed. S.J.M.

**A75-35003\***  
**COLLISIONLESS SHOCK WAVES IN SPACE - A VERY HIGH BETA STRUCTURE**

V. Formisano (CNR, Laboratorio per il Plasma nello Spazio, Frascati, Italy), C. T. Russell, J. D. Means (California, University, Los Angeles, Calif.), E. W. Greenstadt, F. L. Scarf (TRW Systems Group, Redondo Beach, Calif.), and M. Neugebauer (California Institute of Technology, Jet Propulsion Laboratory, Pasadena, Calif.) 1 Jun. 1975 10 p refs Journal of Geophysical Research, vol. 80, June 1, 1975, p. 2013-2022.

(Contracts NASw-2513; NAS7-100; Grant NGR-05-007-004)

Measurements from six OGO-5 particle and field experiments are used to examine the structure of the earth's bow shock during a period of extremely high beta (the ratio of plasma thermal to magnetic energy density), as determined from simultaneous measurements of the upstream plasma on board the HEOS satellite. Even though the interplanetary field is nearly perpendicular to the shock normal, the shock is extremely turbulent. Large field increases are observed up to a factor of 20 above the upstream values. Ahead of these large enhancements, smaller magnetic effects accompanied by electrostatic noise, electron heating, and ion deflection are observed for several minutes. These observations suggest that a steady-state shock may not be able to form at very high beta. Further, they show that while the magnetic energy density may be relatively unimportant in the upstream flow, it can become very significant within the shock structure, and hence the magnetic field should not be ignored in theoretical treatments of very high beta shocks. (Author)

**A75-35005\***  
**CURRENT-DRIVEN PLASMA INSTABILITIES AT HIGH LATITUDES**

F. L. Scarf, R. W. Fredricks (TRW Systems Group, Redondo Beach, Calif.), C. T. Russell, M. Kivelson (California, University, Los Angeles, Calif.), M. Neugebauer (California Institute of Technology, Jet Propulsion Laboratory, Pasadena, Calif.), and C. R. Chappell (NASA, Marshall Space Flight Center, Huntsville, Ala.) 1 Jun. 1975 11 p refs Journal of Geophysical Research, vol. 80, June 1, 1975, p. 2030-2040.

(Contracts NASw-2659; NAS5-9092; NAS7-100; Grant NGR-05-007-004)

Earlier OGO 5 discussions of high-latitude magnetospheric wave-particle interaction phenomena associated with field aligned current systems are extended by considering some September 7, 1968, out-bound measurements and corresponding March 11, 1969, observations, when the spacecraft was traversing auroral L shells in midafternoon. It is shown that during moderate magnetospheric disturbances the most intense waves and currents were detected near sharp boundaries in the density of polar cleft electrons, and it is possible that local wave-particle interactions produced anomalous resistivity. Some observed changes in the electron distribution functions might be explained in terms

of local acceleration, but significant causal questions about the dynamics remain open if one can use only local data from a single spacecraft in this region. (Author)

**A75-35007\***  
**IDENTIFICATIONS OF THE POLAR CAP BOUNDARY AND THE AURORAL BELT IN THE HIGH-ALTITUDE MAGNETOSPHERE - A MODEL FOR FIELD-ALIGNED CURRENTS**

M. Sugiura (NASA, Goddard Space Flight Center, Laboratory for Planetary Atmospheres, Greenbelt, Md.) 1 Jun. 1975 12 p refs Journal of Geophysical Research, vol. 80, June 1, 1975, p. 2057-2068.

**A75-35036**  
**DIFFERENTIAL ROTATION OF THE MAGNETOSPHERIC PLASMA AS CAUSE OF THE SVALGAARD-MANSUROV EFFECT**

H. Volland (Bonn, Universitaet, Bonn, West Germany) 1 Jun. 1975 5 p refs Journal of Geophysical Research, vol. 80, June 1, 1975, p. 2311-2315.

A correspondence between the geomagnetic variations at the geomagnetic poles and the sector polarity of the interplanetary magnetic field was discovered independently by Svalgaard (1968) and by Mansurov (1969). Heppner (1972) noted a dawn-dusk asymmetry in the magnetospheric electric convection field observed by the OGO 6 satellite within the polar caps at ionospheric altitudes. This asymmetry is also related to the sector polarity of the interplanetary magnetic field. It is shown that both effects can be consistently explained by differential rotation of the magnetospheric plasma with respect to the earth. V.P.

**A75-35040\***  
**REMOTE SENSING OF THE IONOSPHERIC F LAYER BY USE OF O I 6300-A AND O I 1356-A OBSERVATIONS**

S. Chandra, E. I. Reed (NASA, Goddard Space Flight Center, Laboratory for Planetary Atmospheres, Greenbelt, Md.), R. R. Meier, C. B. O'Pal, and G. T. Hicks (U.S. Navy, E. O. Hulbert Center for Space Research, Washington, D.C.) 1 Jun. 1975 6 p refs Journal of Geophysical Research, vol. 80, June 1, 1975, p. 2327-2332.

The possibility of using airglow techniques for estimating the electron density and height of the F layer is studied on the basis of a simple relationship between the height of the F2 peak and the column emission rates of the O I 6300 A and O I 1356 A lines. The feasibility of this approach is confirmed by a numerical calculation of F2 peak heights and electron densities from simultaneous measurements of O I 6300 A and O I 1356 A obtained with earth-facing photometers carried by the OGO 4 satellite. Good agreement is established with the F2 peak heights estimates from top-side and bottom-side ionospheric sounding. V.P.

**A75-35537\*#**  
**IMPULSIVE SOLAR FLARE X-RAYS GREATER THAN 10 keV AND SOME CHARACTERISTICS OF COSMIC GAMMA-RAY BURSTS**

S. R. Kane (California, University, Berkeley, Calif.) 1975 35 p In: International Conference on X-Rays in Space - Cosmic, Solar, and Auroral X-Rays, Calgary, Alberta, Canada, August 14-21, 1974, Proceedings, Volume 1. (A75-35526 16-88) Calgary, Alberta, Canada, University of Calgary, 1975, p. 271-305. (Grants NGR-05-003-510; NGL-05-003-017)

Observations of impulsive solar flare X-rays greater than 10 keV are summarized and their interpretation in terms of nonthermal and thermal electron spectra is discussed. This is followed by a brief consideration of models of the hard X-ray source and the requirements of the electron acceleration process during the flash phase of solar flares. Finally, the characteristics of the recently discovered cosmic gamma-ray bursts are compared with those of the impulsive solar X-ray bursts. If both types of emissions are interpreted

as bremsstrahlung from energetic electrons, then the electron spectra must be widely different in the two cases. For example, in case of solar flares, most of the energy is carried by electrons with energies of about 5 keV. On the other hand, electrons with kinetic energy of about 300 keV carry most of the energy in the cosmic source. (Author)

A75-36977

#### A REVIEW OF IN SITU OBSERVATIONS OF THE PLASMAPAUSE

M. J. Rycroft (Southampton, University, Southampton, England; Houston, University, Houston, Tex.) Mar. 1975 16 p ref (European Geophysical Society, Physics of the Plasmopause Symposium, 2nd, Trieste, Italy, Sept. 23-26, 1974.) Annales de Geophysique, vol. 31, Jan.-Mar. 1975, p. 1-16.

First reviewed are early in situ measurements of the thermal plasma density decrease, and corresponding temperature increase, at the plasmopause. Attention is then concentrated on the modus operandi of and results obtained by three instruments aboard OGO 5, namely the NASA GSFC retarding potential analyzer, the Lockheed light ion mass spectrometer, and the UCL MSSL Langmuir probe. The detection of the plasmopause near the equatorial plane by other techniques, such as LF upper hybrid resonance noise, ELF/VLF electromagnetic waves, DC electric fields and energetic charged particle phenomena, is also mentioned. Variations of the plasmopause position with local time and changing geomagnetic activity are considered. Some suggestions are made for future work.

(Author)

A75-36982

#### PROBING THE PLASMAPAUSE BY GEOMAGNETIC PULSATIONS

D. Orr (York, University, York, England) Mar. 1975 15 p refs (European Geophysical Society, Physics of the Plasmopause Symposium, 2nd, Trieste, Italy, Sept. 23-26, 1974.) Annales de Geophysique, vol. 31, Jan.-Mar. 1975, p. 77-91. Science Research Council (Contracts SRC-SG/R/21/2; SRC-SG/R/00589)

OGO 5 proton density data are used to predict possible geomagnetic pulsation periods for different L shells using the simplifying assumption that the excited mode of oscillation is either the axisymmetric toroidal mode or the guided poloidal mode. The effect of the plasmopause on pulsations can be observed in several ways: in situ satellite measurements; ground based statistical studies; and polarization and amplitude studies along a chain of stations. Information from these approaches is reviewed. The plasmopause position during the daytime can be estimated from the previous nighttime Kp index; an enhancement in the detection of Pc 3 when the geomagnetic field line associated with the observatory links the plasmatrough has been found, while Pc 4 amplitudes are increased within the plasmasphere. A similar study with Pc 1 indicates that the source of these events is often at the plasmopause. The large plasma density change at the plasmopause could result in surface waves being generated there from impulsive disturbances; the anticipated polarization pattern at different latitudes is discussed and compared with Pi 2 observations.

(Author)

A75-36988

#### VLF AND ELF EMISSIONS

T. R. Kaiser and K. Bullough (Sheffield, University, Sheffield, England) Mar. 1975 5 p refs (European Geophysical Society, Physics of the Plasmopause Symposium, 2nd, Trieste, Italy, Sept. 23-26, 1974.) Annales de Geophysique, vol. 31, Jan.-Mar. 1975, p. 137-141.

The mutual interaction of waves and particles in the presence of ambient plasma plays a dominant role in the physics of the magnetosphere; the principal processes appear to be resonant interactions of the cyclotron and Heaviside (Cerenkov) type. The mechanisms operative in the vicinity of the plasmopause are briefly outlined and recent results

from magnetospheric and near-earth satellites are reviewed. Thus ELF hiss appears to fill the plasmasphere while chorus is limited to the region between the plasmopause and trapping boundaries. The nature of the observed emissions is also dependent on the propagation characteristics between the generation region and the satellite, in which the plasmopause boundary may play an important role. VLF observations have revealed longitudinal structure in the outer plasmasphere which may have a lifetime of a day or so as well as a marked maximum of emissions at midlatitudes in the American hemisphere. Storm-time variations in the emissions are related to changes in both particle populations and the magnetospheric and plasmaspheric configurations. (Author)

A75-37031\*

#### ACCESS OF SOLAR ELECTRONS TO THE POLAR REGIONS

E. Nielsen and M. A. Pomerantz (Franklin Institute, Bartol Research Foundation, Swarthmore, Pa.) Jun. 1975 10 p refs Planetary and Space Science, vol. 23, June 1975, p. 945-954. NASA-supported research.

Riometric and forward-scatter radio-wave absorption measurements at high polar latitudes in both hemispheres are compared with absorption calculations based on satellite observations in the magnetosheath to determine whether a north-south asymmetry in the solar electron flux occurred during a polar-cap absorption (PCA) event. Detection of solar electrons in interplanetary space is shown to have occurred simultaneously with detection of HF radio-wave absorption, indicating that the initial stage of the PCA was due to the arrival of solar electrons. A north-south asymmetry is observed in the electron flux, and it is found that the flux precipitating over the South Pole did not exceed the mean unidirectional intensity of the electrons detected in space. The ratio between fluxes in the low and high polar latitude regions over Antarctica during a period of solar electron anisotropy is found to be comparable with that obtained during periods of isotropy. These results are shown to be consistent with the idea of an open magnetosphere and with the conclusion that an anisotropic solar electron flux may be rendered isotropic at the magnetopause. F.G.M.

A75-37352\*

#### IMPULSIVE /FLASH/ PHASE OF SOLAR FLARES - HARD X-RAY, MICROWAVE, EUV AND OPTICAL OBSERVATIONS

S. R. Kane (California, University, Berkeley, Calif.) 1974 37 p refs In: Coronal disturbances; Proceedings of the Symposium, Surfer's Paradise, Queensland, Australia, September 7-11, 1973. Dordrecht, D. Reidel Publishing Co., 1974, p. 105-141; Discussion, p. 141. (Grants NGL-05-003-017; NGR-05-003-510)

A75-38275

#### PLASMA FLOW HYPOTHESIS IN THE MAGNETOSPHERE RELATING TO FREQUENCY SHIFT OF ELECTROSTATIC PLASMA WAVES

H. Oya (Tohoku University, Sendai, Japan) 1 Jul. 1975 7 p refs Journal of Geophysical Research, vol. 80, July 1, 1975, p. 2783-2789.

The frequency dynamic spectrum indicating a monotonic frequency shift of the electrostatic electron cyclotron harmonic wave emissions in the data of VLF electric field observations by OGO 5 has been detected in the midnight and dawn meridians outside the plasmopause; the emissions are produced from turbulent areas in the plasma states that include the temperature anisotropy, loss cone velocity distribution, of the double hump in the velocity distribution function. The frequency shift is also observed for the case of the emissions in the magnetosheath near the subsolar point. These frequency shifts are interpreted on a hypothesis of the Doppler effects of the plasma waves due to the plasma flow with respect to the satellite frame. The speeds of the plasma flow are obtained and have a range from 150 to 300 km/sec. Disruption of the plasma flow due to the

magnetic field bumps may produce the turbulent source generating the Harris type or beam type instabilities that generate the electrostatic electron cyclotron harmonic waves. (Author)

## A75-41805\*

**ANGULAR DISTRIBUTIONS OF SOLAR PROTONS AND ELECTRONS**

E. Nielsen, M. A. Pomerantz (Franklin Institute, Bartol Research Foundation, Swarthmore, Pa.), and H. L. West, Jr. (California, University, Livermore, Calif.) Aug. 1975 16 p refs Planetary and Space Science, vol. 23, Aug. 1975, p. 1179-1194.

(Grants NGR-39-005-105; NSG-7109)

High angular-resolution measurements of directional fluxes of solar particles in space have been obtained with detectors aboard OGO-5 during the cosmic ray event of Nov. 18, 1968. This is the only case on record for which sharply-defined directional observations of protons and electrons covering a wide rigidity range (0.3 MV to 1.5 GV) are available. The satellite experiment provided data for determining pitch-angle distributions with respect to the direction of the local interplanetary magnetic field lines during the lengthy highly anisotropic phase of the event. The results have been interpreted in the light of the temporal flux profiles and the state of the interplanetary medium. (Author)

## A75-42726\*

**THE GLOBAL CHARACTERISTICS OF ATMOSPHERIC EMISSIONS IN THE LOWER THERMOSPHERE AND THEIR AERONOMIC IMPLICATIONS**

E. L. Reed and S. Chandra (NASA, Goddard Space Flight Center, Laboratory for Planetary Atmospheres, Greenbelt, Md.) 1 Aug. 1975 10 p refs Journal of Geophysical Research, vol. 80, Aug. 1, 1975, p. 3053-3062.

The green line (555.7 nm) of atomic oxygen and the Herzberg bands of molecular oxygen (measured between 250 and 280 nm) as observed from the OGO 4 airglow photometer from August 1967 through January 1968 are discussed in terms of their spatial and temporal distributions and their relation to the atomic oxygen content in the lower thermosphere. Daily maps of the distribution of emissions show considerable structure (cells, patches, and bands) with appreciable changes from day to day. When data are averaged over periods of several days in length, the resulting patterns have only occasional tendencies to follow geomagnetic parallels. The seasonal variation is characterized by maxima in both the Northern and Southern Hemispheres in October, the Northern Hemisphere having substantially higher emission rates. These maxima tend to move toward the poles, leaving very low values of emission at low latitudes in December and January. Noting the similarity of the atomic oxygen profiles in the lower thermosphere to the profile of a Chapman distribution, formulae are derived relating the vertical column emission rates of the green line and the Herzberg bands to the atomic oxygen peak density. (Author)

## A75-42744\*

**PIONEER 9 AND OGO 5 OBSERVATIONS OF AN INTERPLANETARY MULTIPLE SHOCK ENSEMBLE ON FEBRUARY 2, 1969**

M. Dryer, Z. K. Smith (NOAA, Space Environment Laboratory, Boulder, Colo.), T. Unti (California Institute of Technology, Jet Propulsion Laboratory, Pasadena, Calif.), J. D. Mihalov, B. F. Smith, J. H. Wolfe, D. S. Colburn (NASA, Ames Research Center, Moffett Field, Calif.), and C. P. Sonett (Arizona, University, Tucson, Ariz.) 1 Aug. 1975 10 p refs Journal of Geophysical Research, vol. 80, Aug. 1, 1975, p. 3225-3234.

A multiple shock system was observed upstream (0.13 au) of the earth by Pioneer 9 on February 2, 1969. The same system was observed at earth by OGO 5 and was reported separately in the literature. This paper compares the two sets of observations in still further detail. Both magnetic-field and plasma data are used in a least-squares best-fit method to compute the characteristics of the fast

forward shock wave (Pioneer 9 only) and two fast reverse shock waves. Nearly all major features (shock, piston, and tangential discontinuity) retained their characteristics during the transit of the shock ensemble from Pioneer 9 to OGO 5. The genesis of the ensemble is believed to be due to a complex stream-stream interaction. A substantial density increase (including a large rise of alpha/proton abundance) at OGO 5, but unobserved at Pioneer 9, is explained by a sudden meridional shift to a flow from below the ecliptic plane while the streams were en route to earth. This study demonstrates a spatial and temporal plasma inhomogeneity which is superimposed on the persistent major features. (Author)

## A75-42748\*

**MAGNETOSPHERIC CHORUS - AMPLITUDE AND GROWTH RATE**

W. J. Burtis and R. A. Helliwell (Stanford University, Stanford, Calif.) 1 Aug. 1975 6 p refs Journal of Geophysical Research, vol. 80, Aug. 1, 1975, p. 3265-3270. (Grant NGL-05-020-008)

A new study of the amplitude of magnetospheric chorus with 1966-1967 data from the Stanford University/Stanford Research Institute VLF receivers on OGO 1 and OGO 3 has confirmed the band-limited character of magnetospheric chorus in general and the double-banding of near-equatorial chorus. Chorus amplitude tended to be inversely correlated with frequency, implying lower intensities at lower L values. Individual chorus emissions often showed a characteristic amplitude variation, with rise times of 10 to 300 ms, a short duration at peak amplitude, and decay times of 100 to 3000 msec. Growth was often approximately exponential, with rates from 200 to nearly 2000 dB/sec. Rate of change of frequency was found in many cases to be independent of emission amplitude, in agreement with the cyclotron feedback theory of chorus (Helliwell, 1967, 1970). (Author)

## A75-43792\*

**SLOW X-RAY BURSTS AND FLARES WITH FILAMENT DISRUPTION**

J.-R. Roy (Utrecht, Rijksuniversiteit, Utrecht, Netherlands) and F. Tang (Big Bear Solar Observatory, Pasadena, Calif.) Jun. 1975 15 p refs Solar Physics, vol. 42, June 1975, p. 425-439.

(Grant NGR-05-002-294; Contract F19628-73-C-0085)

The data from OGO-5 and OSO-7 X-ray experiments have been compared with optical data from six chromospheric flares with filament disruption associated with slow thermal X-ray bursts. Filament activation accompanied by a slight X-ray enhancement precedes the first evidence of H-alpha flare by a few minutes. Rapid increase of the soft X-ray flux accompanies the phase of fastest expansion of the filament. Plateau or slow decay phases in the X-ray flux are associated with slowing and termination of filament expansion. The soft X-ray flux increases as F approaches  $(A + Bh)h$ , where h is the height of the disrupted prominence at any given time and A and B are constants. We suggest that the soft X-ray emission originates from a growing shell of roughly constant thickness of high-temperature plasma due to the compression of the coronal gas by the expanding prominence. (Author)

## A75-46232

**SUBSTORM EFFECTS ON THE NEUTRAL SHEET INSIDE 10 EARTH RADII**

B. T. Thomas and P. C. Hedgecock (Imperial College of Science and Technology, London, England) 1975 16 p refs In: The magnetospheres of the Earth and Jupiter; Proceedings of the Neil Brice Memorial Symposium, Frascati, Italy, May 28-June 1, 1974. (A75-46227 23-91) Dordrecht, D. Reidel Publishing Co., 1975, p. 55-70. Research supported by the Science Research Council of England.

Magnetic field and substorm activity data from OGO 5, HEOS 1, and ATS 1 are analyzed along with ground magnetograms which show that a well-defined neutral sheet

can be observed near midnight at geocentric distances as small as 7-8 earth radii. Comparison of observations with auroral electrojet indices shows that the neutral sheet was observed inside 10 earth radii following the onset of a substorm and during generally disturbed periods. It was absent during late recovery phase of substorms or during quiet periods. The observations also indicate that during the growth phase of a substorm the plasma sheet thins at geocentric distances near 10 earth radii, and prior to the onset it can be less than 0.5 earth radii in half thickness. P.T.H.

**A75-46238\***  
**EVIDENCE FOR MAGNETIC FIELD LINE RECONNECTION IN THE SOLAR WIND**

V. Formisano (CNR, Laboratorio per il Plasma nello Spazio, Frascati, Italy) and E. Amata (Imperial College of Science and Technology, London, England) 1975 13 p refs In: The magnetospheres of the Earth and Jupiter; Proceedings of the Neil Brice Memorial Symposium, Frascati, Italy, May 28-June 1, 1974. Dordrecht, D. Reidel Publishing Co., 1975, p. 205-217. Research supported by the Consiglio Nazionale delle Ricerche and Science Research Council of England. (Grant NGR-05-007-004)

The basic scheme of Petschek's (1963) models for slow and fast magnetic reconnection in the solar wind is reviewed in order to determine what sort of results one would expect from satellite observations of possible reconnection processes. Data from HEOS 1 and OGO 5 are then analyzed, in which four observations of neutral sheet structures with large change of magnetic field direction were made. All four may be interpreted as indicating magnetic line reconnections rather than as D-sheets because they all show two distinct discontinuities which bound a lower magnetic field intensity region. The geometry of the magnetic field in the reconnection region appears to be similar to that described by Petschek. In one case the reconnection rate is in agreement with Petschek's prediction, but in the other three cases it is much larger than his limit. The reconnection rates observed do, however, agree with Sonnerup's (1972) limit. P.T.H.

**A75-46269\***  
**EXOSPHERIC TEMPERATURE INFERRED FROM THE AEROS-A NEUTRAL COMPOSITION MEASUREMENT**  
S. Chandra and N. W. Spencer (NASA, Goddard Space Flight Center, Laboratory for Planetary Atmospheres, Greenbelt, Md.) 1 Sep. 1975 7 p refs Journal of Geophysical Research, vol. 80, Sept. 1, 1975, p. 3615-3621.

The derivation of exospheric temperature from satellite drag measurements is based on an assumption of invariant conditions of the neutral atmosphere at 120 km. Since it has been established that atomic oxygen, which is usually the major neutral constituent in the region of drag measurements, is subject to considerable variability with season, latitude, and solar and geomagnetic activity in the altitude region of 120 km, its value as an indicator of exospheric temperature is questionable. OGO 6 neutral mass spectrometer measurements revealed that molecular nitrogen is a better indicator of exospheric temperature, since it is not subject to changes caused by eddy mixing and is therefore relatively less variable near the turbopause. However, theoretical arguments show that argon, even though it is a minor constituent, is relatively less variable with respect to changes in eddy diffusion coefficient and hence a better indicator of exospheric temperature than O and N<sub>2</sub>. In this paper the relative merits of these gases for deriving exospheric temperature are investigated by using observational data from the Aeros-A Nate experiment. (Author)

**A75-46285\***  
**THE DOMINANT MODE OF STANDING ALFVEN WAVES AT THE SYNCHRONOUS ORBIT**

W. D. Cummins, C. Countee, D. Lyons, and W. Wiley, III (Grambling State University, Grambling, La.) 1 Sep. 1975 4 p Journal of Geophysical Research, vol. 80, Sept. 1, 1975, p. 3705-3708.

(Grant NGR-19-011-007)

Low-frequency oscillations of the earth's magnetic field recorded by a magnetometer on board ATS 1 have been examined for the 6-month interval between January and June 1968. Using evidence from OGO 5 and ATS 5 as well as the data from ATS 1, it is argued that the dominant mode at ATS 1 must be the fundamental rather than the second harmonic of a standing Alfvén wave. It is concluded that these transverse oscillations are more accurately associated with magnetically disturbed days than with quiet days. From 14 instances when oscillations of distinctly different periods occurred during the same time interval at ATS 1, it is also concluded that higher harmonics can exist. The period ratio in seven of the 14 cases corresponds to the simultaneous occurrence of the second harmonic with the fundamental, and four other cases could be identified as the simultaneous occurrence of the fourth harmonic with the fundamental. (Author)

**A75-46289\***  
**SATELLITE MEASUREMENTS OF NITRIC OXIDE IN THE POLAR REGION**

D. W. Rusch (Michigan, University, Ann Arbor, Mich.) and C. A. Barth (Colorado, University, Boulder, Colo.) 1 Sep. 1975 3 p Journal of Geophysical Research, vol. 80, Sept. 1, 1975, p. 3719-3721.

(Grant NGR-06-003-127)

Ultraviolet measurements of the (1, 0) gamma band of nitric oxide in fluorescence by a satellite at high latitudes show nitric oxide concentrations which are highly variable in both time and space. The average nitric oxide concentration is 3 to 4 times higher at high latitudes than at midlatitudes. If auroral activity is responsible for the larger nitric oxide densities and if the reaction N(2D) + O<sub>2</sub> is the source of NO, then auroral processes must be more efficient in the production of N(2D) atoms than dayglow processes. (Author)

**A75-46822\***  
**ORIGIN AND COMPOSITION OF HEAVY NUCLEI BETWEEN 10 AND 60 MeV PER NUCLEON DURING INTERPLANETARY QUIET TIMES IN 1968-1972**

A. Mogro-Campero and J. A. Simpson (Chicago, University, Chicago, Ill.) 15 Sep. 1975 14 p refs Astrophysical Journal, vol. 200, Sept. 15, 1975, pt. 1, p. 773-786.

(Contract NASS-9366; Grants NGL-14-001-006 NSF GA-38913X;)

Results are reported for measurements of the relative abundances of nuclei from boron through iron in the energy range between 10 and 60 MeV/nucleon which were made with an instrument on board OGO 5 during the period of changing solar modulation from 1968 to 1971. The investigation was conducted to determine whether the heavy nuclei in this energy range were of solar or galactic origin. It is found that the relative abundances are in good agreement with the nuclear abundances of galactic cosmic rays, that the differential energy spectra of carbon and oxygen at these energies diverged from the characteristic modulated galactic spectrum, that changes in the C + N + O flux during this period underwent a temporal phase lag with respect to high-energy galactic cosmic rays, and that this phase lag was the same as that for helium nuclei of galactic origin with energies of 30 to 100 MeV/nucleon. It is concluded that the experimental evidence favors a galactic origin for the present nuclei. Some implications of the energy-spectrum results for cosmic-ray modulation theory are discussed. F.G.M.

**A76-10136\***  
**THERMAL AND NONTHERMAL INTERPRETATIONS OF FLARE X-RAY BURSTS**

S. Kahler (American Science and Engineering, Inc., Cambridge, Mass.) 1975 21 p ref In: Solar gamma-, X-, and EUV radiation; Proceedings of the Symposium, Buenos Aires, Argentina, June 11-14, 1974. Dordrecht, D. Reidel Publishing Co., 1975, p. 211-231.

Various authors have presented arguments for either the

thermal or the nonthermal interpretations of impulsive E greater than 20 KeV X-ray bursts and slowly varying E less than 10 keV X-ray bursts. Arguments are presented for and against the prevailing opinion that the impulsive bursts are nonthermal and the slowly varying bursts are thermal. For the impulsive bursts, the spectra, electron mean free paths, center-to-limb distributions of both the numbers of events and spectra of events, and polarization data as relevant criteria are discussed. For the slowly varying events, electron self collision times, distribution of X-ray temporal parameters, associated gradual rise and fall radio bursts, spectral and time profiles of special events and center-to-limb distributions of numbers of events as the relevant criteria are examined. (Author)

A76-12272

#### WAVES AND WAVE-PARTICLE INTERACTIONS IN THE MAGNETOSPHERE - A REVIEW

R. Gendrin (Groupe de Recherches Ionosphériques, Issy-les-Moulineaux, Hauts-de-Seine, France) Nov. 1975 56 p refs Space Science Reviews, vol. 18, Nov. 1975, p. 145-200.

Recent space observations of waves, both electromagnetic and electrostatic, are reviewed and the role which they can play in the dynamics of magnetospheric particles is stressed. Wave particle interactions (WPI) in the exo- and intra-plasmaspheric media depend on the exact process of particle injection under the influence of magnetospheric electric fields, and on the spatial distribution of the cold plasma particles; these two aspects of the problem are studied to some extent. The concepts of optimum cold plasma density, critical energy, limiting flux, marginal stability, steady-state equilibrium are critically discussed. The nonlinear aspects - both experimental and theoretical - of WPI's are reviewed and a special section is devoted to active experiments in space. An attempt is made to outline which kind of experiments could be made at high-latitudes, in conjunction with IMS spacecrafts, in order to arrive at a better understanding of magnetospheric processes involving waves and particles. (Author)

A76-14318

#### STRUCTURE OF ELECTRODYNAMIC AND PARTICLE HEATING IN THE UNDISTURBED POLAR THERMOSPHERE

D. R. Tausch and B. B. Hinton (Michigan, University, Ann Arbor, Mich.) 1 Nov. 1975 5 p Journal of Geophysical Research, vol. 80, Nov. 1, 1975, p. 4346-4350. (Grant NSF 75-01486)

This paper describes the variations in N<sub>2</sub> densities in the polar regions above 400-km altitude as measured by the Ogo 6 neutral atmospheric composition experiment. These variations are magnetically controlled and have persistent features which are associated with localized heating effects. These are identified with electrodynamic and particle heating sources. Neutral N<sub>2</sub> enhancements are a persistent feature in the polar cusp and postmidnight westward electrojet. Regions of the N<sub>2</sub> density variability are localized in magnetic local time. (Author)

A76-14838

#### VLF PROPAGATION IN THE MAGNETOSPHERE DURING SUNRISE AND SUNSET HOURS

F. Walter (Instituto Tecnológico de Aeronáutica, Sao Jose dos Campos, Sao Paulo, Brazil) and R. R. Scarabucci (Campinas, Universidade Estadual, Campinas, Sao Paulo, Brazil) Nov. 1975 7 p refs Radio Science, vol. 10, Nov. 1975, p. 965-971. Research supported by the Instituto de Atividades Espaciais.

Whistlers observed on records of the OGO-4 satellite during the sunset/sunrise hours show evidence of both the proresonance (PR) and prolongitudinal (PL) mode of propagation. By tracing rays in a model magnetosphere suitable for these hours, the whistlers observed on these records are reproduced. The upper cutoff frequency presented in the walking trace whistlers appears naturally as a

consequence of the inclusion of latitudinal gradients in the electron density model. A new whistler trace is predicted which appears as a consequence of the transition from the PR to the PL mode of propagation. (Author)

A76-16501\*

#### THE TEMPERATURE GRADIENT BETWEEN 100 AND 120 KM

T. M. Donahue and G. R. Carignan (Michigan, University, Ann Arbor, Mich.) 1 Dec. 1975 5 p refs Journal of Geophysical Research, vol. 80, Dec. 1, 1975, p. 4565-4569. (Contract NAS5-11077; Grants NGR-39-011-155; NSF DES-74-21598)

Oxygen density profiles inferred from OGO 6 green nightglow emission vary too sharply between 100 and 120 km to be consistent with temperature gradients in standard model atmospheres, and the eddy diffusion coefficient K determined from these observations reaches its maximum below 115 km. For three atomic oxygen profiles obtained at geographic latitudes of -27.69, +48.89, and +59.10 the temperature profiles required to create a downward flux that varies with altitude as the integrated photolytic production rate above that altitude are calculated, assuming K to be invariant with altitude and latitude. The oxygen distribution can be reconciled with a constant eddy coefficient above 100 km if the temperature gradient reaches a value between 10 and 20 deg K/km for low values of the eddy coefficient (about 500,000 sq cm/sec) or between 30 and 50 deg K/km for a higher eddy coefficient (about 1.6 million sq cm/sec). The maximum gradient for the Jacchia (1971) model is about 10 deg K/km. These temperature profiles predict Ar/N ratios consistent with those measured by sounding rockets. The low K profiles are large enough to remove a large part of the solar energy deposited below 120 km by thermal conduction. C.K.D.

A76-16507\*

#### PROPERTIES OF ELF ELECTROMAGNETIC WAVES IN AND ABOVE THE EARTH'S IONOSPHERE DEDUCED FROM PLASMA WAVE EXPERIMENTS ON THE OVI-17 AND OGO 6 SATELLITES

M. C. Kelley (Cornell University, Ithaca, N.Y.), B. T. Tsurutani (California Institute of Technology, Jet Propulsion Laboratory, Pasadena, Calif.), and F. S. Mozer (California, University, Berkeley, Calif.) 1 Dec. 1975 9 p refs Journal of Geophysical Research, vol. 80, Dec. 1, 1975, p. 4603-4611.

(Contract NAS7-100; Grants N00014-69-A-0200-1015; N00014-75-C-0780)

A76-16514\*

#### A COMPARISON OF ELECTRIC AND MAGNETIC FIELD DATA FROM THE OGO 6 SPACECRAFT

R. A. Langel (NASA, Goddard Space Flight Center, Geophysics Branch, Greenbelt, Md.) 1 Dec. 1975 13 p refs Journal of Geophysical Research, vol. 80, Dec. 1, 1975, p. 4661-4673.

Previous studies of OGO 6 electric-field data and magnetic-field magnitude observations have indicated a distinct dependence of disturbance characteristics on interplanetary-sector polarity. Examination of simultaneous data below 600 km over the summer polar cap shows that changes in electric-field patterns and the disturbance patterns in magnetic-field magnitude are highly correlated. This correlation extends to pattern shapes, boundary locations, and the amplitudes of the correlated quantities. In the winter hemisphere at altitudes above 800 km, correlations between boundaries exist, pattern correlations are present but not as strong as at low altitudes in summer, and amplitude correlations are essentially absent. These studies verify that below 600 km, the region of positive magnetic-field magnitude, from 2200 to 1000 magnetic local time (MLT), receives a significant contribution from both ionospheric and nonionospheric sources. Above 800 km, the nonionospheric sources dominate. These data are also consistent with the

existence of a latitudinally broad current system at sunlit magnetic local times as the source of the negative-magnitude region between 1000 and 2200 MLT. In this region, broad structures in electric-field patterns and in magnetic-field magnitude patterns are highly correlated. Multiple peaks in the negative-magnitude, presumably identified with the multiple peaks in negative electric-field magnitude found by Langel (1973) in average surface data, occur when the electric-field pattern has multiple reversals near dusk.

(Author)

**A76-16522\*****A NEW INTERPRETATION OF SUBPROTONOSPHERIC WHISTLER CHARACTERISTICS**

R. Raghuram (Stanford University, Stanford, Calif.) 1 Dec. 1975 3 p refs Journal of Geophysical Research, vol. 80, Dec. 1, 1975, p. 4729-4731.  
(Grant NGL-05-020-008)

Propagation paths of subprotonospheric (SP) whistlers are studied on the basis of OGO 4 satellite data and ray tracing. SP whistler components picked up at a point in the ionosphere are associated with wave packets entering the lower ionosphere at different latitudes and traversing different paths. Reflection of a downcoming SP whistler component near the ion cutoff frequency is accompanied by a tone whose frequency increases with time. Horizontal gradients in the ionosphere are shown to play a major role in reflection of ELF waves at heights of about 1000 km. The combination of SP whistler and rising-tone component is examined as a possible useful diagnostic probe of the plasma structure of the ionosphere.

R.D.V.

**A76-18436\*****OGO-6 OBSERVATIONS OF 5577 A**

T. M. Donahue (Pittsburgh, University, Pittsburgh, Pa.) 1975 19 p refs In: Atmospheres of Earth and the planets; Proceedings of the Summer Advanced Study Institute, Liege, Belgium, July 29-August 9, 1974. Dordrecht, D. Reidel Publishing Co., 1975, p. 289-307.  
(Contract NAS5-11077; Grants NGR-39-011-155; NSF GA-27638; NSF GA-37744)

A brief review is given of the data obtained by the horizon-scanning 5577-A airglow photometer flown aboard OGO 6. Data are presented which show the contributions to the 5577-A emission from the F-1 region and the Chapman airglow layer. Emission rates are calculated for both regions on the basis of the dissociative-recombination and Chapman reactions, and the atomic oxygen density and downward flux are inferred from the emission rates and several assumptions concerning the temperature dependence of the rate constants. Latitude variations in the emission rates are discussed along with variations in the altitude of the 5577-A airglow. It is shown that there is a large semiannual variation in the average effective transport properties of the lower thermosphere, that the atomic oxygen profiles near 110 km suggest a maximum in eddy diffusion at about that altitude, and that systematic variations in the altitude of the atomic oxygen maximum probably do not exceed 2 km.

F.G.M.

**A76-19613\*****POLAR ENHANCEMENTS OF NIGHTGLOW EMISSIONS NEAR 6230A**

E. I. Reed (NASA, Goddard Space Flight Center, Laboratory for Planetary Atmospheres, Greenbelt, Md.) Jan. 1976 4 p ref Geophysical Research Letters, vol. 3, Jan. 1976, p. 5-8.

Night airglow emissions near 6230A, as observed from the OGO 4 spacecraft in 1967-8, show enhancements at polar latitudes by more than a factor of ten over mid and low latitude values. The enhancements are generally not symmetrical with either the north pole or the auroral oval. They are attributed in part to increases in the Meinel band emissions of OH, particularly as associated with a stratospheric warming event, and in part to increases in nitric oxide densities in the lower thermosphere.

(Author)

**A76-19838\*****THE ROLE OF COULOMB COLLISIONS IN LIMITING DIFFERENTIAL FLOW AND TEMPERATURE DIFFERENCES IN THE SOLAR WIND**

M. Neugebauer (California Institute of Technology, Jet Propulsion Laboratory, Pasadena, Calif.) 1 Jan. 1976 5 p refs Journal of Geophysical Research, vol. 81, Jan. 1, 1976, p. 78-82.

(Contract NAS7-100)

Data obtained by OGO 5 are used to confirm IMP 6 observations of an inverse dependence of the helium-to-hydrogen temperature ratio in the solar wind on the ratio of solar-wind expansion time to the Coulomb-collision equipartition time. The analysis is then extended to determine the relation of the difference between the hydrogen and helium bulk velocities (the differential flow vector) with the ratio between the solar-wind expansion time and the time required for Coulomb collisions to slow down a beam of ions passing through a plasma. It is found that the magnitude of the differential flow vector varies inversely with the time ratio when the latter is small and approaches zero when it is large. These results are shown to suggest a model of continuous preferential heating and acceleration of helium (or cooling and deceleration of hydrogen), which is cancelled or limited by Coulomb collisions by the time the plasma has reached 1 au. Since the average dependence of the differential flow vector on the time ratio cannot explain all the systematic variations of the vector observed in corotating high-velocity streams, it is concluded that additional helium acceleration probably occurs on the leading edge of such streams.

F.G.M.

**A76-19839\*****SATELLITE MEASUREMENTS OF HIGH-ALTITUDE TWILIGHT MG(PLUS) EMISSION**

J.-C. Gerard (Liege, Universite, Ougree, Belgium) 1 Jan. 1976 5 p refs Journal of Geophysical Research, vol. 81, Jan. 1, 1976, p. 83-87.

(Grant NGR-06-003-127)

Observations made by the ultraviolet spectrometer on board the orbiting geophysical observatory OGO 4 confirmed the presence of resonance scattering at 2800 A of Mg(plus) ions in the twilight subtropical ionosphere. The column density reached 4 billion ions/sq cm above 160 km. Photometric measurements by the ESRO TD 1 satellite revealed a maximum of the Mg(plus) abundance at equinoxes in the top side F region. The interhemisphere asymmetries observed in the intensity distribution are essentially attributed to the effect of eastward thermospheric winds. The 2800-A doublet was also detected by OGO 4 at middle and high latitudes from 110 to 250 km. The brightness of the emission and other evidence indicate that evaporation of meteoritic matter cannot explain the abundance of ions at 200 km. Therefore Mg(plus) ions are probably transported upward from the 100-km permanent source layer.

(Author)

**A76-19854\*****THE UPPER- AND LOWER-FREQUENCY CUTOFFS OF MAGNETOSPHERICALLY REFLECTED WHISTLERS**

B. C. Edgar (Aerospace Corp., Laboratory Operations, Los Angeles, Calif.) 1 Jan. 1976 7 p refs Journal of Geophysical Research, vol. 81, Jan. 1, 1976, p. 205-211.

(Contract F04701-74-C-0075; Grant NGL-05-020-008)

**A76-21456****AN EXPLANATION OF THE LONGITUDINAL VARIATION OF THE O1D (630 NM) TROPICAL NIGHTGLOW INTENSITY**

G. Thuillier (CNRS, Service d'Aeronomie, Verrieres-le-Buisson, Essonne, France), J. W. King, and A. J. Slater (Science Research Council, Appleton Laboratory, Slough, Berks., England) Feb. 1976 4 p Journal of Atmospheric and Terrestrial Physics, vol. 38, Feb. 1976, p. 155-158.

A76-22081

A76-22081\*

**ON THE CAUSES OF SPECTRAL ENHANCEMENTS IN SOLAR WIND POWER SPECTRA**

T. Unti (California Institute of Technology, Jet Propulsion Laboratory, Pasadena, Calif.) and C. T. Russell (California, University, Los Angeles, Calif.) 1 Feb. 1976 14 p refs Journal of Geophysical Research, vol. 81, Feb. 1, 1976, p. 469-482.

(Contract NAS7-100)

Enhancements in power spectra of the solar-wind ion flux in the frequency neighborhood of 0.5 Hz had been noted by Unti et al. (1973). It was speculated that these were due to convected small-scale density irregularities. In this paper, 54 flux spectra calculated from OGO 5 data are examined. It is seen that the few prominent spectral peaks which occur were not generated by density irregularities, but were due to several different causes, including convected discontinuities and propagating transverse waves. A superposition of many spectra, however, reveals a moderate enhancement at a frequency corresponding to convected features with a correlation length of a proton gyroradius, consistent with the results of Neugebauer (1975). (Author)

A76-22086\*

**NEW RESULTS ON THE CORRELATION BETWEEN LOW-ENERGY ELECTRONS AND AURORAL HISS**

T. Laaspere (Dartmouth College, Hanover, N.H.) and R. A. Hoffman (NASA, Goddard Space Flight Center, Greenbelt, Md.) 1 Feb. 1976 7 p ref Journal of Geophysical Research, vol. 81, Feb. 1, 1976, p. 524-530. (Grant NGR-30-001-041)

The results of a VLF (0.3-18 kHz) experiment aboard OGO 4 are compared with simultaneous data obtained by the satellite on precipitating electrons at 0.7, 2.3, and 7.3 keV to determine the source of the auroral hiss band in the night side auroral zone. At these energies the correlation with VLF auroral hiss is best at 0.7 keV and worst at 7.3 keV. Auroral electrons in the keV range may enhance the intensity of VLF auroral hiss on the night side, but the predominant source of night side hiss appears to be electrons of energies below 0.7 keV. Auroral hiss tends to occur simultaneously over a broad range of frequencies. A study based on OGO 6 data has revealed a lack of correlation between keV electrons and LF auroral hiss. These observations suggest that hiss of all frequencies is generated by electrons with energies below about 1 keV. The excellent correlation between auroral hiss and 0.7 keV electrons in the day time cleft is apparently maintained when the region of very soft electron precipitation is in motion. C.K.D.

A76-22092

**OBSERVATIONS OF PROTONS WITH ENERGIES EXCEEDING 100 keV IN THE EARTH'S MAGNETOSHEATH**

H. I. West, Jr. and R. M. Buck (California, University, Livermore, Calif.) 1 Feb. 1976 16 p refs Journal of Geophysical Research, vol. 81, Feb. 1, 1976, p. 569-584. ERDA-sponsored research.

A comprehensive study of energetic protons (100 to 1300 keV) in the magnetosheath is presented, based on OGO 5 observations of bursts of such protons in the sheath and in the upstream wave region beyond the earth's bow shock during periods of generally enhanced solar and geomagnetic activity in 1968. A summary of the described observations shows that: (1) the major bursts tend to appear near the magnetopause in the afternoon magnetosheath, (2) the proton bursts often correlate with depressions in the sheath magnetic field and usually correlate with enhanced magnetic-field turbulence, (3) the directional distributions generally coincide with the plasma flow direction, (4) the flux intensities show a fairly good correlation with Kp index, (5) the peak unidirectional spectra and fluxes in the sheath near the magnetopause are often quite similar to those in the nearby magnetosphere, (6) the main fluxes of upstream protons usually come from the solar-wind direction, and (7) magnetopause boundary-layer effects are often associated with

the fluxes. It is shown that many features of the directional distributions can be explained through a combination of the Compton-Getting effect, proton-flux spatial gradients, and free streaming of protons along field lines away from the source region. Possible sources of the sheath protons considered include escape from the magnetosphere, acceleration in the magnetosheath, acceleration in the bow shock, and acceleration in the upstream wave region with leakage into the magnetosheath. F.G.M.

A76-22105\*

**HIGH-LATITUDE TROUGHS AND THE POLAR CAP BOUNDARY**

J. M. Grebowsky, A. J. Chen, and H. A. Taylor, Jr. (NASA, Goddard Space Flight Center, Greenbelt, Md.) 1 Feb. 1976 5 p refs Journal of Geophysical Research, vol. 81, Feb. 1, 1976, p. 690-694.

OGO 6 observations of troughs in the thermal plasma densities in the topside ionosphere are discussed. Ion mass spectrometer measurements were correlated with energetic electron detector and electric field measurements. It is shown that the variation of ion composition at high latitudes is complex and frequently characterized by mid-latitude and high-latitude density depression. Prominent high-latitude troughs in the atomic ion (H, He, O) distributions were seen to lie frequently near the polar cap boundary. This indicates that these troughs are unrelated to the plasmopause which is found on closed magnetic field lines away from the trapping boundary. The production of the high-latitude troughs is shown to be related to enhancements in the soft electron flux and/or to the convection electric field. B.J.

A76-22107\*

**DEPENDENCE OF THE LATITUDE OF THE CLEFT ON THE INTERPLANETARY MAGNETIC FIELD AND SUBSTORM ACTIVITY**

Y. Kamide (Alaska, University, Fairbanks, Alaska; Cooperative Institute for Research in Environmental Sciences, Boulder, Colo.), J. L. Burch (NASA, Marshall Space Flight Center, Magnetospheric and Plasma Physics Branch, Huntsville, Ala.), J. D. Winningham (Texas, University, Richardson, Tex.), and S.-I. Akasofu (Alaska, University, Fairbanks, Alaska) 1 Feb. 1976 7 p refs Journal of Geophysical Research, vol. 81, Feb. 1, 1976, p. 698-704. (Grant NGR-44-044-150; Contract F19628-75-C-0032; Grants NSF GA-33094; NSF DES-74-23832)

The latitudinal motion of the cleft (the polar cusp) associated with the southward interplanetary magnetic field (IMF) and substorm activity is examined. The cleft location is identified on the basis of the location of midday auroras and of electron precipitation by the OGO 4 and ISIS 1 satellites. It is found that the IMF and substorm activity control independently the latitude of the cleft and that they can shift the cleft location by 3 or 4 deg under average conditions. (Author)

A76-22490\*

**BEHAVIOR OF THE SODIUM AND HYDROXYL NIGHTTIME EMISSIONS DURING A STRATOSPHERIC WARMING**

J. D. Walker (Cleveland State University, Cleveland, Ohio) and E. I. Reed (NASA, Goddard Space Flight Center, Laboratory for Planetary Atmospheres, Greenbelt, Md.) Jan. 1976 13 p refs (American Meteorological Society, Meeting on the Upper Atmosphere, Atlanta, Ga., Sept. 30-Oct. 4, 1974.) Journal of the Atmospheric Sciences, vol. 33, Jan. 1976, p. 118-130.

The behavior of the sodium and hydroxyl nighttime emissions during a stratospheric warming has been studied principally by use of data from the airglow photometers on the OGO 4 satellite. During the late stages of a major warming, both emissions increased appreciably, with the sodium emission returning to normal values prior to the decrease in the hydroxyl emission. The emission behaviors are attributed to temperature and density variations from 70 to 94 km, and a one-dimensional hydrostatic model for

that altitude range is used to calculate the effects on the emissions and on the mesospheric ozone densities. These results support the existence of a warming in the upper part of the mesosphere that is correlated with a major stratospheric warming. (Author)

**A76-26524\***  
**COMPARISON OF THE SAN MARCO 3 NACE NEUTRAL COMPOSITION DATA WITH THE EXTRAPOLATED OGO 6 EMPIRICAL MODEL**

W. T. Kasprzak and G. P. Newton (NASA, Goddard Space Flight Center, Greenbelt, Md.) 1 Mar. 1976 3 p refs Journal of Geophysical Research, vol. 81, Mar. 1, 1976, p. 1404-1406.

An investigation is conducted concerning the feasibility to extrapolate the data of the OGO 6 empirical composition model to altitudes which are lower than 450 km. Extrapolated OGO 6 model densities are, therefore, compared with data obtained in the Neutral Atmospheric Composition Experiment (NACE) carried out during the time from April to November 1971. The results of the investigation support the conclusions of an earlier comparison of OGO 6 and NACE data conducted by Newton et al. (1973). G.R.

**A76-26886\*#**  
**ON THE QUIET-TIME INCREASES OF LOW ENERGY COSMIC RAY ELECTRONS**

J. Lheureux (Arizona, University, Tucson, Ariz.) and P. Meyer (Chicago, University, Chicago, Ill.) 1975 4 p In: International Cosmic Ray Conference, 14th, Munich, West Germany, August 15-29, 1975, Conference Papers. Volume 2. Munich, Max-Planck-Institut fuer extraterrestrische Physik, 1975, p. 748-751.

(Contracts NAS5-9096; NAS5-11444; Grant NSF DES-74-00944)

With a detector on board the OGO-5 satellite, the flux and energy spectrum of electrons in the 10-30 MeV range has been continuously monitored from 1968 to 1972. Sudden increases by factors of up to 300 percent have been observed during solar quiet periods. These 'Quiet-Time Increases' abruptly die out above 30 MeV and correlate well with identical increases reported at lower energies leading to a flat relative energy spectrum. A large fraction of these electrons is most likely of Jovian origin. (Author)

**A76-26907\*#**  
**MODULATION OF LOW ENERGY ELECTRONS AND PROTONS NEAR SOLAR MAXIMUM**

J. Lheureux (Arizona, University, Tucson, Ariz.) and P. Meyer (Chicago, University, Chicago, Ill.) 1975 6 p refs In: International Cosmic Ray Conference, 14th, Munich, West Germany, August 15-29, 1975, Conference Papers. Volume 3. (A76-26851 11-93) Munich, Max-Planck-Institut fuer extraterrestrische Physik, 1975, p. 979-984.

(Contracts NAS5-9096; NAS5-11444; Grant NSF DES-74-00944)

The intensities of cosmic-ray electrons in the energy range from 24 to 235 MeV and of protons in the ranges 40 to 150 MeV and greater than 700 MeV are compared with the neutron intensity data over the period 1968 to 1972. Correlation plots between these various components show a marked break following the June 9, 1969 Forbush decrease. The resulting hysteresis curve is best explained as a sudden change in the rigidity dependence of solar modulation. A variation in the size of the solar cavity is also possible but not likely. (Author)

**A76-28486\***  
**SATELLITE MEASUREMENTS OF ION COMPOSITION AND TEMPERATURES IN THE TOPSIDE IONOSPHERE DURING MEDIUM SOLAR ACTIVITY**

M. K. Goel, B. C. N. Rao (National Physical Laboratory of India, New Delhi, India), S. Chandra, and E. J. Maier (NASA, Goddard Space Flight Center, Greenbelt, Md.) Apr. 1976 6 p ref Journal of Atmospheric and Terrestrial Physics, vol. 38, Apr. 1976, p. 389-394.

Information on both ion density and temperature is obtained from analysis of Retarding Potential Analyzer data from the OGO-4 and Explorer-31 satellites. Results obtained from data in the altitude range of 700-2000 km during medium solar activity are presented. An attempt is made to describe the major altitude variations of ion densities and temperatures at middle and low latitudes. The transition heights, where the heavier and lighter ions are equal, are found to be about 1600 and 1300 km at middle and low latitudes, respectively, for daytime and 700 km at night for middle latitudes. Based on the observed data and using diffusive equilibrium as a first-order approximation, topside ionospheric composition models are given for medium solar activity. (Author)

**A76-28988\***  
**GLOBAL ATOMIC HYDROGEN DENSITY DERIVED FROM OGO-6 LYMAN-ALPHA MEASUREMENTS**

G. E. Thomas and D. E. Anderson, Jr. (Colorado, University, Boulder, Colo.) Apr. 1976 10 p refs Planetary and Space Science, vol. 24, Apr. 1976, p. 303-312.

(Grants NGR-06-003-127; NGR-06-003-052; NSF GA-40992)

The paper analyzes a one-year set of Lyman-alpha airglow data measured in the local zenith at altitudes from 400 to 1100 km by a UV photometer aboard OGO-6. The zenith-intensity data are fitted to theoretical airglow calculations in four spherically symmetric models of the hydrogen geocorona to determine both the Ly-alpha solar flux at line center and the average atomic hydrogen column density. After correcting for a loss of instrument sensitivity, the Ly-alpha flux is found to be linearly correlated with daily Zurich sunspot number. It is also found that the hydrogen density is inversely correlated with Jacchia exospheric temperature, but the dependence is not that predicted by steady-state models with Jeans evaporative escape as the only loss mechanism. It is suggested that charge-exchange production of fast hydrogen atoms from 'hot' ionospheric protons might provide the additional loss this result requires. F.G.M.

**A76-28989\***  
**GLOBAL ATOMIC OXYGEN DENSITY DERIVED FROM OGO-6 1304 A AIRGLOW MEASUREMENTS**

D. J. Strickland and G. E. Thomas (Colorado, University, Boulder, Colo.) Apr. 1976 14 p refs Planetary and Space Science, vol. 24, Apr. 1976, p. 313-326.

(Grants NGR-06-003-127; NGR-06-003-052)

Results are presented for analysis of data on the atomic oxygen 1304-A triplet in the earth's dayglow between 400 and 1100 km which were obtained with the OGO-6 UV photometer during a 40-day period that included both quiet and disturbed conditions. Variations in the atomic oxygen column density are analyzed by obtaining best-fit models in which the 1304-A emission is produced by solar resonance scattering and photoelectron excitation. It is shown that the column density can be determined uniquely from the measured 1304-A intensity, provided the excitation processes can be described quantitatively. The values of the excitation parameters are determined directly from the data, and the deduced variations in column density over the daytime atmosphere are found to agree well with the Jacchia (1971) models. The latitudinal dependence of the column-density variations during a geomagnetic storm are discussed, the results are compared with recent measurements of the solar 1304-A fluxes as well as with calculations of the photoelectron excitation, and a method is suggested for determining the absolute atomic oxygen densities. F.G.M.

**A76-28990**  
**THE INTENSITY VARIATION OF THE ATOMIC OXYGEN RED LINE DURING MORNING AND EVENING TWILIGHT ON 9-10 APRIL 1969**

R. G. Roble (National Center for Atmospheric Research, Boulder, Colo.), J. F. Noxon (NOAA, Aeronomy Laboratory, Boulder, Colo.), and J. V. Evans (MIT, Lexington, Mass.)



Apr. 1976 14 p ref Planetary and Space Science, vol. 24, Apr. 1976, p. 327-340. USAF-Army-supported research (Grant NSF GA-28371)

## A76-31317\*

**THE INTERPRETATIONS OF ULTRAVIOLET OBSERVATIONS OF COMETS**

H. U. Keller May 1976 44 p refs Space Science Reviews, vol. 18, Mar.-May 1976, p. 641-684. (Grant NGL-06-003-052)

The paper summarizes recent cometary UV observations, most of which were made in Ly-alpha light with instruments aboard earth-orbiting satellites. These include OAO-2 observations of comets Bennett and Tago-Sato-Kosaka, OGO-5 observations of comets Bennett and Encke, and numerous observations of comet Kohoutek. Models for the production of cometary hydrogen atoms are described, including the fountain, syndyname, and parent-daughter models. Calculations of emission line profiles and multiple-scattering effects are also discussed. Results of observations and interpretations are reviewed for each cited comet, far-UV observations in other emission lines are noted, and the use of comets as solar-wind probes is considered. It is concluded that the results of the present cometary Ly-alpha observations strongly support the concept of an icy conglomerate solid cometary nucleus and suggest water to be one of the most abundant molecules in comets. F.G.M.

## A76-33057\*

**MAGNETOSHEATH LION ROARS**

E. J. Smith and B. T. Tsurutani (California Institute of Technology, Jet Propulsion Laboratory, Pasadena, Calif.) 1 May 1976 6 p refs Journal of Geophysical Research, vol. 81, May 1, 1976, p. 2261-2266. (Contract NAS7-100)

The characteristics of lion roars, which are intense packets of electromagnetic waves characteristically found in the magnetosheath, are studied. The average frequency of the emissions is 120 Hz, with over 90% occurring between 90 and 160 Hz (which is near one-half the local electron gyrofrequency); over 70% of all emissions last a mere 2 sec or less; the maximum amplitude of lion roars has an average value of 85 milligamma, over 80% being between 40 and 160 milligamma. Occurrence of lion roars is related to the level of geomagnetic activity, measured by Kp. The probability of occurrence ranges from 10% during magnetically quiet intervals to 75% during disturbed periods. Polarization and wave normal direction of lion roars, determined by variance analysis of triaxial wave forms, are right-handed circularly polarized, with propagation essentially along the ambient magnetic field. V.P.

## A76-33058\*

**ELF HISS ASSOCIATED WITH PLASMA DENSITY ENHANCEMENTS IN THE OUTER MAGNETOSPHERE**

K.-W. Chan and R. E. Holzer (California, University, Los Angeles, Calif.) 1 May 1976 8 p refs Journal of Geophysical Research, vol. 81, May 1, 1976, p. 2267-2274. (Grant NGR-05-007-276)

The low-frequency narrow hiss bands associated with plasma-density enhancements in the magnetosphere near and beyond  $L = 4$  have been studied with the search coil magnetometer and ion mass spectrometer data from OGO 5. ELF hiss is found to accompany most of the detached plasmas in the outer magnetosphere and to be sharply limited by the steep ion-density gradient at their boundary. The observations indicate that the hiss originates in and is ducted by the plasma-density enhancements. In a particularly favorable case after an interval of low AE and Dst indices, a series of enhanced plasma-density peaks was observed between  $L = 4$  and  $L = 6$  in the afternoon local-time sector. In this case, it was possible to develop an empirical

relation among hiss amplitude, plasma density, and L by using in situ simultaneous measurements. (Author)

## A76-35289

**ENERGETIC ELECTRONS IN THE INNER BELT IN 1968**

H. I. West, Jr. and R. M. Buck (California, University, Livermore, Calif.) Jul. 1976 13 p refs Planetary and Space Science, vol. 24, July 1976, p. 643-655. (Contract W-7405-ENG-48)

Pitch-angle data were obtained by the scanning magnetic electron spectrometer on OGO 5 during its traversals of the inner belt in 1968. Data from the five lowest-energy channels 79-822 keV, were analyzed in terms of j-perpendicular vs invariant latitude, time-decay rates, and spectral shapes at constant L. The inner-belt electron injection following two storm periods was observed; the first was the mild storm of June 11 and the second the more intense storms of October 31 and November 1. Comparisons with other data indicate that only a small Starfish residual (at more than 1 MeV) still remained in the heart of the inner belt; hence, the results are indicative of the normal inner belt. The data are discussed in terms of current ideas regarding the source and loss of particles in the inner belt. (Author)

## A76-35348

**HYSTERESIS OF PRIMARY COSMIC RAYS ASSOCIATED WITH FORBUSH DECREASES**

R. S. Rajan Mar. 1976 7 p Australian Journal of Physics, vol. 29, Mar. 1976, p. 89-95.

A variation of quasi-steady primary-cosmic-ray intensities during Forbush events is reported which was detected in data obtained by a neutron monitor, the OGO 1 and 3 ion chambers, and daily observations of upper-atmosphere intensities recorded with standardized Geiger-Mueller counters. A regression plot of the intensities of high- and low-rigidity primaries is found to exhibit hysteresis loops during Forbush decreases, indicating a differential modulation between the two intensities. It is shown that this effect is superposed on the 11-year variation of primary intensities, which is known to exhibit a hysteresis as a function of sunspot number. The existence of loops during Forbush events is explained in terms of a long-range order for the magnetic inhomogeneities in the modulation region. F.G.M.

## A76-36276\*

**FIELD-ALIGNED PRECIPITATION OF GREATER THAN 30-keV ELECTRONS**

D. J. Williams (NOAA, Space Environment Laboratory, Boulder, Colo.) and H. Trefall 1 Jun. 1976 4 p refs Journal of Geophysical Research, vol. 81, June 1, 1976, p. 2927-2930. (NASA ORDER S-50026-A)

A search through 2-3 months of data from OGO 6 has revealed about 10 cases of field-aligned precipitation of electrons at energies greater than 30 keV. Brief descriptions are given of the four most spectacular of these events, in which the ratio between precipitated and trapped fluxes reached about 100 in one case. Preliminary indications are that such events occur mainly in the evening and midnight sectors and at high geomagnetic latitudes (usually at or above the trapping boundary for electrons with energies greater than 30 keV). (Author)

## A76-39128\*

**SATELLITE OBSERVATION OF THE MESOSPHERIC SCATTERING LAYER AND IMPLIED CLIMATIC CONSEQUENCES**

J. R. Hummel and J. J. Olivero (Pennsylvania State University, University Park, Pa.) 1 Jul. 1976 2 p refs Journal of Geophysical Research, vol. 81, July 1, 1976, p. 3177, 3178. (Grant NGL-39-009-003)

Recent satellite photometry of the airglow has detected an extensive, though tenuous, scattering layer above the summer polar cap. Located near the mesopause, the layer

persists throughout the summer season poleward of about 75 deg latitude. By employing a simple growth model for the layer a time dependent radiative transfer model has been developed to examine radiative temperature perturbations. As was anticipated, the global temperature perturbations are negligible. However, in the polar region the impact is probably nonnegligible, the temperature decrease being of the order of a few tenths of a degree. The climatological implications of the layer on the polar region are discussed. (Author)

**A76-39130**  
**LONG-TERM COSMIC RAY MODULATION IN THE PERIOD 1966-1972 AND INTERPLANETARY MAGNETIC FIELDS**

C. N. Winkler (Leiden, Rijksuniversiteit, Leiden, Netherlands) and P. J. Bedijn (Leiden, Sterrewacht, Leiden, Netherlands) 1 Jul. 1976 9 p refs Journal of Geophysical Research, vol. 81, July 1, 1976, p. 3198-3206.

A nonseparable model of the interplanetary diffusion coefficient is presented which provides a simultaneous explanation for the available observations of cosmic ray electrons and nuclei of galactic origin measured around the last solar maximum. Changes in the energy spectra of cosmic ray electrons, protons, and alpha particles above roughly 50 MeV/nucleon are theoretically reproduced by numerical solutions of the steady-state transport equation for cosmic rays in the solar system. Changes in the diffusion coefficient are introduced by smooth variations of four independent parameters. It is shown that this model matches also the observed power spectra of the interplanetary magnetic field fluctuations reasonably well. S.D.

**A76-39145**  
**THE THEORY OF VLF DOPPLER SIGNATURES AND THEIR RELATION TO MAGNETOSPHERIC DENSITY STRUCTURE**

B. C. Edgar (Aerospace Corp., Space Science Laboratory, Los Angeles, Calif.) 1 Jul. 1976 13 p refs Journal of Geophysical Research, vol. 81, July 1, 1976, p. 3327-3339. (Contract F04701-75-C-0076; Grant NSF GA-37730)

When signals from a ground-based VLF transmitter travel through the magnetosphere and arrive at a low-altitude satellite in the conjugate hemisphere, they may undergo a spectral distortion due to Doppler shift by the satellite velocity. The paper presents a VLF ray tracing study of published VLF Doppler data samples. It is shown that the density structure of the plasmasphere leaves its imprint or signature in the observed Doppler shift pattern. Large positive and negative Doppler shifts (about 100 Hz) are reproduced by a strong decreasing electron density gradient interacting with the magnetic field curvature gradient between L roughly 2 and L roughly 3. VLF Doppler signatures can detect whether short-scale gradients dominate the density structure or merely perturb the long-scale gradient. The ray path calculations also allow one to map the signals observed by the satellite back to their excitation point in the lower ionosphere and thus estimate the effective transmitter coverage in the excitation hemisphere. S.D.

**A76-41210\***  
**DIURNAL VARIATION OF THERMAL PLASMA IN THE PLASMASPHERE**

A. J. Chen (Aiken Industries, Inc., College Park, Md.), J. M. Grebowsky (NASA, Goddard Space Flight Center, Laboratory for Planetary Atmospheres, Greenbelt; Aiken Industries, Inc., College Park, Md.), and K. Marubashi (Aiken Industries, Inc., College Park, Md.; Radio Research Laboratories, Tokyo, Japan) Aug. 1976 5 p refs Planetary and Space Science, vol. 24, Aug. 1976, p. 765-769.

All of the OGO-5 light ion density measurements were used to determine the average global topology of the equatorial plasmasphere density distribution. The variation of the light ion equatorial density at L less than or equal to 3.2 with local time was deduced by determining the average density observed within one hour of a specific local time and within 0.1 of a given L coordinate. The average H(+)

density showed a semidiurnal variation with peaks near noon and midnight. The He(+) observations also revealed multiple peaks throughout the day but with smaller amplitudes than those of H(+). At L above 3.2 plasma trough conditions increase the scatter of densities. The average variation of the H(+) density with L within the plasmasphere is found to be steepest near midnight and can be least-squares fitted equally well to either an exponential variation or to a power law. (Author)

**A76-41914\***  
**CHARACTERISTICS OF INSTABILITIES IN THE MAGNETOSPHERE DEDUCED FROM WAVE OBSERVATIONS**

F. L. Scarf (TRW Systems Group, Redondo Beach, Calif.) 1975 19 p refs In: Physics of the hot plasma in the magnetosphere; Proceedings of the Thirtieth Nobel Symposium, Kiruna, Sweden, April 2-4, 1975. (A76-41901 21-46) New York, Plenum Press, 1975, p. 271-289. (Contract NASw-2659)

A general summary is presented of the types of unstable plasma distributions encountered in the magnetosphere. It is shown that gyroresonant interactions play an important role in magnetospheric dynamics. Electrostatic instabilities not driven by currents are considered and a description is presented of observations related to current-driven instabilities. Attention is also given to aspects of mode coupling. It is pointed out that during the last decade much progress has been made in the identification of specific instabilities. Better measurements of magnetospheric plasma distribution functions are needed for the solution of remaining problems. G.R.

**A76-42390#**  
**EXPERIMENTAL MODEL OF THE EXOSPHERIC TEMPERATURE BASED ON OPTICAL MEASUREMENTS ON BOARD THE OGO 6 SATELLITE**

G. Thuillier (CNRS, Service d'Aeronomie, Verrieres-le-Buisson, Essonne, France), J. L. Falin, and C. Wachtel (CERGA, Grasse, Alpes-Maritimes, France) Jun. 1976 22 p ref COSPAR, Plenary Meeting, 19th, Philadelphia, Pa., June 8-19, 1976, Paper. 22 p. Centre National de la Recherche Scientifique (Contract CNRS-RCP-336)

The Fabry-Perot interferometer on board the OGO 6 satellite measures the spectral profile of the 630 nm airglow line. The neutral temperature is deduced directly from the Doppler linewidth. The global thermospheric temperature is represented by a set of coefficients based on the results of a spherical harmonics analysis. Comparisons are made with temperatures measured by incoherent scatter radar and temperatures deduced from N2 densities. The present model applies to quiet and moderate magnetic activity and to high solar activity. (Author)

**A76-42683\***  
**TROPICAL F REGION WINDS FROM O I 1356-A AND FORBIDDEN O I 6300-A EMISSIONS. II - ANALYSIS OF OGO 4 DATA**

J. A. Bittencourt (Texas, University, Richardson, Tex.; Instituto de Pesquisas Espaciais, Sao Jose dos Campos, Brazil), B. A. Tinsley (Texas, University, Richardson, Tex.), G. T. Hicks (U.S. Navy, E. O. Hulburt Center for Space Research, Washington, D.C.), and E. I. Reed (NASA, Goddard Space Flight Center, Laboratory for Planetary Atmospheres, Greenbelt, Md.) 1 Aug. 1976 5 p refs Journal of Geophysical Research, vol. 81, Aug. 1, 1976, p. 3786-3790. Research supported by the Instituto de Pesquisas Espaciais (Grants NGR-44-004-142; NSF DES-74-7651)

The OGO 4 tropical nightglow data on the O I 1356-A and forbidden O I 6300-A emissions during several months in the fall of 1967 are analyzed in conjunction with theoretical models. From the latitudinal asymmetry present in the tropical emissions the neutral wind velocities in the magnetic meridian at the time of the observations are found to reach 150 m/s

near 2000 LT in the Pacific sector and 110 m/s in the Indian sector. The longitudinal dependence of the emissions indicates a strong zonal component (referred to geographic coordinates) and allows the resolution of the inferred wind velocities into geographic zonal and meridional wind components. The geographic zonal component reaches a maximum velocity of 260 m/s near 2200 LT. (Author)

A76-42697

**THE TEMPERATURE GRADIENT DRIFT INSTABILITY AT THE EQUATORWARD EDGE OF THE IONOSPHERIC PLASMA TROUGH**

M. K. Hudson (California, University, Berkeley, Calif.) and M. C. Kelley (Cornell University, Ithaca, N.Y.) 1 Aug. 1976 6 p refs Journal of Geophysical Research, vol. 81, Aug. 1, 1976, p. 3913-3918. (Contracts N00014-69-A-0200-1015; N00014-75-C-0780; NOAA-04-5-002-16)

The paper examined the fluid equations relevant to the ionosphere above 400 km in a region of horizontal gradients in plasma density and electron temperature such as those detected near the ionospheric projection of the plasmapause. The equations are unstable to growth of the temperature gradient drift mode. Electric field fluctuations have been observed in this region of the ionosphere by two independent electric field experiments flown on separate satellites. In one case (OGO 6) simultaneous measurements of density and electron temperature were made. By using these data the growth rate of the temperature gradient drift mode is calculated and plotted as a function of distance along the trajectory and is shown to peak in the region where the irregularities were detected. It is concluded that the temperature gradient drift mode may contribute to the growth of irregularities at the equatorward edge of the ionospheric plasma trough. (Author)

A76-44653

**A STUDY OF ELECTRON SPECTRA IN THE INNER BELT**

H. I. West, Jr. and R. M. Buck (California, University, Livermore, Calif.) 1 Sep. 1976 5 p Journal of Geophysical Research, vol. 81, Sept. 1, 1976, p. 4696-4700. (Contract W-7405-ENG-48)

Comparisons are made between energetic electron spectra obtained in the inner belt ( $L = 1.3-2.4$ ) by the OGO 5 satellite during 1968 and spectra acquired by other magnetic spectrometer experiments before and after the Starfish high-altitude nuclear detonation on July 9, 1962. The post-Starfish data show a continual decay at the higher energies (at least 0.5 for 1962 to at least 1 MeV for 1968). Electrons of 2-MeV energy at  $L = 1.4$  showed a mean life of 1 year. By 1968, only a high-energy residual greater than 1 MeV remained in the inner belt ( $L$  is about 1.4). A pre-Starfish spectrum obtained in 1961 at  $L = 1.38$  is almost identical with the 1968 results for the same region. By 1968, Starfish electrons were no longer important as an aspect of inner-belt dynamics. (Author)

A76-44665\*

**CRITICAL ELECTRON PITCH ANGLE ANISOTROPY NECESSARY FOR CHORUS GENERATION**

R. K. Burton (California, University, Los Angeles, Calif.) 1 Sep. 1976 3 p refs Journal of Geophysical Research, vol. 81, Sept. 1, 1976, p. 4779-4781. (Grant NGR-05-007-276)

Simultaneous wave, resonant-particle, and ambient-plasma data from OGO 5 for chorus emissions on August 15, 1968, were found consistent with the theoretical critical pitch-angle-anisotropy condition for whistler-mode instability by Doppler-shifted electron cyclotron resonance. Local generation, as determined by wave normal measurements, occurred only when the pitch-angle anisotropy of resonant electrons required for instability substantially exceeded the critical anisotropy defined by Kennel and Petschek (1966). (Author)

A76-47884

**THINNING OF THE NEAR-EARTH (10 TO ABOUT 15 EARTH RADII) PLASMA SHEET PRECEDING THE SUBSTORM EXPANSION PHASE**

A. Nishida and K. Fujii (Tokyo, University, Tokyo, Japan) Sep. 1976 7 p refs Planetary and Space Science, vol. 24, Sept. 1976, p. 849-853.

The timing of plasma-sheet thinning relative to the onset of the expansion phase of substorms is examined by analysis of OGO 5 electron and proton data with the aid of simultaneous magnetic-field observations. It is found that the timing of the thinning is significantly dependent on distance. At distances less than or about equal to 15 earth radii, the thinning often starts before the onset; at distances greater than that, it tends to occur after the onset. The thinning that precedes the expansion-phase onset has been found to reduce the thickness to about 1 earth radius, and further thinning may occur in a spatially limited region. Hence it is conceivable that formation of the neutral line characterizing the substorm expansion phase is a consequence of the thinning of the plasma sheet in the near-earth region. (Author)

A77-11219\*

**OGO 5 OBSERVATIONS OF PC 5 WAVES - GROUND-MAGNETOSPHERE CORRELATIONS**

S. Kokubun, R. L. McPherron, and C. T. Russell (California, University, Los Angeles, Calif.) 1 Oct. 1976 9 p refs Journal of Geophysical Research, vol. 81, Oct. 1, 1976, p. 5141-5149.

(Grant NGR-05-007-004; Contract N000-69-A-200-4016; Grants NSF GA-341484; NSF DES-74-23464)

A77-11488

**OBSERVATIONS OF HYDROGEN IN THE UPPER ATMOSPHERE**

J. L. Bertaux (CNRS, Service d'Aeronomie, Verrieres-le-Buisson, Essonne, France) Aug. 1976 7 p refs Journal of Atmospheric and Terrestrial Physics, vol. 38, Aug. 1976, p. 821-827.

Observations of hydrogen in the upper atmosphere which were reported since January 1974 are reviewed in the light of four basic questions. The most important results are the following. At the exobase level, the diurnal variation of density in low latitude regions is in agreement with current theories, whereas the latitude variation is not clearly understood. The hydrogen temperature at the exobase level is equal to the temperature of neutral atmosphere as derived by satellite drag data measurements. In the exosphere, the distribution of hydrogen atoms in satellite orbits is largely affected by Lyman-alpha radiation pressure. The absolute value of the thermal escape (Jeans escape flux) is lower than expected from current aeronomical theories, and its variations as a function of solar activity indicates that non-thermal escape mechanisms must exist with a significant contribution to total loss of H from the planet. (Author)

A77-11489\*

**DYNAMICAL EFFECTS IN THE DISTRIBUTION OF HELIUM IN THE THERMOSPHERE**

C. A. Reber (NASA, Goddard Space Flight Center, Greenbelt, Md.) Aug. 1976 12 p refs Journal of Atmospheric and Terrestrial Physics, vol. 38, Aug. 1976, p. 829-840.

The paper discusses some phenomena, mainly observed by satellites, which illustrate the use of helium as a tracer for studying the morphology and history of atmospheric responses to energy inputs of varying amplitudes and durations. The effects observed include (1) the annual north-south excursion of the sub-solar point producing the winter helium bulge, (2) the 24-hour diurnal variation, where the helium density peak is phase-shifted to the morning in the lower thermosphere, (3) high latitude magnetospheric heating of the thermosphere, with helium indicating regions of probable upwelling of the heated gas, and (4) gravity

wave formation and propagation, with the attendant implications for transport of energy from one region of the atmosphere to another. P.T.H.

**A77-11692\***  
**QUIET-TIME INCREASES OF LOW-ENERGY ELECTRONS - THE JOVIAN ORIGIN**

J. Lheureux (Arizona, University, Tucson, Ariz.) and P. Meyer (Chicago, University, Chicago, Ill.) 1 Nov. 1976 6 p refs *Astrophysical Journal*, vol. 209, Nov. 1, 1976, pt. 1, p. 955-960.

(Contracts NASS-11444; NASS-9096; Grant NSF DES-74-00944)

With a detector on board the OGO-5 satellite, the flux and energy spectrum of electrons in the 10-200-MeV range has been continuously measured from 1968 to 1971. Sudden increases in intensity by factors of up to 300% have been observed during solar quiet times. It is shown that these increases are nearly independent of energy up to about 25 MeV and disappear rapidly above that energy. The frequency of the increases peaks every 13 months at a time following the crossing by earth of the interplanetary magnetic-field line which passes the vicinity of the planet Jupiter. Most of the increases occur in a period of 3 to 5 months following this crossing and often appear to be 27 days apart. A Jovian origin for these electrons and their mode of transport to the inner solar system are discussed. (Author)

**A77-12057**  
**MODEL OF EQUATORIAL SCINTILLATIONS FROM IN-SITU MEASUREMENTS**

S. Basu, S. Basu, and B. K. Khan (Calcutta, University, Calcutta, India) Oct. 1976 12 p refs *Radio Science*, vol. 11, Oct. 1976, p. 821-832. Research sponsored by the Indian Space Research Organization.

OGO-6 retarding potential analyzer measurements of F-region irregularity amplitude and ambient electron density have been used in developing a model of equatorial scintillations in the framework of diffraction theory. The percentage occurrence contours of estimated equatorial scintillations not less than 4.5 dB at 140 MHz during 1900-2300 LMT for the period November-December 1969 and 1970 have been derived, and the model is found to depict a pronounced longitude variation with scintillation belt width, percentage occurrence being maximum over the African sector. The latitude extent of the scintillation belt narrows over the American sector without much decrease in scintillation occurrence, while over the Indian and Far Eastern sectors both the extent and occurrence are found to decrease. B.J.

**A77-15786**  
**CORRELATED MEASUREMENTS OF SCINTILLATIONS AND IN-SITU F-REGION IRREGULARITIES FROM OGO-6**

S. Basu (USAF, Geophysics Laboratory, Bedford, Mass.) and S. Basu Nov. 1976 4 p refs (COSPAR, Symposium on the Geophysical Use of Satellite Beacon Observations, Boston, Mass., June 1976.) *Geophysical Research Letters*, vol. 3, Nov. 1976, p. 681-684.

Scintillation estimates obtained from in-situ irregularity measurements by OGO-6 are compared with simultaneous 137 MHz and 6 GHz scintillations recorded at equatorial stations in the American and African sectors. In this first such correlated study, it is found that the equatorial irregularity amplitudes in these sectors are so large that for a moderately thick irregularity layer the commonly observed monotonic power law spectrum with outer scale dimensions much larger than the Fresnel dimension at VHF can explain the observed GHz scintillations and can locate the VHF band in the saturated scintillation regime. This finding is in contrast to other numerical modelling attempts which usually call for artificial tailoring of irregularity spectra to account for the observed GHz scintillations. (Author)

**A77-16238\***  
**MAGNETOSPHERIC CHORUS - OCCURRENCE PATTERNS AND NORMALIZED FREQUENCY**

W. J. Burtis and R. A. Helliwell (Stamford University, Stamford, Calif.) Nov. 1976 22 p *Planetary and Space Science*, vol. 24, Nov. 1976, p. 1007-1024. (Grant NGL-05-020-008)

Over 400 hours of continuous broadband data obtained by the OGO 3 satellite are analyzed to provide a statistically accurate description of band-limited (magnetospheric) chorus. Certain aspects of the chorus frequency distribution are interpreted in terms of a gyroresonant electron feedback model of generation. An example of high chorus activity during an outbound pass through the noon magnetosphere is examined in detail, the spectral complexity of some chorus is illustrated, and the diurnal variation of chorus occurrence is investigated. The frequency and bandwidth distributions of chorus are analyzed. The results indicate that chorus occurrence depends strongly on local time and dipole latitude, the general region of maximum chorus occurrence approximates the previously reported zone of 'hard' electron precipitation, and the normalized chorus frequency is strongly dependent on dipole latitude. It is shown how a change in the curvature of the whistler-mode refractive-index surface affects focusing of radiation along magnetic field lines and how interference can occur between modes with slightly different ray velocities. It is concluded that most magnetospheric chorus consists of rising emissions which are probably generated by gyroresonant electrons slightly off the equator. F.G.M.

**A77-16240\***  
**GEOMAGNETIC STORM EFFECTS ON THE THERMOSPHERE AND THE IONOSPHERE REVEALED BY IN SITU MEASUREMENTS FROM OGO 6**

K. Marubashi, C. A. Reber, and H. A. Taylor, Jr. (NASA, Goddard Space Flight Center, Laboratory for Planetary Atmospheres, Greenbelt, Md.) Nov. 1976 11 p refs *Planetary and Space Science*, vol. 24, Nov. 1976, p. 1031-1041.

The temporal response of the densities of upper-atmospheric ion and neutral constituents to a particular geomagnetic storm is studied using simultaneous ion and neutral-composition data obtained by the OGO 6 satellite during consecutive orbits at altitudes greater than 400 km. The investigated constituents include H(+), O(+), N<sub>2</sub>, O, He, and H. Derivation of the H density is reviewed, and the main effects of the storm are discussed, particularly temporal and global variations in the densities. It is found that: (1) the H and He densities began to decrease near the time of sudden commencement, with the decrease amounting to more than 40% of the quiet-time densities during the maximum stage at high latitudes; (2) the O and N<sub>2</sub> densities exhibited an overall increase which began later than the change in H and He densities; (3) the H(+) density decreased differently in two distinct regions separated near the low-latitude boundary of the light-ion trough; and (4) the O(+) density showed an increase during earlier stages of the storm and decreased only in the Northern Hemisphere during the recovery phase. Certain physical and chemical processes are suggested which play principal roles in the ionospheric response to the storm. F.G.M.

**A77-16243\***  
**OGO-4 OBSERVATIONS OF THE ULTRAVIOLET AURORAL SPECTRUM**

J.-C. Gerard and C. A. Barth (Colorado, University, Boulder, Colo.) Nov. 1976 5 p refs *Planetary and Space Science*, vol. 24, Nov. 1976, p. 1059-1063. (Grant NGR-06-003-127)

Auroral ultraviolet spectra in the range from 1200 to 3200 Å have been obtained by the spectrometer on board the OGO-4 satellite. Emissions of N<sub>2</sub>, H, O, and N are readily identified. Atomic and molecular intensities are deduced from the comparison with a synthetic spectrum and compare reasonably well with some previous

measurements and calculations. A feature at 2150 Å is assigned to the (1-0) NO gamma band. Taking into consideration the various excitation mechanisms of NO(A2 Sigma), it is proposed that energy transfer from N2 metastable molecules to oxygen accounts for the excitation of the NO gamma bands. In particular, it is suggested that the resonant reaction between O2 and highly metastable N2 molecules may be a major source of NO(A2 Sigma).

(Author)

**A77-16850\***  
**CHARACTERISTICS OF COSMIC X-RAY BURSTS OBSERVED WITH THE OGO-5 SATELLITE**

S. R. Kane and K. A. Anderson (California, University, Berkeley, Calif.) 15 Dec. 1976 14 p refs Astrophysical Journal, vol. 210, Dec. 15, 1976, pt. 1, p. 875-888. (Grant NGL-05-003-017)

Observations of 11 cosmic X-ray bursts made with the solar X-ray spectrometer aboard OGO 5 are presented. Their identification as cosmic events is based on good time coincidence with observations of cosmic gamma-ray bursts reported in the literature. The OGO-5 experiment is most sensitive to cosmic X-ray sources located in the sunward hemisphere. When this condition was satisfied and the OGO-5 experiment was operating normally, almost every cosmic gamma-ray burst reported by other observers was detected at X-ray energies of at least 32 keV. In three events the spectrum was observed down to about 10 keV. Two intense events were observed with 0.288-s time resolution, and large time variations were observed to occur in times not exceeding 0.3 s. Evidence is found that most cosmic gamma-ray bursts have photon spectra extending down to about 10 keV. The origin of these cosmic events in processes similar to those believed to occur in solar flares is briefly examined.

(Author)

**A77-16868\***  
**MULTIPLE-SATELLITE STUDIES OF MAGNETOSPHERIC SUBSTORMS - RADIAL DYNAMICS OF THE PLASMA SHEET**

T. Pytte (California, University Los Angeles, Calif.; Bergen, Universitet, Bergen, Norway), R. L. McPherron, M. G. Kivelson (California, University, Los Angeles, Calif.), H. I. West, Jr. (California, University, Livermore, Calif.), and E. W. Hones, Jr. (California, University, Los Alamos, N. Mex.) 1 Dec. 1976 13 p Journal of Geophysical Research, vol. 81, Dec. 1, 1976, p. 5921-5933. ERDA-supported research (Grant NGL-05-007-004; Contract N00014-69-AL-0200-4016; Grant NSF DES-75-10678)

The radial dynamics of the nighttime plasma sheet during substorms is examined. The spatial dependence of plasma sheet variations at different radial distances is studied on the basis of simultaneous recordings from two closely spaced satellites. The simultaneous measurements of the plasma sheet behavior earthward and tailward of  $r = 15$  earth radii confirm substorm models which predict a thinning of the near-earth plasma sheet before the formation of an X-type neutral line, followed by a thickening on the earthward side and a further thinning on the tailward side. Temporal correlations between the plasma sheet variations and substorm development on the ground are studied by obtaining accurate timing of individual substorm expansion onsets. In particular, during multiple onset storms, the near-earth plasma sheet is found to experience a series of multiple expansions and contractions, which usually occur in a one-to-one relationship with ground Pi 2 bursts and are well correlated with auroral zone and low-altitude magnetic disturbances.

V.P.

**A77-17124\***  
**FIELD-ALIGNED CURRENTS OBSERVED BY THE OGO 5 AND TRIAD SATELLITES**

M. Sugiura (NASA, Goddard Space Flight Center, Laboratory for Planetary Atmospheres, Greenbelt, Md.) Sep. 1976 10 p ref (International Union of Geodesy and Geophysics, General Assembly, 16th, Grenoble, France, Aug.

25-Sept. 6, 1975.) Annales de Geophysique, vol. 32, July-Sept. 1976, p. 267-276.

The Triad (at a height of 800 km) and OGO 5 (in the high altitude magnetosphere) magnetic field observations have shown the existence of a field-aligned current system consisting of currents flowing in the polar cap boundary layer and those flowing in another layer located equatorward of the former. In the polar cap boundary layer (identified as the high-latitude boundary of the plasma sheet in the nightside magnetosphere), the current flows into the ionosphere on the morning side and away from the ionosphere on the afternoon side. In the lower-latitude layer, the current directions are reversed. The current in the polar cap boundary layer is considered as the primary field-aligned current system.

B.J.

**A77-18572\***  
**NON-THERMAL PROCESSES DURING THE 'BUILD-UP' PHASE OF SOLAR FLARES AND IN ABSENCE OF FLARES**

S. R. Kane (California, University, Berkeley, Calif.) and M. Pick (Paris, Observatoire, Meudon, Hauts-de-Seine, France) Mar. 1976 12 p refs (NASA, IAU, IUGG, and International Council of Scientific Unions, Workshop on Flare Build-up Study, Falmouth, Mass., Sept. 8-11, 1975.) Solar Physics, vol. 47, Mar. 1976, p. 293-304.

(Grants NGL-05-003-017; NSG-7092; Contract N00014-67-A-0112-0068)

Hard X-ray and radio observations indicate production of non-thermal electrons as a common phenomenon of the active sun. A preliminary analysis of three hard X-ray bursts observed with the OGO-5 satellite and radio observations indicate that non-thermal particles are present in the flare region prior to the impulsive (flash) phase and also during the gradual rise and fall (GRF) bursts which are usually explained in terms of purely 'thermal' radiation. The principal difference between the non-thermal electrons observed before the flash phase and during the flash phase appears to be in their total number rather than in the hardness of their energy spectrum. Basic characteristics of the two acceleration processes are probably similar although the total energy converted into non-thermal electrons is considerably larger in the flash phase. Transient absorbing H-alpha features and filament activations are discussed in terms of their ability to produce energetic particle events and magnetic energy release.

(Author)

**A77-20886**  
**ALTITUDE PROFILES OF THE PHOTOELECTRON INDUCED O 1D (6300 Å) PREDAWN ENHANCEMENT BY OBSERVATION AND THEORY**

G. Thuillier, J. E. Blamont (CNRS, Service d'Aeronomie, Verrieres-le-Buisson, Essonne, France), and G. Lejeune (Grenoble, Universite, Grenoble, France) Dec. 1976 10 p refs Planetary and Space Science, vol. 24, Dec. 1976, p. 1141-1150.

Emission profiles of the 6300-Å line are determined from OGO 4 data in the dark ionosphere during conjugate sunrise. From electron-density profile measurements, it is shown that, for two cases studied, recombination cannot account for the measured O 1D emission profiles. However, direct photoelectron-oxygen excitation can reproduce the data. If the photoelectron escape flux in the sunlit ionosphere, computed from standard photoelectron production, is transmitted through the field tube with an additional attenuation of 0.6 due to angular diffusion through photoelectron-electron and photoelectron-ion Coulomb collisions, the Hinteregger (1965) solar-flux data must be increased by a factor 2, which agrees with previous results.

(Author)

**A77-21093\***  
**TRIGGERING OF SUBSTORMS BY SOLAR WIND DISCONTINUITIES**

S. Kokubun (California, University, Los Angeles, Calif.; Tokyo, University, Tokyo, Japan), R. L. McPherron, and

C. T. Russell (California, University, Los Angeles, Calif.) 1 Jan. 1977 13 p ref Journal of Geophysical Research, vol. 82, Jan. 1, 1977, p. 74-86.  
(Grant NGR-05-007-004; Contract N00014-69-A-200-40160; Grant NSF GA-341484)

The probability of triggering of polar substorms by a large-scale magnetospheric compression associated with a discontinuity in the solar wind has been examined statistically using ground magnetogram data, AE index data and satellite geomagnetic data on 125 sudden storm commencements observed during 1967-1970. The triggering probability was found to depend on the amplitude of the sudden storm commencement and on the degree of preceding AE activity. In almost all cases the triggering occurred when the B-Z component of the interplanetary magnetic field was negative or decreasing during the 30 min before the passage of the discontinuity. Transient geomagnetic responses with a time scale of Alfvén wave propagation in the polar cap also depend on interplanetary magnetic field conditions. B.J.

A77-21504

**SHOCKS, SOLITONS AND THE PLASMAPAUSE**

H. Kikuchi (Nihon University, Tokyo; Nagoya University, Nagoya, Japan) Nov. 1976 6 p refs (International Union of Radio Science and International Association of Geomagnetism and Aeronomy, Symposium on the Physics of the Plasmopause, Grenoble, France, Aug.-Sept. 1975.) Journal of Atmospheric and Terrestrial Physics, vol. 38, Nov. 1976, p. 1055-1060.

An ideal yet plausible mathematical model is developed for the local formation of the nightside equatorial plasmopause. It is assumed that the plasmopause is an electrostatic laminar shock with a plane boundary. The model is based on the idea that the thermal plasma inside the plasmopause is of terrestrial origin, while the plasma beyond the plasmopause is essentially of solar wind origin. An approximate description of the model is presented in terms of a combined form of the Korteweg-de Vries (1895) and Burgers (1940) equation. S.D.

A77-21512

**INSTABILITY PHENOMENA IN DETACHED PLASMA REGIONS**

M. G. Kivelson (California, University, Los Angeles, Calif.) Nov. 1976 12 p refs (International Union of Radio Science and International Association of Geomagnetism and Aeronomy, Symposium on the Physics of the Plasmopause, Grenoble, France, Aug.-Sept. 1975.) Journal of Atmospheric and Terrestrial Physics, vol. 38, Nov. 1976, p. 1115-1126. (Grant NSF DES-74-23464)

Wave-propagation characteristics, such as plasma frequency and Alfvén velocity, are significantly modified by changes in the cold plasma density. Consequently, regions of so-called detached plasma that drift through the plasma trough beyond the plasmopause are highly correlated with waves which develop in a wide range of frequencies and which are observed by spacecraft experiments. In particular, for low-frequency ELF signals, the association is sufficiently close to suggest that the waves are locally generated within the detached plasma. Hence, the observations can be used to test theoretical models of wave generation, especially by examining the dependence of the observed frequencies and amplitudes on position in the dipole field (L-shell) and on the measured particle distributions. ULF waves are frequently observed in detached-plasma regions. At times it is possible to use the OGO-5 plasma measurements to determine one component of the electric field of these ULF waves, and thereby to infer that the waves are standing-mode oscillations of field lines. (Author)

A77-21513

**MICROPULSATIONS AND THE PLASMAPAUSE**

H. Kikuchi (Nihon University, Tokyo; Nagoya University, Nagoya, Japan) Nov. 1976 8 p (International Union of Radio Science and International Association of Geomagnetism and Aeronomy, Symposium on the Physics

of the Plasmopause, Grenoble, France, Aug.-Sept. 1975.) Journal of Atmospheric and Terrestrial Physics, vol. 38, Nov. 1976, p. 1127-1134.

A correlative study was performed of the plasmopause and associated irregularities, the proton ring current and micropulsations from OGO and ground Pc 1 observations. It is shown that plasmopause-associated irregularities are well correlated in space and time with the proton ring current and the Pc 1 micropulsations during the post-storm recovery. This indicates that the plasmopause and associated plasma irregularities may serve as a possible source mechanism for short-period micropulsations and as a MHD waveguide. An ideal model is presented of Pc 1 generation as an active Fabry-Perot resonator which presents the possibility of the combined effect of universal and cyclotron instabilities. B.J.

A77-21523

**DETAILED ANALYSIS OF MAGNETOSPHERIC ELF CHORUS - PRELIMINARY RESULTS**

N. Cornilleau-Wehrin, J. Etcheto (CNET, Centre de Recherches en Physique de l'Environnement, Issy-les-Moulineaux, Hauts-de-Seine, France), and R. K. Burton Nov. 1976 10 p refs (International Union of Radio Science and International Association of Geomagnetism and Aeronomy, Symposium on the Physics of the Plasmopause, Grenoble, France, Aug.-Sept. 1975.) Journal of Atmospheric and Terrestrial Physics, vol. 38, Nov. 1976, p. 1201-1210.

Individual ELF chorus elements are analyzed in detail using OGO 5 search coil magnetometer data. The chorus studied was detected in the equatorial region at L of about 6-7 on the nightside. The evolution of frequency, amplitude, and wave normal direction is studied inside the elements. Isolated rising tones, a period of change from rising to falling tones, and a period of burstlike structure are analyzed. There is nearly always a time structure but no fine structure in frequency. The amplitude variations are very quick. The wave normal direction may turn inside an element. Falling tones seem to present higher values of wave-vector angle than rising ones. The results are preliminary. (Author)

A77-23201

**STRUCTURE OF ELECTRODYNAMIC AND PARTICLE HEATING IN THE DISTURBED POLAR THERMOSPHERE**

D. R. Tausch (Michigan, University, Ann Arbor, Mich.) 1 Feb. 1977 6 p refs Journal of Geophysical Research, vol. 82, Feb. 1, 1977, p. 455-460. (Grant NSF DES-75-01484)

Molecular nitrogen density measurements obtained from the neutral atmospheric composition experiment on board OGO 6 satellite are used to study the morphology of the polar energy deposition during periods of magnetic disturbances. The data presented were obtained for eight families of polar perigee passes during 1969 and 1970. The data show a strong magnetic local time and invariant latitude dependence, the majority of the energy deposition being in the night sectors, extending down from the pole well into the mid-invariant latitude regions. (Author)

A77-23205\*

**MULTIPLE SATELLITE OBSERVATIONS OF PULSATION RESONANCE STRUCTURE IN THE MAGNETOSPHERE**

W. J. Hughes, R. L. McPherron, and C. T. Russell (California, University, Los Angeles, Calif.) 1 Feb. 1977 7 p refs Journal of Geophysical Research, vol. 82, Feb. 1, 1977, p. 492-498.

(Contract NAS5-11674; Grant NGL-05-007-004; LC90A4330F)

Data from two intervals when pulsation activity was simultaneously observed on both ATS 1 and OGO 5 satellites are presented. The first example, a Pc 4, indicates that this pulsation is caused by a field line near L = 7 resonating in its second-harmonic mode. This is inferred from both plasma density measurements and polarization characteristics. The

wave was not observed at three ground stations in the vicinity of the satellite conjugate points. This indicates that Pc 4 waves are very localized in latitude and that a close array (less than 100 km) is needed to perform effective correlation with satellites. The second event, which is also in the Pc 4 band, can again be inferred to be a field line resonance from the polarization characteristics (Author)

**A77-23211\***  
**COMPARISONS OF IONOGRAM AND OGO 6 SATELLITE OBSERVATIONS OF SMALL-SCALE F REGION INHOMOGENEITIES**

J. W. Wright (NOAA, Space Environment Laboratory, Boulder, Colo.), J. P. McClure, and W. B. Hanson (Texas, University, Richardson, Tex.) 1 Feb. 1977 7 p ref Journal of Geophysical Research, vol. 82, Feb. 1, 1977, p. 548-554. (Grants NGR-44-004-120; NSF DES-71-0555-A02; NGL-44-004-001)

**A77-23220\***  
**STRUCTURE OF A QUASI-PARALLEL, QUASI-LAMINAR BOW SHOCK**

E. W. Greenstadt, F. L. Scarf (TRW Systems, Space Sciences Dept., Redondo Beach, Calif.), C. T. Russell, R. E. Holzer (California, University, Los Angeles, Calif.), V. Formisano (CNR, Laboratorio per il Plasma nello Spazio, Frascati, Italy), P. C. Hedgecock (Imperial College of Science and Technology, London, England), and M. Neugebauer (California Institute of Technology, Jet Propulsion Laboratory, Pasadena, Calif.) 1 Feb. 1977 16 p refs Journal of Geophysical Research, vol. 82, Feb. 1, 1977, p. 651-666. (Contract NASw-2398)

A thick quasi-parallel bow shock structure was observed on February 14, 1969, with field and particle detectors of both HEOS 1 and OGO 5. The typical magnetic pulsation structure was at least 1-2 R-E thick radially and was accompanied by irregular but distinct (average) plasma distributions characteristic of neither the solar wind nor the magnetosheath. There appeared to be a separate 'interpulsation' regime occurring between bursts of large amplitude oscillations. This regime was magnetically similar to the upstream wave region but was characterized by disturbed plasma flux and enhanced noise around the ion plasma frequency. The shock structure appeared to be largely of an oblique whistler type, probably complicated by counterstreaming high-energy protons. (Author)

**A77-23222\***  
**HIGH-LATITUDE NITRIC OXIDE IN THE LOWER THERMOSPHERE**

J.-C. Gerard and C. A. Barth (Colorado, University, Boulder, Colo.) 1 Feb. 1977 7 p ref Journal of Geophysical Research, vol. 82, Feb. 1, 1977, p. 674-680. (Grants NGR-06-003-127; NGL-06-003-052)

High-latitude observations of fluorescent nitric oxide gamma bands were made before and during a strong magnetic storm with the OGO 4 ultraviolet spectrometer. Brightness measurements of the (1-0) gamma band of nitric oxide indicate a slow buildup of NO during the disturbed period. The NO column density reaches a value as high as a factor of 8 greater than the midlatitude value and shows no correlation with the brightness of the instantaneous aurora. A time-dependent model calculation indicates that the ionization and dissociation of N<sub>2</sub> by auroral electrons can increase the NO and N(4S) densities. This increase is dependent on the intensity and duration of the auroral precipitation and on the branching ratio of N(2-D) production by dissociation of N<sub>2</sub>. A steady state is not reached for NO until 100,000 sec in an aurora characterized by an energy flux of 10 ergs per sq cm sec. Dissociation by the solar ultraviolet radiation competes with horizontal and vertical transport as a loss process for the nitric oxide produced by the aurora. A high NO(+)/O<sub>2</sub>(+) ratio is to be expected in the period following a strong auroral precipitation. (Author)

**A77-23987#**  
**AEROS A ATOMIC OXYGEN PROFILES COMPARED WITH THE OGO 6 MODEL**

B. Rawer, K. Rawer, G. Schmidtke, R. Matzke, and CH. Muenther (Fraunhofer-Gesellschaft zur Foerderung der angewandten Forschung, Institut fuer physikalische Weltraumforschung, Freiburg im Breisgau, West Germany) 1976 7 p refs In: Space research XVI; Proceedings of the Open Meetings of Working Groups on Physical Sciences, May 29-June 7, 1975, and Symposium and Workshop on Results from Coordinated Upper Atmosphere Measurement Programs, Varna, Bulgaria, May 29-31, 1975. Berlin, East Germany, Akademie-Verlag GmbH, 1976, p. 251-257. Research sponsored by the Bundesministerium fuer Forschung und Technologie.

The two model atmospheres established by the OGO 6 group can now be compared with many atomic oxygen profiles in the height range 200-450 km obtained with a satellite occultation experiment under ground sunrise conditions. It appears that for such conditions densities and temperatures given by the models are higher than found from the measurements. Smoothing over the day, as applied in the models, may be responsible for a part of this difference. Up to 400 km the second (non-isothermal) OGO 6 model fits the data better than does the isothermal one. (Author)

**A77-24016#**  
**THE MORPHOLOGY OF EQUATORIAL IRREGULARITIES IN THE AFRO-ASIAN SECTOR FROM OGO 6 OBSERVATIONS**

S. Basu, S. Basu, J. N. Bhar, and B. K. Guhathakurta (Calcutta, University, Calcutta, India) 1976 7 p refs In: Space research XVI; Proceedings of the Open Meetings of Working Groups on Physical Sciences, May 29-June 7, 1975, and Symposium and Workshop on Results from Coordinated Upper Atmosphere Measurement Programs, Varna, Bulgaria, May 29-31, 1975. Berlin, East Germany, Akademie-Verlag GmbH, 1976, p. 427-433. Research supported by the Indian Space Research Organization.

The morphology of equatorial irregularities in the Afro-Asian sector delimited between 40 deg W and 160 deg E longitudes is assessed on the basis of in-situ data obtained from the retarding potential analyzer aboard the OGO 6 satellite, including a high-resolution mode of operation specifically designed to measure the amplitude and scale sizes of ionospheric irregularities. Equivalent VHF scintillation indices are obtained within the framework of a suitable scattering theory. Smoothed contours of percentage occurrence of estimated scintillations of at least 1 dB on quiet days are determined for overhead observations on a geographic longitude and dip latitude grid. Significant longitudinal variation of the estimated scintillations is revealed, with maximum occurrence being observed in the African sector. S.D.

**A77-25183\***  
**GLOBAL EXOSPHERIC TEMPERATURES AND DENSITIES UNDER ACTIVE SOLAR CONDITIONS**

J. S. Nisbet (Pennsylvania State University, University Park, Pa.), B. J. Wydra (Rockwell International Corp., Anaheim, Calif.), C. A. Reber (NASA, Goddard Space Flight Center, Greenbelt, Md.), and J. M. Luton (CNRS, Service d'Aeronomie, Verrieres-le-Buisson, Essonne, France) Jan. 1977 11 p refs Planetary and Space Science, vol. 25, Jan. 1977, p. 59-69. (Grant NGL-39-009-003; N00014-67-A-0385-0017)

Temperatures measured by the OGO-6 satellite using the 6300 A airglow spectrum are compared with temperatures derived from total densities and N<sub>2</sub> densities. It is shown that while the variation of the total densities with latitude and magnetic activity agree well with values used for CIRA (1972), the temperature behavior is very different. While the temperatures derived from the N<sub>2</sub> density were in much better agreement there were several important differences which radically affect the pressure gradients. The variation of temperature with magnetic activity showed seasonal and

local time variations. Neutral temperature, density, pressure and boundary oxygen variations for the storm of 8 March 1970 are presented. (Author)

**A77-27317\***  
**EMPIRICAL MODELS OF HIGH-LATITUDE ELECTRIC FIELDS**

J. P. Heppner (NASA, Goddard Space Flight Center, Greenbelt, Md.) 1 Mar. 1977 11 p refs Journal of Geophysical Research, vol. 82, Mar. 1, 1977, p. 1115-1125.

Observational models of high-latitude dawn-dusk electric fields, quantitatively based on OGO 6 measurements, are presented for the two Northern Hemisphere (summer) distributions that occur, respectively, when the interplanetary magnetic field is in the -Y or +Y hemisphere in solar ecliptic coordinates. Both models are representative of conditions which produce magnetic disturbance levels corresponding to Kp of approximately 3. Model cross sections are also given for two selected time periods when the fields were exceptionally weak or strong and were accompanied by magnetic conditions corresponding to Kp of zero or AE of about 1000, respectively. An attempt is made to construct convection patterns resembling the original idealizations of Axford and Hines (1961) in order to obtain convective continuity within the observed boundaries. Since the result is not realistic in representing observations near the Harang discontinuity in the nightside auroral belt, the pattern is modified to fit typical conditions near that discontinuity.

F.G.M.

**A77-27318\***  
**MAGNETIC STORM EFFECTS ON THE TROPICAL ULTRAVIOLET AIRGLOW**

J.-C. Gerard (Colorado, University, Boulder, Colo.), D. N. Anderson (NOAA, Space Environment Laboratory, Boulder, Colo.), and S. Matsushita (High Altitude Observatory, Boulder, Colo.) 1 Mar. 1977 11 p refs Journal of Geophysical Research, vol. 82, Mar. 1, 1977, p. 1126-1136. (Grants NGR-06-003-127; NGL-06-003-052)

OGO 4 measurements of the UV equatorial airglow made during a period which included a major magnetic storm are analyzed and used as an indicator of wind direction and velocity as well as ExB drift magnitude and phase. Some features of the airglow intensity and distribution are explained in terms of storm-induced changes in vertical drift velocity, neutral composition, or both. The observations are shown to be consistent with an eastward neutral wind that transports ionization from the Southern to the Northern Hemisphere while raising the F layer in the South and lowering it in the North. Theoretical modeling of the low-latitude F-region ionosphere indicates that an eastward wind with velocity approaching 300 m/s at 2100 LT can qualitatively produce the observed hemispheric asymmetries in airglow emission rates.

F.G.M.

**A77-31391\***  
**THE LOCAL TIME VARIATION OF ELF EMISSIONS DURING PERIODS OF SUBSTORM ACTIVITY**

R. M. Thorne, S. R. Church, W. J. Malloy (California, University, Los Angeles, Calif.), and B. T. Tsurutani (California Institute of Technology, Jet Propulsion Laboratory, Pasadena, Calif.) 1 Apr. 1977 6 p refs Journal of Geophysical Research, vol. 82, Apr. 1, 1977, p. 1585-1590.

(Contract NAS7-100; Grants NSF DES-75-14923; NSF DES-75-13792)

A statistical study is reported concerning the occurrence probability of ELF emissions observed on the low-altitude polar-orbiting satellite OGO 6 during periods of substorm activity. Over 160 individual substorm periods have been selected and analyzed during the period from June 1969 to October 1970. The statistical results are discussed, taking into account ELF response to substorm activity and emissions during the recovery phase of magnetic storms. G.R.

**A77-34326\***  
**VARIATIONAL ELECTRIC FIELDS AT LOW LATITUDES AND THEIR RELATION TO SPREAD-F AND PLASMA IRREGULARITIES**

J. A. Holtet, N. C. Maynard, and J. P. Heppner (NASA, Goddard Space Flight Center, Laboratory for Planetary Atmospheres, Greenbelt, Md.) Mar. 1977 16 p refs Journal of Atmospheric and Terrestrial Physics, vol. 39, Mar. 1977, p. 247-262.

In situ measurements of variational electric fields at low latitudes, taken by OGO 6 satellite instruments, are analyzed. The observations are compared with other data on F region and spread-F structures. Conformity of the electric field fluctuations with the overall picture of low-latitude irregularities is examined empirically and theoretically, and candidate processes for generation of the observed irregularities are considered. Three distinct types of irregularities are delineated and compared. R.D.V.

**A77-34901**  
**EXPERIMENTAL GLOBAL MODEL OF THE EXOSPHERIC TEMPERATURE BASED ON MEASUREMENTS FROM THE FABRY-PEROT INTERFEROMETER ON BOARD THE OGO-6 SATELLITE - DISCUSSION OF THE DATA AND PROPERTIES OF THE MODEL**

G. Thuillier (CNRS, Service d'Aeronomie, Verrieres-le-Buisson, Essonne, France), J. L. Falin, and C. Wachtel (Centre d'Etudes et de Recherches Geodynamiques et Astronomiques, Grasse, Alpes-Maritimes, France) Apr. 1977 16 p refs Journal of Atmospheric and Terrestrial Physics, vol. 39, Apr. 1977, p. 399-414. Centre National de la Recherche Scientifique (Contract CNRS-RCP-336)

The Fabry-Perot interferometer on board of the OGO-6 satellite measures the spectral profile of the 630 nm airglow line. The Doppler width leads to a direct measurement of the thermospheric temperature. A careful analysis of the data has been performed. The global thermospheric temperature is represented by a set of coefficients based on the results of an analysis in spherical harmonics. Comparisons with measured temperatures by incoherent scatter ground stations and by N2 density are made. The model refers to quiet and moderate magnetic activity and to high solar activity.

(Author)

**A77-37153\***  
**A GLOBAL THERMOSPHERIC MODEL BASED ON MASS SPECTROMETER AND INCOHERENT SCATTER DATA MSIS. I - N2 DENSITY AND TEMPERATURE**

A. E. Hedin, C. A. Reber, G. P. Newton, N. W. Spencer (NASA, Goddard Space Flight Center, Greenbelt, Md.), J. E. Salah, J. V. Evans (MIT, Lexington, Mass.), D. C. Kayser (Minnesota, University, Minneapolis, Minn.), D. Alayde (Centre d'Etudes Spatiales des Rayonnements, Toulouse, France), P. Bauer (Centre de Recherches en Physique de l'Environnement, Issy-les-Moulineaux, Hauts-de-Seine, France), L. Cogger (Calgary, University, Calgary, Alberta, Canada) et al 1 Jun. 1977 9 p refs Journal of Geophysical Research, vol. 82, June 1, 1977, p. 2139-2147.

Measurements of neutral nitrogen density from mass spectrometers on five satellites (AE-B, OGO 6, San Marco 3, Aeos A, and AE-C) and neutral temperatures inferred from incoherent scatter measurements at four ground stations are combined to produce a model of thermospheric neutral temperatures and nitrogen densities similar to the OGO 6 empirical model (Hedin et al., 1974). This global model is designated MSIS (mass spectrometer and incoherent scatter). The global average temperature, the annual temperature variation, lower bound density, and lower bound temperature are discussed. The data set covers the time period from the end of 1965 to mid-1975 and also a wide range of solar activities. Diurnal and semidiurnal variations in lower bound density and temperature are considered, as is magnetic activity. M.L.



A77-37154\*

**A GLOBAL THERMOSPHERIC MODEL BASED ON MASS SPECTROMETER AND INCOHERENT SCATTER DATA MSIS. II - COMPOSITION**

A. E. Hedin, C. A. Reber, G. P. Newton, N. W. Spencer, H. C. Brinton, H. G. Mayr (NASA, Goddard Space Flight Center, Greenbelt, Md.), and W. E. Potter (Minnesota, University, Minneapolis, Minn.) 1 Jun. 1977 9 p refs Journal of Geophysical Research, vol. 82, June 1, 1977, p. 2148-2156.

Measurements of O, He, and Ar from neutral gas mass spectrometers on four satellites (OGO 6, San Marco 3, AEROS A, and AEC-C) and inferred oxygen and hydrogen densities from an ion mass spectrometer on AE-C have been combined with a neutral temperature and nitrogen density model to produce a global model of thermospheric composition in terms of inferred variations at 120 km. The data set covers the time period from mid-1969 to mid-1975. The MSIS (mass spectrometer and incoherent scatter data) model is compared with the OGO 6 model (Hedin et al., 1974). Ar variations at 120 km tend to be in phase with temperature variations and inverse to the He, O, and H variations. M.L.

on the OGO-5 and OSO-6 satellites. Spectra for five of the six bursts have been determined using measurements from both satellites in order to reduce ambiguities due to uncertain source locations. A significant fraction, about 20-60%, of the energy of the bursts falls in the hard X-ray range (20-130 keV). The time-integrated spectra have been fitted by power-law, exponential, and thermal-bremsstrahlung functions. They are consistent with power laws which steepen at energies of at least 150 keV, as reported earlier for two other bursts. Evidence for spectral variability from event to event in the hard X-ray region is presented. For a power-law representation, the power-law index has values ranging from approximately unity to 2.5. The hard X-ray spectra of the gamma-ray bursts differ significantly from those of the recently discovered 1-15-keV X-ray bursts.

(Author)

A77-42295\*

**OGO 5 OBSERVATIONS OF PC 5 WAVES - PARTICLE FLUX MODULATIONS**

S. Kokubun, M. G. Kivelson, R. L. McPherron, C. T. Russell (California, University, Los Angeles, Calif.), and H. I. West, Jr. (California, University, Livermore, Calif.) 1 Jul. 1977 13 p refs Journal of Geophysical Research, vol. 82, July 1, 1977, p. 2774-2786. ERDA-sponsored research (Grant NGR-05-007-004; Contract N00014-69-A-200-4016; Grants NSF DES-74-23464; NSF GA-34148 NSF GA-34148)

An investigation is conducted concerning the modulations of particle fluxes associated with Pc 5 waves in the region beyond the plasmapause. A study of thermal flux modulations indicates that some of the density enhancements observed are not spatial structures but are spurious features caused by temporal flux variations associated with hydromagnetic waves. A resonance model of the energetic particle flux modulations is discussed. Energetic particle modulations are also considered. The reported observations reveal that modulations are dominant at energies of about 100 keV for electrons and at 100 keV to 1 MeV for protons. This may indicate that the bounce resonance interaction is not important for Pc 5 waves. G.R.

A77-42297\*

**LIGHT ION AND ELECTRON TROUGHS OBSERVED IN THE MID-LATITUDE TOPSIDE IONOSPHERE ON TWO PASSES OF OGO 6 COMPARED TO COINCIDENT EQUATORIAL ELECTRON DENSITY DEDUCED FROM WHISTLERS**

M. G. Morgan, P. E. Brown, W. C. Johnson (Dartmouth College, Hanover, N.H.), and H. A. Taylor, Jr. (NASA, Goddard Space Flight Center, Laboratory for Planetary Atmospheres, Greenbelt, Md.) 1 Jul. 1977 4 p Journal of Geophysical Research, vol. 82, July 1, 1977, p. 2797-2800.

(Contract NAS5-9305; Contract NGR-30-001-031)

A78-10580\*

**HARD X-RAY SPECTRA OF COSMIC GAMMA-RAY BURSTS**

S. R. Kane (California, University, Berkeley, Calif.) and G. H. Share (U.S. Navy, E. O. Hulbert Center for Space Research, Washington, D.C.) 15 Oct. 1977 16 p refs Astrophysical Journal, Part 1, vol. 217, Oct. 15, 1977, p. 549-564. Navy-supported research. (Grant NGL-05-003-017)

Hard X-ray measurements of six gamma-ray bursts observed during the period from October 1969 to April 1971 are presented. The measurements were made with detectors

## B. Literature Cited in STAR

The "N" at the beginning of these accession numbers which end with a five digit number less than 70001 represents a series announced in *Scientific and Technical Aerospace Reports (STAR)*. This series contains scientific and technical reports issued by NASA and its contractors, other Government agencies, corporations, universities, and research organizations throughout the world.

**N68-33302\*#** California Univ., Berkeley. Space Sciences Lab.

**EXPERIMENT DATA ANALYSIS REPORT. OGO-A EXPERIMENT NO. 1**

K. A. Anderson 10 Jun. 1968 6 p *Its ser. 9, issue 10*  
(Contract NAS5-2222)  
(NASA-CR-96278) Avail: NTIS

A scintillation counter on the OGO-A satellite, consisting of a CsI crystal surrounded by a plastic anticoincidence shield, was used in an experiment to detect 3 to 90 MeV protons in solar cosmic rays. Typical background counting rates of the OGO-A detector are indicated, and the various observed proton events are listed. The main problems in dealing with these data are that the anticoincidence shield did not function and that much of the time coverage of the events was very fragmentary.

M.W.R.

**N71-25288\*#** National Aeronautics and Space Administration. Goddard Space Flight Center, Greenbelt, Md.  
**RELATIVISTIC INTERPLANETARY ELECTRONS AND POSITRONS**

T. L. Cline 1970 6 p *In its Significant Accomplishments in Sci. and Technol. at Goddard Space Flight Center 1970* p 134-139  
Avail: NTIS

Comparison between electron and positron intensities in interplanetary regions show that, in the energy interval of 2 to 10 MeV, positrons are only a few percent as numerous as electrons so that the 2 to 10 MeV electrons indeed form a separate component in the interplanetary electron population. Time variation analyses of electron intensities establish the presence of four coherent populations: solar flare electrons, storm particles, quiet time electrons, and anomalous electron intensity variations during quiet times; the latter correlate inversely with proton intensities.

G.G.

**N73-17947\*** National Aeronautics and Space Administration. Goddard Space Flight Center, Greenbelt, Md.

**A NEW VIEW OF THE RING CURRENT**

M. Sugiura 1972 5 p *In its Significant Accomplishments in Sci., 1971* p 62-66

The OGO 3 and 5 observations provided reliable magnetic field data on the inner magnetosphere, including the intensity and distribution of the quiettime ring current. The field energy density associated with the minimum Delta B (about -40 nT) is found to be greater than the plasma energy density estimated from the available thermal plasma observations by a factor of 10 or more.

J.A.M.

**N74-25869\*#** Faraday Labs., Inc., La Jolla, Calif.  
**OGO-6 GAS-SURFACE ENERGY TRANSFER EXPERIMENT Final Report, 8 Aug. 1968 - 31 Dec. 1973**  
D. McKeown, R. S. Dummer, J. M. Bowyer, Jr., and W.

E. Corbin, Jr. 31 Dec. 1973 57 p

(Contract NAS5-11163)

(NASA-CR-139009; FAR-GF73-013) Avail: NTIS

The kinetic energy flux of the upper atmosphere was analyzed using OGO-6 data. Energy transfer between 10 microwatts/sq cm and 0.1 W/sq cm was measured by short-term frequency changes of temperature-sensitive quartz crystals used in the energy transfer probe. The condition of the surfaces was continuously monitored by a quartz crystal microbalance to determine the effect surface contamination had on energy accommodation. Results are given on the computer analysis and laboratory tests performed to optimize the operation of the energy transfer probe. Data are also given on the bombardment of OGO-6 surfaces by high energy particles. The thermoelectrically-cooled quartz crystal microbalance is described in terms of its development and applications.

Author

**N74-26848** Maryland Univ., College Park.

**THE EFFECT OF EXTRATERRESTRIAL DUST, STRATOSPHERIC WARMINGS, AND LOWER THERMOSPHERIC PRESSURE SYSTEMS ON OGO-4 MEASURED NIGHTGLOWS IN THE EARTH'S ATMOSPHERE (80 TO 100 KM) Ph.D. Thesis**

J. D. Walker, Jr. 1973 204 p

Photometric measurements of four upper D and lower E region nightglows are investigated. World-wide maps of the night-glow distribution and deviations from daily zonal averages are given, and analysis of the variation in nightglow intensities is made. From this distribution, pressure systems operating in the nightglow altitudes are deduced, though the source of these systems is not determined.

Dissert. Abstr.

**N74-28251\*** National Aeronautics and Space Administration. Goddard Space Flight Center, Greenbelt, Md.

**AE-LEE MEASUREMENTS AT LOW AND MID LATITUDE**

R. A. Hoffman, J. L. Burch, and R. J. Janetzke May 1974 14 p *In its Proc. of the Workshop on Electron Contamination in X-ray Astronomy Expt.*

Shortly after the Low Energy Electron Experiment (LEE) on the Atmosphere Explorer-C was turned on following launch, an unexpected phenomenon was encountered at mid-latitudes, a counting rate was acquired with one maximum per roll. Recent analysis shows that these counting rates occur when the detectors are looking in the ram direction of the spacecraft and the spacecraft is near perigee, and are indeed not due to properly analyzed charged particles. After showing the probable cause of these counting rates, some upper limits to true fluxes at low altitudes in the energy range 200 eV to 25 keV from the LEE experiment are

shown. OGO-4 data taken at mid-latitudes are included.

Author

**N74-29091\*** National Aeronautics and Space Administration. Goddard Space Flight Center, Greenbelt, Md.  
**HIGH LATITUDE IONOSPHERIC WINDS RELATED TO SOLAR-INTERPLANETARY CONDITIONS**  
 J. P. Heppner 15 Feb. 1974 6 p *In its Possible Relationships between Solar Activity and Meteorol. Phenomena* p 266-271

Two recent results imply that the distribution of winds in the polar ionosphere should change as a function of the direction of the interplanetary magnetic field. From the motions of chemically released ion and neutral clouds, it is apparent that neutral winds in the high latitude ionosphere are driven principally by ion drag forces. OGO-6 electric field measurements have demonstrated that there are definite relationships between the time latitude distribution of ionospheric plasma convection and interplanetary magnetic field parameters, and also that the distribution is most sensitive to the azimuthal angle of the interplanetary field. The lower altitude, meteorological effects of these externally driven ionospheric winds are not known. However, observations of infrasonic waves following sudden ionization enhancements indicate the existence of momentum transfer.

Author

**N74-29255\*#** Temple Univ., Philadelphia, Pa.  
**REDUCTION AND ANALYSIS OF DATA FROM COSMIC DUST EXPERIMENTS ON MARINER 4, OGO 3, AND LUNAR EXPLORER 35** Final Technical Report  
 27 Jun. 1974 95 p  
 (Grant NGR-39-012-001)  
 (NASA-CR-138866) Avail: NTIS

The analysis of data from the cosmic dust experiment on three NASA missions is discussed. These missions were Mariner IV, OGO III, and Lunar Explorer 35. The analysis effort has included some work in the laboratory of the physics of microparticle hypervelocity impact. This laboratory effort was initially aimed at the calibration and measurements of the different sensors being used in the experiment. The latter effort was conducted in order to better understand the velocity and mass distributions of the picogram sized ejecta particles.

Author

**N74-30528** California Univ., Los Angeles.  
**EXTREMELY LOW FREQUENCY HISS EMISSIONS IN THE MAGNETOSPHERE** Ph.D. Thesis  
 K. W. Chan 1974 210 p

The extremely low frequency hiss emissions in the magnetosphere were studied, using the data from the UCLA/JPL triaxial search coil magnetometer experiment on OGO-5 and OGO-6. In supplement of the wave observations, simultaneous measurements of ion density, ambient magnetic field, and energetic electron flux from the complementary experiments on OGO-5 were analyzed. In regions of the detached ion density enhancements outside the plasmasphere, a narrow band of hiss emission (Dp hiss) between 50 and 200 Hz was detected consistently. This is of distinctly lower frequency than the hiss between 200 and 500 Hz observed inside the plasmasphere. The occurrence patterns, spectral characteristics, wave polarization, and normal vector direction of the DP hiss are presented for the first time.

Dissert. Abstr.

**N74-35223** California Univ., Los Angeles.  
**ENERGETIC ELECTRONS IN THE NEAR GEOMAGNETIC TAIL AND AT SYNCHRONOUS ORBIT: SPATIAL DISTRIBUTIONS AND ACCELERATION MECHANISMS** Ph.D. Thesis  
 R. J. Walker 1973 133 p

The results of a study of the energetic (E50 keV) electron population in the near geomagnetic tail and a model for the acceleration of outer radiation zone electrons are presented. Energetic electron data and magnetic field data from electron spectrometer and fluxgate magnetometer

experiments on OGO-5 formed the basis for the magnetotail electrons study. The spatial distribution of energetic plasma sheet electrons out to a radial distance of 24 RE is presented. The energetic electron population is of nearly constant thickness as a function of the solar magnetospheric Y coordinate. This observation contrasts those from the Vela satellites in which the distribution thickens near the dawn magnetopause.

Dissert. Abstr.

**N75-12873\*#** National Aeronautics and Space Administration. Goddard Space Flight Center, Greenbelt, Md.  
**FEATURES OF POLAR CUSP ELECTRON PRECIPITATION ASSOCIATED WITH A LARGE MAGNETIC STORM**

F. W. Berko Nov. 1974 25 p Submitted for publication (NASA-TM-X-70792; X-626-74-326) Avail: NTIS

Measurements of precipitating electrons made by the OGO-4 satellite reveal several interesting phenomena in the polar cusp. Extremely high fluxes of 0.7 keV electrons were observed in the polar cusp ninety minutes following the sudden commencement of a very large magnetic storm. Structured, fairly high fluxes of 7.3 keV electrons were also observed in the cusp region, accompanied by very strong search coil magnetometer fluctuations, indicative of strong field-aligned currents. The observations confirm previously reported latitudinal shifts in the location of the polar cusp in response to southward interplanetary magnetic fields.

Author

**N75-17020\*#** Franklin Inst., Swarthmore, Pa. Bartol Research Foundation  
**ANALYSIS OF PROTON AND ELECTRON SPECTROMETER DATA FROM OGO-5 SPACECRAFT** Final Report,  
 1 Jul. 1973 - 31 Jul. 1974

M. A. Pomerantz 13 Feb. 1975 95 p  
 (Contract NGR-39-005-105)  
 (NASA-CR-142078) Avail: NTIS

The interaction between the geomagnetic and interplanetary magnetic fields is studied through its effects upon the intensities of solar electrons reaching the polar caps during times of strongly anisotropic electron fluxes in the magnetosheath. During the particle event of November 18, 1968, electrons of solar origin were observed outside the magnetopause with detectors aboard OGO-5. Correlative studies of these satellite observations and concurrent measurements by riometers and ionospheric forward scatter systems in both polar regions revealed that the initial stage of the associated polar cap absorption event is attributable to the arrival of solar electrons. Evidence of a north-south asymmetry in the solar electron flux, at a time when the interplanetary magnetic field vector was nearly parallel with the ecliptic plane, supports an open magnetospheric model. The analysis indicates that an anisotropic electron flux may be isotropized at the magnetopause before propagating into the polar regions.

Author

**N75-17277\*#** California Inst. of Tech., Pasadena.  
**ANALYSIS OF OGO-5 AND OSO-7 X-RAY DATA** Final Report

R. L. Moore Feb. 1975 8 p  
 (Contract NGR-05-002-294)  
 (NASA-CR-142131) Avail: NTIS

The physical nature of solar flares implied by the data was studied. The empirical results were obtained primarily from the OGO-5 and OSO-7 X-ray data in combination with optical data. The principal conclusions regarding the physics of flares are the following. (1) Flares are produced by magnetic field reconnection. (2) The resulting thermal X-ray plasma is cooled primarily by heat conduction rather than by radiative cooling. (3) The heating and cooling of the thermal X-ray plasma are approximately in balance during the maximum phase of the flare.

Author

**N75-17281\*#** California Inst. of Tech., Pasadena. Big Bear Solar Observatory.  
**SLOW X-RAY BURSTS AND CHROMOSPHERIC FLARES WITH FILAMENT DISRUPTION**

J. R. Roy and F. Tang 1975 31 p  
(Grant NGR-05-002-294)

(NASA-CR-142151; BBSO-0141) Avail: NTIS

The data from OGO-5 and OSO-7 X-ray experiments have been analyzed to study six chromospheric flares with filament disruption associated with slow thermal X-ray bursts. Filament activation accompanied by a slight X-ray enhancement precedes the first evidence of H alpha flare by a few minutes. Rapid increase of the soft X-ray flux is accompanied by a sudden brightening of the filament when viewed on-band H alpha. Thereafter the bright chromospheric strands reach their maximum brightness with maximum X-ray flux. Any plateau or slow decay phase in the X-ray flux is accompanied by a quieting in filament activity and even by filament re-appearance. The height of the disrupted prominence is proportional to the soft X-ray flux for the August 3, 1970 limb occulted event. Author

N75-17877\*# Lockheed Missiles and Space Co., Palo Alto, Calif. Space Sciences Lab.

**A MULTI-SATELLITE STUDY OF THE NATURE OF WAVELIKE STRUCTURES IN THE MAGNETOSPHERIC PLASMA** Final Report

E. G. Shelley 22 Aug. 1974 30 p

(Contract NASw-2551)

(NASA-CR-143680; LMSC-D405375;

NSSDC-ID-68-014A-18-PM) Avail: NTIS

An intercomparison is made of the wavelike structures in the data from the light ion mass spectrometer and the fluxgate magnetometer on OGO 5. The wavelike structures appear simultaneously in the data from both experiments. The waves contain both transverse and compressional modes and exhibit periods of 100 to 200 seconds. The waves are usually observed outside the plasmopause and are located primarily on the dayside of the magnetosphere. One possible cause of the apparent density fluctuation is a velocity modulation of the thermal plasma which causes the particles to drift into and out of the ion spectrometer. Author

N75-18144\*# Aerospace Corp., Los Angeles, Calif.

**SOLAR X-RAY STUDIES** Final Report

J. A. Vorpahl 5 Jan. 1975 3 p

(Grant NGR-05-084-002)

(NASA-CR-142164) Avail: NTIS

The hard X-ray component in the impulsive phase of solar flares is reported. Observations from OGO-5 and OSO-7 show no center-to-limb effect of soft X-ray flare. These soft events were plotted separately as a function of solar longitude. M.C.F.

N75-19114\*# Michigan Univ., Ann Arbor. Radio Astronomy Observatory.

**OGO-V RADIO BURST ANALYSIS**

F. T. Haddock Feb. 1975 3 p

(Grant NGR-23-005-549)

(NASA-CR-142232; UM/RAO-75-1) Avail: NTIS

An analysis is presented of data on the km-wave type-3 bursts associated with H alpha flares. A list of published papers based on previous analysis is also presented. M.J.S.

N75-19882 Pittsburgh Univ., Pa.

**OBSERVATIONS FROM THE ORBITING GEOPHYSICAL OBSERVATORY 6 OF MESOSPHERIC AIRGLOW AND SCATTERING LAYERS** Ph.D. Thesis

B. W. Guenther 1974 98 p

Data obtained from an horizon scanning photometer flown onboard the Orbiting Geophysical Observatory-6 are presented. The photometer had a field of 7.5' of arc in the vertical, to yield an extremely fine altitude resolution (usually 6 km or less) through the region about the mesopause near 95 km. Interference filters, one centered near 557.7 nm designed to detect the O(S)-O(D) atomic oxygen emission, and one centered near 589.3 nm designed to detect the resonance radiation from free atomic sodium, were alternately displayed between a telescope and a photomultiplier tube. Several latitude profiles of the maximum integrated slant

emission rate of 557.7 and 589.0-589.6 nm nightglow are presented, showing generally an oscillatory behavior for both lines, with a generally anticorrelative amplitude. The green line of atomic oxygen near 97 km in the mesosphere shows a strong tendency for a relatively deep trough at low latitudes near the equator. Sodium day airglow, known to emit in a narrow layer about 92 km, was investigated. Several plots of sodium dayglow brightness displayed against latitude are presented. At high latitudes, during local summers, a narrow but bright particle scattering layer was detected.

Dissert. Abstr.

N75-20195 Stanford Univ., Calif.

**LOW-ENERGY RADIO EMISSIONS FROM THE EARTH AND SUN** Ph.D. Thesis

N. Dunkel 1974 178 p

New features of solar type 3 bursts, plasma-wave emissions and high-pass or earth noise (also called terrestrial kilometeric radiation) are revealed by a sensitive sweeping receiver operating in the 10 to 100 kHz range on the OGO-1 and OGO-3 satellites. A new feature of the study was the comparison of the dynamic spectra of type 3 bursts with the azimuthal distribution of density in the interplanetary medium. Dynamic spectra observed at times when the associated flare was in a position to illuminate a dense interplanetary region with energetic particles suggest that generation took place in this dense region. Shocks propagating in the interplanetary medium can cause enhancements in the type 3 burst spectra. The relative times of arrival at 1 AU of energetic particles and low-frequency type 3 bursts indicate that the exciting particles are electrons not protons. The effects on the emitted wave of refraction and reduced velocity due to the coronal density are shown to be minimal. Dissert. Abstr.

N75-22959 Stanford Univ., Calif.

**MAGNETOSPHERIC CHORUS** Ph.D. Thesis

W. J. Burtis 1974 179 p

Characteristics of VLF chorus in the outer magnetosphere are investigated in a survey based on 400 hr of broadband data collected by OGO 3 during 1966-67. Bandlimited whistler-mode emissions constitute the dominant form of radiation, and the detailed description provides a starting point for a realistic theory of wave-particle interactions beyond the plasmopause. Spectrograms illustrate typical and unusual examples of magnetospheric chorus. The observations are interpreted in terms of whistler-mode propagation theory and a gyroresonant feedback interaction model. An exact expression is derived for the critical frequency at which the curvature of the refractive index surface vanishes at zero wave normal angle. Near this frequency rays with initial wave normal angles between 0 deg and -20 deg are focused along the initial field line for thousands of km, enhancing the phase-bunching of incoming gyroresonant electrons. The upper peak in the bimodal normalized frequency distribution is attributed to this enhancement near the critical frequency. The observations seem to be consistent with gyroresonant generation of emissions at low latitudes, followed by spreading of the radiation over a range of L shells farther down the field lines. Dissert. Abstr.

N75-24202 Pennsylvania State Univ., University Park.

**THE ROLE OF ICE PARTICULATES IN THE ELECTRIFICATION OF THE AIR IN THE MESOSPHERE** Ph.D. Thesis

E. T. Chesworth 1974 126 p

The observations of noctilucent clouds, the measurements of hydrated ions, and the light-scattering layer detected by the OGO-6 satellite suggest the presence of ice crystals in the mesosphere. The correlation between temperature and positive ion mobility where the vapor pressure over ice becomes greater than atmospheric pressure just above the stratopause indicates the presence of ice crystals throughout the mesosphere at all latitudes during all seasons. Confirmation of this theory is provided by the numerical value of the logarithmic derivative of positive ion conductivity being

within 8% of the specific entropy change when ice sublimates. It is shown that 1000 to 10,000 ice crystals per cu cm of order 100 A in diameter dominate electron loss processes in the upper mesosphere. The theory explains the ledge at 83 km and validates the positive ion density measurements of Hale. Dissert. Abstr.

**N75-24593\*#** Michigan Univ., Ann Arbor.  
**DATA USER'S NOTES OF THE RADIO ASTRONOMY EXPERIMENT ABOARD THE OGO-V SPACECRAFT**  
F. T. Haddock and S. L. Breckenridge 20 Apr. 1970  
46 p

(Contract NAS5-9099)  
(NASA-CR-143696; UM/RAO-70-3) Avail: NTIS  
General information concerning the low-frequency radiometer, instrument package launching and operation, and scientific objectives of the flight are provided. Calibration curves and correction factors, with general and detailed information on the preflight calibration procedure are included. The data acquisition methods and the format of the data reduction, both on 35 mm film and on incremental computer plots, are described. L.B.

**N75-32651** Michigan Univ., Ann Arbor.  
**MAGNETICALLY ORDERED HEATING IN THE POLAR REGIONS OF THE THERMOSPHERE** Ph.D. Thesis  
B. B. Hinton 1975 206 p

Geomagnetically controlled perturbations in the composition and temperature of the upper atmosphere were studied for magnetically quiet and ordinary days using data from the Neutral Atmosphere Composition Experiment on the OGO-6 satellite. Two mechanisms were considered for producing this effect: heating with an associated free convection and horizontal forced convection driven by ion drag. It is concluded, from study of the experimental data, that the first mechanism is the dominant one. Two one-dimensional models are proposed; these represent complementary approximations of the importance of the horizontal mass flux divergence to the continuity of total mass density. Maps of the horizontal distribution of the column integrated energy input rate were produced from comprehensive global composition data using a selected altitude profile of heating. Global average input rates for this heating were also obtained. It follows that polar heating is extremely significant to global thermospheric structure. Dissert. Abstr.

**N75-32995\*#** Chicago Univ., Ill. Lab. for Astrophysics and Space Research.  
**OGO-5 EXPERIMENT E-09 COSMIC RAY ELECTRONS**  
Final Report

P. Meyer 5 Jun. 1975 3 p  
(Contract NAS5-9096)  
(NASA-CR-144668) Avail: NTIS

Cosmic ray spectra and solar electron data in the 10 to 200 MeV range, as measured by experiment E-09 on OGO-5, are reported. E.H.W.

**N76-10603** Texas Univ., Dallas.  
**DETERMINATION OF TROPICAL F-REGION WINDS FROM ATOMIC OXYGEN AIRGLOW EMISSIONS** Ph.D. Thesis

J. A. Bittencourt 1975 268 p  
The nighttime variation, longitudinal behavior, and latitudinal asymmetry in the 01 1356 A and 01 6300 A emissions, measured from OGO 4, were analysed in conjunction with theoretical computer generated models. The nighttime variation of the column emission rates of both emissions from about 25 deg N. to 25 deg S. dip latitude in the ionospheric F-region was theoretically calculated by numerically solving the time-dependent, coupled, non-linear system of equations for the ionic concentrations, taking into account production, loss, and transport of ionization. The ratio of the square roots of the 1356 A to the 6300 A intensities is found to be a single valued function of the height of the F2-peak, with a small dependence on exospheric tempera-

ture. The inferred zonal velocity has an amplitude of about 280 meter/sec occurring near 21:30-22:00 LT. Dissert. Abstr.

**N76-10610\*#** Pennsylvania State Univ., University Park. Ionosphere Research Lab.  
**GLOBAL EXOSPHERIC TEMPERATURES AND DENSITIES UNDER ACTIVE SOLAR CONDITIONS**  
B. J. Wydra 3 Oct. 1975 98 p  
(Grant NGL-39-009-003; Contract N00014-67-A-0385-0017) (NASA-CR-145394; PSU-IRL-SCI-436) Avail: NTIS

Temperatures measured by the OGO-6 satellite using the 6300 A airglow spectrum are compared with temperatures derived from total densities and N2 densities. It is shown that while the variation of the total densities with latitude and magnetic activity agree well with values used for CIRA (1972), the temperature behavior is very different. While the temperatures derived from the N2 density were in much better agreement there were several important differences which radically affect the pressure gradients. The variation of temperature with magnetic activity indicated a seasonal and local time effect and also a latitude and delay time variation different from previous density derived temperatures. A new magnetic index is proposed that is better correlated with the observed temperatures. The temperature variations at high latitudes were examined for three levels of magnetic activity for both solstices and equinox conditions. A temperature maximum in the pre-midnight sector and a minimum in the noon sector were noted and seasonal and geomagnetic time and latitude effects discussed. Neutral temperature, density, pressure and boundary oxygen variations for the great storm of March 8, 1970 are presented. Author

**N76-21066\*** Colorado Univ., Boulder.  
**ON THE COMETARY HYDROGEN COMA AND FAR UV EMISSION**  
H. U. Keller 1976 42 p In NASA. Goddard Space Flight Center. The Study of Comets, Part 1 p 287-314  
(Grant NGR-06-003-179)

Cometary hydrogen observations are reviewed with emphasis on observations of comet Bennett. The results are theoretically interpreted and a brief summary of ultraviolet observations other than Lyman alpha is given. Author

**N76-27744** Pittsburgh Univ., Pa.  
**LATITUDINAL DEPENDENCE OF ATOMIC OXYGEN DENSITY BETWEEN 90 AND 120 KILOMETERS AS DERIVED FROM OGO-6 OBSERVATIONS OF THE 5577 A NIGHTGLOW** Ph.D. Thesis  
B. Wasser 1975 99 p

A photometer on board OGO-6 was used to study atomic oxygen densities between 80 and 120 km altitude during November, 1969. Densities were inferred from the 5577 A emission observed in nightglow. To take account of density variations below the altitude of maximum slant emission rate, data from several consecutive scans in a vertical plane were used to produce near synoptic maps of volume emission rates and atomic oxygen densities. The profiles showed peaks at about 97 km with densities that varied between  $2.1 \times 10$  to the 11th power and  $3.5 \times 10$  to the 11th power atoms/cu cm. The densities at 90 km varied between  $2.0 \times 10$  to the 10th power and  $1.7 \times 10$  to the 11th power atoms/cu cm. The deduced atomic oxygen density profiles between 90 km and 100 km were then compared with the solution to the continuity equation in the same range. The theoretical curves agreed to within 20-25% of the curves deduced from the nightglow observations. In addition, mechanisms for atomic oxygen loss and atmospheric heating were considered. Dissert. Abstr.

**N76-33787#** Laboratorio di Ricerca e Tecnologia per lo Studio del Plasma nello Spazio, Frascati (Italy).  
**THE MAGNETOPAUSE. PART I: MULTISATELLITE SIMULTANEOUS OBSERVATIONS OF BOW SHOCK AND MAGNETOPAUSE POSITIONS**  
V. Formisano Aug. 1975 14 p

(LPS-75-23-PT-1) Avail: NTIS

Simultaneous multisatellite observations of the earth's bow shock and magnetopause positions were made in order to calculate gamma, the solar wind specific heat ratio. The satellites used were OGO-5 and HEOS-1. On six occasions OGO-5 crossed the bow shock and HEOS-1 observed the magnetopause; in seven cases the opposite occurred. The measured values of the gamma range from 1.36 to 2.05, with some indication that low values relate to low frequency (0.05 Hz) upstream waves, whereas high values were obtained when no upstream waves were observed. The average value is exactly 1.666. In the laminar magnetosheath cases very high gamma values were obtained. ESA

N76-33788# Laboratorio di Ricerca e Tecnologia per lo Studio del Plasma nello Spazio, Frascati (Italy).  
**THE MAGNETOPAUSE: PART 2: MAGNETOPAUSE POSITION AND THE RECONNECTION PROBLEM**  
 V. Formisano Aug. 1975 31 p  
 (LPS-75-24-PT-2) Avail: NTIS

OGO-5 magnetic field data were used to locate the magnetopause, while HEOS-1 (or sometimes Explorer 33) plasma data were used to measure the solar wind dynamic pressure and to study the actual response of the magnetosphere (through the location of the magnetopause) to different solar wind pressures. The OGO-5 magnetopause positions were divided into two groups, one relating to observations close to the ecliptic plane, the other having a sun-earth-satellite angle greater than 56.5 deg. Results show that not only is the interplanetary magnetic field latitude important for the magnetopause position (and therefore for the reconnection process) but also the presence or absence of magnetosheath turbulence and the proton number density are important. ESA

N76-33793# Laboratorio di Ricerca e Tecnologia per lo Studio del Plasma nello Spazio, Frascati (Italy).  
**THE OUTER MAGNETOSPHERE. PART 1: A MULTI-SATELLITE STUDY OF THE MAGNETOPAUSE POSITION IN RELATION WITH SOME IMPORTANT FLUID DYNAMIC PARAMETERS**  
 V. Formisano Feb. 1976 32 p  
 (LPS-76-2-PT-1) Avail: NTIS

Simultaneous observations by OGO-5 and HEOS-1 of the magnetopause and the earth's bow shock give a measurement of the magnetosheath thickness, allowing a determination of the magnetosheath specific heats ratio. A statistical study of the magnetopause position, normalized with respect to the solar wind dynamical pressure, allows the determination of  $f_2/K$  and, in a few cases, of  $f$  and  $K$  separately. The quantity  $f_2/K$  varies over a large range and, on average, has the value  $f_2/K = 1.55$ . The geomagnetic field compression factor  $f$  has the value  $f = 1.53$ , while the stagnation pressure factor  $K$  is  $K$  approximately = 2.9, a value much larger than predicted, probably because of the presence of the magnetic field in the solar wind, and, possibly, of erosion of the day-side magnetosphere. Both the fluid dynamic approach and the current sheet model of the solar wind confinement of the earth magnetic field appear to be insufficient. Author (ESA)

N76-33795# Laboratorio di Ricerca e Tecnologia per lo Studio del Plasma nello Spazio, Frascati (Italy).  
**THE OUTER MAGNETOSPHERE. PART 3: SIMULTANEOUS MULTISATELLITE OBSERVATIONS OF THE MAGNETOPAUSE.**  
 V. Formisano Mar. 1976 29 p  
 (LPS-76-4-PT-2) Avail: NTIS

Differences between local structures Simultaneous observations of magnetopause structure with HEOS-1 and OGO-5 (Day 341, 350 1969) or Explorer 35 (Day 300, 1969) are studied. It is shown that the magnetopause structure is similar over a large portion of space if similar conditions are present. In one case (Day 350, 1969) the structure observed at HEOS-1 (reconnected magnetopause close to the diffusion zone) is very different from the two discontinuity structure

observed at OGO-5 (reconnected magnetopause away from the diffusion zone). At HEOS-1 the magnetic field intensity appears to be enhanced on both sides of the magnetopause, by at least 10 gammas, compared with ambient field intensity. The magnetospheric magnetic field (at about 95 deg to the magnetosheath magnetic field) appears to be distorted, with respect to the meridian plane, in the opposite sense compared with the magnetospheric models.

Author (ESA)

N77-13587\*# National Aeronautics and Space Administration. Goddard Space Flight Center, Greenbelt, Md.  
**MAGNETIC ANOMALY MAP OF NORTH AMERICA SOUTH OF 50 DEGREES NORTH FROM POGO DATA**  
 M. A. Mayhew Aug. 1976 22 p Presented at 2d Intern. Conf. on the New Basement Tectonics, Univ. of Delaware, Jul. 1976  
 (NASA-TM-X-71229; X-922-76-201) Avail: NTIS

A magnetic anomaly map produced from Pogo data for North America and adjacent ocean areas is presented. At satellite elevations anomalies have wavelengths measured in hundreds of kilometers, and reflect regional structures on a large scale. Prominent features of the map are: (1) a large east-west high through the mid-continent, breached at the Mississippi Embayment; (2) a broad low over the Gulf of Mexico; (3) a strong gradient separating these features, which follows the Southern Appalachian-Ouachita curvature; and (4) a high over the Antilles-Bahamas Platform which extends to northern Florida. A possible relationship between the high of the mid-continent and the 38th parallel lineament is noted. Author

N77-23648\*# Smithsonian Astrophysical Observatory, Cambridge, Mass.  
**THERMOSPHERIC TEMPERATURE, DENSITY, AND COMPOSITION: NEW MODELS**  
 L. G. Jacchia 15 Mar. 1977 112 p Sponsored by NASA (NASA-CR-153049; SAO-Special-Rept-375) Avail: NTIS

The models essentially consist of two parts: the basic static models, which give temperature and density profiles for the relevant atmospheric constituents for any specified exospheric temperature, and a set of formulae to compute the exospheric temperature and the expected deviations from the static models as a result of all the recognized types of thermospheric variation. For the basic static models, tables are given for heights from 90 to 2,500 km and for exospheric temperatures from 500 to 2600 K. In the formulae for the variations, an attempt has been made to represent the changes in composition observed by mass spectrometers on the OGO 6 and ESRO 4 satellites. Author

N78-11543# Maine Univ., Orono.  
**A STUDY OF THE HEAT FLUX REVERSAL REGION UPSTREAM FROM THE EARTH'S BOW SHOCK, USING DATA FROM THE OGO 5 ELECTRON SPECTROMETER**  
 Ph.D. Thesis  
 D. J. Hei, Jr. Ann Arbor, Mich. Univ. Microfilms International, 1977 213 p  
 Avail: NTIS

Interplanetary data from the OGO 5 electron spectrometer experiment were analyzed to understand the cause of non-monotonic spectral features at suprathermal energies. It was found that the source for these features has one terminus at the bow shock surface skirted by the interplanetary magnetic field. The source region termed the heat flux reversal region (HFR) was found to be approximately located at the boundary between connecting and missing field geometries. Plasma determined to be in the HFR was shown to have reduced magnetic field magnitude compared to data taken adjacent to it. This plasma also was shown to have perpendicular electron pressure within the average range expected for the solar wind. These results were explained in terms of an interaction occurring within the HFR involving suprathermal electrons which produced the reduced magnetic field magnitude and the regulated perpendicular pressure. Author

N78-12583

N78-12583\* Colorado Univ., Boulder.

**SATELLITE OBSERVATIONS OF THE GLOBAL DISTRIBUTION OF STRATOSPHERIC OZONE**

J. London, J. E. Frederick, and G. P. Anderson 30 Apr. 1976 19 p Presented at Intern. Ozone Symp., Dresden, 9-17 Aug. 1976 Submitted for publication *In its Observed and Theoretical Variations of Atmospheric Ozone* (Grants NGR-06-003-127; NSG-2126; NSG-7224; NSF GA-38134X2)

Avail: NTIS

Observations of backscattered radiation from an Orbiting Geophysical Observatory (OGO) Satellite were used to determine the global distribution of ozone in different layers in the middle and upper stratosphere. The derived distributions show significant seasonal and geographic variations with important differences indicated between winter and summer hemisphere distributions. The OGO derived distributions are compared with other observations (rocket and satellite) and with photochemical calculations. It is suggested that the increased ozone mixing ratio in the high latitude winter hemisphere can be accounted for by transport processes up to about 40-45 km and by the effects of seasonal variations of NO<sub>x</sub>, HO<sub>x</sub> and temperature in the region above. Author

### C. Literature Cited in Other Series

The following "N" series citations identified by accession numbers N...-70001 through N...-89999 for the years 1967 through the present year represent technical reports that were relatively old at the time of processing or those that contained preliminary or fragmentary information.

**N75-70676\*** Smithsonian Astrophysical Observatory, Cambridge, Mass.  
**THE MICROMETEOROID EXPERIMENT ON THE OGO 4 SATELLITE Final Report**  
C. S. Nilsson Jul. 1969 38 p  
(Contract NAS5-11007)  
(NASA-CR-141948)

**N75-76086** California Univ., Los Angeles. Inst. of Geophysics and Planetary Physics.  
**PRODUCTION PROCESSING OF THE DATA OBTAINED BY THE UCLA OGO-5 FLUXGATE MAGNETOMETER**  
C. T. Russell Mar. 1971 24 p ref  
(PUBL-905)

**N76-71877** National Aeronautics and Space Administration. Goddard Space Flight Center, Greenbelt, Md.  
**MAGNETIC FIELD VARIATIONS ABOVE 60 DEGREES INVARIANT LATITUDE AT THE POGO SATELLITES**  
R. A. Langel Sep. 1973 20 p *In* Intern. Union of Geodesy and Geophys. Symp. on Low Level Satellite Surv. p 21-40

**N76-71880\*** National Aeronautics and Space Administration. Goddard Space Flight Center, Greenbelt, Md.  
**LOW LATITUDE VARIATIONS OF THE MAGNETIC FIELD**  
J. C. Cain and W. M. Davis Sep. 1973 17 p Sponsored in part by USGS *In* Intern. Union of Geodesy and Geophys. Symp. on Low Level Satellite Surv. p 67-83

**N76-71883** Bundesanstalt fuer Bodenforschung, Hannover (West Germany).  
**COMPARISON OF A MAGNETIC LOCAL ANOMALY MEASURED BY OGO-6 AND A CRUSTAL FEATURE**  
A. Hahn Sep. 1973 4 p *In* Intern. Union of Geodesy and Geophys. Symp. on Low Level Satellite Surv. p 123-126

**N77-84176** Leiden Univ. (Netherlands).  
**LONG-TERM SOLAR MODULATION OF COSMIC-RAY ELECTRONS WITH ENERGIES ABOVE 0.5 GEV**  
J. J. Burger and B. N. SWanenburg 1971 6 p Presented at the 12th Intern. Conf. on Cosmic Rays, Hobart, Australia, 16-25 Aug. 1971

**N77-84177** Leiden Univ. (Netherlands). Cosmic-ray Working Group.  
**SHORT-TERM VARIATIONS OF THE COSMIC-RAY PROTON AND ELECTRON INTENSITIES IN 1968 AND 1969**  
C. Baixeras-Aiguabella 1971 6 p Presented at the 12th Intern. Conf. on Cosmic Rays, Hobart, Tasmania, Australia, 16-25 Aug. 1971

**N77-86006** Naval Research Lab., Washington, D. C.  
**TROPICAL UV ARCS: COMPARISON OF BRIGHTNESS WITH f SUB 0 F SUB 2**  
R. R. Meier and C. B. Opal 1 Jun. 1973 5 p Repr. from *J. Geophys. Res.*, v. 78, no. 16, 1 Jun. 1973 p 3189-3193

**N77-86268\*** New Mexico Univ., Albuquerque. Dept. of Physics and Astronomy.  
**ULTRAVIOLET SOLAR ENERGY SURVEY ON OGO-6 Final Report**  
V. H. Regener 31 Mar. 1975 25 p ref  
(Contract NAS5-9314)  
(NASA-CR-155088)

**N78-70070** Academy of Sciences (USSR), Moscow.  
**AURORAL OVAL AND MAGNETOSPHERIC CUSPS**  
Y. I. Feldstein 1975 *In* Aurora and Airglow, No. 22 p77-99  
*In* RUSSIAN: ENGLISH summary

**N78-70785** McDonnell-Douglas Astronautics Co., Huntington Beach, Calif.  
**SOLAR COSMIC RAY OBSERVATIONS DURING 1969**  
A. J. Masley 1970 3 p Repr. from Antarctic J. US, v. 5, no. 6, Sep. - Oct. 1970 p 172 Sponsored by NSF  
(MDAC-WD-1448)

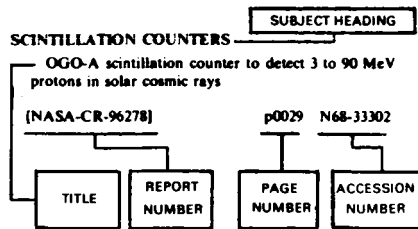
**N78-71246** Centre National de la Recherche Scientifique, Verrieres-le-Buisson (France).  
**INTERPRETATION OF HYDROGEN LYMAN-ALPHA OBSERVATIONS OF COMETS BENNET AND ENCKE**  
J. L. Bertaux, J. E. Blamont and M. Festou 1973 16 p Repr. from *Astron. and Astrophys.*, v. 25, 1973 p 415-430



# VI. INDEXES TO ADDITIONAL LITERATURE CITATIONS AND ABSTRACTS

## A. SUBJECT INDEX

### Typical Subject Index Listing



This index is arranged alphabetically by subject term. A brief description of the document, e.g., title plus title extension, or Notation of Content, (NOC) is included in each subject entry to indicate the type of document cited. The page number identifies the page in the abstract section (V) on which the citation appears.

### A

#### ABUNDANCE

The solar cycle variation of the solar wind helium abundance  
[NSSDC-ID-68-014A-17-OS] p0010 A75-16631  
Solar particle events with anomalously large relative abundance of He-3  
p0013 A75-34018  
Origin and composition of heavy nuclei between 10 and 60 MeV per nucleon during interplanetary quiet times in 1968-1972  
p0017 A75-46822

#### AERIAL EXPLOSIONS

A study of electron spectra in the inner belt  
p0024 A76-44653

#### AEROS SATELLITE

AEROS A atomic oxygen profiles compared with the OGO 6 model  
p0028 A77-23987

#### AIRGLOW

Atomic oxygen 1304-A day airglow observed from OGO-D spacecraft, attributing subsonic emission rates to photoelectron impact excitation  
p0002 A71-33964  
An upper limit to the product of NO and O densities from 105 to 120 km  
[NSSDC-ID-69-051A-26-PM] p0008 A75-11227  
F region wind components in the magnetic meridian from OGO 4 tropical airglow observations  
p0011 A75-22671  
Remote sensing of the ionospheric F layer by use of O I 6300-A and O I 1356-A observations  
p0014 A75-35040  
OGO-6 observations of 5577 A --- airglow measurements  
p0019 A76-18436  
Global atomic hydrogen density derived from OGO-6 Lyman-alpha measurements  
p0021 A76-28988  
Global atomic oxygen density derived from OGO-6 1304 A airglow measurements  
p0021 A76-28989  
Satellite observation of the mesospheric scattering layer and implied climatic consequences  
p0022 A76-39128  
Altitude profiles of the photoelectron induced O I D (6300 A) predawn enhancement by observation and theory  
p0026 A77-20886  
Magnetic storm effects on the tropical ultraviolet airglow  
p0029 A77-27318

Observations from the Orbiting Geophysical Observatory 6 of mesospheric airglow and scattering layers  
p0033 N75-19882

#### ALPHA PARTICLES

Solar energetic particle event with He-3/He-4 greater than 1  
p0009 A75-15342  
Relation of solar wind fluctuations to differential flow between protons and alphas  
p0013 A75-28004

#### ANGULAR DISTRIBUTION

Pitch angle distributions of energetic electrons in the equatorial regions of the outer magnetosphere - OGO-5 observations  
p0011 A75-22759  
Angular distributions of solar protons and electrons  
p0016 A75-41805

#### ANNUAL VARIATIONS

Thermospheric 'temperatures' --- discrepancies in inferred and satellite measured values  
p0007 A74-36747  
Dependence of field-aligned electron precipitation occurrence on season and altitude  
p0007 A74-43679  
North-south asymmetries in the thermosphere during the last maximum of the solar cycle  
p0009 A75-16449  
The global characteristics of atmospheric emissions in the lower thermosphere and their aeronomic implications  
p0016 A75-42726

#### ARTIFICIAL CLOUDS

Magnetospheric electric fields convective motions measurement by Ba ion cloud tracking and symmetric double probe floating potential technique  
p0003 A73-15333

#### ASTRONOMICAL MODELS

A cometary hydrogen model - Comparison with OGO-5 measurements of Comet Bennett (1970 II)  
p0013 A75-32382

#### ASTROPHYSICS

Recent advances in cometary physics and chemistry  
p0009 A75-13176

#### ATMOSPHERIC CHEMISTRY

OGO-6 observations of 5577 A --- airglow measurements  
p0019 A76-18436

#### ATMOSPHERIC CIRCULATION

Tropical F region winds from O I 1356-A and forbidden O I 6300-A emissions. II - Analysis of OGO 4 data  
p0023 A76-42683  
Dynamical effects in the distribution of helium in the thermosphere  
p0024 A77-11489

#### ATMOSPHERIC COMPOSITION

Variations in thermospheric composition - A model based on mass spectrometer and satellite drag data  
p0006 A74-30667  
Comparison of the San Marco 3 Nace neutral composition data with the extrapolated Ogo 6 empirical model --- Neutral Atmospheric Composition Experiment  
p0021 A76-26524  
Observations of hydrogen in the upper atmosphere  
p0024 A77-11488  
A global thermospheric model based on mass spectrometer and incoherent scatter data MSIS. II - Composition  
p0029 A77-37154  
Satellite observations of the global distribution of stratospheric ozone  
p0036 N78-12583

#### ATMOSPHERIC DENSITY

Recent improvements in our knowledge of neutral atmosphere structure from satellite drag measurements  
[BMBW-WRK-226] p0005 A74-23676  
Observed variations of the exospheric hydrogen density with the exospheric temperature  
p0012 A75-23721  
Global exospheric temperatures and densities under active solar conditions  
p0028 A77-25183

#### ATMOSPHERIC ELECTRICITY

Empirical models of high-latitude electric fields  
p0029 A77-27317

#### ATMOSPHERIC HEAT BUDGET

Dynamical effects in the distribution of helium in the thermosphere  
p0024 A77-11489

#### ATMOSPHERIC HEATING

Magnetic storm dynamics of the thermosphere  
p0008 A75-12453  
Structure of electrodynamic and particle heating in the undisturbed polar thermosphere  
p0018 A76-14318  
Behavior of the sodium and hydroxyl nighttime emissions during a stratospheric warming  
p0020 A76-22490  
Structure of electrodynamic and particle heating in the disturbed polar thermosphere  
p0027 A77-23201

#### ATMOSPHERIC IONIZATION

High latitude minor ion enhancements - A clue for studies of magnetosphere-atmosphere coupling  
p0008 A75-12439  
F region wind components in the magnetic meridian from OGO 4 tropical airglow observations  
p0011 A75-22671

#### ATMOSPHERIC MODELS

Magnetospheric thermal plasma and hydrogen cation density profile characteristics in different local time regions explained by time-varying convection model  
p0003 A73-13879  
Theory of the phase anomaly in the thermosphere --- radar temperature-satellite drag density phase difference  
p0005 A74-12645  
Density and temperature distributions in non-uniform rotating planetary exospheres with applications to earth  
p0005 A74-14224  
Exospheric models of the topside ionosphere --- emphasizing escape of light gases  
p0006 A74-28723  
Variations in thermospheric composition - A model based on mass spectrometer and satellite drag data  
p0006 A74-30667  
The solar wind and magnetospheric dynamics  
p0010 A75-19127  
Identifications of the polar cap boundary and the auroral belt in the high-altitude magnetosphere - A model for field-aligned currents  
p0014 A75-35007  
Comparison of the San Marco 3 Nace neutral composition data with the extrapolated Ogo 6 empirical model --- Neutral Atmospheric Composition Experiment  
p0021 A76-26524  
Model of equatorial scintillations from in-situ measurements --- based on OGO-6 observed F region irregularity  
p0025 A77-12057  
AEROS A atomic oxygen profiles compared with the OGO 6 model  
p0028 A77-23987

SUBJECT

**ATMOSPHERIC RADIATION**

Experimental global model of the exospheric temperature based on measurements from the Fabry-Perot interferometer on board the OGO-6 satellite - Discussion of the data and properties of the model

p0029 A77-34901

A global thermospheric model based on mass spectrometer and incoherent scatter data MSIS. I - N2 density and temperature

p0029 A77-37153

A global thermospheric model based on mass spectrometer and incoherent scatter data MSIS. II - Composition

p0029 A77-37154

**ATMOSPHERIC RADIATION**

VLF and ELF emissions --- in magnetosphere

p0015 A75-36988

The global characteristics of atmospheric emissions in the lower thermosphere and their aeronomic implications

p0016 A75-42726

Magnetospheric chorus - Amplitude and growth rate

p0016 A75-42748

The local time variation of ELF emissions during periods of substorm activity

p0029 A77-31391

Tropical UV arcs: Comparison of brightness with f sub 0 F sub 2

p0037 N77-86006

**ATMOSPHERIC SCATTERING**

Noctilucent clouds in daytime - Circumpolar particulate layers near the summer mesopause.

p0003 A72-42515

Satellite observation of the mesospheric scattering layer and implied climatic consequences

p0022 A76-39128

**ATMOSPHERIC STRATIFICATION**

Noctilucent clouds in daytime - Circumpolar particulate layers near the summer mesopause.

p0003 A72-42515

**ATMOSPHERIC TEMPERATURE**

Neutral wind velocities calculated from temperature measurements during a magnetic storm and the observed ionospheric effects.

p0004 A73-36150

Diurnal variation of the neutral thermospheric winds determined from incoherent scatter radar data

p0006 A74-36735

Thermospheric 'temperatures' --- discrepancies in inferred and satellite measured values

p0007 A74-36747

Observed variations of the exospheric hydrogen density with the exospheric temperature

p0012 A75-23721

Exospheric temperature inferred from the Aeros-A neutral composition measurement

p0017 A75-46269

Experimental model of the exospheric temperature based on optical measurements on board the OGO 6 satellite

p0023 A76-42390

Global exospheric temperatures and densities under active solar conditions

p0028 A77-25183

Experimental global model of the exospheric temperature based on measurements from the Fabry-Perot interferometer on board the OGO-6 satellite - Discussion of the data and properties of the model

p0029 A77-34901

**ATMOSPHERIC TURBULENCE**

Steady ELF plasmaspheric hiss, studying whistler mode turbulence, band limitation, power spectra and peak intensities

p0004 A73-26984

**ATMOSPHERICS**

Detailed analysis of magnetospheric ELF chorus - preliminary results

p0027 A77-21523

**ATOMIC SPECTRA**

OGO-4 observations of the ultraviolet auroral spectrum

p0025 A77-16243

**AURORAL IRRADIATION**

'Hislers' - Quasi-periodic (T approximately equal to 2 sec) VLF noise forms at auroral latitudes

p0009 A75-16440

**AURORAL SPECTROSCOPY**

OGO-4 observations of the ultraviolet auroral spectrum

p0025 A77-16243

**AURORAL ZONES**

Ionospheric and magnetospheric electric field strength measurements in auroral and polar cap regions by Ba ion cloud and double floating probe techniques

p0003 A72-39543

Is the red arc a good indicator of ionosphere-magnetosphere conditions

[NSSDC-ID-69-051A-02-PM] p0008 A75-11226

Electric field measurements across the Harang discontinuity --- in auroral zone

p0010 A75-16634

Identifications of the polar cap boundary and the auroral belt in the high-altitude magnetosphere - A model for field-aligned currents

p0014 A75-35007

New results on the correlation between low-energy electrons and auroral hiss

p0020 A76-22086

Field-aligned precipitation of greater than 30-keV electrons

p0022 A76-36276

High-latitude nitric oxide in the lower thermosphere

p0028 A77-23222

**AURORAS**

Electron precipitation patterns and substorm morphology.

[NSSDC-ID-67-073A-11-PM] p0004 A73-33434

Simultaneous particle and field observations of field-aligned currents --- in magnetosphere

p0011 A75-19330

Auroral oval and magnetospheric cusps

p0037 N78-70070

**B**

**BARIUM**

Magnetospheric electric fields convective motions measurement by Ba ion cloud tracking and symmetric double probe floating potential technique

p0003 A73-15333

**BERYLLIUM**

Measurements of the cosmic-ray Be/B ratio and the age of cosmic rays

p0006 A74-30187

**BORON**

Measurements of the cosmic-ray Be/B ratio and the age of cosmic rays

p0006 A74-30187

**BOUNDARY LAYERS**

Field-aligned currents observed by the OGO 5 and Triad satellites

p0026 A77-17124

**BOW WAVES**

Earth collisionless plasma bow shock oblique structure assessment by pulsation index Ip devised from empirical results

p0003 A72-44511

On the local time dependence of the bow shock wave structure

p0005 A74-24759

The earth's bow shock fine structure

p0011 A75-19138

Plasma instability modes related to the earth's bow shock

p0011 A75-22774

Structure of the quasi-perpendicular laminar bow shock --- earth-solar wind interaction

p0012 A75-23707

Collisionless shock waves in space - A very high beta structure --- solar wind measurements

p0014 A75-35003

Structure of a quasi-parallel, quasi-laminar bow shock

p0028 A77-23220

The magnetopause. Part I: Multisatellite simultaneous observations of bow shock and magnetopause positions

[LPS-75-23-PT-1] p0034 N76-33787

A study of the heat flux reversal region upstream from the earth's bow shock, using data from the OGO 5 electron spectrometer

p0035 N78-11543

**BREMSSTRAHLUNG**

Magnetic fields, bremsstrahlung and synchrotron emission in impulsive flare of 24 October 1969

p0002 A71-43849

**BURSTS**

Hard X-ray spectra of cosmic gamma-ray bursts

p0030 A78-10580

**SUBJECT INDEX**

**C**

**CHEMICAL COMPOSITION**

Recent advances in cometary physics and chemistry

p0009 A75-13176

Thermospheric temperature, density, and composition: New models

[NASA-CR-153049] p0035 N77-23648

**CHROMOSPHERE**

Slow X-ray bursts and chromospheric flares with filament disruption

[NASA-CR-142151] p0032 N75-17281

**CHRONOLOGY**

Measurements of the cosmic-ray Be/B ratio and the age of cosmic rays

p0006 A74-30187

**CISLUNAR SPACE**

Explorer 35 and OGO 3 data on picogram size dust particle distribution in cislunar and selenocentric space, showing fluctuations during meteor shower periods

p0002 A72-31937

**CLIMATOLOGY**

Satellite observation of the mesospheric scattering layer and implied climatic consequences

p0022 A76-39128

**COLD PLASMAS**

Detached plasma regions in the magnetosphere

p0006 A74-30660

The measurement of cold ion densities in the plasma trough --- in magnetosphere

[NSSDC-ID-68-014A-18-PM] p0010 A75-16637

Instability phenomena in detached plasma regions --- in magnetosphere

p0027 A77-21512

**COLLISIONLESS PLASMAS**

Earth collisionless plasma bow shock oblique structure assessment by pulsation index Ip devised from empirical results

p0003 A72-44511

On the local time dependence of the bow shock wave structure

p0005 A74-24759

Exospheric models of the topside ionosphere --- emphasizing escape of light gases

p0006 A74-28723

Collisionless shock waves in space - A very high beta structure --- solar wind measurements

p0014 A75-35003

Characteristics of instabilities in the magnetosphere deduced from wave observations

p0023 A76-41914

Structure of a quasi-parallel, quasi-laminar bow shock

p0028 A77-23220

**COMET HEADS**

A cometary hydrogen model - Comparison with OGO-5 measurements of Comet Bennett (1970 II)

p0013 A75-32382

**COMET NUCLEI**

The interpretations of ultraviolet observations of comets

p0022 A76-31317

**COMETS**

Recent advances in cometary physics and chemistry

p0009 A75-13176

The interpretations of ultraviolet observations of comets

p0022 A76-31317

On the cometary hydrogen coma and far UV emission

p0034 N76-21066

**CONVECTIVE FLOW**

High latitude electric fields and the modulations related to interplanetary magnetic field parameters

p0005 A74-14272

**CORRELATION**

The outer magnetosphere. Part 3: Simultaneous multisatellite observations of the magnetopause. [LPS-76-4-PT-2]

p0035 N76-33795

**CORRELATION COEFFICIENTS**

Relation of variations in total magnetic field at high latitude with the parameters of the interplanetary magnetic field and with DP 2 fluctuations

p0013 A75-28743

**COSMIC DUST**

Reduction and analysis of data from cosmic dust experiments on Mariner 4, OGO 3, and Lunar Explorer 35

[NASA-CR-138866] p0032 N74-29255

**COSMIC RAYS**

Measurements of the cosmic-ray Be/B ratio and the age of cosmic rays

p0006 A74-30187

**SUBJECT INDEX**

- Impulsive solar flare X-rays greater than 10 keV and some characteristics of cosmic gamma-ray bursts  
p0014 A75-35537
- On the quiet-time increases of low energy cosmic ray electrons  
p0021 A76-26886
- Modulation of low energy electrons and protons near solar maximum  
p0021 A76-26907
- Long-term cosmic ray modulation in the period 1966-1972 and interplanetary magnetic fields  
p0023 A76-39130
- OGO-5 experiment E-09 cosmic ray electrons [NASA-CR-144668]  
p0034 N75-32995
- Long-term solar modulation of cosmic-ray electrons with energies above 0.5 GeV  
p0037 N77-84176
- Short-term variations of the cosmic-ray proton and electron intensities in 1968 and 1969  
p0037 N77-84177
- COSMIC X RAYS**
- Characteristics of cosmic X-ray bursts observed with the OGO-5 satellite  
p0026 A77-16850
- Hard X-ray spectra of cosmic gamma-ray bursts  
p0030 A78-10580
- COULOMB COLLISIONS**
- The role of Coulomb collisions in limiting differential flow and temperature differences in the solar wind  
p0019 A76-19838
- CROSS CORRELATION**
- On the causes of spectral enhancements in solar wind power spectra  
p0020 A76-22081
- CURRENT SHEETS**
- Simultaneous particle and field observations of field-aligned currents --- in magnetosphere  
p0011 A75-19330
- CUSPS (MATHEMATICS)**
- Auroral oval and magnetospheric cusps  
p0037 N78-70070
- CYCLOTRON RESONANCE**
- Critical electron pitch angle anisotropy necessary for chorus generation --- Doppler-shifted cyclotron resonance  
p0024 A76-44665

**D**

- DATA BASES**
- Production processing of the data obtained by the UCLA OGO-5 fluxgate magnetometer [PUBL-905]  
p0037 N75-76086
- DATA CORRELATION**
- Correlation of 'satellite estimates' of the equatorial electrojet intensity with ground observations at Addis Ababa.  
p0004 A73-31771
- Relation of variations in total magnetic field at high latitude with the parameters of the interplanetary magnetic field and with DP 2 fluctuations  
p0013 A75-28743
- DATA PROCESSING**
- Production processing of the data obtained by the UCLA OGO-5 fluxgate magnetometer [PUBL-905]  
p0037 N75-76086
- DAWN CHORUS**
- Intensity variation of ELF hiss and chorus during isolated substorms [NSSDC-ID-69-051A-22-PM]  
p0007 A74-44202
- Critical electron pitch angle anisotropy necessary for chorus generation --- Doppler-shifted cyclotron resonance  
p0024 A76-44665
- Magnetospheric chorus - Occurrence patterns and normalized frequency  
p0025 A77-16238
- Magnetospheric chorus  
p0033 N75-22959
- DAYGLOW**
- Atomic oxygen 1304-A day airglow observed from OGO-D spacecraft, attributing subsolar emission rates to photoelectron impact excitation  
p0002 A71-33964
- DAYTIME**
- Noctilucent clouds in daytime - Circumpolar particulate layers near the summer mesopause.  
p0003 A72-42515
- DENSE PLASMAS**
- Detached plasma regions in the magnetosphere  
p0006 A74-30660

- DENSITY DISTRIBUTION**
- Interpretation of Ogo 5 Lyman alpha measurements in the upper geocorona.  
[NSSDC-ID-68-014A-22-PM] p0004 A73-19233
- Density and temperature distributions in non-uniform rotating planetary exospheres with applications to earth  
p0005 A74-14224
- The temperature gradient between 100 and 120 km  
p0018 A76-16501
- Thermospheric temperature, density, and composition: New models [NASA-CR-153049]  
p0035 N77-23648
- DENSITY MEASUREMENT**
- Structure of electrodynamic and particle heating in the disturbed polar thermosphere  
p0027 A77-23201
- DIFFUSION COEFFICIENT**
- Long-term cosmic ray modulation in the period 1966-1972 and interplanetary magnetic fields  
p0023 A76-39130
- DIURNAL VARIATIONS**
- Recent satellite measurements of the morphology and dynamics of the plasmasphere.  
p0003 A73-13709
- Magnetospheric thermal plasma and hydrogen cation density profile characteristics in different local time regions explained by time-varying convection model  
p0003 A73-13879
- Magnetospheric field morphology at magnetically quiet times  
p0005 A74-14270
- Diurnal variation of the neutral thermospheric winds determined from incoherent scatter radar data  
p0006 A74-36735
- Thermospheric 'temperatures' --- discrepancies in inferred and satellite measured values  
p0007 A74-36747
- Magnetic storm dynamics of the thermosphere  
p0008 A75-12453
- Diurnal variation of thermal plasma in the plasmasphere  
p0023 A76-41210
- Field-aligned currents observed by the OGO 5 and Triad satellites  
p0026 A77-17124
- AEROS A atomic oxygen profiles compared with the OGO 6 model  
p0028 A77-23987
- DOPPLER EFFECT**
- The theory of VLF Doppler signatures and their relation to magnetospheric density structure  
p0023 A76-39145
- Critical electron pitch angle anisotropy necessary for chorus generation --- Doppler-shifted cyclotron resonance  
p0024 A76-44665

- DRAG MEASUREMENT**
- Recent improvements in our knowledge of neutral atmosphere structure from satellite drag measurements [BMW-WRK-226]  
p0005 A74-23676

**E**

- E REGION**
- Ionospheric E-layer formation, investigating role of solar X-ray control by electron production rate and density calculations  
p0001 A70-34943
- EARTH ATMOSPHERE**
- Density and temperature distributions in non-uniform rotating planetary exospheres with applications to earth  
p0005 A74-14224
- The effect of extraterrestrial dust, stratospheric warmings, and lower thermospheric pressure systems on OGO-4 measured nightglows in the earth's atmosphere (80 to 100 km)  
p0031 N74-26848
- EARTH SURFACE**
- Ogo 5 observations of Pc 5 waves - Ground-magnetosphere correlations  
p0024 A77-11219
- ELECTRIC FIELD STRENGTH**
- Ionospheric and magnetospheric electric field strength measurements in auroral and polar cap regions by Ba ion cloud and double floating probe techniques  
p0003 A72-39543

**ELECTRON ENERGY**

- ELECTRIC FIELDS**
- Magnetospheric electric fields convective motions measurement by Ba ion cloud tracking and symmetric double probe floating potential technique  
p0003 A73-15333
- High latitude electric fields and the modulations related to interplanetary magnetic field parameters  
p0005 A74-14272
- Electric field measurements across the Harang discontinuity --- in auroral zone  
p0010 A75-16634
- Empirical models of high-latitude electric fields  
p0029 A77-27317
- Variational electric fields at low latitudes and their relation to spread-F and plasma irregularities  
p0029 A77-34326
- ELECTRIC POTENTIAL**
- Magnetospheric electric fields convective motions measurement by Ba ion cloud tracking and symmetric double probe floating potential technique  
p0003 A73-15333
- ELECTRODYNAMICS**
- Structure of electrodynamic and particle heating in the undisturbed polar thermosphere  
p0018 A76-14318
- ELECTROJETS**
- Magnetic field variations above 60 degrees invariant latitude at the POGO satellites  
p0037 N76-71877
- ELECTROMAGNETIC INTERACTIONS**
- Waves and wave-particle interactions in the magnetosphere - A review  
p0018 A76-12272
- ELECTROMAGNETIC NOISE**
- Noise signals in earth magnetosheath interpreted as electromagnetic waves propagating in whistler mode  
p0001 A69-31985
- Properties of ELF electromagnetic waves in and above the earth's ionosphere deduced from plasma wave experiments on the OV1-17 and Ogo 6 satellites  
p0018 A76-16507
- ELECTROMAGNETIC WAVE TRANSMISSION**
- Noise signals in earth magnetosheath interpreted as electromagnetic waves propagating in whistler mode  
p0001 A69-31985
- ELECTRON ACCELERATORS**
- Acceleration of electrons in absence of detectable optical flares deduced from type III radio bursts, H alpha activity and soft X-ray emission [NSSDC-ID-68-014A-04-PS]  
p0009 A75-16217
- ELECTRON DECAY RATE**
- Electromagnetic hiss and relativistic electron losses in the inner zone --- of magnetosphere  
p0012 A75-23716
- Energetic electrons in the inner belt in 1968  
p0022 A76-35289
- ELECTRON DENSITY (CONCENTRATION)**
- The theory of VLF Doppler signatures and their relation to magnetospheric density structure  
p0023 A76-39145
- ELECTRON DENSITY PROFILES**
- AE-LEE measurements at low and mid latitude  
p0031 N74-28251
- ELECTRON DISTRIBUTION**
- AE-LEE measurements at low and mid latitude  
p0031 N74-28251
- ELECTRON EMISSION**
- Ion density and electron acceleration region location from satellite-borne solar flare X-ray measurements  
p0003 A72-32790
- Quiet-time increases of low-energy electrons - The Jovian origin  
p0025 A77-11692
- ELECTRON ENERGY**
- Electron temperature and emission measures during solar X-ray flares, studying effects of gradual and rapid radiation flux increases  
p0002 A72-29722
- New results on the correlation between low-energy electrons and auroral hiss  
p0020 A76-22086
- Modulation of low energy electrons and protons near solar maximum  
p0021 A76-26907
- A study of electron spectra in the inner belt  
p0024 A76-44653
- Non-thermal processes during the 'build-up' phase of solar flares and in absence of flares  
p0026 A77-18572
- Relativistic electron and positron intensity distributions in interplanetary regions  
p0031 N71-25288

**ELECTRON FLUX DENSITY**

Long-term solar modulation of cosmic-ray electrons with energies above 0.5 GeV  
p0037 N77-84176

Short-term variations of the cosmic-ray proton and electron intensities in 1968 and 1969  
p0037 N77-84177

**ELECTRON FLUX DENSITY**

Access of solar electrons to the polar regions  
p0015 A75-37031

On the quiet-time increases of low energy cosmic ray electrons  
p0021 A76-26886

Quiet-time increases of low-energy electrons - The Jovian origin  
p0025 A77-11692

OGO 5 observations of Pc 5 waves - Particle flux modulations  
p0030 A77-42295

**ELECTRON IMPACT**

Atomic oxygen 1304-A day airglow observed from OGO-D spacecraft, attributing subsolar emission rates to photoelectron impact excitation  
p0002 A71-33964

**ELECTRON PRECIPITATION**

Electron precipitation patterns and substorm morphology.  
[NSSDC-ID-67-073A-11-PM] p0004 A73-33434

Dependence of field-aligned electron precipitation occurrence on season and altitude  
p0007 A74-43679

Simultaneous particle and field observations of field-aligned currents --- in magnetosphere  
p0011 A75-19330

New results on the correlation between low-energy electrons and auroral hiss  
p0020 A76-22086

Field-aligned precipitation of greater than 30-keV electrons  
p0022 A76-36276

Features of polar cusp electron precipitation associated with a large magnetic storm  
[NASA-TM-X-70792] p0032 N75-12873

**ELECTRON RADIATION**

Critical electron pitch angle anisotropy necessary for chorus generation --- Doppler-shifted cyclotron resonance  
p0024 A76-44665

**ELECTROSTATIC WAVES**

Plasma flow hypothesis in the magnetosphere relating to frequency shift of electrostatic plasma waves  
p0015 A75-38275

Waves and wave-particle interactions in the magnetosphere - A review  
p0018 A76-12272

Characteristics of instabilities in the magnetosphere deduced from wave observations  
p0023 A76-41914

**EMISSION SPECTRA**

Solar low energy X-ray spectra observation during impulsive bursts, discussing thermal and nonthermal emission properties  
p0002 A71-40425

Electron temperature and emission measures during solar X-ray flares, studying effects of gradual and rapid radiation flux increases  
p0002 A72-29722

Altitude profiles of the photoelectron induced O I D (6300 A) predawn enhancement by observation and theory  
p0026 A77-20886

On the cometary hydrogen coma and far UV emission  
p0034 N76-21066

**ENERGY DISSIPATION**

Long-term solar modulation of cosmic-ray electrons with energies above 0.5 GeV  
p0037 N77-84176

**ENERGY SPECTRA**

Origin and composition of heavy nuclei between 10 and 60 MeV per nucleon during interplanetary quiet times in 1968-1972  
p0017 A75-46822

A study of electron spectra in the inner belt  
p0024 A76-44653

Quiet-time increases of low-energy electrons - The Jovian origin  
p0025 A77-11692

**ENERGY TRANSFER**

OGO-6 gas-surface energy transfer experiment  
[NASA-CR-139009] p0031 N74-25869

**EQUATORIAL ELECTROJET**

Correlation of 'satellite estimates' of the equatorial electrojet intensity with ground observations at Addis Ababa.  
p0004 A73-31771

**EXOSPHERE**

Density and temperature distributions in non-uniform rotating planetary exospheres with applications to earth  
p0005 A74-14224

Recent improvements in our knowledge of neutral atmosphere structure from satellite drag measurements  
[BMW-WRK-226] p0005 A74-23676

Exospheric models of the topside ionosphere --- emphasizing escape of light gases  
p0006 A74-28723

Diurnal variation of the neutral thermospheric winds determined from incoherent scatter radar data  
p0006 A74-36735

Observed variations of the exospheric hydrogen density with the exospheric temperature  
p0012 A75-23721

Exospheric temperature inferred from the Aeros-A neutral composition measurement  
p0017 A75-46269

Experimental model of the exospheric temperature based on optical measurements on board the OGO 6 satellite  
p0023 A76-42390

Observations of hydrogen in the upper atmosphere  
p0024 A77-11488

Global exospheric temperatures and densities under active solar conditions  
p0028 A77-25183

Experimental global model of the exospheric temperature based on measurements from the Fabry-Perot interferometer on board the OGO-6 satellite - Discussion of the data and properties of the model  
p0029 A77-34901

**EXPERIMENTAL DESIGN**

OGO-5 experiment E-09 cosmic ray electrons  
[NASA-CR-144668] p0034 N75-32995

**EXPLORER 3 SATELLITE**

AE-LEE measurements at low and mid latitude  
p0031 N74-28251

**EXTRATERRESTRIAL MATTER**

The effect of extraterrestrial dust, stratospheric warmings, and lower thermospheric pressure systems on OGO-4 measured nightglows in the earth's atmosphere (80 to 100 km)  
p0031 N74-26848

Reduction and analysis of data from cosmic dust experiments on Mariner 4, OGO 3, and Lunar Explorer 35  
[NASA-CR-138866] p0032 N74-29255

**EXTRATERRESTRIAL RADIATION**

AE-LEE measurements at low and mid latitude  
p0031 N74-28251

**EXTREMELY LOW FREQUENCIES**

Steady ELF plasmaspheric hiss, studying whistler mode turbulence, band limitation, power spectra and peak intensities  
p0004 A73-26984

Intensity variation of ELF hiss and chorus during isolated substorms  
[NSSDC-ID-69-051A-22-PM] p0007 A74-44202

ELF hiss associated with plasma density enhancements in the outer magnetosphere  
p0022 A76-33058

Detailed analysis of magnetospheric ELF chorus - preliminary results  
p0027 A77-21523

Extremely low frequency hiss emissions in the magnetosphere --- using OGO 5 and 6 observations  
p0032 N74-30528

**EXTREMELY LOW RADIO FREQUENCIES**

A relation between ELF hiss amplitude and plasma density in the outer plasmasphere  
p0006 A74-30677

Electromagnetic hiss and relativistic electron losses in the inner zone --- of magnetosphere  
p0012 A75-23716

VLF and ELF emissions --- in magnetosphere  
p0015 A75-36988

Properties of ELF electromagnetic waves in and above the earth's ionosphere deduced from plasma wave experiments on the OV1-17 and Ogo 6 satellites  
p0018 A76-16507

The local time variation of ELF emissions during periods of substorm activity  
p0029 A77-31391

**SUBJECT INDEX**

**F**

**F REGION**

F region wind components in the magnetic meridian from OGO 4 tropical airglow observations  
p0011 A75-22671

Remote sensing of the ionospheric F layer by use of O I 6300-A and O I 1356-A observations  
p0014 A75-35040

Tropical F region winds from O I 1356-A and forbidden O I 6300-A emissions. II - Analysis of OGO 4 data  
p0023 A76-42683

Model of equatorial scintillations from in-situ measurements --- based on OGO-6 observed F region irregularity  
p0025 A77-12057

Correlated measurements of scintillations and in-situ F-region irregularities from OGO-6  
p0025 A77-15786

Comparisons of ionogram and OGO 6 satellite observations of small-scale F region inhomogeneities  
p0028 A77-23211

Determination of tropical F-region winds from atomic oxygen airglow emissions  
p0034 N76-10603

**F 2 REGION**

Neutral wind velocities calculated from temperature measurements during a magnetic storm and the observed ionospheric effects.  
p0004 A73-36150

**FABRY-PEROT INTERFEROMETERS**

Experimental model of the exospheric temperature based on optical measurements on board the OGO 6 satellite  
p0023 A76-42390

Experimental global model of the exospheric temperature based on measurements from the Fabry-Perot interferometer on board the OGO-6 satellite - Discussion of the data and properties of the model  
p0029 A77-34901

**FAR ULTRAVIOLET RADIATION**

Thermal plasma origin of solar X-ray emission and far UV flash observation during 28 August 1966 proton flare  
p0002 A72-20013

Impulsive /flash/ phase of solar flares - Hard X-ray, microwave, EUV and optical observations  
p0015 A75-37352

On the cometary hydrogen coma and far UV emission  
p0034 N76-21066

**FILAMENTS**

Slow X-ray bursts and chromospheric flares with filament disruption  
[NASA-CR-142151] p0032 N75-17281

**FINE STRUCTURE**

The earth's bow shock fine structure  
p0011 A75-19138

An explanation of the longitudinal variation of the O I D (630 nm) tropical nightglow intensity  
p0019 A76-21456

**FLUID DYNAMICS**

The outer magnetosphere. Part I: A multisatellite study of the magnetopause position in relation with some important fluid dynamic parameters  
[LPS-76-2-PT-1] p0035 N76-33793

**FORBUSH DECREASES**

Hysteresis of primary cosmic rays associated with Forbush decreases  
p0022 A76-35348

**FREQUENCY DISTRIBUTION**

Magnetospheric chorus - Occurrence patterns and normalized frequency  
p0025 A77-16238

**FREQUENCY RANGES**

The upper- and lower-frequency cutoffs of magnetospherically reflected whistlers  
p0019 A76-19854

**FREQUENCY SHIFT**

Plasma flow hypothesis in the magnetosphere relating to frequency shift of electrostatic plasma waves  
p0015 A75-38275

**G**

**GAMMA RAY ASTRONOMY**

Hard X-ray spectra of cosmic gamma-ray bursts  
p0030 A78-10580

**SUBJECT INDEX**

**GAMMA RAYS**  
 Impulsive solar flare X-rays greater than 10 keV and some characteristics of cosmic gamma-ray bursts p0014 A75-35537  
 Characteristics of cosmic X-ray bursts observed with the OGO-5 satellite p0026 A77-16850

**GAS DENSITY**  
 An upper limit to the product of NO and O densities from 105 to 120 km [NSSDC-ID-69-051A-26-PM] p0008 A75-11227  
 Satellite measurements of nitric oxide in the polar region p0017 A75-46289  
 Global atomic hydrogen density derived from OGO-6 Lyman-alpha measurements p0021 A76-28988  
 Global atomic oxygen density derived from OGO-6 1304 A airglow measurements p0021 A76-28989  
 Observations of hydrogen in the upper atmosphere p0024 A77-11488  
 Geomagnetic storm effects on the thermosphere and the ionosphere revealed by in situ measurements from OGO 6 p0025 A77-16240  
 A global thermospheric model based on mass spectrometer and incoherent scatter data MSIS. I - N2 density and temperature p0029 A77-37153  
 A global thermospheric model based on mass spectrometer and incoherent scatter data MSIS. II - Composition p0029 A77-37154

**GAS TEMPERATURE**  
 A global thermospheric model based on mass spectrometer and incoherent scatter data MSIS. I - N2 density and temperature p0029 A77-37153

**GEOCORONAL EMISSIONS**  
 Interpretation of Ogo 5 Lyman alpha measurements in the upper geocorona. [NSSDC-ID-68-014A-22-PM] p0004 A73-19233

**GEOLOGICAL SURVEYS**  
 A global magnetic anomaly map p0012 A75-24043

**GEOMAGNETIC LATITUDE**  
 The equatorial helium ion trough and the geomagnetic anomaly p0011 A75-20360

**GEOMAGNETIC MICROPULSATIONS**  
 Micropulsations and the plasmopause p0027 A77-21513

**GEOMAGNETIC PULSATIONS**  
 Earth collisionless plasma bow shock oblique structure assessment by pulsation index Ip devised from empirical results p0003 A72-44511  
 Probing the plasmopause by geomagnetic pulsations p0015 A75-36982  
 The dominant mode of standing Alfvén waves at the synchronous orbit p0017 A75-46285  
 Ogo 5 observations of Pc 5 waves - Ground-magnetosphere correlations p0024 A77-11219  
 Multiple satellite observations of pulsation resonance structure in the magnetosphere p0027 A77-23205  
 Structure of a quasi-parallel, quasi-laminar bow shock p0028 A77-23220

**GEOMAGNETIC TAIL**  
 Plasma tail interpretations of pronounced detached plasma regions measured by Ogo 5 p0007 A74-43691  
 Substorm and interplanetary magnetic field effects on the geomagnetic tail lobes p0011 A75-19349  
 Thinning of the near-earth (10 to about 15 earth radii) plasma sheet preceding the substorm expansion phase p0024 A76-47884  
 Multiple-satellite studies of magnetospheric substorms - Radial dynamics of the plasma sheet p0026 A77-16868  
 Energetic electrons in the near geomagnetic tail and at synchronous orbit: Spatial distributions and acceleration mechanisms p0032 N74-35223

**GEOMAGNETISM**  
 Proton measurements in ring current by OGO-3 satellite compared with geomagnetic field data at low and high latitudes p0002 A71-33663  
 Recent satellite measurements of the morphology and dynamics of the plasmasphere. p0003 A73-13709  
 Magnetospheric field morphology at magnetically quiet times p0005 A74-14270  
 Substorms in space - The correlation between ground and satellite observations of the magnetic field p0005 A74-14285  
 Dependence of field-aligned electron precipitation occurrence on season and altitude p0007 A74-43679  
 Magnetopause rotational forms [NSSDC-ID-68-014A-15-PM] p0008 A75-11221  
 Variation with interplanetary sector of the total magnetic field measured at the OGO 2, 4 and 6 satellites p0008 A75-12368  
 Differential rotation of the magnetospheric plasma as cause of the Svalgaard-Mansurov effect --- relationship between geomagnetic variables and IMF polarity p0014 A75-35036  
 Access of solar electrons to the polar regions p0015 A75-37031  
 A comparison of electric and magnetic field data from the OGO 6 spacecraft p0018 A76-16514  
 Magnetic storm effects on the tropical ultraviolet airglow p0029 A77-27318  
 Low latitude variations of the magnetic field p0037 N76-71880

**GEOPHYSICS**  
 Auroral oval and magnetospheric cusps p0037 N78-70070

**GROUND STATIONS**  
 Correlation of 'satellite estimates' of the equatorial electrojet intensity with ground observations at Addis Ababa. p0004 A73-31771

**H**

**H ALPHA LINE**  
 Acceleration of electrons in absence of detectable optical flares deduced from type III radio bursts, H alpha activity and soft X-ray emission [NSSDC-ID-68-014A-04-PS] p0009 A75-16217  
 OGO-V radio burst analysis --- h alpha line [NASA-CR-142232] p0033 N75-19114

**HARMONIC ANALYSIS**  
 The dominant mode of standing Alfvén waves at the synchronous orbit p0017 A75-46285

**HEAT FLUX**  
 A study of the heat flux reversal region upstream from the earth's bow shock, using data from the OGO 5 electron spectrometer p0035 N78-11543

**HEAVY NUCLEI**  
 Origin and composition of heavy nuclei between 10 and 60 MeV per nucleon during interplanetary quiet times in 1968-1972 p0017 A75-46822

**HELIUM**  
 The solar cycle variation of the solar wind helium abundance [NSSDC-ID-68-014A-17-OS] p0010 A75-16631  
 Dynamical effects in the distribution of helium in the thermosphere p0024 A77-11489

**HELIUM IONS**  
 The equatorial helium ion trough and the geomagnetic anomaly p0011 A75-20360

**HELIUM ISOTOPES**  
 Solar energetic particle event with He-3/He-4 greater than 1 p0009 A75-15342  
 Solar particle events with anomalously large relative abundance of He-3 p0013 A75-34018

**HEOS A SATELLITE**  
 The magnetopause: Part 2: Magnetopause position and the reconnection problem [LPS-75-24-PT-2] p0035 N76-33788

**HYSTERESIS**

**HIGH ENERGY ELECTRONS**  
 Relativistic electron events in interplanetary space p0007 A74-37632  
 Pitch angle distributions of energetic electrons in the equatorial regions of the outer magnetosphere - OGO-5 observations p0011 A75-22759  
 Electromagnetic hiss and relativistic electron losses in the inner zone --- of magnetosphere p0012 A75-23716  
 On the quiet-time increases of low energy cosmic ray electrons p0021 A76-26886  
 Energetic electrons in the inner belt in 1968 p0022 A76-35289  
 Field-aligned precipitation of greater than 30-keV electrons p0022 A76-36276

**HIGH TEMPERATURE PLASMAS**  
 Diurnal variation of thermal plasma in the plasmasphere p0023 A76-41210

**HISS**  
 Steady ELF plasmaspheric hiss, studying whistler mode turbulence, band limitation, power spectra and peak intensities p0004 A73-26984  
 A relation between ELF hiss amplitude and plasma density in the outer plasmasphere p0006 A74-30677  
 Intensity variation of ELF hiss and chorus during isolated substorms [NSSDC-ID-69-051A-22-PM] p0007 A74-44202  
 'Hisslers' - Quasi-periodic (T approximately equal to 2 sec) VLF noise forms at auroral latitudes p0009 A75-16440  
 Electromagnetic hiss and relativistic electron losses in the inner zone --- of magnetosphere p0012 A75-23716  
 New results on the correlation between low-energy electrons and auroral hiss p0020 A76-22086  
 ELF hiss associated with plasma density enhancements in the outer magnetosphere p0022 A76-33058

**HYDROGEN**  
 Observed variations of the exospheric hydrogen density with the exospheric temperature p0012 A75-23721  
 Observations of hydrogen in the upper atmosphere p0024 A77-11488  
 On the cometary hydrogen coma and far UV emission p0034 N76-21066

**HYDROGEN ATOMS**  
 Interpretation of Ogo 5 Lyman alpha measurements in the upper geocorona. [NSSDC-ID-68-014A-22-PM] p0004 A73-19233  
 Variation of the solar wind flux with heliographic latitude, deduced from its interaction with interplanetary hydrogen p0013 A75-28032  
 Global atomic hydrogen density derived from OGO-6 Lyman-alpha measurements p0021 A76-28988  
 Geomagnetic storm effects on the thermosphere and the ionosphere revealed by in situ measurements from OGO 6 p0025 A77-16240

**HYDROGEN CLOUDS**  
 A cometary hydrogen model - Comparison with OGO-5 measurements of Comet Bennett (1970 II) p0013 A75-32382

**HYDROGEN IONS**  
 Magnetospheric thermal plasma and hydrogen cation density profile characteristics in different local time regions explained by time-varying convection model p0003 A73-13879  
 Multiple satellite observations of pulsation resonance structure in the magnetosphere p0027 A77-23205

**HYDROXYL EMISSION**  
 Polar enhancements of nightglow emissions near 6230A. p0019 A76-19613  
 Behavior of the sodium and hydroxyl nighttime emissions during a stratospheric warming p0020 A76-22490

**HYSTERESIS**  
 Hysteresis of primary cosmic rays associated with Forbush decreases p0022 A76-35348

## I

## ICE

The role of ice particulates in the electrification of the air in the mesosphere — using OGO 6 data  
p0033 N75-24202

## INCOHERENT SCATTERING

A global thermospheric model based on mass spectrometer and incoherent scatter data MSIS. I - N2 density and temperature  
p0029 A77-37153

A global thermospheric model based on mass spectrometer and incoherent scatter data MSIS. II - Composition  
p0029 A77-37154

## INNER RADIATION BELT

Energetic electrons in the inner belt in 1968  
p0022 A76-35289

## INTERPLANETARY DUST

Explorer 35 and OGO 3 data on picogram size dust particle distribution in cis-lunar and selenocentric space, showing fluctuations during meteor shower periods  
p0002 A72-31937

## INTERPLANETARY MAGNETIC FIELDS

High latitude electric fields and the modulations related to interplanetary magnetic field parameters  
p0005 A74-14272

Variation with interplanetary sector of the total magnetic field measured at the OGO 2, 4 and 6 satellites  
p0008 A75-12368

Dependence of the magnetopause position on the southward interplanetary magnetic field  
p0008 A75-12370

OGO-5 observations of the magnetopause  
p0010 A75-19134

The earth's bow shock fine structure  
p0011 A75-19138

Substorm and interplanetary magnetic field effects on the geomagnetic tail lobes  
p0011 A75-19349

Instabilities connected with neutral sheets in the solar wind  
p0013 A75-28015

Relation of variations in total magnetic field at high latitude with the parameters of the interplanetary magnetic field and with DP 2 fluctuations  
p0013 A75-28743

Collisionless shock waves in space - A very high beta structure — solar wind measurements  
p0014 A75-35003

Differential rotation of the magnetospheric plasma as cause of the Svalgaard-Mansurov effect — relationship between geomagnetic variables and IMF polarity  
p0014 A75-35036

Access of solar electrons to the polar regions  
p0015 A75-37031

Angular distributions of solar protons and electrons  
p0016 A75-41805

Pioneer 9 and OGO 5 observations of an interplanetary multiple shock ensemble on February 2, 1969  
p0016 A75-42744

Evidence for magnetic field line reconnection in the solar wind  
p0017 A75-46238

A comparison of electric and magnetic field data from the OGO 6 spacecraft  
p0018 A76-16514

Dependence of the latitude of the cleft on the interplanetary magnetic field and substorm activity  
p0020 A76-22107

Long-term cosmic ray modulation in the period 1966-1972 and interplanetary magnetic fields  
p0023 A76-39130

Thinning of the near-earth (10 to about 15 earth radii) plasma sheet preceding the substorm expansion phase  
p0024 A76-47884

High latitude ionospheric winds related to solar-interplanetary conditions  
p0032 N74-29091

## INTERPLANETARY MEDIUM

Variation of the solar wind flux with heliographic latitude, deduced from its interaction with interplanetary hydrogen  
p0013 A75-28032

Relativistic electron and positron intensity distributions in interplanetary regions  
p0031 N71-25288

## INTERSTELLAR GAS

Solar radiation asymmetries and heliospheric gas heating influencing extraterrestrial UV data  
p0009 A75-13173

## INVARIANCE

Magnetic field variations above 60 degrees invariant latitude at the POGO satellites  
p0037 N76-71877

## ION CONCENTRATION

Satellite measurements of ion composition and temperatures in the topside ionosphere during medium solar activity  
p0021 A76-28486

## ION DENSITY (CONCENTRATION)

Ion density and electron acceleration region location from satellite-borne solar flare X-ray measurements  
p0003 A72-32790

High-latitude proton precipitation and light ion density profiles during the magnetic storm initial phase.  
[NSSDC-ID-67-073A-11-PM] p0004 A73-45114

Diurnal variation of thermal plasma in the plasmasphere  
p0023 A76-41210

## ION TEMPERATURE

The measurement of cold ion densities in the plasma trough — in magnetosphere  
[NSSDC-ID-68-014A-18-PM] p0010 A75-16637

The role of Coulomb collisions in limiting differential flow and temperature differences in the solar wind  
p0019 A76-19838

Satellite measurements of ion composition and temperatures in the topside ionosphere during medium solar activity  
p0021 A76-28486

## IONIZATION

The role of ice particulates in the electrification of the air in the mesosphere — using OGO 6 data  
p0033 N75-24202

## IONOGRAMS

Comparisons of ionogram and OGO 6 satellite observations of small-scale F region inhomogeneities  
p0028 A77-23211

## IONOSPHERE

Variational electric fields at low latitudes and their relation to spread-F and plasma irregularities  
p0029 A77-34326

## IONOSPHERIC COMPOSITION

The temperature gradient between 100 and 120 km  
p0018 A76-16501

Satellite measurements of ion composition and temperatures in the topside ionosphere during medium solar activity  
p0021 A76-28486

## IONOSPHERIC CURRENTS

Ionospheric and magnetospheric electric field strength measurements in auroral and polar cap regions by Ba ion cloud and double floating probe techniques  
p0003 A72-39543

Variation with interplanetary sector of the total magnetic field measured at the OGO 2, 4 and 6 satellites  
p0008 A75-12368

Electric field measurements across the Harang discontinuity — in auroral zone  
p0010 A75-16634

Current-driven plasma instabilities at high latitudes — Ogo-5 observations  
p0014 A75-35005

Identifications of the polar cap boundary and the auroral belt in the high-altitude magnetosphere - A model for field-aligned currents  
p0014 A75-35007

Differential rotation of the magnetospheric plasma as cause of the Svalgaard-Mansurov effect — relationship between geomagnetic variables and IMF polarity  
p0014 A75-35036

A comparison of electric and magnetic field data from the OGO 6 spacecraft  
p0018 A76-16514

Field-aligned currents observed by the OGO 5 and Triad satellites  
p0026 A77-17124

High latitude ionospheric winds related to solar-interplanetary conditions  
p0032 N74-29091

## IONOSPHERIC DISTURBANCES

In-situ observations of irregular ionospheric structure associated with the plasmopause  
p0008 A75-11853

Magnetic storm dynamics of the thermosphere  
p0008 A75-12453

North-south asymmetries in the thermosphere during the last maximum of the solar cycle  
p0009 A75-16449

The temperature gradient drift instability at the equatorward edge of the ionospheric plasma trough  
p0024 A76-42697

Correlated measurements of scintillations and in-situ F-region irregularities from OGO-6  
p0025 A77-15786

## IONOSPHERIC ELECTRON DENSITY

Ionospheric E-layer formation, investigating role of solar X-ray control by electron production rate and density calculations  
p0001 A70-34943

Neutral wind velocities calculated from temperature measurements during a magnetic storm and the observed ionospheric effects.  
p0004 A73-36150

Is the red arc a good indicator of ionosphere-magnetosphere conditions  
[NSSDC-ID-69-051A-02-PM] p0008 A75-11226

Remote sensing of the ionospheric F layer by use of O I 6300-A and O I 1356-A observations  
p0014 A75-35040

A study of electron spectra in the inner belt  
p0024 A76-44653

Model of equatorial scintillations from in-situ measurements — based on OGO-6 observed F region irregularity  
p0025 A77-12057

Altitude profiles of the photoelectron induced O I D (6300 A) predawn enhancement by observation and theory  
p0026 A77-20886

Light ion and electron troughs observed in the mid-latitude topside ionosphere on two passes of OGO 6 compared to coincident equatorial electron density deduced from whistlers  
p0030 A77-42297

## IONOSPHERIC HEATING

Magnetically ordered heating in the polar regions of the thermosphere  
p0034 N75-32651

## IONOSPHERIC ION DENSITY

In-situ observations of irregular ionospheric structure associated with the plasmopause  
p0008 A75-11853

High latitude minor ion enhancements - A clue for studies of magnetosphere-atmosphere coupling  
p0008 A75-12439

The measurement of cold ion densities in the plasma trough — in magnetosphere  
[NSSDC-ID-68-014A-18-PM] p0010 A75-16637

The equatorial helium ion trough and the geomagnetic anomaly  
p0011 A75-20360

Ion composition irregularities and ionosphere-plasmasphere coupling - Observations of a high latitude ion trough  
p0013 A75-28356

Satellite measurements of high-altitude twilight Mg(plus) emission  
p0019 A76-19839

High-latitude troughs and the polar cap boundary  
p0020 A76-22105

Geomagnetic storm effects on the thermosphere and the ionosphere revealed by in situ measurements from OGO 6  
p0025 A77-16240

## IONOSPHERIC PROPAGATION

Properties of ELF electromagnetic waves in and above the earth's ionosphere deduced from plasma wave experiments on the OVI-17 and Ogo 6 satellites  
p0018 A76-16507

A new interpretation of subprotonospheric whistler characteristics  
p0019 A76-16522

The morphology of equatorial irregularities in the Afro-Asian sector from OGO 6 observations  
p0028 A77-24016

## IONOSPHERIC SOUNDING

Correlation of 'satellite estimates' of the equatorial electrojet intensity with ground observations at Addis Ababa.  
p0004 A73-31771

F region wind components in the magnetic meridian from OGO 4 tropical airglow observations  
p0011 A75-22671

Remote sensing of the ionospheric F layer by use of O I 6300-A and O I 1356-A observations  
p0014 A75-35040

OGO 6 observations of 5577 A — airglow measurements  
p0019 A76-18436

**SUBJECT INDEX**

**IONOSPHERIC TEMPERATURE**

North-south asymmetries in the thermosphere during the last maximum of the solar cycle  
 p0009 A75-16449  
 The temperature gradient between 100 and 120 km  
 p0018 A76-16501  
 The temperature gradient drift instability at the equatorward edge of the ionospheric plasma trough  
 p0024 A76-42697  
 Global exospheric temperatures and densities under active solar conditions --- measured by OGO-6  
 [NASA-CR-145394] p0034 N76-10610

**J**

**JUPITER (PLANET)**

Quiet-time increases of low-energy electrons - The Jovian origin  
 p0025 A77-11692

**K**

**KINETIC ENERGY**

Relativistic electron and positron intensity distributions in interplanetary regions  
 p0031 N71-25288

**KINETIC THEORY**

Exospheric models of the topside ionosphere --- emphasizing escape of light gases  
 p0006 A74-28723

**L**

**LAMINAR FLOW**

Structure of the quasi-perpendicular laminar bow shock --- earth-solar wind interaction  
 p0012 A75-23707

**LATITUDE**

North-south asymmetries in the thermosphere during the last maximum of the solar cycle  
 p0009 A75-16449  
 Dependence of the latitude of the cleft on the interplanetary magnetic field and substorm activity  
 p0020 A76-22107

**LIGHT ELEMENTS**

High-latitude proton precipitation and light ion density profiles during the magnetic storm initial phase.  
 [NSSDC-ID-67-073A-11-PM] p0004 A73-45114

**LIGHT EMISSION**

Impulsive /flash/ phase of solar flares - Hard X-ray, microwave, EUV and optical observations  
 p0015 A75-37352

**LINES OF FORCE**

Evidence for magnetic field line reconnection in the solar wind  
 p0017 A75-46238

**LONG TERM EFFECTS**

Long-term cosmic ray modulation in the period 1966-1972 and interplanetary magnetic fields  
 p0023 A76-39130

**LONGITUDE**

An explanation of the longitudinal variation of the OI(630 nm) tropical nightglow intensity  
 p0019 A76-21456

**LOW FREQUENCIES**

Low-energy radio emissions from the earth and sun --- solar type 3 bursts  
 p0033 N75-20195

**LUMINOUS INTENSITY**

The intensity variation of the atomic oxygen red line during morning and evening twilight on 9-10 April 1969  
 p0021 A76-28990

**LUNAR ORBITS**

Explorer 35 and OGO 3 data on picogram size dust particle distribution in cislunar and selenocentric space, showing fluctuations during meteor shower periods  
 p0002 A72-31937

**LYMAN ALPHA RADIATION**

Interpretation of Ogo 5 Lyman alpha measurements in the upper geocorona.  
 [NSSDC-ID-68-014A-22-PM] p0004 A73-19233  
 Solar radiation asymmetries and heliospheric gas heating influencing extraterrestrial UV data  
 p0009 A75-13173  
 Variation of the solar wind flux with heliographic latitude, deduced from its interaction with interplanetary hydrogen  
 p0013 A75-28032

Global atomic hydrogen density derived from OGO-6 Lyman-alpha measurements  
 p0021 A76-28988

The interpretations of ultraviolet observations of comets  
 p0022 A76-31317

**M**

**MAGNESIUM**

Satellite measurements of high-altitude twilight Mg(plus) emission  
 p0019 A76-19839

**MAGNETIC ANOMALIES**

The equatorial helium ion trough and the geomagnetic anomaly  
 p0011 A75-20360  
 A global magnetic anomaly map  
 p0012 A75-24043  
 Magnetic anomaly map of North America south of 50 degrees north from Pogo data  
 [NASA-TM-X-71229] p0035 N77-13587  
 Comparison of a magnetic local anomaly measured by OGO-6 and a crustal feature  
 p0037 N76-71883

**MAGNETIC DISTURBANCES**

Electric field measurements across the Harang discontinuity --- in auroral zone  
 p0010 A75-16634  
 Simultaneous particle and field observations of field-aligned currents --- in magnetosphere  
 p0011 A75-19330  
 Relation of variations in total magnetic field at high latitude with the parameters of the interplanetary magnetic field and with DP 2 fluctuations  
 p0013 A75-28743  
 A comparison of electric and magnetic field data from the OGO 6 spacecraft  
 p0018 A76-16514

**MAGNETIC EFFECTS**

Energetic electrons in the inner belt in 1968  
 p0022 A76-35289  
 Field-aligned precipitation of greater than 30-keV electrons  
 p0022 A76-36276  
 Magnetically ordered heating in the polar regions of the thermosphere  
 p0034 N75-32651

**MAGNETIC EQUATOR**

The equatorial helium ion trough and the geomagnetic anomaly  
 p0011 A75-20360  
 F region wind components in the magnetic meridian from OGO 4 tropical airglow observations  
 p0011 A75-22671  
 Pitch angle distributions of energetic electrons in the equatorial regions of the outer magnetosphere - OGO-5 observations  
 p0011 A75-22759

**MAGNETIC FIELD CONFIGURATIONS**

Magnetospheric field morphology at magnetically quiet times  
 p0005 A74-14270  
 Variation with interplanetary sector of the total magnetic field measured at the OGO 2, 4 and 6 satellites  
 p0008 A75-12368  
 OGO-5 observations of the magnetopause  
 p0010 A75-19134  
 Evidence for magnetic field line reconnection in the solar wind  
 p0017 A75-46238

**MAGNETIC FIELDS**

Magnetic field variations above 60 degrees invariant latitude at the POGO satellites  
 p0037 N76-71877  
 Low latitude variations of the magnetic field  
 p0037 N76-71880

**MAGNETIC FLUX**

Dependence of the magnetopause position on the southward interplanetary magnetic field  
 p0008 A75-12370  
 Substorm and interplanetary magnetic field effects on the geomagnetic tail lobes  
 p0011 A75-19349

**MAGNETIC MEASUREMENT**

ELF hiss associated with plasma density enhancements in the outer magnetosphere  
 p0022 A76-33058  
 Detailed analysis of magnetospheric ELF chorus - preliminary results  
 p0027 A77-21523

**MAGNETOHYDRODYNAMIC STABILITY**

**MAGNETIC SIGNATURES**

Magnetopause rotational forms  
 [NSSDC-ID-68-014A-15-PM] p0008 A75-11221

**MAGNETIC STORMS**

Electron precipitation patterns and substorm morphology.  
 [NSSDC-ID-67-073A-11-PM] p0004 A73-33434  
 Neutral wind velocities calculated from temperature measurements during a magnetic storm and the observed ionospheric effects.  
 p0004 A73-36150  
 High-latitude proton precipitation and light ion density profiles during the magnetic storm initial phase.  
 [NSSDC-ID-67-073A-11-PM] p0004 A73-45114  
 Substorms in space - The correlation between ground and satellite observations of the magnetic field  
 p0005 A74-14285  
 Magnetic storm dynamics of the thermosphere  
 p0008 A75-12453  
 Magnetospheric substorm associated with SC --- sudden commencements at OGO-5  
 p0011 A75-22613

Electromagnetic hiss and relativistic electron losses in the inner zone --- of magnetosphere  
 p0012 A75-23716

Substorm effects on the neutral sheet inside 10 earth radii  
 p0016 A75-46232

Dependence of the latitude of the cleft on the interplanetary magnetic field and substorm activity  
 p0020 A76-22107

Energetic electrons in the inner belt in 1968  
 p0022 A76-35289

Geomagnetic storm effects on the thermosphere and the ionosphere revealed by in situ measurements from OGO 6  
 p0025 A77-16240

High-latitude nitric oxide in the lower thermosphere  
 p0028 A77-23222

Magnetic storm effects on the tropical ultraviolet airglow  
 p0029 A77-27318

The local time variation of ELF emissions during periods of substorm activity  
 p0029 A77-31391

Features of polar cusp electron precipitation associated with a large magnetic storm  
 [NASA-TM-X-70792] p0032 N75-12873

**MAGNETIC SURVEYS**

A global magnetic anomaly map  
 p0012 A75-24043

**MAGNETIC VARIATIONS**

Substorms in space - The correlation between ground and satellite observations of the magnetic field  
 p0005 A74-14285  
 Variation with interplanetary sector of the total magnetic field measured at the OGO 2, 4 and 6 satellites  
 p0008 A75-12368  
 Relation of variations in total magnetic field at high latitude with the parameters of the interplanetary magnetic field and with DP 2 fluctuations  
 p0013 A75-28743  
 Differential rotation of the magnetospheric plasma as cause of the Svalgaard-Mansurov effect --- relationship between geomagnetic variables and IMF polarity  
 p0014 A75-35036

**MAGNETOACOUSTIC WAVES**

Excitation of magnetosonic waves with discrete spectrum in the equatorial vicinity of the plasmapause  
 p0012 A75-27679

**MAGNETOHYDRODYNAMIC FLOW**

Exospheric models of the topside ionosphere --- emphasizing escape of light gases  
 p0006 A74-28723  
 Plasma flow hypothesis in the magnetosphere relating to frequency shift of electrostatic plasma waves  
 p0015 A75-38275

**MAGNETOHYDRODYNAMIC STABILITY**

Plasma instability modes related to the earth's bow shock  
 p0011 A75-22774  
 Instabilities connected with neutral sheets in the solar wind  
 p0013 A75-28015  
 The enhancement of solar wind fluctuations with scale size near the proton gyroradius  
 p0013 A75-28038  
 Micropulsations and the plasmapause  
 p0027 A77-21513

MAGNETOHYDRODYNAMIC WAVES

MAGNETOHYDRODYNAMIC WAVES

The dominant mode of standing Alfvén waves at the synchronous orbit  
 p0017 A75-46285  
 Ogo 5 observations of Pc 5 waves -  
 Ground-magnetosphere correlations  
 p0024 A77-11219  
 Instability phenomena in detached plasma regions  
 --- in magnetosphere  
 p0027 A77-21512

**MAGNETOMETERS**  
 Production processing of the data obtained by the UCLA OGO-5 fluxgate magnetometer  
 [PUBL-905] p0037 N75-76086

**MAGNETOFAUSE**  
 Magnetopause rotational forms  
 [NSSDC-ID-68-014A-15-PM] p0008 A75-11221  
 Dependence of the magnetopause position on the southward interplanetary magnetic field  
 p0008 A75-12370  
 OGO-5 observations of the magnetopause  
 p0010 A75-19134  
 Access of solar electrons to the polar regions  
 p0015 A75-37031  
 The magnetopause. Part 1: Multisatellite simultaneous observations of bow shock and magnetopause positions  
 [LPS-75-23-PT-1] p0034 N76-33787  
 The magnetopause. Part 2: Magnetopause position and the reconnection problem  
 [LPS-75-24-PT-2] p0035 N76-33788

**MAGNETOSONIC RESONANCE**  
 Excitation of magnetosonic waves with discrete spectrum in the equatorial vicinity of the plasmopause  
 p0012 A75-27679

**MAGNETOSPHERE**  
 Noise signals in earth magnetosheath interpreted as electromagnetic waves propagating in whistler mode  
 p0001 A69-31985  
 Ionospheric and magnetospheric electric field strength measurements in auroral and polar cap regions by Ba ion cloud and double floating probe techniques  
 p0003 A72-39543  
 Recent satellite measurements of the morphology and dynamics of the plasmasphere.  
 p0003 A73-13709  
 Magnetospheric electric fields convective motions measurement by Ba ion cloud tracking and symmetric double probe floating potential technique  
 p0003 A73-15333  
 Steady ELF plasmaspheric hiss, studying whistler mode turbulence, band limitation, power spectra and peak intensities  
 p0004 A73-26984  
 Magnetospheric field morphology at magnetically quiet times  
 p0005 A74-14270  
 Substorms in space - The correlation between ground and satellite observations of the magnetic field  
 p0005 A74-14285  
 On the local time dependence of the bow shock wave structure  
 p0005 A74-24759  
 Detached plasma regions in the magnetosphere  
 p0006 A74-30660  
 A relation between ELF hiss amplitude and plasma density in the outer plasmasphere  
 p0006 A74-30677  
 Is the red arc a good indicator of ionosphere-magnetosphere conditions  
 [NSSDC-ID-69-051A-02-PM] p0008 A75-11226  
 High latitude minor ion enhancements - A clue for studies of magnetosphere-atmosphere coupling  
 p0008 A75-12439  
 Correlated satellite measurements of proton precipitation and plasma density --- in magnetosphere  
 p0009 A75-16437  
 The solar wind and magnetospheric dynamics  
 p0010 A75-19127  
 Simultaneous particle and field observations of field-aligned currents --- in magnetosphere  
 p0011 A75-19330  
 Electromagnetic hiss and relativistic electron losses in the inner zone --- of magnetosphere  
 p0012 A75-23716  
 Identifications of the polar cap boundary and the auroral belt in the high-altitude magnetosphere - A model for field-aligned currents  
 p0014 A75-35007  
 Differential rotation of the magnetospheric plasma as cause of the Svalgaard-Mansurov effect --- relationship between geomagnetic variables and IMF polarity  
 p0014 A75-35036

Probing the plasmopause by geomagnetic pulsations  
 p0015 A75-36982  
 VLF and ELF emissions --- in magnetosphere  
 p0015 A75-36988  
 Plasma flow hypothesis in the magnetosphere relating to frequency shift of electrostatic plasma waves  
 p0015 A75-38275  
 Waves and wave-particle interactions in the magnetosphere - A review  
 p0018 A76-12272  
 VLF propagation in the magnetosphere during sunrise and sunset hours  
 p0018 A76-14838  
 Properties of ELF electromagnetic waves in and above the earth's ionosphere deduced from plasma wave experiments on the OV1-17 and Ogo 6 satellites  
 p0018 A76-16507  
 A new interpretation of subprotonospheric whistler characteristics  
 p0019 A76-16522  
 The upper- and lower-frequency cutoffs of magnetospherically reflected whistlers  
 p0019 A76-19854  
 Magnetosheath lion roars --- strongest whistler mode signals  
 p0022 A76-33057  
 ELF hiss associated with plasma density enhancements in the outer magnetosphere  
 p0022 A76-33058  
 The theory of VLF Doppler signatures and their relation to magnetospheric density structure  
 p0023 A76-39145  
 Ogo 5 observations of Pc 5 waves - Ground-magnetosphere correlations  
 p0024 A77-11219  
 Magnetospheric chorus - Occurrence patterns and normalized frequency  
 p0025 A77-16238  
 Field-aligned currents observed by the OGO 5 and Triad satellites  
 p0026 A77-17124  
 Multiple satellite observations of pulsation resonance structure in the magnetosphere  
 p0027 A77-23205  
 Empirical models of high-latitude electric fields  
 p0029 A77-27317  
 OGO 5 observations of Pc 5 waves - Particle flux modulations  
 p0030 A77-42295  
 OGO 3 and 5 observations of inner magnetosphere and ring currents  
 p0031 N73-17947  
 Extremely low frequency hiss emissions in the magnetosphere --- using OGO 5 and 6 observations  
 p0032 N74-30528  
 A multi-satellite study of the nature of wavelike structures in the magnetospheric plasma  
 [NASA-CR-143680] p0033 N75-17877  
 Magnetospheric chorus  
 p0033 N75-22959  
 The outer magnetosphere. Part 1: A multisatellite study of the magnetopause position in relation with some important fluid dynamic parameters  
 [LPS-76-2-PT-1] p0035 N76-33793  
 The outer magnetosphere. Part 3: Simultaneous multisatellite observations of the magnetopause.  
 [LPS-76-4-PT-2] p0035 N76-33795  
 Auroral oval and magnetospheric cusps  
 p0037 N78-70070

**MAGNETOSPHERIC ELECTRON DENSITY**  
 Pitch angle distributions of energetic electrons in the equatorial regions of the outer magnetosphere - OGO-5 observations  
 p0011 A75-22759  
 Thinning of the near-earth (10 to about 15 earth radii) plasma sheet preceding the substorm expansion phase  
 p0024 A76-47884

**MAGNETOSPHERIC INSTABILITY**  
 Electron precipitation patterns and substorm morphology.  
 [NSSDC-ID-67-073A-11-PM] p0004 A73-33434  
 The measurement of cold ion densities in the plasma trough --- in magnetosphere  
 [NSSDC-ID-68-014A-18-PM] p0010 A75-16637  
 OGO-5 observations of the magnetopause  
 p0010 A75-19134  
 Substorm and interplanetary magnetic field effects on the geomagnetic tail lobes  
 p0011 A75-19349  
 Magnetospheric substorm associated with SC --- sudden commencements at OGO-5  
 p0011 A75-22613

SUBJECT INDEX

Plasma instability modes related to the earth's bow shock  
 p0011 A75-22774  
 Current-driven plasma instabilities at high latitudes --- Ogo-5 observations  
 p0014 A75-35005  
 Magnetospheric chorus - Amplitude and growth rate  
 p0016 A75-42748  
 The dominant mode of standing Alfvén waves at the synchronous orbit  
 p0017 A75-46285  
 Dependence of the latitude of the cleft on the interplanetary magnetic field and substorm activity  
 p0020 A76-22107  
 Characteristics of instabilities in the magnetosphere deduced from wave observations  
 p0023 A76-41914  
 Multiple-satellite studies of magnetospheric substorms - Radial dynamics of the plasma sheet  
 p0026 A77-16868  
 Triggering of substorms by solar wind discontinuities  
 p0026 A77-21093  
 Shocks, solitons and the plasmopause  
 p0027 A77-21504  
 Instability phenomena in detached plasma regions --- in magnetosphere  
 p0027 A77-21512  
 Detailed analysis of magnetospheric ELF chorus - preliminary results  
 p0027 A77-21523

**MAGNETOSPHERIC ION DENSITY**  
 Magnetospheric thermal plasma and hydrogen cation density profile characteristics in different local time regions explained by time-varying convection model  
 p0003 A73-13879  
 Plasma tail interpretations of pronounced detached plasma regions measured by Ogo 5  
 p0007 A74-43691  
 The measurement of cold ion densities in the plasma trough --- in magnetosphere  
 [NSSDC-ID-68-014A-18-PM] p0010 A75-16637  
 Dynamics of Mid-latitude light ion trough and plasma tails  
 p0012 A75-27383  
 Multiple satellite observations of pulsation resonance structure in the magnetosphere  
 p0027 A77-23205

**MAGNETOSPHERIC PROTON DENSITY**  
 Observations of protons with energies exceeding 100 keV in the earth's magnetosheath  
 p0020 A76-22092

**MAPS**  
 A global magnetic anomaly map  
 p0012 A75-24043  
 Magnetic anomaly map of North America south of 50 degrees north from Pogo data  
 [NASA-TM-X-71229] p0035 N77-13587

**MASS SPECTROSCOPY**  
 Variations in thermospheric composition - A model based on mass spectrometer and satellite drag data  
 p0006 A74-30667  
 A global thermospheric model based on mass spectrometer and incoherent scatter data MSIS. I - N2 density and temperature  
 p0029 A77-37153  
 A global thermospheric model based on mass spectrometer and incoherent scatter data MSIS. II - Composition  
 p0029 A77-37154  
 A multi-satellite study of the nature of wavelike structures in the magnetospheric plasma  
 [NASA-CR-143680] p0033 N75-17877

**MESOPAUSE**  
 Noctilucent clouds in daytime - Circumpolar particulate layers near the summer mesopause.  
 p0003 A72-42515

**MESOSPHERE**  
 Satellite observation of the mesospheric scattering layer and implied climatic consequences  
 p0022 A76-39128  
 Observations from the Orbiting Geophysical Observatory 6 of mesospheric airglow and scattering layers  
 p0033 N75-19882  
 The role of ice particulates in the electrification of the air in the mesosphere --- using OGO 6 data  
 p0033 N75-24202

**METAL IONS**  
 Magnetospheric electric fields convective motions measurement by Ba ion cloud tracking and symmetric double probe floating potential technique  
 p0003 A73-15333



**SUBJECT INDEX**

**METEOROID SHOWERS**

Explorer 35 and OGO 3 data on picogram size dust particle distribution in cislunar and selenocentric space, showing fluctuations during meteor shower periods p0002 A72-31937

**MICROMETEORIODS**

The micrometeoroid experiment on the OGO 4 satellite [NASA-CR-141948] p0037 N75-70676

**MICROWAVE EMISSION**

Impulsive /flash/ phase of solar flares - Hard X-ray, microwave, EUV and optical observations p0015 A75-37352

**MIDLATITUDE ATMOSPHERE**

Is the red arc a good indicator of ionosphere-magnetosphere conditions [NSSDC-ID-69-051A-02-PM] p0008 A75-11226  
Dynamics of Mid-latitude light ion trough and plasma tails p0012 A75-27383

The intensity variation of the atomic oxygen red line during morning and evening twilight on 9-10 April 1969 p0021 A76-28990

**MODELS**

Thermospheric temperature, density, and composition: New models [NASA-CR-153049] p0035 N77-23648

**MODULATION**

High latitude electric fields and the modulations related to interplanetary magnetic field parameters p0005 A74-14272

Modulation of low energy electrons and protons near solar maximum p0021 A76-26907

**MOLECULAR IONS**

High latitude minor ion enhancements - A clue for studies of magnetosphere-atmosphere coupling p0008 A75-12439

**MOLECULAR SPECTRA**

OGO-4 observations of the ultraviolet auroral spectrum p0025 A77-16243

**N**

**NEUTRAL SHEETS**

Instabilities connected with neutral sheets in the solar wind p0013 A75-28015

Substorm effects on the neutral sheet inside 10 earth radii p0016 A75-46232

**NEUTRON FLUX DENSITY**

A search for solar neutrons during solar flares p0010 A75-18717

**NIGHT SKY**

New results on the correlation between low-energy electrons and auroral hiss p0020 A76-22086

Altitude profiles of the photoelectron induced O I D (6300 A) predawn enhancement by observation and theory p0026 A77-20886

Magnetic storm effects on the tropical ultraviolet airglow p0029 A77-27318

**NIGHTGLOW**

Vertical red line 6300 A distribution and tropical nightglow morphology in quiet magnetic conditions p0004 A74-11523

Polar enhancements of nightglow emissions near 6230A p0019 A76-19613

An explanation of the longitudinal variation of the O I D (630 nm) tropical nightglow intensity p0019 A76-21456

Behavior of the sodium and hydroxyl nighttime emissions during a stratospheric warming p0020 A76-22490

The effect of extraterrestrial dust, stratospheric warmings, and lower thermospheric pressure systems on OGO-4 measured nightglows in the earth's atmosphere (80 to 100 km) p0031 N74-26848

Determination of tropical F-region winds from atomic oxygen airglow emissions p0034 N76-10603

Latitudinal dependence of atomic oxygen density between 90 and 120 kilometers as derived from OGO-6 observations of the 5577 A nightglow p0034 N76-27744

**NITRIC OXIDE**

An upper limit to the product of NO and O densities from 105 to 120 km [NSSDC-ID-69-051A-26-PM] p0008 A75-11227  
Satellite measurements of nitric oxide in the polar region p0017 A75-46289

OGO-4 observations of the ultraviolet auroral spectrum p0025 A77-16243

High-latitude nitric oxide in the lower thermosphere p0028 A77-23222

**NITROGEN**

Structure of electrodynamic and particle heating in the disturbed polar thermosphere p0027 A77-23201

A global thermospheric model based on mass spectrometer and incoherent scatter data MSIS. I - N2 density and temperature p0029 A77-37153

**NOCTILUCENT CLOUDS**

Noctilucent clouds in daytime - Circumpolar particulate layers near the summer mesopause. p0003 A72-42515

**NORTH AMERICA**

Magnetic anomaly map of North America south of 50 degrees north from Pogo data [NASA-TM-X-71229] p0035 N77-13587

**NUCLEAR EXPLOSIONS**

A study of electron spectra in the inner belt p0024 A76-44653

**NUCLEONS**

Origin and composition of heavy nuclei between 10 and 60 MeV per nucleon during interplanetary quiet times in 1968-1972 p0017 A75-46822

**O**

**OBLIQUE SHOCK WAVES**

Earth collisionless plasma bow shock oblique structure assessment by pulsation index Ip devised from empirical results p0003 A72-44511

**OSO-7**

Analysis of OGO-5 and OSO-7 X-ray data --- physical nature of solar flares [NASA-CR-142131] p0032 N75-17277

**OXYGEN AFTERGLOW**

The temperature gradient between 100 and 120 km p0018 A76-16501

**OXYGEN ATOMS**

Atomic oxygen 1304-A day airglow observed from OGO-D spacecraft, attributing subsolar emission rates to photoelectron impact excitation p0002 A71-33964

An upper limit to the product of NO and O densities from 105 to 120 km [NSSDC-ID-69-051A-26-PM] p0008 A75-11227

Global atomic oxygen density derived from OGO-6 1304 A airglow measurements p0021 A76-28989

AEROS A atomic oxygen profiles compared with the OGO 6 model p0028 A77-23987

Determination of tropical F-region winds from atomic oxygen airglow emissions p0034 N76-10603

Latitudinal dependence of atomic oxygen density between 90 and 120 kilometers as derived from OGO-6 observations of the 5577 A nightglow p0034 N76-27744

**OXYGEN SPECTRA**

Remote sensing of the ionospheric F layer by use of O I 6300-A and O I 1356-A observations p0014 A75-35040

The global characteristics of atmospheric emissions in the lower thermosphere and their aeronomic implications p0016 A75-42726

OGO-6 observations of 5577 A --- airglow measurements p0019 A76-18436

An explanation of the longitudinal variation of the O I D (630 nm) tropical nightglow intensity p0019 A76-21456

The intensity variation of the atomic oxygen red line during morning and evening twilight on 9-10 April 1969 p0021 A76-28990

**PLASMA DENSITY**

Tropical F region winds from O I 1356-A and forbidden O I 6300-A emissions. II - Analysis of OGO 4 data p0023 A76-42683

**OZONE**

Satellite observations of the global distribution of stratospheric ozone p0036 N78-12583

**P**

**PARTICLE ACCELERATION**

Acceleration of electrons in absence of detectable optical flares deduced from type III radio bursts, H alpha activity and soft X-ray emission [NSSDC-ID-68-014A-04-PS] p0009 A75-16217

**PARTICLE DIFFUSION**

Long-term cosmic ray modulation in the period 1966-1972 and interplanetary magnetic fields p0023 A76-39130

**PARTICLE INTENSITY**

Modulation of low energy electrons and protons near solar maximum p0021 A76-26907

**PARTICLE INTERACTIONS**

Waves and wave-particle interactions in the magnetosphere - A review p0018 A76-12272

**PARTICLE SIZE DISTRIBUTION**

Explorer 35 and OGO 3 data on picogram size dust particle distribution in cislunar and selenocentric space, showing fluctuations during meteor shower periods p0002 A72-31937

**PERIODIC VARIATIONS**

Variations in thermospheric composition - A model based on mass spectrometer and satellite drag data p0006 A74-30667

The solar cycle variation of the solar wind helium abundance [NSSDC-ID-68-014A-17-OS] p0010 A75-16631

OGO 5 observations of Pc 5 waves - Particle flux modulations p0030 A77-42295

**PHASE DEVIATION**

Theory of the phase anomaly in the thermosphere --- radar temperature-satellite drag density phase difference p0005 A74-12645

**PHOTOELECTRONS**

Atomic oxygen 1304-A day airglow observed from OGO-D spacecraft, attributing subsolar emission rates to photoelectron impact excitation p0002 A71-33964

Altitude profiles of the photoelectron induced O I D (6300 A) predawn enhancement by observation and theory p0026 A77-20886

**PITCH (INCLINATION)**

Pitch angle distributions of energetic electrons in the equatorial regions of the outer magnetosphere - OGO-5 observations p0011 A75-22759

Critical electron pitch angle anisotropy necessary for chorus generation --- Doppler-shifted cyclotron resonance p0024 A76-44665

**PLANETARY ATMOSPHERES**

Density and temperature distributions in non-uniform rotating planetary exospheres with applications to earth p0005 A74-14224

**PLANETARY RADIATION**

Quiet-time increases of low-energy electrons - The Jovian origin p0025 A77-11692

**PLASMA COMPOSITION**

The solar cycle variation of the solar wind helium abundance [NSSDC-ID-68-014A-17-OS] p0010 A75-16631

**PLASMA DENSITY**

A relation between ELF hiss amplitude and plasma density in the outer plasmasphere p0006 A74-30677

Plasma tail interpretations of pronounced detached plasma regions measured by Ogo 5 p0007 A74-43691

Correlated satellite measurements of proton precipitation and plasma density --- in magnetosphere p0009 A75-16437

A review of in situ observations of the plasmapause p0015 A75-36977

**PLASMA DIAGNOSTICS**

Probing the plasmopause by geomagnetic pulsations p0015 A75-36982  
 High-latitude troughs and the polar cap boundary p0020 A76-22105  
 ELF hiss associated with plasma density enhancements in the outer magnetosphere p0022 A76-33058  
 The temperature gradient drift instability at the equatorward edge of the ionospheric plasma trough p0024 A76-42697

**PLASMA DIAGNOSTICS**

Detached plasma regions in the magnetosphere p0006 A74-30660  
 Correlated satellite measurements of proton precipitation and plasma density --- in magnetosphere p0009 A75-16437  
 Structure of the quasi-perpendicular laminar bow shock --- earth-solar wind interaction p0012 A75-23707  
 A review of in situ observations of the plasmopause p0015 A75-36977  
 Probing the plasmopause by geomagnetic pulsations p0015 A75-36982

**PLASMA DYNAMICS**

The measurement of cold ion densities in the plasma trough --- in magnetosphere [NSSDC-ID-68-014A-18-PM] p0010 A75-16637  
 The solar wind and magnetospheric dynamics p0010 A75-19127

**PLASMA FLUX MEASUREMENTS**

Multiple-satellite studies of magnetospheric substorms - Radial dynamics of the plasma sheet p0026 A77-16868

**PLASMA FREQUENCIES**

Instability phenomena in detached plasma regions --- in magnetosphere p0027 A77-21512

**PLASMA INTERACTIONS**

Instabilities connected with neutral sheets in the solar wind p0013 A75-28015

**PLASMA LAYERS**

Substorm effects on the neutral sheet inside 10 earth radii p0016 A75-46232  
 Thinning of the near-earth (10 to about 15 earth radii) plasma sheet preceding the substorm expansion phase p0024 A76-47884

**PLASMA OSCILLATIONS**

The enhancement of solar wind fluctuations at the proton thermal gyroradius p0012 A75-27387

**PLASMA PHYSICS**

Variational electric fields at low latitudes and their relation to spread-F and plasma irregularities p0029 A77-34326

**PLASMA TEMPERATURE**

A review of in situ observations of the plasmopause p0015 A75-36977

**PLASMA TURBULENCE**

Characteristics of instabilities in the magnetosphere deduced from wave observations p0023 A76-41914

**PLASMA WAVES**

On the local time dependence of the bow shock wave structure p0005 A74-24759  
 Plasma instability modes related to the earth's bow shock p0011 A75-22774

Plasma flow hypothesis in the magnetosphere relating to frequency shift of electrostatic plasma waves p0015 A75-38275  
 Pioneer 9 and OGO 5 observations of an interplanetary multiple shock ensemble on February 2, 1969 p0016 A75-42744

Characteristics of instabilities in the magnetosphere deduced from wave observations p0023 A76-41914

A multi-satellite study of the nature of wavelike structures in the magnetospheric plasma [NASA-CR-143680] p0033 N75-17877

**PLASMA-ELECTROMAGNETIC INTERACTION**

A relation between ELF hiss amplitude and plasma density in the outer plasmasphere p0006 A74-30677  
 Magnetospheric chorus - Occurrence patterns and normalized frequency p0025 A77-16238

**PLASMA-PARTICLE INTERACTIONS**

Waves and wave-particle interactions in the magnetosphere - A review p0018 A76-12272

**PLASMAPAUSE**

Recent satellite measurements of the morphology and dynamics of the plasmasphere. p0003 A73-13709

Plasma tail interpretations of pronounced detached plasma regions measured by Ogo 5 p0007 A74-43691

In-situ observations of irregular ionospheric structure associated with the plasmopause p0008 A75-11853

Correlated satellite measurements of proton precipitation and plasma density --- in magnetosphere p0009 A75-16437

Dynamics of Mid-latitude light ion trough and plasma tails p0012 A75-27383

Excitation of magnetosonic waves with discrete spectrum in the equatorial vicinity of the plasmopause p0012 A75-27679

Ion composition irregularities and ionosphere-plasmasphere coupling - Observations of a high latitude ion trough p0013 A75-28356

A review of in situ observations of the plasmopause p0015 A75-36977

Probing the plasmopause by geomagnetic pulsations p0015 A75-36982

VLF and ELF emissions --- in magnetosphere p0015 A75-36988

Thinning of the near-earth (10 to about 15 earth radii) plasma sheet preceding the substorm expansion phase p0024 A76-47884

Sirocks, solitons and the plasmopause p0027 A77-21504

Instability phenomena in detached plasma regions --- in magnetosphere p0027 A77-21512

Micropulsations and the plasmopause p0027 A77-21513

Light ion and electron troughs observed in the mid-latitude topside ionosphere on two passes of OGO 6 compared to coincident equatorial electron density deduced from whistlers p0030 A77-42297

**PLASMAS (PHYSICS)**

Critique on existence of one hundred million degree K solar flare plasma p0001 A71-20944

**POGO**

Magnetic anomaly map of North America south of 50 degrees north from Pogo data [NASA-TM-X-71229] p0035 N77-13587

Magnetic field variations above 60 degrees invariant latitude at the POGO satellites p0037 N76-71877

**POLAR CAPS**

Ionospheric and magnetospheric electric field strength measurements in auroral and polar cap regions by Ba ion cloud and double floating probe techniques p0003 A72-39543

High latitude electric fields and the modulations related to interplanetary magnetic field parameters p0005 A74-14272

Identifications of the polar cap boundary and the auroral belt in the high-altitude magnetosphere - A model for field-aligned currents p0014 A75-35007

Access of solar electrons to the polar regions p0015 A75-37031

High-latitude troughs and the polar cap boundary p0020 A76-22105

Satellite observation of the mesospheric scattering layer and implied climatic consequences p0022 A76-39128

Field-aligned currents observed by the OGO 5 and Triad satellites p0026 A77-17124

**POLAR REGIONS**

Proton measurements in ring current by OGO-3 satellite compared with geomagnetic field data at low and high latitudes p0002 A71-33663

High-latitude proton precipitation and light ion density profiles during the magnetic storm initial phase. [NSSDC-ID-67-073A-11-PM] p0004 A73-45114

High latitude minor ion enhancements - A clue for studies of magnetosphere-atmosphere coupling p0008 A75-12439

**SUBJECT INDEX**

Ion composition irregularities and ionosphere-plasmasphere coupling - Observations of a high latitude ion trough p0013 A75-28356

Relation of variations in total magnetic field at high latitude with the parameters of the interplanetary magnetic field and with DP 2 fluctuations p0013 A75-28743

Current-driven plasma instabilities at high latitudes --- Ogo-5 observations p0014 A75-35005

Satellite measurements of nitric oxide in the polar region p0017 A75-46289

Structure of electrodynamic and particle heating in the undisturbed polar thermosphere p0018 A76-14318

Polar enhancements of nightglow emissions near 6230A p0019 A76-19613

Structure of electrodynamic and particle heating in the disturbed polar thermosphere p0027 A77-23201

Empirical models of high-latitude electric fields p0029 A77-27317

High latitude ionospheric winds related to solar-interplanetary conditions p0032 N74-29091

Features of polar cusp electron precipitation associated with a large magnetic storm [NASA-TM-X-70792] p0032 N75-12873

Magnetically ordered heating in the polar regions of the thermosphere p0034 N75-32651

**POLAR SUBSTORMS**

Intensity variation of ELF hiss and chorus during isolated substorms [NSSDC ID 69-051A-22-PM] p0007 A74-44202

Substorm and interplanetary magnetic field effects on the geomagnetic tail lobes p0011 A75-19349

Thinning of the near-earth (10 to about 15 earth radii) plasma sheet preceding the substorm expansion phase p0024 A76-47884

Multiple-satellite studies of magnetospheric substorms - Radial dynamics of the plasma sheet p0026 A77-16868

Triggering of substorms by solar wind discontinuities p0026 A77-21093

**POLARITY**

Dependence of the magnetopause position on the southward interplanetary magnetic field p0008 A75-12370

**POSITION (LOCATION)**

The magnetopause: Part 2: Magnetopause position and the reconnection problem [LPS-75-24-PT-2] p0035 N76-33788

The outer magnetosphere. Part 1: A multisatellite study of the magnetopause position in relation with some important fluid dynamic parameters [LPS-76-2-PT-1] p0035 N76-33793

**POSITRONS**

Relativistic electron and positron intensity distributions in interplanetary regions p0031 N71-25288

**POWER SPECTRA**

Steady ELF plasmaspheric hiss, studying whistler mode turbulence, band limitation, power spectra and peak intensities p0004 A73-26984

The enhancement of solar wind fluctuations at the proton thermal gyroradius p0012 A75-27387

Excitation of magnetosonic waves with discrete spectrum in the equatorial vicinity of the plasmopause p0012 A75-27679

The enhancement of solar wind fluctuations with scale size near the proton gyroradius p0013 A75-28038

On the causes of spectral enhancements in solar wind power spectra p0020 A76-22081

**PRESSURE**

Thermospheric temperature, density, and composition: New models [NASA-CR-153049] p0035 N77-23648

**PRIMARY COSMIC RAYS**

Origin and composition of heavy nuclei between 10 and 60 MeV per nucleon during interplanetary quiet times in 1968-1972 p0017 A75-46822

## SUBJECT INDEX

- Hysteresis of primary cosmic rays associated with Forbush decreases p0022 A76-35348
- PROBABILITY DISTRIBUTION FUNCTIONS**  
Dependence of field-aligned electron precipitation occurrence on season and altitude p0007 A74-43679
- PROPAGATION MODES**  
The dominant mode of standing Alfvén waves at the synchronous orbit p0017 A75-46285  
Magnetosheath lion roars --- strongest whistler mode signals p0022 A76-33057
- PROTON BELTS**  
Micropulsations and the plasmopause p0027 A77-21513
- PROTON ENERGY**  
The enhancement of solar wind fluctuations at the proton thermal gyroradius p0012 A75-27387  
Observations of protons with energies exceeding 100 keV in the earth's magnetosheath p0020 A76-22092  
Modulation of low energy electrons and protons near solar maximum p0021 A76-26907  
Short-term variations of the cosmic-ray proton and electron intensities in 1968 and 1969 p0037 N77-84177
- PROTON FLUX DENSITY**  
Proton measurements in ring current by OGO-3 satellite compared with geomagnetic field data at low and high latitudes p0002 A71-33663  
OGO 5 observations of Pc 5 waves - Particle flux modulations p0030 A77-42295
- PROTON PRECIPITATION**  
High-latitude proton precipitation and light ion density profiles during the magnetic storm initial phase. [NSSDC-ID-67-073A-11-PM] p0004 A73-45114  
Correlated satellite measurements of proton precipitation and plasma density --- in magnetosphere p0009 A75-16437
- PROTONS**  
OGO-A scintillation counter to detect 3 to 90 MeV protons in solar cosmic rays [NASA-CR-96278] p0031 N68-33302
- ## R
- RADAR MEASUREMENT**  
Theory of the phase anomaly in the thermosphere --- radar temperature-satellite drag density phase difference p0005 A74-12645  
Diurnal variation of the neutral thermospheric winds determined from incoherent scatter radar data p0006 A74-36735
- RADIAL DISTRIBUTION**  
A search for solar wind velocity changes between 0.7 and 1 au p0013 A75-28750
- RADIANT FLUX DENSITY**  
Electron temperature and emission measures during solar X-ray flares, studying effects of gradual and rapid radiation flux increases p0002 A72-29722  
Intensity variation of ELF hiss and chorus during isolated substorms [NSSDC-ID-69-051A-22-PM] p0007 A74-44202
- RADIATION BELTS**  
A study of electron spectra in the inner belt p0024 A76-44653  
Magnetospheric chorus p0033 N75-22959
- RADIATION DISTRIBUTION**  
Solar radiation asymmetries and heliospheric gas heating influencing extraterrestrial UV data p0009 A75-13173  
Pitch angle distributions of energetic electrons in the equatorial regions of the outer magnetosphere - OGO-5 observations p0011 A75-22759
- RADIATION MEASURING INSTRUMENTS**  
Ultraviolet solar energy survey on OGO-6 [NASA-CR-155088] p0037 N77-86268
- RADIATIVE RECOMBINATION**  
Tropical UV arcs: Comparison of brightness with f sub 0 F sub 2 p0037 N77-86006

- RADIO ASTRONOMY**  
Non-thermal processes during the 'build-up' phase of solar flares and in absence of flares p0026 A77-18572  
Data user's notes of the radio astronomy experiment aboard the OGO-V spacecraft [NASA-CR-143696] p0034 N75-24593
- RADIO ATTENUATION**  
The upper- and lower-frequency cutoffs of magnetospherically reflected whistlers p0019 A76-19854
- RADIO EMISSION**  
Non-relativistic solar electrons [NSSDC-ID-68-014A-04-08] p0007 A74-37631  
Relativistic electron events in interplanetary space p0007 A74-37632  
Magnetospheric chorus - Amplitude and growth rate p0016 A75-42748  
The local time variation of ELF emissions during periods of substorm activity p0029 A77-31391
- RADIO SCATTERING**  
Correlated measurements of scintillations and in-situ F-region irregularities from OGO-6 p0025 A77-15786  
The morphology of equatorial irregularities in the Afro-Asian sector from OGO 6 observations p0028 A77-24016
- RADIO SOURCES (ASTRONOMY)**  
On the causes of spectral enhancements in solar wind power spectra p0020 A76-22081
- RAREFIED GASES**  
Exospheric temperature inferred from the Aeros-A neutral composition measurement p0017 A75-46269
- RAY TRACING**  
The upper- and lower-frequency cutoffs of magnetospherically reflected whistlers p0019 A76-19854
- RED ARCS**  
Vertical red line 6300 Å distribution and tropical nightglow morphology in quiet magnetic conditions p0004 A74-11523  
Is the red arc a good indicator of ionosphere-magnetosphere conditions [NSSDC-ID-69-051A-02-PM] p0008 A75-11226
- RELATIVISTIC EFFECTS**  
Relativistic electron events in interplanetary space p0007 A74-37632
- REMOTE SENSORS**  
Remote sensing of the ionospheric F layer by use of O I 6300-Å and O I 1356-Å observations p0014 A75-35040
- RESISTANCE HEATING**  
Magnetic storm dynamics of the thermosphere p0008 A75-12453
- RING CURRENTS**  
Proton measurements in ring current by OGO-3 satellite compared with geomagnetic field data at low and high latitudes p0002 A71-33663  
Micropulsations and the plasmopause p0027 A77-21513  
Empirical models of high-latitude electric fields p0029 A77-27317  
OGO 3 and 5 observations of inner magnetosphere and ring currents p0031 N73-17947
- ROTATING PLASMAS**  
Magnetopause rotational forms [NSSDC-ID-68-014A-15-PM] p0008 A75-11221  
Differential rotation of the magnetospheric plasma as cause of the Svalgaard-Mansurov effect --- relationship between geomagnetic variables and IMF polarity p0014 A75-35036
- ## S
- SAN MARCO 3 SATELLITE**  
Comparison of the San Marco 3 Nace neutral composition data with the extrapolated Ogo 6 empirical model --- Neutral Atmospheric Composition Experiment p0021 A76-26524
- SATELLITE DRAG**  
Theory of the phase anomaly in the thermosphere --- radar temperature-satellite drag density phase difference p0005 A74-12645

## SATELLITE OBSERVATION

- Recent improvements in our knowledge of neutral atmosphere structure from satellite drag measurements [BMW-WRK-226] p0005 A74-23676  
Variations in thermospheric composition - A model based on mass spectrometer and satellite drag data p0006 A74-30667  
Exospheric temperature inferred from the Aeros-A neutral composition measurement p0017 A75-46269
- SATELLITE OBSERVATION**  
Ion density and electron acceleration region location from satellite-borne solar flare X-ray measurements p0003 A72-32790  
Recent satellite measurements of the morphology and dynamics of the plasmasphere. p0003 A73-13709  
Interpretation of Ogo 5 Lyman alpha measurements in the upper geocorona. [NSSDC-ID-68-014A-22-PM] p0004 A73-19233  
Correlation of 'satellite estimates' of the equatorial electrojet intensity with ground observations at Addis Ababa. p0004 A73-31771  
High-latitude proton precipitation and light ion density profiles during the magnetic storm initial phase. [NSSDC-ID-67-073A-11-PM] p0004 A73-45114  
Substorms in space - The correlation between ground and satellite observations of the magnetic field p0005 A74-14285  
Detached plasma regions in the magnetosphere p0006 A74-30660  
A relation between ELF hiss amplitude and plasma density in the outer plasmasphere p0006 A74-30677  
Dependence of field-aligned electron precipitation occurrence on season and altitude p0007 A74-43679  
Plasma tail interpretations of pronounced detached plasma regions measured by Ogo 5 p0007 A74-43691  
Intensity variation of ELF hiss and chorus during isolated substorms [NSSDC-ID-69-051A-22-PM] p0007 A74-44202  
Magnetopause rotational forms [NSSDC-ID-68-014A-15-PM] p0008 A75-11221  
An upper limit to the product of NO and O densities from 105 to 120 km [NSSDC-ID-69-051A-26-PM] p0008 A75-11227  
In-situ observations of irregular ionospheric structure associated with the plasmopause p0008 A75-11853  
Variation with interplanetary sector of the total magnetic field measured at the OGO 2, 4 and 6 satellites p0008 A75-12368  
Recent advances in cometary physics and chemistry p0009 A75-13176  
Correlated satellite measurements of proton precipitation and plasma density --- in magnetosphere p0009 A75-16437  
'Hissers' - Quasi-periodic (T approximately equal to 2 sec) VLF noise forms at auroral latitudes p0009 A75-16440  
A search for solar neutrons during solar flares p0010 A75-18717  
OGO-5 observations of the magnetopause p0010 A75-19134  
Simultaneous particle and field observations of field-aligned currents --- in magnetosphere p0011 A75-19330  
Structure of the quasi-perpendicular laminar bow shock --- earth-solar wind interaction p0012 A75-23707  
A global magnetic anomaly map p0012 A75-24043  
Dynamics of Mid-latitude light ion trough and plasma tails p0012 A75-27383  
The enhancement of solar wind fluctuations at the proton thermal gyroradius p0012 A75-27387  
Excitation of magnetosonic waves with discrete spectrum in the equatorial vicinity of the plasmopause p0012 A75-27679  
Ion composition irregularities and ionosphere-plasmasphere coupling - Observations of a high latitude ion trough p0013 A75-28356  
A search for solar wind velocity changes between 0.7 and 1 au p0013 A75-28750

**SATELLITE-BORNE INSTRUMENTS**

Current-driven plasma instabilities at high latitudes --- Ogo-5 observations p0014 A75-35005

A review of in situ observations of the plasmapause p0015 A75-36977

Probing the plasmapause by geomagnetic pulsations p0015 A75-36982

Satellite measurements of nitric oxide in the polar region p0017 A75-46289

Properties of ELF electromagnetic waves in and above the earth's ionosphere deduced from plasma wave experiments on the OVI-17 and Ogo 6 satellites p0018 A76-16507

A comparison of electric and magnetic field data from the OGO 6 spacecraft p0018 A76-16514

OGO-6 observations of 5577 A --- airglow measurements p0019 A76-18436

Polar enhancements of nightglow emissions near 6230A p0019 A76-19613

Satellite measurements of high-altitude twilight Mg(plus) emission p0019 A76-19839

Behavior of the sodium and hydroxyl nighttime emissions during a stratospheric warming p0020 A76-22490

On the quiet-time increases of low energy cosmic ray electrons p0021 A76-26886

Satellite measurements of ion composition and temperatures in the topside ionosphere during medium solar activity p0021 A76-28486

Satellite observation of the mesospheric scattering layer and implied climatic consequences p0022 A76-39128

Ogo 5 observations of Pc 5 waves - Ground-magnetosphere correlations p0024 A77-11219

Model of equatorial scintillations from in-situ measurements --- based on OGO-6 observed F region irregularity p0025 A77-12057

OGO-4 observations of the ultraviolet auroral spectrum p0025 A77-16243

Characteristics of cosmic X-ray bursts observed with the OGO-5 satellite p0026 A77-16850

Multiple-satellite studies of magnetospheric substorms - Radial dynamics of the plasma sheet p0026 A77-16868

Structure of electrodynamic and particle heating in the disturbed polar thermosphere p0027 A77-23201

Multiple satellite observations of pulsation resonance structure in the magnetosphere p0027 A77-23205

Comparisons of ionogram and OGO 6 satellite observations of small-scale F region inhomogeneities p0028 A77-23211

Structure of a quasi-parallel, quasi-laminar bow shock p0028 A77-23220

AEROS A atomic oxygen profiles compared with the OGO 6 model p0028 A77-23987

Experimental global model of the exospheric temperature based on measurements from the Fabry-Perot interferometer on board the OGO-6 satellite - Discussion of the data and properties of the model p0029 A77-34901

OGO 5 observations of Pc 5 waves - Particle flux modulations p0030 A77-42295

Magnetic anomaly map of North America south of 50 degrees north from Pogo data [NASA-TM-X-71229] p0035 N77-13587

**SATELLITE-BORNE INSTRUMENTS**

Hysteresis of primary cosmic rays associated with Forbush decreases p0022 A76-35348

Field-aligned currents observed by the OGO 5 and Triad satellites p0026 A77-17124

Detailed analysis of magnetospheric ELF chorus - preliminary results p0027 A77-21523

High-latitude nitric oxide in the lower thermosphere p0028 A77-23222

A multi-satellite study of the nature of wavelike structures in the magnetospheric plasma [NASA-CR-143680] p0033 N75-17877

**SCATTERING CROSS SECTIONS**

Observations from the Orbiting Geophysical Observatory 6 of mesospheric airglow and scattering layers p0033 N75-19882

**SCINTILLATION**

Model of equatorial scintillations from in-situ measurements --- based on OGO-6 observed F region irregularity p0025 A77-12057

Correlated measurements of scintillations and in-situ F-region irregularities from OGO-6 p0025 A77-15786

The morphology of equatorial irregularities in the Afro-Asian sector from OGO 6 observations p0028 A77-24016

**SCINTILLATION COUNTERS**

OGO-A scintillation counter to detect 3 to 90 MeV protons in solar cosmic rays [NASA-CR-96278] p0031 N68-33302

**SHOCK WAVE INTERACTION**

The earth's bow shock fine structure p0011 A75-19138

**SHOCK WAVE PROFILES**

Earth collisionless plasma bow shock oblique structure assessment by pulsation index Ip devised from empirical results p0003 A72-44511

On the local time dependence of the bow shock wave structure p0005 A74-24759

**SHOCK WAVE PROPAGATION**

Structure of the quasi-perpendicular laminar bow shock --- earth-solar wind interaction p0012 A75-23707

Collisionless shock waves in space - A very high beta structure --- solar wind measurements p0014 A75-35003

Pioneer 9 and OGO 5 observations of an interplanetary multiple shock ensemble on February 2, 1969 p0016 A75-42744

Shocks, solitons and the plasmapause p0027 A77-21504

**SHOCK WAVES**

Plasma instability modes related to the earth's bow shock p0011 A75-22774

Structure of a quasi-parallel, quasi-laminar bow shock p0028 A77-23220

The magnetopause. Part I: Multisatellite simultaneous observations of bow shock and magnetopause positions [LPS-75-23-PT-1] p0034 N76-33787

**SIGNAL TRANSMISSION**

The theory of VLF Doppler signatures and their relation to magnetospheric density structure p0023 A76-39145

**SODIUM**

Behavior of the sodium and hydroxyl nighttime emissions during a stratospheric warming p0020 A76-22490

**SOLAR ACTIVITY**

Solar activity study based on solar X-ray spectra observation, considering flare mechanism p0001 A70-16719

Global exospheric temperatures and densities under active solar conditions --- measured by OGO-6 [NASA-CR-145394] p0034 N76-10610

Solar cosmic ray observations during 1969 [MDAC-WD-1448] p0037 N78-70785

**SOLAR ACTIVITY EFFECTS**

Ionospheric E-layer formation, investigating role of solar X-ray control by electron production rate and density calculations p0001 A70-34943

Observations of protons with energies exceeding 100 keV in the earth's magnetosheath p0020 A76-22092

Modulation of low energy electrons and protons near solar maximum p0021 A76-26907

Satellite measurements of ion composition and temperatures in the topside ionosphere during medium solar activity p0021 A76-28486

Global atomic hydrogen density derived from OGO-6 Lyman-alpha measurements p0021 A76-28988

Triggering of substorms by solar wind discontinuities p0026 A77-21093

Global exospheric temperatures and densities under active solar conditions p0028 A77-25183

**SOLAR CELLS**

The Engineering design of the Orbiting Geophysical Observatories. [NSSDC-ID-64-054A-00-PC] p0001 A63-21528

**SOLAR CORONA**

Solar flare trigger mechanism, proposing inner corona thermal runaway of radiative power function p0001 A71-12761

**SOLAR CORPUSCULAR RADIATION**

Non-relativistic solar electrons [NSSDC-ID-68-014A-04-OS] p0007 A74-37631

A search for solar neutrons during solar flares p0010 A75-18717

Solar particle events with anomalously large relative abundance of He-3 p0013 A75-34018

**SOLAR COSMIC RAYS**

Solar energetic particle event with He-3/He-4 greater than 1 p0009 A75-15342

OGO-A scintillation counter to detect 3 to 90 MeV protons in solar cosmic rays [NASA-CR-96278] p0031 N68-33302

Solar cosmic ray observations during 1969 [MDAC-WD-1448] p0037 N78-70785

**SOLAR CYCLES**

North-south asymmetries in the thermosphere during the last maximum of the solar cycle p0009 A75-16449

The solar cycle variation of the solar wind helium abundance [NSSDC-ID-68-014A-17-OS] p0010 A75-16631

**SOLAR ELECTRONS**

Non-relativistic solar electrons [NSSDC-ID-68-014A-04-OS] p0007 A74-37631

Access of solar electrons to the polar regions p0015 A75-37031

Angular distributions of solar protons and electrons p0016 A75-41805

Non-thermal processes during the 'build-up' phase of solar flares and in absence of flares p0026 A77-18572

Analysis of proton and electron spectrometer data from OGO-5 spacecraft [NASA-CR-142078] p0032 N75-17020

OGO-5 experiment E-09 cosmic ray electrons [NASA-CR-144668] p0034 N75-32995

**SOLAR FLARES**

Solar flare trigger mechanism, proposing inner corona thermal runaway of radiative power function p0001 A71-12761

Critique on existence of one hundred million degree K solar flare plasma p0001 A71-20944

Magnetic fields, bremsstrahlung and synchrotron emission in impulsive flare of 24 October 1969 p0002 A71-43849

Thermal plasma origin of solar X-ray emission and far UV flash observation during 28 August 1966 proton flare p0002 A72-20013

Electron temperature and emission measures during solar X-ray flares, studying effects of gradual and rapid radiation flux increases p0002 A72-29722

Ion density and electron acceleration region location from satellite-borne solar flare X-ray measurements p0003 A72-32790

Relativistic electron events in interplanetary space p0007 A74-37632

Solar energetic particle event with He-3/He-4 greater than 1 p0009 A75-15342

Acceleration of electrons in absence of detectable optical flares deduced from type III radio bursts, H alpha activity and soft X-ray emission [NSSDC-ID-68-014A-04-PS] p0009 A75-16217

A search for solar neutrons during solar flares p0010 A75-18717

Solar particle events with anomalously large relative abundance of He-3 p0013 A75-34018

**SUBJECT INDEX**

**SUBJECT INDEX**

Impulsive solar flare X-rays greater than 10 keV and some characteristics of cosmic gamma-ray bursts p0014 A75-35537

Impulsive /flash/ phase of solar flares - Hard X-ray, microwave, EUV and optical observations p0015 A75-37352

Slow X-ray bursts and flares with filament disruption p0016 A75-43792

Thermal and nonthermal interpretations of flare X-ray bursts p0017 A76-10136

Non-thermal processes during the 'build-up' phase of solar flares and in absence of flares p0026 A77-18572

Analysis of OGO-5 and OSO-7 X-ray data --- physical nature of solar flares [NASA-CR-142131] p0032 N75-17277

Slow X-ray bursts and chromospheric flares with filament disruption [NASA-CR-142151] p0032 N75-17281

Solar X-ray studies [NASA-CR-142164] p0033 N75-18144

**SOLAR FLUX**  
Relation of solar wind fluctuations to differential flow between protons and alphas p0013 A75-28004

**SOLAR HEATING**  
Solar radiation asymmetries and heliospheric gas heating influencing extraterrestrial UV data p0009 A75-13173

**SOLAR LONGITUDE**  
Solar radiation asymmetries and heliospheric gas heating influencing extraterrestrial UV data p0009 A75-13173

**SOLAR MAGNETIC FIELD**  
Magnetic fields, bremsstrahlung and synchrotron emission in impulsive flare of 24 October 1969 p0002 A71-43849

**SOLAR PHYSICS**  
Long-term solar modulation of cosmic-ray electrons with energies above 0.5 GeV p0037 N77-84176

**SOLAR PROMINENCES**  
Slow X-ray bursts and flares with filament disruption p0016 A75-43792

**SOLAR PROTONS**  
Thermal plasma origin of solar X-ray emission and far UV flash observation during 28 August 1966 proton flare p0002 A72-20013

Relation of solar wind fluctuations to differential flow between protons and alphas p0013 A75-28004

The enhancement of solar wind fluctuations with scale size near the proton gyroradius p0013 A75-28038

Angular distributions of solar protons and electrons p0016 A75-41805

Solar cosmic ray observations during 1969 [MDAC-WD-1448] p0037 N78-70785

**SOLAR RADIATION**  
Solar radiation asymmetries and heliospheric gas heating influencing extraterrestrial UV data p0009 A75-13173

**SOLAR RADIO BURSTS**  
Solar low energy X-ray spectra observation during impulsive bursts, discussing thermal and nonthermal emission properties p0002 A71-40425

**SOLAR SPECTRA**  
Solar activity study based on solar X-ray spectra observation, considering flare mechanism p0001 A70-16719

Solar low energy X-ray spectra observation during impulsive bursts, discussing thermal and nonthermal emission properties p0002 A71-40425

Ultraviolet solar energy survey on OGO-6 [NASA-CR-155088] p0037 N77-86268

**SOLAR TEMPERATURE**  
Critique on existence of one hundred million degree K solar flare plasma p0001 A71-20944

**SOLAR WIND**  
Dependence of the magnetopause position on the southward interplanetary magnetic field p0008 A75-12370

The solar wind and magnetospheric dynamics p0010 A75-19127

OGO-5 observations of the magnetopause p0010 A75-19134

The earth's bow shock fine structure p0011 A75-19138

Structure of the quasi-perpendicular laminar bow shock --- earth-solar wind interaction p0012 A75-23707

The enhancement of solar wind fluctuations at the proton thermal gyroradius p0012 A75-27387

Instabilities connected with neutral sheets in the solar wind p0013 A75-28015

Variation of the solar wind flux with heliographic latitude, deduced from its interaction with interplanetary hydrogen p0013 A75-28032

The enhancement of solar wind fluctuations with scale size near the proton gyroradius p0013 A75-28038

Collisionless shock waves in space - A very high beta structure --- solar wind measurements p0014 A75-35003

Pioneer 9 and OGO 5 observations of an interplanetary multiple shock ensemble on February 2, 1969 p0016 A75-42744

Evidence for magnetic field line reconnection in the solar wind p0017 A75-46238

The role of Coulomb collisions in limiting differential flow and temperature differences in the solar wind p0019 A76-19838

Triggering of substorms by solar wind discontinuities p0026 A77-21093

High latitude ionospheric solar-interplanetary conditions p0032 N74-29091

The magnetopause. Part I: Multisatellite simultaneous observations of bow shock and magnetopause positions [LPS-75-23-PT-1] p0034 N76-33787

**SOLAR WIND VELOCITY**  
The solar cycle variation of the solar wind helium abundance [NSSDC-ID-68-014A-17-OS] p0010 A75-16631

Relation of solar wind fluctuations to differential flow between protons and alphas p0013 A75-28004

A search for solar wind velocity changes between 0.7 and 1 au p0013 A75-28750

On the causes of spectral enhancements in solar wind power spectra p0020 A76-22081

**SOLAR X-RAYS**  
Solar activity study based on solar X-ray spectra observation, considering flare mechanism p0001 A70-16719

Ionospheric E-layer formation, investigating role of solar X-ray control by electron production rate and density calculations p0001 A70-34943

Solar low energy X-ray spectra observation during impulsive bursts, discussing thermal and nonthermal emission properties p0002 A71-40425

Thermal plasma origin of solar X-ray emission and far UV flash observation during 28 August 1966 proton flare p0002 A72-20013

Electron temperature and emission measures during solar X-ray flares, studying effects of gradual and rapid radiation flux increases p0002 A72-29722

Ion density and electron acceleration region location from satellite-borne solar flare X-ray measurements p0003 A72-32790

Non-relativistic solar electrons p0007 A74-37631

Relativistic electron events in interplanetary space p0007 A74-37632

A coacceleration of electrons in absence of detectable optical flares deduced from type III radio bursts, H alpha activity and soft X-ray emission [NSSDC-ID-68-014A-04-PS] p0009 A75-16217

Impulsive solar flare X-rays greater than 10 keV and some characteristics of cosmic gamma-ray bursts p0014 A75-35537

Impulsive /flash/ phase of solar flares - Hard X-ray, microwave, EUV and optical observations p0015 A75-37352

Slow X-ray bursts and flares with filament disruption p0016 A75-43792

**STRATOSPHERE**

Thermal and nonthermal interpretations of flare X-ray bursts p0017 A76-10136

Non-thermal processes during the 'build-up' phase of solar flares and in absence of flares p0026 A77-18572

Analysis of OGO-5 and OSO-7 X-ray data --- physical nature of solar flares [NASA-CR-142131] p0032 N75-17277

Slow X-ray bursts and chromospheric flares with filament disruption [NASA-CR-142151] p0032 N75-17281

Solar X-ray studies [NASA-CR-142164] p0033 N75-18144

**SOLITARY WAVES**  
Shocks, solitons and the plasmopause p0027 A77-21504

**SPACE DEBRIS**  
Reduction and analysis of data from cosmic dust experiments on Mariner 4, OGO 3, and Lunar Explorer 35 [NASA-CR-138866] p0032 N74-29255

**SPACEBORNE ASTRONOMY**  
Variation of the solar wind flux with heliographic latitude, deduced from its interaction with interplanetary hydrogen p0013 A75-28032

The interpretations of ultraviolet observations of comets p0022 A76-31317

Non-thermal processes during the 'build-up' phase of solar flares and in absence of flares p0026 A77-18572

Hard X-ray spectra of cosmic gamma-ray bursts p0030 A78-10580

Data user's notes of the radio astronomy experiment aboard the OGO-V spacecraft [NASA-CR-143696] p0034 N75-24593

**SPACECRAFT DESIGN**  
The Engineering design of the Orbiting Geophysical Observatories. [NSSDC-ID-64-054A-00-PC] p0001 A63-21528

**SPECIFIC HEAT**  
The magnetopause. Part I: Multisatellite simultaneous observations of bow shock and magnetopause positions [LPS-75-23-PT-1] p0034 N76-33787

**SPECTRAL ENERGY DISTRIBUTION**  
Polar enhancements of nightglow emissions near 6230A p0019 A76-19613

Energetic electrons in the inner belt in 1968 p0022 A76-35289

**SPECTROMETERS**  
Analysis of proton and electron spectrometer data from OGO-5 spacecraft [NASA-CR-142078] p0032 N75-17020

A study of the heat flux reversal region upstream from the earth's bow shock, using data from the OGO 5 electron spectrometer p0035 N78-11543

**SPECTRUM ANALYSIS**  
Vertical red line 6300 A distribution and tropical nightglow morphology in quiet magnetic conditions p0004 A74-11523

**SPREAD F**  
Comparisons of ionogram and OGO 6 satellite observations of small-scale F region inhomogeneities p0028 A77-23211

Variational electric fields at low latitudes and their relation to spread-F and plasma irregularities p0029 A77-34326

**STANDING WAVES**  
The dominant mode of standing Alfvén waves at the synchronous orbit p0017 A75-46285

**STATISTICAL ANALYSIS**  
Dependence of the magnetopause position on the southward interplanetary magnetic field p0008 A75-12370

**STATISTICAL CORRELATION**  
Ogo 5 observations of Pc 5 waves Ground-magnetosphere correlations p0024 A77-11219

**STRATOSPHERE**  
Behavior of the sodium and hydroxyl nighttime emissions during a stratospheric warming p0020 A76-22490

The effect of extraterrestrial dust, stratospheric warmings, and lower thermospheric pressure systems on OGO-4 measured nightglows in the earth's atmosphere (80 to 100 km) p0031 N74-26848

## STRUCTURES

- Satellite observations of the global distribution of stratospheric ozone  
p0036 N78-12583
- STRUCTURES**  
The outer magnetosphere. Part 3: Simultaneous multisatellite observations of the magnetopause. [LPS-76-4-PT-2]  
p0035 N76-33795
- SUDDEN ENHANCEMENT OF ATMOSPHERICS**  
ELF hiss associated with plasma density enhancements in the outer magnetosphere  
p0022 A76-33058
- SUDDEN STORM COMMENCEMENTS**  
Magnetospheric substorm associated with SC --- sudden commencements at OGO-5  
p0011 A75-22613  
Triggering of substorms by solar wind discontinuities  
p0026 A77-21093
- SUMMER**  
Noctilucent clouds in daytime - Circumpolar particulate layers near the summer mesopause.  
p0003 A72-42515
- SUNRISE**  
VLF propagation in the magnetosphere during sunrise and sunset hours  
p0018 A76-14838
- SUNSET**  
VLF propagation in the magnetosphere during sunrise and sunset hours  
p0018 A76-14838
- SUNSPOT CYCLE**  
Hysteresis of primary cosmic rays associated with Forbush decreases  
p0022 A76-35348
- SYNCHROTRON RADIATION**  
Magnetic fields, bremsstrahlung and synchrotron emission in impulsive flare of 24 October 1969  
p0002 A71-43849
- SYNOPTIC MEASUREMENT**  
The global characteristics of atmospheric emissions in the lower thermosphere and their aeronomic implications  
p0016 A75-42726  
Experimental global model of the exospheric temperature based on measurements from the Fabry-Perot interferometer on board the OGO-6 satellite - Discussion of the data and properties of the model  
p0029 A77-34901

## T

- TELEMETRY**  
The Engineering design of the Orbiting Geophysical Observatories.  
[NSSDC-ID-64-054A-00-PC] p0001 A63-21528
- TELLURIC CURRENTS**  
High latitude electric fields and the modulations related to interplanetary magnetic field parameters  
p0005 A74-14272
- TEMPERATURE**  
Thermospheric temperature, density, and composition: New models  
[NASA-CR-153049] p0035 N77-23648
- TEMPERATURE DISTRIBUTION**  
Density and temperature distributions in non-uniform rotating planetary exospheres with applications to earth  
p0005 A74-14224
- TEMPERATURE EFFECTS**  
Solar flare trigger mechanism, proposing inner corona thermal runaway of radiative power function  
p0001 A71-12761  
Observed variations of the exospheric hydrogen density with the exospheric temperature  
p0012 A75-23721
- TEMPERATURE GRADIENTS**  
The temperature gradient between 100 and 120 km  
p0018 A76-16501  
The temperature gradient drift instability at the equatorward edge of the ionospheric plasma trough  
p0024 A76-42697
- TEMPERATURE MEASUREMENT**  
Neutral wind velocities calculated from temperature measurements during a magnetic storm and the observed ionospheric effects.  
p0004 A73-36150  
Thermospheric 'temperatures' --- discrepancies in inferred and satellite measured values  
p0007 A74-36747

- Experimental model of the exospheric temperature based on optical measurements on board the OGO 6 satellite  
p0023 A76-42390
- TERRESTRIAL RADIATION**  
Low-energy radio emissions from the earth and sun --- solar type 3 bursts  
p0033 N75-20195
- THERMAL EMISSION**  
Solar low energy X-ray spectra observation during impulsive bursts, discussing thermal and nonthermal emission properties  
p0002 A71-40425
- THERMAL ENERGY**  
Thermal and nonthermal interpretations of flare X-ray bursts  
p0017 A76-10136
- THERMAL PLASMAS**  
Thermal plasma origin of solar X-ray emission and far UV flash observation during 28 August 1966 proton flare  
p0002 A72-20013  
Magnetospheric thermal plasma and hydrogen cation density profile characteristics in different local time regions explained by time-varying convection model  
p0003 A73-13879  
A review of in situ observations of the plasmopause  
p0015 A75-36977  
High-latitude troughs and the polar cap boundary  
p0020 A76-22105
- THERMOSPHERE**  
Theory of the phase anomaly in the thermosphere --- radar temperature-satellite drag density phase difference  
p0005 A74-12645  
Recent improvements in our knowledge of neutral atmosphere structure from satellite drag measurements  
[BMBW-WRK-226] p0005 A74-23676  
Variations in thermospheric composition - A model based on mass spectrometer and satellite drag data  
p0006 A74-30667  
Diurnal variation of the neutral thermospheric winds determined from incoherent scatter radar data  
p0006 A74-36735  
Thermospheric 'temperatures' --- discrepancies in inferred and satellite measured values  
p0007 A74-36747  
Magnetic storm dynamics of the thermosphere  
p0008 A75-12453  
North-south asymmetries in the thermosphere during the last maximum of the solar cycle  
p0009 A75-16449  
The global characteristics of atmospheric emissions in the lower thermosphere and their aeronomic implications  
p0016 A75-42726  
Structure of electrodynamic and particle heating in the undisturbed polar thermosphere  
p0018 A76-14318  
Dynamical effects in the distribution of helium in the thermosphere  
p0024 A77-11489  
Geomagnetic storm effects on the thermosphere and the ionosphere revealed by in situ measurements from OGO 6  
p0025 A77-16240  
Structure of electrodynamic and particle heating in the disturbed polar thermosphere  
p0027 A77-23201  
High-latitude nitric oxide in the lower thermosphere  
p0028 A77-23222  
A global thermospheric model based on mass spectrometer and incoherent scatter data MSIS. I - N2 density and temperature  
p0029 A77-37153  
A global thermospheric model based on mass spectrometer and incoherent scatter data MSIS. II - Composition  
p0029 A77-37154  
The effect of extraterrestrial dust, stratospheric warmings, and lower thermospheric pressure systems on OGO-4 measured nightglows in the earth's atmosphere (80 to 100 km)  
p0031 N74-26848  
Magnetically ordered heating in the polar regions of the thermosphere  
p0034 N75-32651  
Thermospheric temperature, density, and composition: New models  
[NASA-CR-153049] p0035 N77-23648

## SUBJECT INDEX

- TIME DEPENDENCE**  
On the local time dependence of the bow shock wave structure  
p0005 A74-24759
- TIME RESPONSE**  
Geomagnetic storm effects on the thermosphere and the ionosphere revealed by in situ measurements from OGO 6  
p0025 A77-16240
- TROPICAL REGIONS**  
Proton measurements in ring current by OGO-3 satellite compared with geomagnetic field data at low and high latitudes  
p0002 A71-33663  
Vertical red line 6300 A distribution and tropical nightglow morphology in quiet magnetic conditions  
p0004 A74-11523  
An explanation of the longitudinal variation of the OI(630 nm) tropical nightglow intensity  
p0019 A76-21456  
Tropical F region winds from O I 1356-A and forbidden O I 6300-A emissions. II - Analysis of OGO 4 data  
p0023 A76-42683  
The temperature gradient drift instability at the equatorward edge of the ionospheric plasma trough  
p0024 A76-42697  
Model of equatorial scintillations from in-situ measurements --- based on OGO-6 observed F region irregularity  
p0025 A77-12057  
The morphology of equatorial irregularities in the Afro-Asian sector from OGO 6 observations  
p0028 A77-24016  
Magnetic storm effects on the tropical ultraviolet airglow  
p0029 A77-27318  
Variational electric fields at low latitudes and their relation to spread-F and plasma irregularities  
p0029 A77-34326  
Determination of tropical F-region winds from atomic oxygen airglow emissions  
p0034 N76-10603
- TWILIGHT GLOW**  
Satellite measurements of high-altitude twilight Mg(plus) emission  
p0019 A76-19839  
The intensity variation of the atomic oxygen red line during morning and evening twilight on 9-10 April 1969  
p0021 A76-28990
- TYPE 3 BURSTS**  
Acceleration of electrons in absence of detectable optical flares deduced from type III radio bursts, H alpha activity and soft X-ray emission  
[NSSDC-ID-68-014A-04-PS] p0009 A75-16217  
OGO-V radio burst analysis --- h alpha line  
[NASA-CR-142232] p0033 N75-19114  
Low-energy radio emissions from the earth and sun --- solar type 3 bursts  
p0033 N75-20195
- U**
- ULTRAVIOLET PHOTOMETRY**  
Global atomic oxygen density derived from OGO-6 1304 A airglow measurements  
p0021 A76-28989
- ULTRAVIOLET RADIATION**  
Tropical UV arcs: Comparison of brightness with f sub 0 F sub 2  
p0037 N77-86006  
Ultraviolet solar energy survey on OGO-6  
[NASA-CR-155088] p0037 N77-86268
- ULTRAVIOLET SPECTRA**  
The interpretations of ultraviolet observations of comets  
p0022 A76-31317  
OGO-4 observations of the ultraviolet auroral spectrum  
p0025 A77-16243  
On the cometary hydrogen coma and far UV emission  
p0034 N76-21066
- ULTRAVIOLET SPECTROMETERS**  
Satellite measurements of high-altitude twilight Mg(plus) emission  
p0019 A76-19839  
High-latitude nitric oxide in the lower thermosphere  
p0028 A77-23222

**SUBJECT INDEX**

**X RAY SPECTROSCOPY**

**ULTRAVIOLET SPECTROSCOPY**

Satellite measurements of nitric oxide in the polar region  
p0017 A75-46289

**UPPER ATMOSPHERE**

High-latitude troughs and the polar cap boundary  
p0020 A76-22105

Diurnal variation of thermal plasma in the plasmasphere  
p0023 A76-41210

Observations of hydrogen in the upper atmosphere  
p0024 A77-11488

**UPPER IONOSPHERE**

In-situ observations of irregular ionospheric structure associated with the plasmopause  
p0008 A75-11853

High latitude minor ion enhancements - A clue for studies of magnetosphere-atmosphere coupling  
p0006 A75-12439

Satellite measurements of ion composition and temperatures in the topside ionosphere during medium solar activity  
p0021 A76-28486

Light ion and electron troughs observed in the mid-latitude topside ionosphere on two passes of OGO 6 compared to coincident equatorial electron density deduced from whistlers  
p0030 A77-42297

**V**

**VELOCITY MEASUREMENT**

A search for solar wind velocity changes between 0.7 and 1 au  
p0013 A75-28750

**VERTICAL DISTRIBUTION**

Vertical red line 6300 A distribution and tropical nightglow morphology in quiet magnetic conditions  
p0004 A74-11523

Dependence of field-aligned electron precipitation occurrence on season and altitude  
p0007 A74-43679

Altitude profiles of the photoelectron induced O 1D (6300 A) predawn enhancement by observation and theory  
p0026 A77-20886

**VERY HIGH FREQUENCIES**

The morphology of equatorial irregularities in the Afro-Asian sector from OGO 6 observations  
p0028 A77-24016

**VERY LOW FREQUENCIES**

'Hislers' - Quasi-periodic (T approximately equal to 2 sec) VLF noise forms at auroral latitudes  
p0009 A75-16440

VLF and ELF emissions --- in magnetosphere  
p0015 A75-36988

Magnetospheric chorus - Amplitude and growth rate  
p0016 A75-42748

VLF propagation in the magnetosphere during sunrise and sunset hours  
p0018 A76-14838

The upper- and lower-frequency cutoffs of magnetospherically reflected whistlers  
p0019 A76-19854

New results on the correlation between low-energy electrons and auroral hiss  
p0020 A76-22086

**W**

**WAVE EXCITATION**

Excitation of magnetosonic waves with discrete spectrum in the equatorial vicinity of the plasmopause  
p0012 A75-27679

**WAVE INTERACTION**

Waves and wave-particle interactions in the magnetosphere - A review  
p0018 A76-12272

**WAVE PACKETS**

Magnetosheath lion roars --- strongest whistler mode signals  
p0022 A76-33057

**WAVE PROPAGATION**

Instability phenomena in detached plasma regions --- in magnetosphere  
p0027 A77-21512

**WAVE REFLECTION**

A new interpretation of subprotonospheric whistler characteristics  
p0019 A76-16522

**WHISTLERS**

Noise signals in earth magnetosheath interpreted as electromagnetic waves propagating in whistler mode  
p0001 A69-31985

Steady ELF plasmaspheric hiss, studying whistler mode turbulence, band limitation, power spectra and peak intensities  
p0004 A73-26984

Magnetospheric chorus - Amplitude and growth rate  
p0016 A75-42748

VLF propagation in the magnetosphere during sunrise and sunset hours  
p0018 A76-14838

A new interpretation of subprotonospheric whistler characteristics  
p0019 A76-16522

The upper- and lower-frequency cutoffs of magnetospherically reflected whistlers  
p0019 A76-19854

Magnetosheath lion roars --- strongest whistler mode signals  
p0022 A76-33057

Magnetospheric chorus - Occurrence patterns and normalized frequency  
p0025 A77-16238

Light ion and electron troughs observed in the mid-latitude topside ionosphere on two passes of OGO 6 compared to coincident equatorial electron density deduced from whistlers  
p0030 A77-42297

**WIDEBAND COMMUNICATION**

The Engineering design of the Orbiting Geophysical Observatories.  
[NSSDC-ID-64-054A-00-PC] p0001 A63-21528

**WIND EFFECTS**

Vertical red line 6300 A distribution and tropical nightglow morphology in quiet magnetic conditions  
p0004 A74-11523

Dynamical effects in the distribution of helium in the thermosphere  
p0024 A77-11489

**WIND PROFILES**

Diurnal variation of the neutral thermospheric winds determined from incoherent scatter radar data  
p0006 A74-36735

F region wind components in the magnetic meridian from OGO 4 tropical airglow observations  
p0011 A75-22671

**WIND VELOCITY**

Neutral wind velocities calculated from temperature measurements during a magnetic storm and the observed ionospheric effects.  
p0004 A73-36150

Determination of tropical F-region winds from atomic oxygen airglow emissions  
p0034 N76-10603

**WIND VELOCITY MEASUREMENT**

Tropical F region winds from O 1 1356-A and forbidden O 1 6300-A emissions. II - Analysis of OGO 4 data  
p0023 A76-42683

**X**

**X RAY ASTRONOMY**

Solar activity study based on solar X-ray spectra observation, considering flare mechanism  
p0001 A70-16719

Impulsive solar flare X-rays greater than 10 keV and some characteristics of cosmic gamma-ray bursts  
p0014 A75-35537

**X RAY DENSITY MEASUREMENT**

Slow X-ray bursts and flares with filament disruption  
p0016 A75-43792

**X RAY SPECTRA**

Thermal and nonthermal interpretations of flare X-ray bursts  
p0017 A76-10136

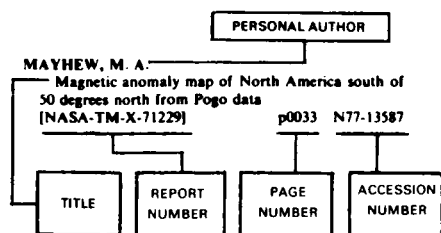
Hard X-ray spectra of cosmic gamma-ray bursts  
p0030 A78-10580

**X RAY SPECTROSCOPY**

Characteristics of cosmic X-ray bursts observed with the OGO-5 satellite  
p0026 A77-16850

# B. PERSONAL AUTHOR INDEX

## Typical Personal Author Index Listing



Listings in this index are arranged alphabetically by personal author. The title of the document provides a brief description of the subject matter. The report number helps to indicate the type of document cited. The page number identifies the page in the abstract section (V) on which the citation appears while the accession number denotes the number by which the citation is identified on that page. Under each author's name the accession numbers are arranged in ascending alphanumeric order.

## A

- AKASOFU, S.-I.**  
Dependence of the latitude of the cleft on the interplanetary magnetic field and substorm activity  
p0020 A76-22107
- ALCAYDE, D.**  
A global thermospheric model based on mass spectrometer and incoherent scatter data MSIS. I - N2 density and temperature  
p0029 A77-37153
- ALEXANDER, W. M.**  
Four years of dust particle measurements in cislunar and selenocentric space from Lunar Explorer 35 and OGO 3.  
p0002 A72-31937
- AMATA, E.**  
Evidence for magnetic field line reconnection in the solar wind  
p0017 A75-46238
- ANDERSON, D. E., JR.**  
Global atomic hydrogen density derived from OGO-6 Lyman-alpha measurements  
p0021 A76-28988
- ANDERSON, D. N.**  
Magnetic storm effects on the tropical ultraviolet airglow  
p0029 A77-27318
- ANDERSON, G. P.**  
Satellite observations of the global distribution of stratospheric ozone  
p0036 N78-12583
- ANDERSON, K. A.**  
Characteristics of cosmic X-ray bursts observed with the OGO-5 satellite  
Experiment data analysis report. OGO-A experiment no. 1  
[NASA-CR-96278]  
p0031 N68-33302
- ARTHUR, C. W.**  
Four years of dust particle measurements in cislunar and selenocentric space from Lunar Explorer 35 and OGO 3.  
p0002 A72-31937

## B

- BAIXERAS-AIGUABELLA, C.**  
Short-term variations of the cosmic-ray proton and electron intensities in 1968 and 1969  
p0037 N77-84177
- BALASUBRAHMANYAN, V. K.**  
Solar particle events with anomalously large relative abundance of He-3  
p0013 A75-34018
- BALASUBRAHMANYAN, V. K.**  
Solar energetic particle event with He-3/He-4 greater than 1  
p0009 A75-15342
- BARLIER, F.**  
North-south asymmetries in the thermosphere during the last maximum of the solar cycle  
p0009 A75-16449
- BARTH, C. A.**  
Satellite measurements of nitric oxide in the polar region  
OGO-4 observations of the ultraviolet auroral spectrum  
p0017 A75-46289  
p0025 A77-16243  
High-latitude nitric oxide in the lower thermosphere  
p0028 A77-23222
- BASU, S.**  
Model of equatorial scintillations from in-situ measurements  
p0025 A77-12057  
Model of equatorial scintillations from in-situ measurements  
p0025 A77-12057  
Correlated measurements of scintillations and in-situ F-region irregularities from OGO-6  
p0025 A77-15786  
Correlated measurements of scintillations and in-situ F-region irregularities from OGO-6  
p0025 A77-15786  
The morphology of equatorial irregularities in the Afro-Asian sector from OGO 6 observations  
p0028 A77-24016  
The morphology of equatorial irregularities in the Afro-Asian sector from OGO 6 observations  
p0028 A77-24016
- BAUER, P.**  
North-south asymmetries in the thermosphere during the last maximum of the solar cycle  
p0009 A75-16449  
A global thermospheric model based on mass spectrometer and incoherent scatter data MSIS. I - N2 density and temperature  
p0029 A77-37153
- BEDIJN, P. J.**  
Long-term cosmic ray modulation in the period 1966-1972 and interplanetary magnetic fields  
p0023 A76-39130
- BERG, L. E.**  
Correlated satellite measurements of proton precipitation and plasma density  
p0009 A75-16437
- BERKO, F. W.**  
Dependence of field-aligned electron precipitation occurrence on season and altitude  
p0007 A74-43679  
Simultaneous particle and field observations of field-aligned currents  
p0011 A75-19330  
Features of polar cusp electron precipitation associated with a large magnetic storm  
[NASA-TM-X-70792]  
p0032 N75-12873
- BERTAUX, J. L.**  
Interpretation of Ogo 5 Lyman alpha measurements in the upper geocorona.  
[NSSDC-ID-68-014A-22-PM]  
p0004 A73-19233  
Observed variations of the exospheric hydrogen density with the exospheric temperature  
p0012 A75-23721  
Observations of hydrogen in the upper atmosphere  
p0024 A77-11488
- BHAR, J. N.**  
The morphology of equatorial irregularities in the Afro-Asian sector from OGO 6 observations  
p0028 A77-24016
- BIERMANN, L.**  
Recent advances in cometary physics and chemistry  
p0009 A75-13176
- BITTENCOURT, J. A.**  
F region wind components in the magnetic meridian from OGO 4 tropical airglow observations  
p0011 A75-22671  
Tropical F region winds from O I 1356-A and forbidden O I 6300-A emissions. II - Analysis of OGO 4 data  
p0023 A76-42683  
Determination of tropical F-region winds from atomic oxygen airglow emissions  
p0034 N76-10603
- BLAMONT, J.**  
Variation of the solar wind flux with heliographic latitude, deduced from its interaction with interplanetary hydrogen  
p0013 A75-28032
- BLAMONT, J. E.**  
Noctilucent clouds in daytime - Circumpolar particulate layers near the summer mesopause.  
Interpretation of Ogo 5 Lyman alpha measurements in the upper geocorona.  
[NSSDC-ID-68-014A-22-PM]  
p0003 A72-42515  
p0004 A73-19233  
Vertical red line 6300 A distribution and tropical nightglow morphology in quiet magnetic conditions  
p0004 A74-11523  
Altitude profiles of the photoelectron induced O I D (6300 A) predawn enhancement by observation and theory  
p0026 A77-20886
- BOHN, J. L.**  
Four years of dust particle measurements in cislunar and selenocentric space from Lunar Explorer 35 and OGO 3.  
p0002 A72-31937
- BOWYER, J. M., JR.**  
OGO-6 gas-surface energy transfer experiment  
[NASA-CR-139009]  
p0031 N74-25869
- BRACE, L. H.**  
Is the red arc a good indicator of ionosphere-magnetosphere conditions  
[NSSDC-ID-69-051A-02-PM]  
p0008 A75-11226
- BRECKENRIDGE, S. L.**  
Data user's notes of the radio astronomy experiment aboard the OGO-V spacecraft  
[NASA-CR-143696]  
p0034 N75-24593
- BRINTON, H. C.**  
A global thermospheric model based on mass spectrometer and incoherent scatter data MSIS. II - Composition  
p0029 A77-37154
- BROWN, J. W.**  
Measurements of the cosmic-ray Be/B ratio and the age of cosmic rays  
p0006 A74-30187
- BROWN, P. E.**  
Light ion and electron troughs observed in the mid-latitude topside ionosphere on two passes of OGO 6 compared to coincident equatorial electron density deduced from whistlers  
p0030 A77-42297
- BUCK, R. M.**  
Pitch angle distributions of energetic electrons in the equatorial regions of the outer magnetosphere - OGO-5 observations  
p0011 A75-22759  
Observations of protons with energies exceeding 100 keV in the earth's magnetosheath  
p0020 A76-22092  
Energetic electrons in the inner belt in 1968  
p0022 A76-35289



**BULLOUGH, K.**

A study of electron spectra in the inner belt  
p0024 A76-44653

**BULLOUGH, K.**

VLF and ELF emissions  
p0015 A75-36988

**BURCH, J. L.**

Electron precipitation patterns and substorm morphology.  
[NSSDC-ID-67-073A-11-PM] p0004 A73-33434  
High-latitude proton precipitation and light ion density profiles during the magnetic storm initial phase.  
[NSSDC-ID-67-073A-11-PM] p0004 A73-45114  
Dependence of the latitude of the cleft on the interplanetary magnetic field and substorm activity  
p0020 A76-22107  
AE-LEE measurements at low and mid latitude  
p0031 N74-28251

**BURGER, J. J.**

Long-term solar modulation of cosmic-ray electrons with energies above 0.5 GeV  
p0037 N77-84176

**BURTIS, W. J.**

Magnetospheric chorus - Amplitude and growth rate  
p0016 A75-42748  
Magnetospheric chorus - Occurrence patterns and normalized frequency  
p0025 A77-16238  
Magnetospheric chorus  
p0033 N75-22959

**BURTON, R. K.**

Plasmaspheric hiss.  
p0004 A73-26984  
Simultaneous particle and field observations of field-aligned currents  
p0011 A75-19330  
Critical electron pitch angle anisotropy necessary for chorus generation  
p0024 A76-44665  
Detailed analysis of magnetospheric ELF chorus - preliminary results  
p0027 A77-21523

**C**

**CAAN, M. N.**

Substorm and interplanetary magnetic field effects on the geomagnetic tail lobes  
p0011 A75-19349

**CAIN, J. C.**

A global magnetic anomaly map  
p0012 A75-24043  
Low latitude variations of the magnetic field  
p0037 N76-71880

**CARIGNAN, G. R.**

The temperature gradient between 100 and 120 km  
p0018 A76-16501

**CARPENTER, D. L.**

'Hislers' - Quasi-periodic (T approximately equal to 2 sec) VLF noise forms at auroral latitudes  
p0009 A75-16440

**CHAN, K. W.**

Extremely low frequency hiss emissions in the magnetosphere  
p0032 N74-30528

**CHAN, K.-W.**

A relation between ELF hiss amplitude and plasma density in the outer plasmasphere  
p0006 A74-30677  
ELF hiss associated with plasma density enhancements in the outer magnetosphere  
p0022 A76-33058

**CHANDRA, S.**

The equatorial helium ion trough and the geomagnetic anomaly  
p0011 A75-20360  
Remote sensing of the ionospheric F layer by use of O I 6300-A and O I 1356-A observations  
p0014 A75-35040  
The global characteristics of atmospheric emissions in the lower thermosphere and their aeronomic implications  
p0016 A75-42726  
Exospheric temperature inferred from the Aeros-A neutral composition measurement  
p0017 A75-46269  
Satellite measurements of ion composition and temperatures in the topside ionosphere during medium solar activity  
p0021 A76-28486

**CHAPPELL, C. R.**

Recent satellite measurements of the morphology and dynamics of the plasmasphere.  
p0003 A73-13709

Thermal ions in the magnetosphere.  
p0003 A73-13879

Detached plasma regions in the magnetosphere  
p0006 A74-30660  
Current-driven plasma instabilities at high latitudes  
p0014 A75-35005

**CHEN, A. J.**

Plasma tail interpretations of pronounced detached plasma regions measured by Ogo 5  
p0007 A74-43691  
Dynamics of Mid-latitude light ion trough and plasma tails  
p0012 A75-27383  
Ion composition irregularities and ionosphere-plasmasphere coupling - Observations of a high latitude ion trough  
p0013 A75-28356

High-latitude troughs and the polar cap boundary  
p0020 A76-22105  
Diurnal variation of thermal plasma in the plasmasphere  
p0023 A76-41210

**CHESWORTH, E. T.**

The role of ice particulates in the electrification of the air in the mesosphere  
p0033 N75-24202

**CHUBB, T. A.**

Evidence that solar X-ray emission is of purely thermal origin (Also observation of far UV flash during 28 August 1966 proton flare).  
p0002 A72-20013

**CHURCH, S. R.**

Intensity variation of ELF hiss and chorus during isolated substorms  
[NSSDC-ID-69-051A-22-PM] p0007 A74-44202  
The local time variation of ELF emissions during periods of substorm activity  
p0029 A77-31391

**CLINE, T. L.**

Relativistic interplanetary electrons and positrons  
p0031 N71-25288

**COGGER, L.**

A global thermospheric model based on mass spectrometer and incoherent scatter data MSIS. I - N2 density and temperature  
p0029 A77-37153

**COLBURN, D. S.**

Pioneer 9 and OGO 5 observations of an interplanetary multiple shock ensemble on February 2, 1969  
p0016 A75-42744

**COLEMAN, P. J., JR.**

Substorms in space - The correlation between ground and satellite observations of the magnetic field  
p0005 A74-14285

**CORBIN, W. E., JR.**

OGO-6 gas-surface energy transfer experiment [NASA-CR-139009] p0031 N74-25869

**CORDIER, G. R.**

In-situ observations of irregular ionospheric structure associated with the mapspause  
p0008 A75-11853

**CORNILLEAU-WEHRLIN, N.**

Detailed analysis of magnetospheric ELF chorus - preliminary results  
p0027 A77-21523

**COUNTREE, C.**

The dominant mode of standing Alfvén waves at the synchronous orbit  
p0017 A75-46285

**CUMMINS, W. D.**

The dominant mode of standing Alfvén waves at the synchronous orbit  
p0017 A75-46285

**D**

**DAVIS, W. M.**

A global magnetic anomaly map  
p0012 A75-24043  
Low latitude variations of the magnetic field  
p0037 N76-71880

**DONAHUE, T. M.**

Noctilucent clouds in daytime - Circumpolar particulate layers near the summer mesopause.  
p0003 A72-42515  
An upper limit to the product of NO and O densities from 105 to 120 km  
[NSSDC ID 69-051A-26-PM] p0008 A75-11227

**PERSONAL AUTHOR INDEX**

The temperature gradient between 100 and 120 km  
p0018 A76-16501  
OGO-6 observations of 5577 A  
p0019 A76-18436

**DRYER, M.**

Pioneer 9 and OGO 5 observations of an interplanetary multiple shock ensemble on February 2, 1969  
p0016 A75-42744

**DUMMER, R. S.**

OGO-6 gas-surface energy transfer experiment [NASA-CR-139009] p0031 N74-25869

**DUNCKEL, N.**

Low-energy radio emissions from the earth and sun  
p0033 N75-20195

**E**

**EDGAR, B. C.**

The upper- and lower-frequency cutoffs of magnetospherically reflected whistlers  
p0019 A76-19854  
The theory of VLF Doppler signatures and their relation to magnetospheric density structure  
p0023 A76-39145

**EMERY, B. A.**

Diurnal variation of the neutral thermospheric winds determined from incoherent scatter radar data  
p0006 A74-36735

**ETCHETO, J.**

Detailed analysis of magnetospheric ELF chorus - preliminary results  
p0027 A77-21523

**EVANS, J. V.**

The intensity variation of the atomic oxygen red line during morning and evening twilight on 9-10 April 1969  
p0021 A76-28990  
A global thermospheric model based on mass spectrometer and incoherent scatter data MSIS. I - N2 density and temperature  
p0029 A77-37153

**F**

**FAHR, H. J.**

Solar radiation asymmetries and heliospheric gas heating influencing extraterrestrial UV data  
p0009 A75-13173

**FALIN, J. L.**

Experimental model of the exospheric temperature based on optical measurements on board the OGO 6 satellite  
p0023 A76-42390  
Experimental global model of the exospheric temperature based on measurements from the Fabry-Perot interferometer on board the OGO-6 satellite - Discussion of the data and properties of the model  
p0029 A77-34901

**FELDSHTEIN, IA. I.**

Ring current asymmetry  
p0002 A71-33663

**FELDSTEIN, Y. I.**

Auroral oval and magnetospheric cusps  
p0037 N78-70070

**FISKE, K. F.**

Intensity variation of ELF hiss and chorus during isolated substorms  
[NSSDC-ID-69-051A-22-PM] p0007 A74-44202

**FORMISANO, V.**

The earth's bow shock fine structure  
p0011 A75-19138  
Structure of the quasi-perpendicular laminar bow shock  
p0012 A75-23707  
Instabilities connected with neutral sheets in the solar wind  
p0013 A75-28015  
Collisionless shock waves in space - A very high beta structure  
p0014 A75-35003  
Evidence for magnetic field line reconnection in the solar wind  
p0017 A75-46238  
Structure of a quasi-parallel, quasi-laminar bow shock  
p0028 A77-23220  
The magnetopause. Part I: Multisatellite simultaneous observations of bow shock and magnetopause positions [LPS-75-23-PT-1] p0034 N76-33787

PERSONAL AUTHOR INDEX

HUMMEL, J. R.

The magnetopause: Part 2: Magnetopause position and the reconnection problem [LPS-75-24-PT-2] p0035 N76-33788  
 The outer magnetosphere. Part 1: A multisatellite study of the magnetopause position in relation with some important fluid dynamic parameters [LPS-76-2-PT-1] p0035 N76-33793  
 The outer magnetosphere. Part 3: Simultaneous multisatellite observations of the magnetopause. [LPS-76-4-PT-2] p0035 N76-33795  
**FREDERICK, J. E.**  
 Satellite observations of the global distribution of stratospheric ozone p0036 N78-12583  
**FREDRICKS, R. W.**  
 Plasma instability modes related to the earth's bow shock p0011 A75-22774  
 Current-driven plasma instabilities at high latitudes p0014 A75-35005  
**FUJII, K.**  
 Thinning of the near-earth (10 to about 15 earth radii) plasma sheet preceding the substorm expansion phase p0024 A76-47884

**G**

**GENDRIN, R.**  
 Waves and wave-particle interactions in the magnetosphere - A review p0018 A76-12272  
**GERARD, J.-C.**  
 Satellite measurements of high-altitude twilight Mg(plus) emission p0019 A76-19839  
 OGO-4 observations of the ultraviolet auroral spectrum p0025 A77-16243  
 High-latitude nitric oxide in the lower thermosphere p0028 A77-23222  
 Magnetic storm effects on the tropical ultraviolet airglow p0029 A77-27318  
**GLEGHORN, G. J.**  
 The Engineering design of the Orbiting Geophysical Observatories. [NSSDC-ID-64-054A-00-PC] p0001 A63-21528  
**GOEL, M. K.**  
 Satellite measurements of ion composition and temperatures in the topside ionosphere during medium solar activity p0021 A76-28486  
**GOUIN, P.**  
 Correlation of 'satellite estimates' of the equatorial electrojet intensity with ground observations at Addis Ababa. p0004 A73-31771  
**GREBOWSKY, J. M.**  
 Plasma tail interpretations of pronounced detached plasma regions measured by Ogo 5 p0007 A74-43691  
 Dynamics of Mid-latitude light ion trough and plasma tails p0012 A75-27383  
 Ion composition irregularities and ionosphere-plasmasphere coupling - Observations of a high latitude ion trough p0013 A75-28356  
 High-latitude troughs and the polar cap boundary p0020 A76-22105  
 Diurnal variation of thermal plasma in the plasmasphere p0023 A76-41210  
**GREENSTADT, E. W.**  
 Binary index for assessing local bow shock obliquity. p0003 A72-44511  
 Structure of the quasi-perpendicular laminar bow shock p0012 A75-23707  
 Collisionless shock waves in space - A very high beta structure p0014 A75-35003  
 Structure of a quasi-parallel, quasi-laminar bow shock p0028 A77-23220  
**GREENSTADT, W. W.**  
 Plasma instability modes related to the earth's bow shock p0011 A75-22774

**GUENTHER, B.**  
 Noctilucent clouds in daytime - Circumpolar particulate layers near the summer mesopause. p0003 A72-42515  
**GUENTHER, B. W.**  
 Observations from the Orbiting Geophysical Observatory 6 of mesospheric airglow and scattering layers p0033 N75-19882  
**GUHATHAKURTA, B. K.**  
 The morphology of equatorial irregularities in the Afro-Asian sector from OGO 6 observations p0028 A77-24016  
**GULEMI, A. V.**  
 Excitation of magnetosonic waves with discrete spectrum in the equatorial vicinity of the plasmapause p0012 A75-27679

**H**

**HADDOCK, F. T.**  
 OGO-V radio burst analysis [NASA-CR-142232] p0033 N75-19114  
 Data user's notes of the radio astronomy experiment aboard the OGO-V spacecraft [NASA-CR-143696] p0034 N75-24593  
**HAHN, A.**  
 Comparison of a magnetic local anomaly measured by OGO-6 and a crustal feature p0037 N76-71883  
**HANSON, W. B.**  
 Is the red arc a good indicator of ionosphere-magnetosphere conditions [NSSDC-ID-69-051A-02-PM] p0008 A75-11226  
 Comparisons of ionogram and OGO 6 satellite observations of small-scale F region inhomogeneities p0028 A77-23211  
**HARRIS, I.**  
 Theory of the phase anomaly in the thermosphere p0005 A74-12645  
 Thermospheric 'temperatures' p0007 A74-36747  
**HARRIS, K. K.**  
 The measurement of cold ion densities in the plasma trough [NSSDC-ID-68-014A-18-PM] p0010 A75-16637  
**HARTLE, R. E.**  
 Density and temperature distributions in non-uniform rotating planetary exospheres with applications to earth p0005 A74-14224  
**HAYS, P. B.**  
 Diurnal variation of the neutral thermospheric winds determined from incoherent scatter radar data p0006 A74-36735  
**HEDGECOCK, P. C.**  
 Instabilities connected with neutral sheets in the solar wind p0013 A75-28015  
 Substorm effects on the neutral sheet inside 10 earth radii p0016 A75-46232  
 Structure of a quasi-parallel, quasi-laminar bow shock p0028 A77-23220  
**HEDIN, A. E.**  
 A global thermospheric model based on mass spectrometer and incoherent scatter data MSIS. I - N2 density and temperature p0029 A77-37153  
 A global thermospheric model based on mass spectrometer and incoherent scatter data MSIS. II - Composition p0029 A77-37154  
**HEI, D. J., JR.**  
 A study of the heat flux reversal region upstream from the earth's bow shock, using data from the OGO 5 electron spectrometer p0035 N78-11543  
**HELLIWELL, R. A.**  
 Magnetospheric chorus - Amplitude and growth rate p0016 A75-42748  
 Magnetospheric chorus - Occurrence patterns and normalized frequency p0025 A77-16238  
**HEPPNER, J. P.**  
 Electric fields in the magnetosphere. p0003 A73-15333  
 High latitude electric fields and the modulations related to interplanetary magnetic field parameters p0005 A74-14272

Empirical models of high-latitude electric fields p0029 A77-27317  
 Variational electric fields at low latitudes and their relation to spread-F and plasma irregularities p0029 A77-34326  
 High latitude ionospheric winds related to solar-interplanetary conditions p0032 N74-29091  
**HICKS, G. T.**  
 F region wind components in the magnetic meridian from OGO 4 tropical airglow observations p0011 A75-22671  
 Remote sensing of the ionospheric F layer by use of O I 6300-A and O I 1356-A observations p0014 A75-35040  
 Tropical F region winds from O I 1356-A and forbidden O I 6300-A emissions. II - Analysis of OGO 4 data p0023 A76-42683  
**HINTON, B. B.**  
 Structure of electrodynamic and particle heating in the undisturbed polar thermosphere p0018 A76-14318  
 Magnetically ordered heating in the polar regions of the thermosphere p0034 N75-32651  
**HIRSHBERG, J.**  
 The solar cycle variation of the solar wind helium abundance [NSSDC-ID-68-014A-17-OS] p0010 A75-16631  
**HOFFMAN, R. A.**  
 Electron precipitation patterns and substorm morphology. [NSSDC-ID-67-073A-11-PM] p0004 A73-33434  
 Dependence of field-aligned electron precipitation occurrence on season and altitude p0007 A74-43679  
 Simultaneous particle and field observations of field-aligned currents p0011 A75-19330  
 New results on the correlation between low-energy electrons and auroral hiss p0020 A76-22086  
 AE-LEE measurements at low and mid latitude p0031 N74-28251  
**HOLTET, J. A.**  
 Variational electric fields at low latitudes and their relation to spread-F and plasma irregularities p0029 A77-34326  
**HOLZER, R. E.**  
 Magnetic emissions in the magnetosheath at frequencies near 100 Hz. p0001 A69-31985  
 On the local time dependence of the bow shock wave structure p0005 A74-24759  
 A relation between ELF hiss amplitude and plasma density in the outer plasmasphere p0006 A74-30677  
 Simultaneous particle and field observations of field-aligned currents p0011 A75-19330  
 ELF hiss associated with plasma density enhancements in the outer magnetosphere p0022 A76-33058  
 Structure of a quasi-parallel, quasi-laminar bow shock p0028 A77-23220  
**HOLZER, R. E.,**  
 Plasmaspheric hiss. p0004 A73-26984  
**HONES, E. W., JR.**  
 Multiple-satellite studies of magnetospheric substorms - Radial dynamics of the plasma sheet p0026 A77-16868  
**HORAN, D. M.**  
 Electron temperature and emission measure variations during solar X-ray flares. p0002 A72-29722  
**HUDSON, M. K.**  
 The temperature gradient drift instability at the equatorward edge of the ionospheric plasma trough p0024 A76-42697  
**HUGHES, W. J.**  
 Multiple satellite observations of pulsation resonance structure in the magnetosphere p0027 A77-23205  
**HUMMEL, J. R.**  
 Satellite observation of the mesospheric scattering layer and implied climatic consequences p0022 A76-39128

I

**IFEDILI, S. O.**  
A search for solar neutrons during solar flares  
p0010 A75-18717

**INTRILIGATOR, D. S.**  
A search for solar wind velocity changes between 0.7 and 1 au  
p0013 A75-28750

J

**JACCHIA, L. G.**  
Variations in thermospheric composition - A model based on mass spectrometer and satellite drag data  
p0006 A74-30667

Thermospheric temperature, density, and composition: New models  
[NASA-CR-153049] p0035 N77-23648

**JAECK, C.**  
North-south asymmetries in the thermosphere during the last maximum of the solar cycle  
p0009 A75-16449

**JANETZKE, R. J.**  
AE-LEE measurements at low and mid latitude  
p0031 N74-28251

**JOHNSON, W. C.**  
Light ion and electron troughs observed in the mid-latitude topside ionosphere on two passes of OGO 6 compared to coincident equatorial electron density deduced from whistlers  
p0030 A77-42297

K

**KAHLER, S.**  
On the existence of solar-flare plasmas of temperature greater than .1 billion deg K  
p0001 A71-20944

Thermal and nonthermal interpretations of flare X-ray bursts  
p0017 A76-10136

**KAHLER, S. W.**  
Thermal runaway as the solar flare trigger mechanism  
p0001 A71-12761

The observation of nonthermal solar X-radiation in the energy range 3 less than E less than 10 keV  
p0002 A71-40425

**KAISER, T. R.**  
VLF and ELF emissions  
p0015 A75-36988

**KAMIDE, Y.**  
Dependence of the latitude of the cleft on the interplanetary magnetic field and substorm activity  
p0020 A76-22107

**KANE, S. R.**  
Location of the electron acceleration region in solar flares.  
p0003 A72-32790

Acceleration of electrons in absence of detectable optical flares deduced from type III radio bursts, H alpha activity and soft X-ray emission  
[NSSDC-ID-68-014A-04-PS] p0009 A75-16217

Impulsive solar flare X-rays greater than 10 keV and some characteristics of cosmic gamma-ray bursts  
p0014 A75-35537

Impulsive /flash/ phase of solar flares - Hard X-ray, microwave, EUV and optical observations  
p0015 A75-37352

Characteristics of cosmic X-ray bursts observed with the OGO-5 satellite  
p0026 A77-16850

Non-thermal processes during the 'build-up' phase of solar flares and in absence of flares  
p0026 A77-18572

Hard X-ray spectra of cosmic gamma-ray bursts  
p0030 A78-10580

**KASPRZAK, W. T.**  
Comparison of the San Marco 3 Nace neutral composition data with the extrapolated Ogo 6 empirical model  
p0021 A76-26524

**KAYSER, D. C.**  
A global thermospheric model based on mass spectrometer and incoherent scatter data MSIS. 1 - N2 density and temperature  
p0029 A77-37153

**KELLER, H. U.**  
A cometary hydrogen model - Comparison with OGO-5 measurements of Comet Bennett (1970 II)  
p0013 A75-32382

The interpretations of ultraviolet observations of comets  
p0022 A76-31317

On the cometary hydrogen coma and far UV emission  
p0034 N76-21066

**KELLEY, M. C.**  
Properties of ELF electromagnetic waves in and above the earth's ionosphere deduced from plasma wave experiments on the OVI-17 and Ogo 6 satellites  
p0018 A76-16507

The temperature gradient drift instability at the equatorward edge of the ionospheric plasma trough  
p0024 A76-42697

**KHAN, B. K.**  
Model of equatorial scintillations from in-situ measurements  
p0025 A77-12057

**KIKUCHI, H.**  
Shocks, solitons and the plasmopause  
p0027 A77-21504

Micropulsations and the plasmopause  
p0027 A77-21513

**KING, J. W.**  
An explanation of the longitudinal variation of the O1D (630 nm) tropical nightglow intensity  
p0019 A76-21456

**KIVELSON, M.**  
Current-driven plasma instabilities at high latitudes  
p0014 A75-35005

**KIVELSON, M. G.**  
Substorms in space - The correlation between ground and satellite observations of the magnetic field  
p0005 A74-14285

OGO-5 observations of the magnetopause  
p0010 A75-19134

Multiple-satellite studies of magnetospheric substorms - Radial dynamics of the plasma sheet  
p0026 A77-16868

Instability phenomena in detached plasma regions  
p0027 A77-21512

OGO 5 observations of Pc 5 waves - Particle flux modulations  
p0030 A77-42295

**KLAINÉ, B. I.**  
Excitation of magnetosonic waves with discrete spectrum in the equatorial vicinity of the plasmopause  
p0012 A75-27679

**KOCKARTS, G.**  
North-south asymmetries in the thermosphere during the last maximum of the solar cycle  
p0009 A75-16449

**KOKUBUN, S.**  
Ogo 5 observations of Pc 5 waves - Ground-magnetosphere correlations  
p0024 A77-11219

Triggering of substorms by solar wind discontinuities  
p0026 A77-21093

OGO 5 observations of Pc 5 waves - Particle flux modulations  
p0030 A77-42295

**KREPLIN, R. W.**  
Solar X-rays - Developing background for comprehensive theory  
p0001 A70-16719

Thermal runaway as the solar flare trigger mechanism  
p0001 A71-12761

The observation of nonthermal solar X-radiation in the energy range 3 less than E less than 10 keV  
p0002 A71-40425

Acceleration of electrons in absence of detectable optical flares deduced from type III radio bursts, H alpha activity and soft X-ray emission  
[NSSDC-ID-68-014A-04-PS] p0009 A75-16217

L

**LAASPERE, T.**  
New results on the correlation between low-energy electrons and auroral hiss  
p0020 A76-22086

**LANGEL, R. A.**  
Variation with interplanetary sector of the total magnetic field measured at the OGO 2, 4 and 6 satellites  
p0008 A75-12368

Relation of variations in total magnetic field at high latitude with the parameters of the interplanetary magnetic field and with DP<sup>2</sup> fluctuations  
p0013 A75-28743

A comparison of electric and magnetic field data from the OGO 6 spacecraft  
p0018 A76-16514

Magnetic field variations above 60 degrees invariant latitude at the POGO satellites  
p0037 N76-71877

**LAY, G.**  
Solar radiation asymmetries and heliospheric gas heating influencing extraterrestrial UV data  
p0009 A75-13173

**LEDLEY, B. G.**  
Magnetopause rotational forms  
[NSSDC-ID-68-014A-15-PM] p0008 A75-11221

**LEJEUNE, G.**  
Altitude profiles of the photoelectron induced O 1D (6300 Å) predawn enhancement by observation and theory  
p0026 A77-20886

**LEMAIRE, J.**  
Exospheric models of the topside ionosphere  
p0006 A74-28723

**LHEUREUX, J.**  
On the quiet-time increases of low energy cosmic ray electrons  
p0021 A76-26886

Modulation of low energy electrons and protons near solar maximum  
p0021 A76-26907

Quiet-time increases of low-energy electrons - The Jovian origin  
p0025 A77-11692

**LIN, R. P.**  
Location of the electron acceleration region in solar flares.  
p0003 A72-32790

Non-relativistic solar electrons  
[NSSDC-ID-68-014A-04-05] p0007 A74-37631

**LONDON, J.**  
Satellite observations of the global distribution of stratospheric ozone  
p0036 N78-12583

**LUTON, J. M.**  
Global exospheric temperatures and densities under active solar conditions  
p0028 A77-25183

**LYONS, D.**  
The dominant mode of standing Alfvén waves at the synchronous orbit  
p0017 A75-46285

M

**MAEZAWA, K.**  
Dependence of the magnetopause position on the southward interplanetary magnetic field  
p0008 A75-12370

**MAHAJAN, K. K.**  
Neutral wind velocities calculated from temperature measurements during a magnetic storm and the observed ionospheric effects.  
p0004 A73-36150

**MAIER, E. J.**  
Satellite measurements of ion composition and temperatures in the topside ionosphere during medium solar activity  
p0021 A76-28486

**MALLOY, W. J.**  
The local time variation of ELF emissions during periods of substorm activity  
p0029 A77-31391

**MARTRES, M. J.**  
Acceleration of electrons in absence of detectable optical flares deduced from type III radio bursts, H alpha activity and soft X-ray emission  
[NSSDC-ID-68-014A-04-PS] p0009 A75-16217

**MARUBASHI, K.**  
Diurnal variation of thermal plasma in the plasmasphere  
p0023 A76-41210

Geomagnetic storm effects on the thermosphere and the ionosphere revealed by in situ measurements from OGO 6  
p0025 A77-16240

**MASLEY, A. J.**  
Solar cosmic ray observations during 1969  
[MDAC-WD-1448] p0037 N78-70785

**MATSUSHITA, S.**  
Magnetic storm effects on the tropical ultraviolet airglow  
p0029 A77-27318

PERSONAL AUTHOR INDEX

RAGHURAM, R.

**MATZKE, R.**  
AEROS A atomic oxygen profiles compared with the OGO 6 model p0028 A77-23987

**MAYHEW, M. A.**  
Magnetic anomaly map of North America south of 50 degrees north from Pogo data [NASA-TM-X-71229] p0035 N77-13587

**MAYNARD, N. C.**  
Electric fields in the ionosphere and magnetosphere. p0003 A72-39543  
Is the red arc a good indicator of ionosphere-magnetosphere conditions [NSSDC-ID-69-051A-02-PM] p0008 A75-11226  
Electric field measurements across the Harang discontinuity p0010 A75-16634  
Variational electric fields at low latitudes and their relation to spread-F and plasma irregularities p0029 A77-34326

**MAYR, H. G.**  
Theory of the phase anomaly in the thermosphere p0005 A74-12645  
Thermospheric 'temperatures' p0007 A74-36747  
Magnetic storm dynamics of the thermosphere p0008 A75-12453  
A global thermospheric model based on mass spectrometer and incoherent scatter data MSIS. II - Composition p0029 A77-37154

**MCCLURE, J. P.**  
Comparisons of ionogram and OGO 6 satellite observations of small-scale F region inhomogeneities p0028 A77-23211

**MCKEOWN, D.**  
OGO-6 gas-surface energy transfer experiment [NASA-CR-139009] p0031 N74-25869

**MCPHERRON**  
Substorm and interplanetary magnetic field effects on the geomagnetic tail lobes p0011 A75-19349

**MCPHERRON, R. L.**  
Substorms in space - The correlation between ground and satellite observations of the magnetic field p0005 A74-14285  
Ogo 5 observations of Pc 5 waves - Ground-magnetosphere correlations p0024 A77-11219  
Multiple-satellite studies of magnetospheric substorms - Radial dynamics of the plasma sheet p0026 A77-16868  
Triggering of substorms by solar wind discontinuities p0026 A77-21093  
Multiple satellite observations of pulsation resonance structure in the magnetosphere p0027 A77-23205  
OGO 5 observations of Pc 5 waves - Particle flux modulations p0030 A77-42295

**MEANS, J. D.**  
Instabilities connected with neutral sheets in the solar wind p0013 A75-28015  
Collisionless shock waves in space - A very high beta structure p0014 A75-35003

**MEIER, R. R.**  
Observations of the O I 1304-A airglow from OGO 4 p0002 A71-33964  
Remote sensing of the ionospheric F layer by use of O I 6300-A and O I 1356-A observations p0014 A75-35040  
Tropical UV arcs: Comparison of brightness with f sub 0 F sub 2 p0037 N77-86006

**MEYER, P.**  
On the quiet-time increases of low energy cosmic ray electrons p0021 A76-26886  
Modulation of low energy electrons and protons near solar maximum p0021 A76-26907  
Quiet-time increases of low-energy electrons - The Jovian origin p0025 A77-11692  
OGO-5 experiment E-09 cosmic ray electrons [NASA-CR-144668] p0034 N75-32995

**MIHALOV, J. D.**  
Pioneer 9 and OGO 5 observations of an interplanetary multiple shock ensemble on February 2, 1969 p0016 A75-42744

**MOGRO-CAMPERO, A.**  
Origin and composition of heavy nuclei between 10 and 60 MeV per nucleon during interplanetary quiet times in 1968-1972 p0017 A75-46822

**MOORE, R. L.**  
Analysis of OGO-5 and OSO-7 X-ray data [NASA-CR-142131] p0032 N75-17277

**MORGAN, M. G.**  
Light ion and electron troughs observed in the mid-latitude topside ionosphere on two passes of OGO 6 compared to coincident equatorial electron density deduced from whistlers p0030 A77-42297

**MOZER, F. S.**  
Properties of ELF electromagnetic waves in and above the earth's ionosphere deduced from plasma wave experiments on the OV1-17 and Ogo 6 satellites p0018 A76-16507

**MUENTHER, CH.**  
AEROS A atomic oxygen profiles compared with the OGO 6 model p0028 A77-23987

**N**

**NAGY, A. F.**  
Is the red arc a good indicator of ionosphere-magnetosphere conditions [NSSDC-ID-69-051A-02-PM] p0008 A75-11226

**NEUGEBAUER, M.**  
OGO-5 observations of the magnetopause p0010 A75-19134  
Structure of the quasi-perpendicular laminar bow shock p0012 A75-23707  
The enhancement of solar wind fluctuations at the proton thermal gyroradius p0012 A75-27387  
Relation of solar wind fluctuations to differential flow between protons and alphas p0013 A75-28004  
The enhancement of solar wind fluctuations with scale size near the proton gyroradius p0013 A75-28038  
A search for solar wind velocity changes between 0.7 and 1 au p0013 A75-28750  
Current-driven plasma instabilities at high latitudes p0014 A75-35005  
The role of Coulomb collisions in limiting differential flow and temperature differences in the solar wind p0019 A76-19838  
Structure of a quasi-parallel, quasi-laminar bow shock p0028 A77-23220

**NEUGEBAUTER, M.**  
Collisionless shock waves in space - A very high beta structure p0014 A75-35003

**NEWTON, G. P.**  
Comparison of the San Marco 3 Nace neutral composition data with the extrapolated Ogo 6 empirical model p0021 A76-26524  
A global thermospheric model based on mass spectrometer and incoherent scatter data MSIS. I - N2 density and temperature p0029 A77-37153  
A global thermospheric model based on mass spectrometer and incoherent scatter data MSIS. II - Composition p0029 A77-37154

**NIELSEN, E.**  
Access of solar electrons to the polar regions p0015 A75-37031  
Angular distributions of solar protons and electrons p0016 A75-41805

**NILSSON, C. S.**  
The micrometeoroid experiment on the OGO 4 satellite [NASA-CR-141948] p0037 N75-70676

**NISBET, J. S.**  
Global exospheric temperatures and densities under active solar conditions p0028 A77-25183

**NISHIDA, A.**  
Thinning of the near-earth (10 to about 15 earth radii) plasma sheet preceding the substorm expansion phase p0024 A76-47884

**NOXON, J. F.**  
The intensity variation of the atomic oxygen red line during morning and evening twilight on 9-10 April 1969 p0021 A76-28990

**O**

**OGILVIE, K. W.**  
The solar cycle variation of the solar wind helium abundance [NSSDC-ID-68-014A-17-OS] p0010 A75-16631

**OLIVERO, J. J.**  
Satellite observation of the mesospheric scattering layer and implied climatic consequences p0022 A76-39128

**OLSON, J. V.**  
On the local time dependence of the bow shock wave structure p0005 A74-24759

**ONDOH, T.**  
Magnetospheric substorm associated with SC p0011 A75-22613

**OPAL, C. B.**  
Remote sensing of the ionospheric F layer by use of O I 6300-A and O I 1356-A observations p0014 A75-35040  
Tropical UV arcs: Comparison of brightness with f sub 0 F sub 2 p0037 N77-86006

**ORR, D.**  
Probing the plasmapause by geomagnetic pulsations p0015 A75-36982

**OYA, H.**  
Plasma flow hypothesis in the magnetosphere relating to frequency shift of electrostatic plasma waves p0015 A75-38275

P

**PICK, M.**  
Acceleration of electrons in absence of detectable optical flares deduced from type III radio bursts, H alpha activity and soft X-ray emission [NSSDC-ID-68-014A-04-PS] p0009 A75-16217  
Non-thermal processes during the 'build-up' phase of solar flares and in absence of flares p0026 A77-18572

**POMERANTZ, M. A.**  
Access of solar electrons to the polar regions p0015 A75-37031  
Angular distributions of solar protons and electrons p0016 A75-41805  
Analysis of proton and electron spectrometer data from OGO-5 spacecraft [NASA-CR-142078] p0032 N75-17020

**POTAPOV, A. S.**  
Excitation of magnetosonic waves with discrete spectrum in the equatorial vicinity of the plasmapause p0012 A75-27679

**POTTER, W. E.**  
A global thermospheric model based on mass spectrometer and incoherent scatter data MSIS. II - Composition p0029 A77-37154

**PRINZ, D. K.**  
Observations of the O I 1304-A airglow from OGO 4 p0002 A71-33964

**PRUSS, G.**  
Magnetic fields, bremsstrahlung and synchrotron emission in the flare of 24 October 1969 p0002 A71-43849

**PYTTE, T.**  
Multiple-satellite studies of magnetospheric substorms - Radial dynamics of the plasma sheet p0026 A77-16868

**R**

**RAGHURAM, R.**  
A new interpretation of subprotonospheric whistler characteristics p0019 A76-16522

**RAJAN, R. S.**

**RAJAN, R. S.**  
Hysteresis of primary cosmic rays associated with Forbush decreases p0022 A76-35348

**RAO, B. C. N.**  
Satellite measurements of ion composition and temperatures in the topside ionosphere during medium solar activity p0021 A76-28486

**RAWER, B.**  
AEROS A atomic oxygen profiles compared with the OGO 6 model p0028 A77-23987

**RAWER, K.**  
AEROS A atomic oxygen profiles compared with the OGO 6 model p0028 A77-23987

**REBER, C. A.**  
Dynamical effects in the distribution of helium in the thermosphere p0024 A77-11489  
Geomagnetic storm effects on the thermosphere and the ionosphere revealed by in situ measurements from OGO 6 p0025 A77-16240  
Global exospheric temperatures and densities under active solar conditions p0028 A77-25183

A global thermospheric model based on mass spectrometer and incoherent scatter data MSIS. I - N2 density and temperature p0029 A77-37153  
A global thermospheric model based on mass spectrometer and incoherent scatter data MSIS. II - Composition p0029 A77-37154

**REED, E. I.**  
Remote sensing of the ionospheric F layer by use of O I 6300-A and O I 1356-A observations p0014 A75-35040  
Polar enhancements of nightglow emissions near 6230A p0019 A76-19613

Behavior of the sodium and hydroxyl nighttime emissions during a stratospheric warming p0020 A76-22490  
Tropical F region winds from O I 1356-A and forbidden O I 6300-A emissions. II - Analysis of OGO 4 data p0023 A76-42683

**REED, E. L.**  
The global characteristics of atmospheric emissions in the lower thermosphere and their aeronomic implications p0016 A75-42726

**REGAN, R. D.**  
A global magnetic anomaly map p0012 A75-24043

**REGENER, V. H.**  
Ultraviolet solar energy survey on OGO-6 [NASA-CR-155088] p0037 N77-86268

**ROBLE, R. G.**  
Diurnal variation of the neutral thermospheric winds determined from incoherent scatter radar data p0006 A74-36735  
The intensity variation of the atomic oxygen red line during morning and evening twilight on 9-10 April 1969 p0021 A76-28990

**ROEMER, M.**  
Recent improvements in our knowledge of neutral atmosphere structure from satellite drag measurements [BMBW-WRK-226] p0005 A74-23676

**ROY, J. R.**  
Slow X-ray bursts and chromospheric flares with filament disruption [NASA-CR-142151] p0032 N75-17281

**ROY, J. R.**  
Slow X-ray bursts and flares with filament disruption p0016 A75-43792

**RUSCH, D. W.**  
Satellite measurements of nitric oxide in the polar region p0017 A75-46289

**RUSSELL, C. T.**  
Magnetic emissions in the magnetosheath at frequencies near 100 Hz. p0001 A69-31985  
Substorms in space - The correlation between ground and satellite observations of the magnetic field p0005 A74-14285

The solar wind and magnetospheric dynamics p0010 A75-19127  
OGO-5 observations of the magnetopause p0010 A75-19134  
Substorm and interplanetary magnetic field effects on the geomagnetic tail lobes p0011 A75-19349

Structure of the quasi-perpendicular laminar bow shock p0012 A75-23707  
Instabilities connected with neutral sheets in the solar wind p0013 A75-28015

Collisionless shock waves in space - A very high beta structure p0014 A75-35003  
Current-driven plasma instabilities at high latitudes p0014 A75-35005

On the causes of spectral enhancements in solar wind power spectra p0020 A76-22081  
Ogo 5 observations of Pc 5 waves - Ground-magnetosphere correlations p0024 A77-11219

Triggering of substorms by solar wind discontinuities p0026 A77-21093  
Multiple satellite observations of pulsation resonance structure in the magnetosphere p0027 A77-23205

Structure of a quasi-parallel, quasi-laminar bow shock p0028 A77-23220  
OGO 5 observations of Pc 5 waves - Particle flux modulations p0030 A77-42295

Production processing of the data obtained by the UCLA OGO-5 fluxgate magnetometer [PUBL-905] p0037 N75-76086

**RYCROFT, M. J.**  
A review of in situ observations of the plasmopause p0015 A75-36977

**S**

**SALAH, J. E.**  
Diurnal variation of the neutral thermospheric winds determined from incoherent scatter radar data p0006 A74-36735  
A global thermospheric model based on mass spectrometer and incoherent scatter data MSIS. I - N2 density and temperature p0029 A77-37153

**SAXENA, O. P.**  
Neutral wind velocities calculated from temperature measurements during a magnetic storm and the observed ionospheric effects. p0004 A73-36150

**SCARABUCCI, R. R.**  
VLF propagation in the magnetosphere during sunrise and sunset hours p0018 A76-14838

**SCARF, F. L.**  
Structure of the quasi-perpendicular laminar bow shock p0012 A75-23707  
Collisionless shock waves in space - A very high beta structure p0014 A75-35003

Current-driven plasma instabilities at high latitudes p0014 A75-35005  
Characteristics of instabilities in the magnetosphere deduced from wave observations p0023 A76-41914

Structure of a quasi-parallel, quasi-laminar bow shock p0028 A77-23220

**SCHERER, M.**  
Exospheric models of the topside ionosphere p0006 A74-28723

**SCHMIDTKE, G.**  
AEROS A atomic oxygen profiles compared with the OGO 6 model p0028 A77-23987

**SENGUPTA, P. R.**  
Solar X-ray control of the E-layer of the ionosphere p0001 A70-34943

**SERLEMITSOS, A. T.**  
Solar energetic particle event with He-3/He-4 greater than 1 p0009 A75-15342

**PERSONAL AUTHOR INDEX**

Solar particle events with anomalously large relative abundance of He-3 p0013 A75-34018

**SHARE, G. H.**  
Hard X-ray spectra of cosmic gamma-ray bursts p0030 A78-10580

**SHELLEY, E. G.**  
A multi-satellite study of the nature of wavelike structures in the magnetospheric plasma [NASA-CR-143680] p0033 N75-17877

**SIMNETT, G. M.**  
Relativistic electron events in interplanetary space p0007 A74-37632

**SIMPSON, J. A.**  
Origin and composition of heavy nuclei between 10 and 60 MeV per nucleon during interplanetary quiet times in 1968-1972 p0017 A75-46822

**SLATER, A. J.**  
An explanation of the longitudinal variation of the OI D (630 nm) tropical nightglow intensity p0019 A76-21456

**SMITH, B. F.**  
Pioneer 9 and OGO 5 observations of an interplanetary multiple shock ensemble on February 2, 1969 p0016 A75-42744

**SMITH, E. J.**  
Magnetic emissions in the magnetosheath at frequencies near 100 Hz. p0001 A69-31985  
Plasmaspheric hiss. p0004 A73-26984

A relation between ELF hiss amplitude and plasma density in the outer plasmasphere p0006 A74-30677  
Intensity variation of ELF hiss and chorus during isolated substorms [NSSDC-ID-69-051A-22-PM] p0007 A74-44202

Electromagnetic hiss and relativistic electron losses in the inner zone p0012 A75-23716  
Magnetosheath lion roars p0022 A76-33057

**SMITH, J. C.**  
Four years of dust particle measurements in cislunar and selenocentric space from Lunar Explorer 35 and OGO 3. p0002 A72-31937

**SMITH, Z. K.**  
Pioneer 9 and OGO 5 observations of an interplanetary multiple shock ensemble on February 2, 1969 p0016 A75-42744

**SONETT, C. P.**  
Pioneer 9 and OGO 5 observations of an interplanetary multiple shock ensemble on February 2, 1969 p0016 A75-42744

**SONNERUP, B. U. O.**  
Magnetopause rotational forms [NSSDC-ID-68-014A-15-PM] p0008 A75-11221

**SORAAS, F.**  
Correlated satellite measurements of proton precipitation and plasma density p0009 A75-16437

**SORU-ESCAUT, I.**  
Acceleration of electrons in absence of detectable optical flares deduced from type III radio bursts, H alpha activity and soft X-ray emission [NSSDC-ID-68-014A-04-PS] p0009 A75-16217

**SPENCER, N. W.**  
Thermospheric 'temperatures' p0007 A74-36747  
Exospheric temperature inferred from the AEROS-A neutral composition measurement p0017 A75-46269

A global thermospheric model based on mass spectrometer and incoherent scatter data MSIS. I - N2 density and temperature p0029 A77-37153

A global thermospheric model based on mass spectrometer and incoherent scatter data MSIS. II - Composition p0029 A77-37154

**STONE, E. C.**  
Measurements of the cosmic-ray Be/B ratio and the age of cosmic rays p0006 A74-30187

**STRICKLAND, D. J.**  
Global atomic oxygen density derived from OGO-6 1304 A airglow measurements p0021 A76-28989

PERSONAL AUTHOR INDEX

ZIRIN, H.

SUGIURA, M.

Magnetospheric field morphology at magnetically quiet times

p0005 A74-14270

Identifications of the polar cap boundary and the auroral belt in the high-altitude magnetosphere - A model for field-aligned currents

p0014 A75-35007

Field-aligned currents observed by the OGO 5 and Triad satellites

p0026 A77-17124

A new view of the ring current

p0031 N73-17947

SWANENBURG, B. N.

Long-term solar modulation of cosmic-ray electrons with energies above 0.5 GeV

p0037 N77-84176

T

TAEUSCH, D. R.

Structure of electrodynamic and particle heating in the undisturbed polar thermosphere

p0018 A76-14318

Structure of electrodynamic and particle heating in the disturbed polar thermosphere

p0027 A77-23201

TANG, F.

Slow X-ray bursts and flares with filament disruption

p0016 A75-43792

Slow X-ray bursts and chromospheric flares with filament disruption [NASA-CR-142151]

p0032 N75-17281

TAYLOR, H. A., JR.

In-situ observations of irregular ionospheric structure associated with the plasmopause

p0008 A75-11853

High latitude minor ion enhancements - A clue for studies of magnetosphere-atmosphere coupling

p0008 A75-12439

Dynamics of Mid-latitude light ion trough and plasma tails

p0012 A75-27383

Ion composition irregularities and ionosphere-plasmasphere coupling - Observations of a high latitude ion trough

p0013 A75-28356

High-latitude troughs and the polar cap boundary

p0020 A76-22105

Geomagnetic storm effects on the thermosphere and the ionosphere revealed by in situ measurements from OGO 6

p0025 A77-16240

Light ion and electron troughs observed in the mid-latitude topside ionosphere on two passes of OGO 6 compared to coincident equatorial electron density deduced from whistlers

p0030 A77-42297

THOMAS, B. T.

Substorm effects on the neutral sheet inside 10 earth radii

p0016 A75-46232

THOMAS, G. E.

A cometary hydrogen model - Comparison with OGO-5 measurements of Comet Bennett (1970 II)

p0013 A75-32382

Global atomic hydrogen density derived from OGO-6 Lyman-alpha measurements

p0021 A76-28988

Global atomic oxygen density derived from OGO-6 1304 A airglow measurements

p0021 A76-28989

THORNE, R. M.

Plasmaspheric hiss.

p0004 A73-26984

Intensity variation of ELF hiss and chorus during isolated substorms

[NSSDC-ID-69-051A-22-PM]

p0007 A74-44202

Electromagnetic hiss and relativistic electron losses in the inner zone

p0012 A75-23716

The local time variation of ELF emissions during periods of substorm activity

p0029 A77-31391

THULLIER, G.

Vertical red line 6300 A distribution and tropical nightglow morphology in quiet magnetic conditions

p0004 A74-11523

An explanation of the longitudinal variation of the OI D (630 nm) tropical nightglow intensity

p0019 A76-21456

Experimental model of the exospheric temperature based on optical measurements on board the OGO 6 satellite

p0023 A76-42390

Altitude profiles of the photoelectron induced O I D (6300 A) predawn enhancement by observation and theory

p0026 A77-20886

Experimental global model of the exospheric temperature based on measurements from the Fabry-Perot interferometer on board the OGO-6 satellite - Discussion of the data and properties of the model

p0029 A77-34901

THULLIER, G.

North-south asymmetries in the thermosphere during the last maximum of the solar cycle

p0009 A75-16449

TINSLEY, B. A.

F region wind components in the magnetic meridian from OGO 4 tropical airglow observations

p0011 A75-22671

Tropical F region winds from O I 1356-A and forbidden O I 6300-A emissions. II - Analysis of OGO 4 data

p0023 A76-42683

TREFALL, H.

Field-aligned precipitation of greater than 30-keV electrons

p0022 A76-36276

TROSHICHEV, O. A.

Ring current asymmetry

p0002 A71-33663

TSURUTANI, B. T.

Electromagnetic hiss and relativistic electron losses in the inner zone

p0012 A75-23716

Properties of ELF electromagnetic waves in and above the earth's ionosphere deduced from plasma wave experiments on the OVI-17 and Ogo 6 satellites

p0018 A76-16507

Magnetosheath lion roars

p0022 A76-33057

The local time variation of ELF emissions during periods of substorm activity

p0029 A77-31391

U

UNGSTRUP, I. M.

'Hislers' - Quasi-periodic (T approximately equal to 2 sec) VLF noise forms at auroral latitudes

p0009 A75-16440

UNTI, T.

Pioneer 9 and OGO 5 observations of an interplanetary multiple shock ensemble on February 2, 1969

p0016 A75-42744

On the causes of spectral enhancements in solar wind power spectra

p0020 A76-22081

V

VOGT, R. E.

Measurements of the cosmic-ray Be/B ratio and the age of cosmic rays

p0006 A74-30187

VOLLAND, H.

Theory of the phase anomaly in the thermosphere

p0005 A74-12645

Magnetic storm dynamics of the thermosphere

p0006 A75-12453

Differential rotation of the magnetospheric plasma as cause of the Svalgaard-Mansurov effect

p0014 A75-35036

VORPAHL, J.

Magnetic fields, bremsstrahlung and synchrotron emission in the flare of 24 October 1969

p0002 A71-43849

VORPAHL, J. A.

Solar X-ray studies

[NASA-CR-142164]

p0033 N75-18144

W

WACHTEL, C.

Experimental model of the exospheric temperature based on optical measurements on board the OGO 6 satellite

p0023 A76-42390

Experimental global model of the exospheric temperature based on measurements from the Fabry-Perot interferometer on board the OGO-6 satellite - Discussion of the data and properties of the model

p0029 A77-34901

WALKER, J. D.

Behavior of the sodium and hydroxyl nighttime emissions during a stratospheric warming

p0020 A76-22490

WALKER, J. D., JR.

The effect of extraterrestrial dust, stratospheric warmings, and lower thermospheric pressure systems on OGO-4 measured nightglows in the earth's atmosphere (80 to 100 km)

p0031 N74-26848

WALKER, R. J.

Energetic electrons in the near geomagnetic tail and at synchronous orbit: Spatial distributions and acceleration mechanisms

p0032 N74-35223

WALTER, F.

VLF propagation in the magnetosphere during sunrise and sunset hours

p0018 A76-14838

WASSER, B.

Latitudinal dependence of atomic oxygen density between 90 and 120 kilometers as derived from OGO-6 observations of the 5577 A nightglow

p0034 N76-27744

WEST, H. I., JR.

Pitch angle distributions of energetic electrons in the equatorial regions of the outer magnetosphere - OGO-5 observations

p0011 A75-22759

Observations of protons with energies exceeding 100 keV in the earth's magnetosheath

p0020 A76-22092

Energetic electrons in the inner belt in 1968

p0022 A76-35289

A study of electron spectra in the inner belt

p0024 A76-44653

Multiple-satellite studies of magnetospheric substorms - Radial dynamics of the plasma sheet

p0026 A77-16868

OGO 5 observations of Pc 5 waves - Particle flux modulations

p0030 A77-42295

WEST, H. L., JR.

Angular distributions of solar protons and electrons

p0016 A75-41805

WILEY, W., III

The dominant mode of standing Alfvén waves at the synchronous orbit

p0017 A75-46285

WILLIAMS, D. J.

Field-aligned precipitation of greater than 30-keV electrons

p0022 A76-36276

WINKLER, C. N.

Long-term cosmic ray modulation in the period 1966-1972 and interplanetary magnetic fields

p0023 A76-39130

WINNINGHAM, J. D.

Dependence of the latitude of the cleft on the interplanetary magnetic field and substorm activity

p0020 A76-22107

WOLFE, J. H.

Pioneer 9 and OGO 5 observations of an interplanetary multiple shock ensemble on February 2, 1969

p0016 A75-42744

WRIGHT, J. W.

Comparisons of ionogram and OGO 6 satellite observations of small-scale F region inhomogeneities

p0028 A77-23211

WYDRA, B. J.

Global exospheric temperatures and densities under active solar conditions

p0028 A77-25183

Global exospheric temperatures and densities under active solar conditions

[NASA-CR-145394]

p0034 N76-10610

Z

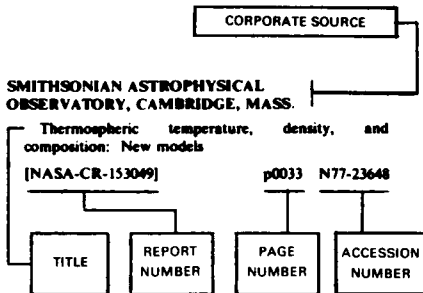
ZIRIN, H.

Magnetic fields, bremsstrahlung and synchrotron emission in the flare of 24 October 1969

p0002 A71-43849

# C. CORPORATE SOURCE INDEX

## Typical Corporate Source Index Listing



Listings in this index are arranged alphabetically by corporate source. The title of the document provides the user with a brief description of the subject matter. The report number helps to indicate the type of document cited. The page number identifies the page in the abstract section (V) on which the citation appears while the accession number denotes the number by which the citation is identified on that page. The titles are arranged under each corporate source in ascending accession number order.

### A

- ACADEMY OF SCIENCES (USSR), MOSCOW.**  
Auroral oval and magnetospheric cusps  
p0037 N78-70070
- AEROSPACE CORP., LOS ANGELES, CALIF.**  
Solar X-ray studies  
[NASA-CR-142164] p0033 N75-18144

### B

- BUNDESANSTALT FUER BODENFORSCHUNG, HANNOVER (WEST GERMANY).**  
Comparison of a magnetic local anomaly measured by OGO-6 and a crustal feature  
p0037 N76-71883

### C

- CALIFORNIA INST. OF TECH., PASADENA.**  
Analysis of OGO-5 and OSO-7 X-ray data  
[NASA-CR-142131] p0032 N75-17277
- Slow X-ray bursts and chromospheric flares with filament disruption  
[NASA-CR-142151] p0032 N75-17281
- CALIFORNIA UNIV., BERKELEY.**  
Experiment data analysis report. OGO-A experiment no. 1  
[NASA-CR-96278] p0031 N68-33302
- CALIFORNIA UNIV., LOS ANGELES.**  
Extremely low frequency hiss emissions in the magnetosphere  
p0032 N74-30528
- Energetic electrons in the near geomagnetic tail and at synchronous orbit: Spatial distributions and acceleration mechanisms  
p0032 N74-35223
- Production processing of the data obtained by the UCLA OGO-5 fluxgate magnetometer  
[PUBL-905] p0037 N75-76086
- CHICAGO UNIV., ILL.**  
OGO-5 experiment E-09 cosmic ray electrons  
[NASA-CR-144668] p0034 N75-32995

### COLORADO UNIV., BOULDER.

- On the cometary hydrogen coma and far UV emission  
p0034 N76-21066
- Satellite observations of the global distribution of stratospheric ozone  
p0036 N78-12583

### F

- FARADAY LABS., INC., LA JOLLA, CALIF.**  
OGO-6 gas-surface energy transfer experiment  
[NASA-CR-139009] p0031 N74-25869
- FRANKLIN INST., SWARTHMORE, PA.**  
Analysis of proton and electron spectrometer data from OGO-5 spacecraft  
[NASA-CR-142078] p0032 N75-17020

### L

- LABORATORIO DI RICERCA E TECNOLOGIA PER LO STUDIO DEL PLASMA NELLO SPAZIO, FRASCATI (ITALY).**  
The magnetopause. Part 1: Multisatellite simultaneous observations of bow shock and magnetopause positions  
[LPS-75-23-PT-1] p0034 N76-33787
- The magnetopause: Part 2: Magnetopause position and the reconnection problem  
[LPS-75-24-PT-2] p0035 N76-33788
- The outer magnetosphere. Part 1: A multisatellite study of the magnetopause position in relation with some important fluid dynamic parameters  
[LPS-76-2-PT-1] p0035 N76-33793
- The outer magnetosphere. Part 3: Simultaneous multisatellite observations of the magnetopause.  
[LPS-76-4-PT-2] p0035 N76-33795

### LEIDEN UNIV. (NETHERLANDS).

- Long-term solar modulation of cosmic-ray electrons with energies above 0.5 GeV  
p0037 N77-84176
- Short-term variations of the cosmic-ray proton and electron intensities in 1968 and 1969  
p0037 N77-84177

### LOCKHEED MISSILES AND SPACE CO., PALO ALTO, CALIF.

- A multi-satellite study of the nature of wavelike structures in the magnetospheric plasma  
[NASA-CR-143680] p0033 N75-17877

### M

#### MAINE UNIV., ORONO.

- A study of the heat flux reversal region upstream from the earth's bow shock, using data from the OGO 5 electron spectrometer  
p0035 N78-11543

#### MARYLAND UNIV., COLLEGE PARK.

- The effect of extraterrestrial dust, stratospheric warmings, and lower thermospheric pressure systems on OGO-4 measured nightglows in the earth's atmosphere (80 to 100 km)  
p0031 N74-26848

#### MCDONNELL-DOUGLAS AERONAUTICS CO., HUNTINGTON BEACH, CALIF.

- Solar cosmic ray observations during 1969  
[MDAC-WD-1448] p0037 N78-70785

#### MICHIGAN UNIV., ANN ARBOR.

- OGO-V radio burst analysis  
[NASA-CR-142232] p0033 N75-19114

- Data user's notes of the radio astronomy experiment aboard the OGO-V spacecraft  
[NASA-CR-143696] p0034 N75-24593

- Magnetically ordered heating in the polar regions of the thermosphere  
p0034 N75-32651

### N

#### NATIONAL AERONAUTICS AND SPACE ADMINISTRATION, GODDARD SPACE FLIGHT CENTER, GREENBELT, MD.

- Relativistic interplanetary electrons and positrons  
p0031 N71-25288
- A new view of the ring current  
p0031 N73-17947
- AE-LEE measurements at low and mid latitude  
p0031 N74-28251
- High latitude ionospheric winds related to solar-interplanetary conditions  
p0032 N74-29091
- Features of polar cusp electron precipitation associated with a large magnetic storm  
[NASA-TM-X-70792] p0032 N75-12873

- Magnetic anomaly map of North America south of 50 degrees north from Pogo data  
[NASA-TM-X-71229] p0035 N77-13587

- Magnetic field variations above 60 degrees invariant latitude at the POGO satellites  
p0037 N76-71877

- Low latitude variations of the magnetic field  
p0037 N76-71880

#### NAVAL RESEARCH LAB., WASHINGTON, D. C.

- Tropical UV arcs: Comparison of brightness with I sub 0 F sub 2  
p0037 N77-86006

#### NEW MEXICO UNIV., ALBUQUERQUE.

- Ultraviolet solar energy survey on OGO-6  
[NASA-CR-155088] p0037 N77-86268

### P

#### PENNSYLVANIA STATE UNIV., UNIVERSITY PARK.

- The role of ice particulates in the electrification of the air in the mesosphere  
p0033 N75-24202

- Global exospheric temperatures and densities under active solar conditions  
[NASA-CR-145394] p0034 N76-10610

#### PITTSBURGH UNIV., PA.

- Observations from the Orbiting Geophysical Observatory 6 of mesospheric airglow and scattering layers  
p0033 N75-19882

- Latitudinal dependence of atomic oxygen density between 90 and 120 kilometers as derived from OGO-6 observations of the 5577 A nightglow  
p0034 N76-27744

### S

#### SMITHSONIAN ASTROPHYSICAL OBSERVATORY, CAMBRIDGE, MASS.

- Thermospheric temperature, density, and composition: New models  
[NASA-CR-153049] p0035 N77-23648
- The micrometeoroid experiment on the OGO 4 satellite  
[NASA-CR-141948] p0037 N75-70676

#### STANFORD UNIV., CALIF.

- Low-energy radio emissions from the earth and sun  
p0033 N75-20195

- Magnetospheric chorus  
p0033 N75-22959

TEMPLE UNIV., PHILADELPHIA, PA.

CORPORATE SOURCE INDEX

T

TEMPLE UNIV., PHILADELPHIA, PA.

Reduction and analysis of data from cosmic dust  
experiments on Mariner 4, OGO 3, and Lunar Explorer  
35

[NASA-CR-138866] p0032 N74-29255

TEXAS UNIV., DALLAS.

Determination of tropical F-region winds from  
atomic oxygen airglow emissions

p0034 N76-10603



1. Report No. NASA SP-7601 (Supp. 1)	2. Government Accession No.	3. Recipient's Catalog No.	
4. Title and Subtitle  OGO Program Summary - Supplement 1		5. Report Date June 1978	6. Performing Organization Code
		8. Performing Organization Report No.	
7. Author(s)  John E. Jackson		10. Work Unit No.	
9. Performing Organization Name and Address National Space Science Data Center Goddard Space Flight Center Greenbelt, MD 20771		11. Contract or Grant No.	
		13. Type of Report and Period Covered	
12. Sponsoring Agency Name and Address National Aeronautics and Space Administration Goddard Space Flight Center Greenbelt, MD 20771		14. Sponsoring Agency Code	
		15. Supplementary Notes	
16. Abstract  <p>This publication supplements the "OGO Program Summary" of December 1975. The Supplement provides a major updating of the bibliographic references in the original publication and contains a comprehensive summary of the scientific results of OGO 5 and OGO 6, which were not fully available in 1975. The Supplement follows the same format as that of the OGO Program Summary; it does not repeat the finalized information in the original publication, which should be consulted for indexes of experiments, experimenters, institutions, and the glossary of Abbreviations and Acronyms.</p> <p>The six Orbiting Geophysical Observatories (OGO's) were launched, one per year, from 1964 to 1969. OGO's 1, 3, and 5 were placed in highly elliptical, low-inclination orbits to retrieve and transmit data on the interplanetary region, shock and transition zones, the magnetosphere, the radiation belts, the ionosphere, cosmic rays, micrometeorites, and geocorona. OGO's 2, 4, and 6 were placed in low-altitude, nearly polar orbits to study the neutral atmosphere, particle influence at the poles, airglow and auroral emissions, and solar flares.</p>			
17. Key Words (Suggested by Author(s)) Artificial Satellites    NASA Programs Bibliographies            OGO Earth Satellites          Summary Geophysical Observations		18. Distribution Statement  Unclassified - Unlimited	
19. Security Classif. (of this report) Unclassified	20. Security Classif. (of this page) Unclassified	21. No. of Pages 126	22. Price* \$6.50 HC